TREATMENT, RECYCLE AND REUSE OF WASTE

FROM HANDMADE PAPER INDUSTRY

Submitted in fulfillment of the requirements of the degree of

DOCTOR OF PHILOSOPHY IN CHEMICAL ENGINEERING

By

SAAKSHY

(2011RCH7109)

SUPERVISOR

Dr. Kailash Singh

Associate Professor

JOINT-SUPERVISOR

Dr. A.B Gupta

Professor

Department of Chemical Engineering

MALAVIYA NATIONAL INSTITUTE OF TECHNOLOGY JAIPUR

May 2017

Malaviya National Institute of Technology Jaipur

2017

All Rights Reserved

MALAVIYA NATIONAL INSTITUTE OF TECHNOLOGY JAIPUR

DEPARTMENT OF CHEMICAL ENGINEERING

JLN MARG, JAIPUR-302017 (RAJASTHAN) INDIA

CERTIFICATE

This is to certify that data presented in the current Ph.D. thesis entitled **"Treatment, Recycle and Reuse of Waste from Handmade Paper Industry"** is the outcome of the study conducted by me for the present work. To the best of my knowledge, these data have not been published anywhere else. The data referred/taken from other papers/reports/ books have been duly acknowledged.

Date: Saakshy

2011RCH7109

This is to certify that the data presented in the current Ph.D. thesis entitled **"Treatment, Recycle and Reuse of Waste from Handmade Paper Industry"** has been completed by Ms. Saakshy, (Student ID: 2011RCH7109) under our supervision. The present work has been carried out at the Department of Chemical Engineering, Malaviya National Institute of Technology Jaipur and is approved for submission for Ph.D. degree. The above statement made by the candidate is correct to the best of our knowledge.

Dr. Kailash Singh
(Supervisor)

Prof. A. B Gupta
(Joint-Supervisor)

ACKNOWLEDGEMENT

First of all, I extend my immeasurable thanks to God Almighty for bestowing his blessings so that I could complete this thesis.

I wish to express my deep sense of gratitude and respect to my supervisor, Dr. Kailash Singh, Associate Professor, Department of Chemical Engineering for his valuable guidance, kind support and co-operation, he has shown to me during the studies especially modelling and simulation studies. My Co-supervisor Prof. A. B. Gupta, Department of Civil Engineering has always been kind enough to guide me at each and every step of the studies. His guidance has been able to inculcate in me the understanding of my topic and to have deep knowledge of the subject. I am lucky enough that they have agreed to be my supervisor and co-supervisor. I would like to thank members of my DREC, Dr. R K Vyas, Associate Professor, Department of Chemical Engineering, MNIT Jaipur & Dr. Prabhat Pandit, Associate Professor, Department of Chemical Engineering for their valuable inputs during progress seminars of the study.

It is my privilege to extend my sincere thanks to Mr. Ashwini Kumar Sharma, Dy. Director KNHPI for his support and technical guidance whenever needed during the study. I am thankful to all the faculty members and technical staff of Department of Chemical Engineering, MNIT Jaipur including staff of Materials Research Centre for their kind support in analysis of the samples. I would like to thanks Dr. Manisha Sharma, Assistant Professor, Department of Chemical Engineering, Manipal University Jaipur, Dr. Jitendra Kumar Singh, Assistant Professor, J K Lakshmipat University Jaipur, Dr. Kavita Verma, Assistant Professor, JECRC Jaipur, Mr. Gaurav Kataria and Mr. Avdhesh Pundir, Research Scholars, Department of Chemical Engineering, MNIT Jaipur for their help and co-operation whenever needed. My thanks are due to my dear and respected mother Dr. Kiran Bala, father Dr. Khem Chand, brother Dr. Salil Raja Agarwal and Bhabhi Mrs. Neha Agarwal who have taken lots of pain in completion of my studies. I have been able to complete my studies due to their unconditional affection and support.

(Saakshy)

2011RCH7109

ABSTRACT

Handmade paper industries use direct dyes to make brilliant coloured paper, which is used in making decorative wedding cards, stationery items etc. resulting in an effluent with intense colour. The handmade paper industry is a small scale industry and cannot afford costly wastewater treatment technologies. The handmade paper making process consumes huge amount of water, which is generally not recovered and hence discharged as a waste stream. In the present day context, handmade paper units are also facing water shortage as ground water level is going down day by day and therefore minimization of water utilization and recycling of treated water using simple treatment methods is needed to conserve this industry. Therefore, a need was felt to carry out detailed investigations emphasizing on treatment and recycling of wastewater in handmade paper sector in order to make it eco-friendly.

Besides dye containing stream, the major constituent of the wastewater generated in a handmade paper industry is lignin containing black liquor. Effluent samples were collected from 30 handmade paper units in Sanganer region of Jaipur district.

The effluent of handmade paper industry was characterized for various pollution parameters like BOD, COD, and colour as per standard testing method of Standard Methods of Examination of Water & Waste water (APHA, 1997). These average characteristic parameters were used to make synthetic samples for laboratory experiments.

Batch studies for adsorption were conducted with 5 g/l of fly ash and dye of 30 to 200 mg/l at various pH, initial concentration and temperature of adsorbate. Three adsorption isotherms were fitted to the data i.e. Langmuir, Freundlich and Temkin isotherm. A comparison of R^2 values of these indicates that Langmuir isotherm fitted the best. In order to describe the fixed bed column behaviour and to scale it up for industrial applications, Bohart and Adams model, Yoon Nelson and Thomas models were used showing the latter to fit the column experimental data better.

The maximum adsorption capacity of 76.33 mg/g was achieved at 318 K in batch studies. The kinetic studies of adsorption of fly ash on direct black dye showed good fitting with first order kinetics. The negative value of ΔG_0 confirmed the feasibility of the process and spontaneous nature of adsorption of fly ash. The results of COD, Colour and BOD values of treated effluent with fly ash were within prescribed limits of CPCB as derived from EPA Notification S.O 64(E), dated 18 Jan 1998. A numerical model for adsorption has also been developed to predict the behaviour of adsorption in column studies with the help of MATLAB. The experimental and predicted values compared and found to fit well.

The SEM studies on fly ash particles showed them to be nearly spherical in shape. Elemental composition of fly ash using SEM-EDX showed the presence of Ti, Fe, Al, Si, O and an additional element K appears prominently after adsorption. The X-ray diffraction (XRD) studies showed that while the fly ash consisted of silicon oxide (SiO_2), Iron oxide (FeO), Sodium aluminium oxide, the adsorbed fly ash comprised Silicon oxide (SiO_2), aluminium silicon oxide and aluminium silicate (Al_2SiO_5). The surface area of fly ash as determined with methylene blue method was about 240 m^2/g.

The adsorbed fly ash was added to the coloured cotton rag pulp in dosages of 1 to 5% and the strength properties of the pulp were evaluated. It was found that the tensile index, double fold, tear index and burst index of the cotton pulp before addition of fly ash were 2.56 Nm/g, 789, 18.79 mN. m^2/g and 1.76 kPa.m^2/g respectively which got modified to 2.51 Nm/g, 750, 17.85 mN.m^2/g and 1.73 kPa.m^2/g respectively after addition of fly ash. Thus, it can safely be added to the pulp for paper making the whole process a closed loop cycle.

The use of fly ash proves economical compared to activated carbon for the treatment of wastewater of handmade paper industry.

Semi-batch ozonation studies of direct red, direct blue dye were conducted at various affecting parameters and initial concentration of dye solution varying from 50 to 1000 mg/l.

The results indicated that decolourization time was reduced from 12 to 4 minutes for blue dye with removal increasing from 59.5% to 99% at pH of 4; the corresponding values were reduction in reaction time from 12 to 6 minutes and removal efficiency increased from 73% to 99% at pH 10 for the red dye at effluent temperature of 313 K. The maximum COD removal of 45 and 54% was achieved for direct blue dye and direct red dye solutions respectively. The decolourization of dye solutions with ozone followed pseudo-first-order reaction with the maximum rate constant for direct red and direct blue dyes as 0.917 and 0.904 min^{-1} respectively, at pH of 10 and temperature of 313 K. Modelling and simulation studies of ozonation treatment in bubble column were conducted with the help of MATLAB software for a deeper understanding of mechanism of the processes and developing design parameters for laboratory scale to pilot plant systems.

The black liquor of Jute fiber with sulphite pulping process having initial COD of 6000 mg/l was biologically treated with different fungal and bacterial biomass in batch studies. The results showed that the maximum decolourization of 86% was achieved with the Phanerochaete Chrysosporium.

The sludge of handmade paper industry (solid fibers) and black liquor (liquid waste) was used for making energy briquettes by which complete recycle of solid waste and highly polluted black liquor is possible.

Thus, it is proved that both ozonation and adsorption with fly ash have a high potential for the treatment of effluent of handmade paper industry.

Table of Contents

LIST OF FIGURES

LIST OF TABLES

LIST OF NOTATIONS

ΔA Difference in absorbance between sample and blank,

ΔG_0 Standard free energy (kJ/mol),

ΔH_0 Standard enthalpy (J/mol),

ΔS_0 Standard entropy (J/mol K),

Δz Bed height, cm

1/n Heterogeneity factor,

a_{MB} Cross section area of one molecule of methylene blue,

A_T Temkin isotherm equilibrium binding constant (L/g),

B Constant related to heat of adsorption (J/mol),

b Path length of cell (cm),

C Concentration of adsorbate at time t (mg/l),

C_b Bulk concentration (mg/l),

C_e Equilibrium concentration of dye (mg/L),

C_o Initial concentration of the adsorbate in the solution (mg/L),

C_t Outlet concentration of black dye at time t (mg/L),

C_s Liquid phase concentration in equilibrium with qs on the surface (mg/l),

C_G Gas phase ozone concentration (mg/l),

C_L Concentration of dissolved ozone in liquid (mg/l),

C_d Concentration of dye (mg/l),

d_p Adsorbent diameter (m),

D_L Axial dispersion coefficient (m^2/s),

D_m Molecular diffusivity of dye in water (m^2/s),

D_{oz} Dispersion coefficient of dissolved ozone in liquid (m^2/s),

D_{dye} Dispersion coefficient of dye in water (m^2/s),

D_G Dispersion coefficient of ozone in gas phase (m^2/s),

E Mean free energy per molecule of adsorbate (kJ/mol),

h Initial adsorption rate (mg/g, min),

k Kinetic constant of ozone decomposition (s^{-1}),

k_0 Bangham constants,

k_1 Pseudo first order rate constant of adsorption (min^{-1}),

k_2 Rate constant of pseudo-second-order adsorption (g/mg min),

k_{AB} K is the kinetic constant (mL/mg, min),

K_f Freundlich constant representing adsorption capacity (mg/g) $(L/mg)^{1/n}$,

k_{id} Intra-particle rate diffusion constant,

K_L Langmuir constant related to energy of adsorption or Langmuir isotherm constant (L/mg),

k_{TH} Thomas rate constant (ml/min.mg),

k_{YN} Yoon Nelson rate constant (min)

k_f Mass transfer coefficient (cm/s),

k_{La} Mass transfer coefficient, m^2/s

L Linear velocity (flow rate/column section area, cm/min),

m Mass of adsorbent (g),

M Weight of adsorbent per liter of solution (g/L),

M_{MB} Molecular weight of methylene blue, i.e. 373.9 (g/mol),

N_0 Saturation concentration (mg/mL),

N_A Avogadro's Number ¼ 6.02×10^{23},

Q Inlet flow rate (ml/min_1) and t is the flow time (min),

q Average adsorbed phase dye concentration (mg/g),

qe Amount of adsorbate adsorbed per unit mass of adsorbent at equilibrium (mg/g),

Qe Capacity of adsorption (mg/g),

Q_{max} Maximum monolayer adsorption capacity (mg/g),

q_{max} Maximum adsorption at monolayer coverage (mg/g),

q_{MB} Maximum number of molecules of methylene blue adsorbed at the monolayer of adsorbent (mg/g),

q_s Theoretical isotherm saturation capacity (mg/g),

q_t Amount of dye adsorbed (mg/g) at any time t,

q_m Langmuir isotherm parameter

r_d Dye reaction rate (s^{-1}),

R Universal gas constant (8.314 J/mol. K),

R_L Separation factor,

R_p Radius of the adsorbent pellet (m),

S Specific surface area, m^{-1}

S_{MB} Surface area of methylene blue (m^2/g),

T Absolute temperature (K),

t Contact time (min),

T Temperature at 298 K,

$t^{1/2}$ Time required for 50% adsorbate breakthrough (minutes),

u_0 Superficial velocity (m/s),

u_G Gas flow rate (m/s),

u_L Liquid flow rate (m/s),

V Volume of adsorbate (mL),

v Interstitial velocity (m/s),

W Mass of adsorbent (g),

Z Bed depth of the column (cm),

z Axial co-ordinate (m),

ε Bed porosity,

τ Time required to achieve 50% breakthrough, minutes

ρ_p Density of adsorbent (kg/m^3),

σ^2 Time distribution variance (min^2),

LIST OF PUBLICATIONS

[1] Saakshy, Kailash Singh, A B Gupta, A K Sharma, 2016, Fly ash as low cost adsorbent for treatment of effluent of handmade paper industry-Kinetic and modelling studies for direct black dye, Journal of Cleaner Production, 112, 1227-1240. [I.F-4.959]

[2] Saakshy, Ashwini Sharma, Kailash Singh, A B Gupta , 2016, Decolonization of direct red and direct blue dye used in handmade paper making by ozonation treatment, Desalination and Water Treatment, 57 (8), 3757-3765. [I.F-1.272]

[3] Saakshy Agarwal, Shashi Yadav, Ashwini Sharma, Kailash Singh, A B Gupta , 2016, Kinetic & equilibrium studies of decolonization of effluent of handmade paper industry by low cost fly ash, Desalination and Water Treatment, 57 (53), 25783-25799. [I.F-1.272]

CHAPTER-1 INTRODUCTION

1.1 Overview of mill made paper and handmade paper industry

The word paper was derived from the Latin word "papyrus" (Kulshrestha et al. 1988). Paper is dilute slurry of fibers in water in which water is drained through a paper making screen so that a mat of interwoven fibers is laid down. The pressing and drying is used from this mat of fibers by pressing and drying. The earliest paper made with hand is called “handmade paper” because this paper was made by hand without help of any machines (www.knhpi.org.in).

The global paper consumption reached 415 million tonnes by 2014 and the global per capita consumption has moved from 54 kgs. in 2000 to 63 kgs. in 2015 (JP world paper demand 2015). In India paper consumption is growing at average of 7.6% Compounded Annual Growth Rate across the segments. The per capita consumption is in excess of 10 kg (Jogarao 2016). There are total 660 paper mills in India (india.paperex-expo.com/Exhibitors/Market-Facts.aspx).

Handmade paper may be termed as a layer of entwined fibers held together by the natural internal bonding of cellulose fibers in which sheets are made by hand. The Indian handmade paper industry has reached a turnover of over Rs. 250 crores and grown outstandingly in the recent past (www.knhpi.org.in).

The production of handmade paper is 5100 MT with export of 4080 MT worth Rs. 53.43 crores (Saakshy et al. 2015). The export of handmade paper has a great potential. This can be fulfilled by lowering the cost of production of handmade paper by making different grades of paper, adopting new technologies, utilizing alternative raw materials, improving the quality of the products and providing gainful employment.

1.2. Manufacturing process of mill made paper and handmade paper

The manufacturing process of the mill made paper industry includes raw material preparation, pulping, bleaching and papermaking.

The process flow diagram of handmade paper making process using cotton rags as raw material is given as Figure-1.1.

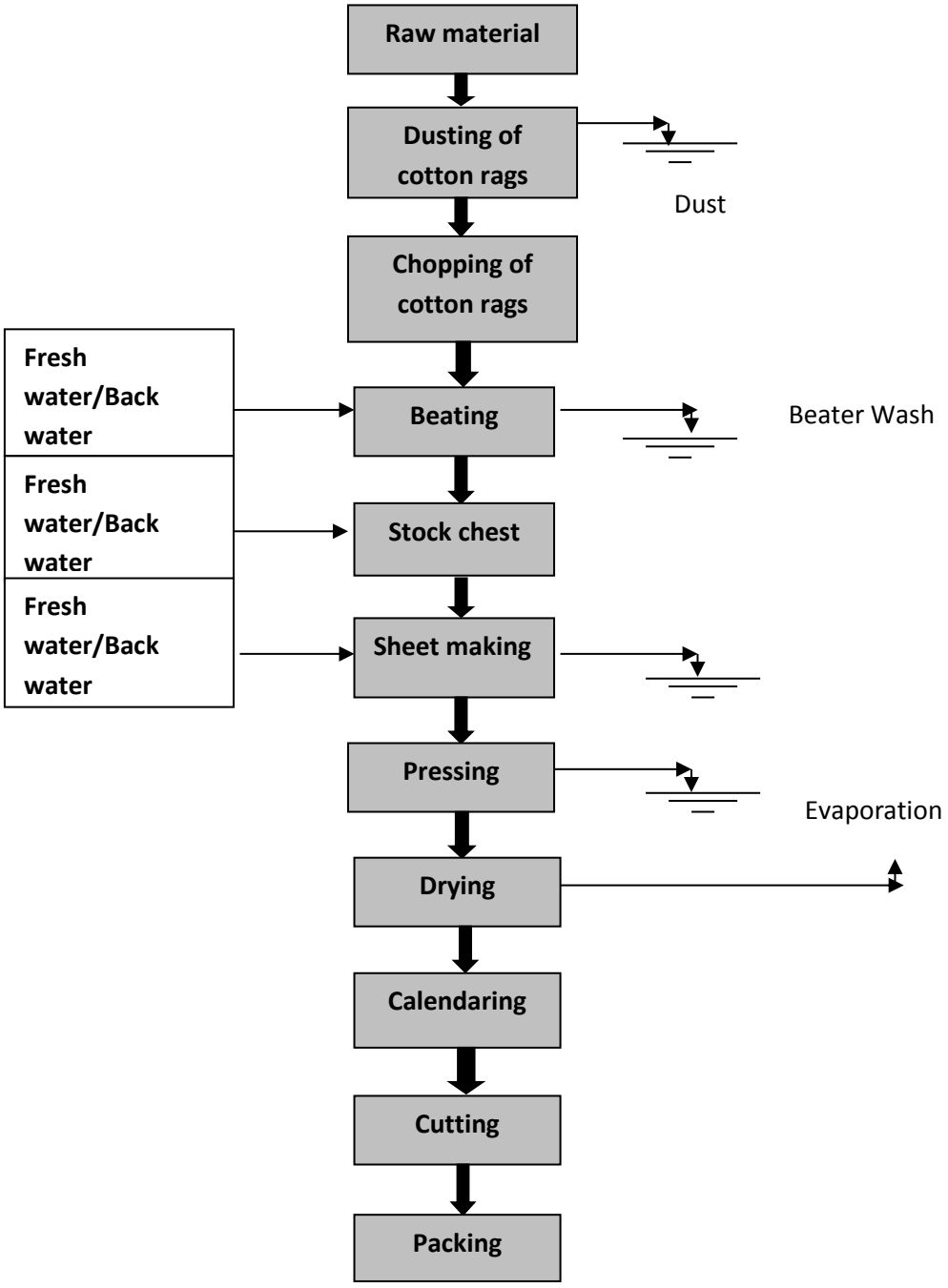

Figure 1.1 Process flow chart of handmade paper making process using cotton rags as raw material (www.knhpi.org.in)

The flow chart for making paper out of alternative ligno-cellulosic raw material is given as Figure-1.2.

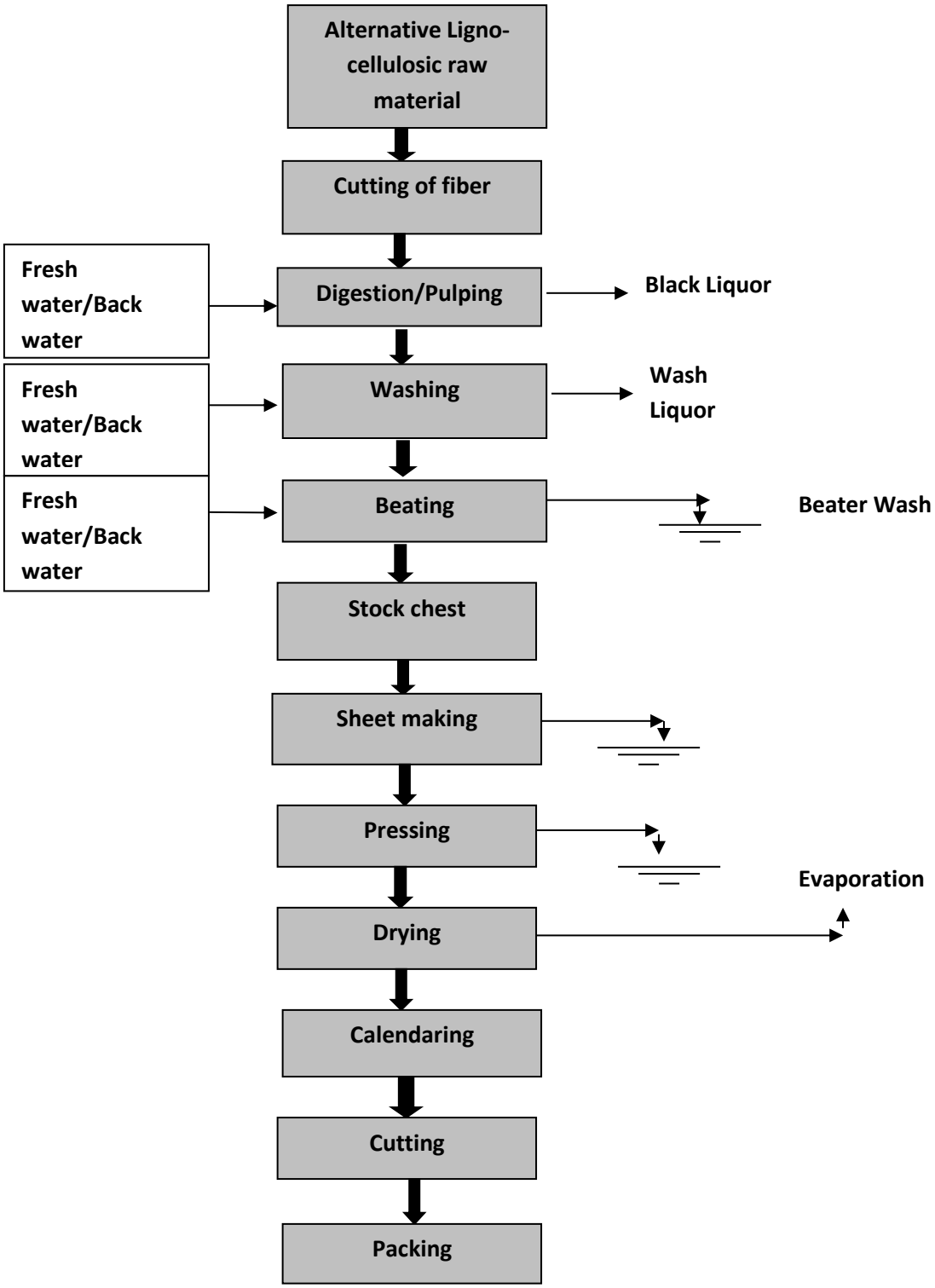

Figure 1.2 Process flow chart of handmade paper making process using alternative ligno-cellulosic raw material (www.knhpi.org.in)

The overall process and details of individual processes followed in paper making are explained in Table 1.1.

Table 1.1 Paper Making Process (Biermann. 2012)

Process	Details of process
Raw material preparation	Dry Debarking system Log washing
Cooking	Delignification/cooking (batch or continuous)
Brown stock washing, screening & cleaning	03 or 04 stage washing using presses or high-efficiency washers.
Bleaching	Elemental chlorine free (ECF) or Total chlorine free (TCF) bleaching
Sheet making	Cylinder mould vat machine,

The major wastes in handmade paper making process come out from dyed water, black liquor and wash liquor.

1. 3. Environmental issues of mill made paper and handmade paper industry

The pulp and paper industry is listed as one of the highest energy consuming and pollution generating sectors. The conventional technology used in Indian Handmade Paper Industry consumes much amount of energy and water, thereby creating high volume of effluents. Incidentally, it is one among the 17 industries identified by the Central Pollution Control Board (CPCB) as highly polluting and compliance to environmental norms are inadequate. Other environmental issues related to Indian Paper Industry which needs to be addressed include highly coloured effluents due to recalcitrant compounds, black liquor management in agro-based mills, ETP sludge disposal and management.

It is said that handmade paper making process is totally eco-friendly, but some chemicals are used at different stages in handmade paper making which are given as Table 1.2. The sizing chemicals, dyes, binders, coating chemicals, etc. contribute to pollution load in effluent.

Table 1.2 Chemicals used in handmade paper making process

Paper making process	Chemicals used
Bleaching	Chlorine as AOX, Hydrogen peroxide
Sizing	Acidic sizing(Rosin + Alum), Alkyl Ketone Dimer
Dyeing	Azo group

The points of effluent generation during the paper making process along with their nature are presented in Table-1.3.

Table 1. 3 Nature of effluents and their source

Process	Main constituents of effluent
Potcher washer	Suspended solids having high concentration of fines
Wash of beater	Mainly having fiber as pulp locked in pockets of agitator
Agitator wash	Mainly having fiber as pulp locked in pockets of agitator
Paper making vat wash (Sanganeri vat or Auto vat)	Having more fibers
Paper making spillage	Spillage having more fibers
Pressing	Pulp fibers
Miscellaneous	Solid waste of sorting and chopping process. Discharge of dyes and chemicals, coloured threads, plastics along with other materials having heavy metals

The suspended solids originating from these points are mainly fibers beaten to a certain freeness level. Efforts are therefore needed to recover these fibers.

Colour

The dyes used to make coloured paper contribute to colour in the effluent. Moreover, residual lignin in black liquor contributes to colour in case of utilization of alternative ligno-cellulosic raw material.

Suspended solids

The fibers spelt during paper making process and washing contributes to suspended solids in the effluent and also contributes to BOD and COD load.

Lignin

Black liquor is responsible for high pollution load in the paper industry (Rodriguez-Mirasol et al. 1996) . Lignin, a major component present in the black liquor, is a mixture of polyphenolic compounds. Lignin is non-biodegradable in nature and resists to traditional biological treatment processes (Zaied and Bellakhal. 2008). Lignin is integral part of the secondary cell walls of plants. Lignin is one of the most abundantly available organic polymers on earth. Lignin provides support to plants through strengthening of wood. The effluent become dark colour due to the presence of Lignin (Bajpai and Bajpai. 1994).

Solids-The solid waste contains about 3-70% moisture content and 1500-2400 calorie/gm solids.

1.4. Treatment techniques of effluent of mill made paper and handmade paper industry

The treatment techniques of mill made paper differ widely with handmade paper industry as the effluent discharged from mill made paper is more polluted than handmade paper industry.

1.4.1 Treatment techniques of paper industry

Acid precipitation

Chemical precipitation involves separation and precipitation of lignin and other inorganic compounds by reducing the pH of the effluent below 6.5. The maximum precipitation occurs in the pH range of 3-4. The technique is easy but it is expensive due to cost of chemicals. There is difficulty in handling of precipitated sludge and difficult in separation of precipitated mass due to hydrophilic nature of lignin.

The precipitation of lignin by acidification is one of the potential treatment of black liquor (Loutfi et al. 1991; Davy et al. 1998; Ohman. 2006; Ohman and Theliander. 2007) using sulfuric acid (Uloth and Wearing. 1989). The sulfuric acid interferes in the liquor cycle chemical balance with excess sulfur (Loutfi et al. 1991). Therefore, CO_2 is preferred for acidification for black liquor (Loutfi et al. 1991; Olsson et al. 2006). The separation of lignin from black liquor is an important step (Ohman and Theliander. 2007). Almost 50 % of the COD in black liquor can be removed after separation of lignin from black liquor (Abacherli et al. 1999).

Biological treatment methods

Biological treatment method is still considered as partial successful alternative for black liquor treatment among the treatment alternatives of black liquor. A selected group of fungi and basidiomycete have been shown to possess ligninolytic enzyme systems (Kirk and Cullen. 1998). The white rot fungus *Trametes versicolour* was found to reduce color of black liquor and effluent effectively (Varasavanan and Sreekrishnan. 2005).

Advanced oxidation

Ozonation

The ozone has a specific sharp odour and can be detected above 0.01 mg/l in air. The ozone gas is a potential germicide and also used as an oxidizing agent. Ozone production from pure oxygen is an appropriate and economical solution. The ozonation treatment needs high capital investment even though the operating cost is low. Ozone is a strong oxidant (E^0 = 2.08 V). Ozone oxidizes the complex aromatic rings of dyestuffs (Fanchiang et al. 2009). The ozone is an unstable molecule and therefore, generated near the site. Ozonation does not yield complete mineralization to CO_2 and H_2O (Assalin et al. 2004)

Chemical coagulation

The chemical coagulation is widely used for wastewater treatment. It is an integral treatment step in the surface or underground water treatment. The most widely used chemicals for chemical coagulation include aluminum chloride, ferric chloride, barium chloride and copper sulphate (Ukiwe et al. 2014)

Adsorption

The adsorption method is effective in removal of trace component from the wastewater. There are various adsorbents including activated carbon, zeolite, charcoal, fly ash etc. for adsorption applications. The fly ash is fine mineral residue collected in electrostatic precipitators collected after the combustion of coal in electricity generating plant. Fly ash is usually slit shaped with size 0.005-–0.074 mm (Heidrich et al. 2013).

1.4.2 Treatment techniques for the effluent of handmade paper industry

In the present scenario, the Indian handmade paper industry normally does not use any treatment techniques and discharge as such without any treatment as this is a small scale industry. Handmade paper industries use direct dyes to make brilliant coloured paper, which is used in making fancy and decorative papers, wedding cards, stationery items etc. These industries use negligible chemicals but due to abundant use of direct dye, the main component in effluent is dye.

The handmade paper industry is a small scale industry and cannot afford the costly or complex wastewater treatment technologies. The low cost fly ash can offer a cost effective technology for handmade paper sector.

1.5. Government legislations

The total waste water discharge standard for pulp and paper mills is given as Table 1.4.

Table 1.4 Discharge standards of small pulp and paper industry (EPA Notification)

Category	Standard for waste water generation
Large pulp & paper mills	200 m^3/ton of paper before 1992 and 100 m^3/ton for paper mills established after 1992.
Large pulp and paper mills (Rayon grade)	150 m^3/ton of paper produced
Waste paper based pulp and paper mills	75 m^3/ton of paper produced 150 m^3/ton for mills established after 1992
Agro based small pulp and paper mills	200 m^3/ton of paper produced 150 m^3/ton for mills established after 1992

Source: EPA Notifications' 64(E), dated 18 Jan 1998; Environment Protection rules 1986

Table 1.5 Environmental standards of pulp and paper industry

Parameter	**Concentration not to exceed, mg/l for small paper mills (production <24000MT/annum)**	**Concentration not to exceed, mg/l for large paper mills(production >24000 MT/annum)**
pH	5.5-9.0	7.0-8.5
Total Suspended solids, mg/l	50 100 (on land)	50
BOD at 27^0C for 3 days	30 100 (on land)	30
COD, mg/l	-	250
AOX, kg/tonne of paper produced	2	1
Sodium absorption ratio	26 (on land)	-

Source: EPA Notifications' 64(E), dated 18 Jan 1998; Environment Protection rules 1986

The Indian government has included pulp and paper industry in "red category". The effluent from pulp and paper mills must meet the standards before discharging into surface bodies or irrigated lands. The wastewater treatment technology for paper industry depend on the raw material, production process and the product. Out of 442 identified industries by the Rajasthan Pollution Control Board, 73 units are of textiles, 19 units of dyes and dye intermediates while 78 units of engineering sector which include paper making, etc. The environmental standards & discharge standards for small pulp and paper industry is given as Table-1.4 & Table-1.5 respectively.

1.6 Origin and significance of the present study

In the present scenario, the physical and biological treatment system are not found adequate enough for the wastewater to meet the prescribed effluent norms and for waste water recycling within the existing process. Therefore, tertiary treatment is the requirement (Charter, Central Pollution Control Board, 2015). Handmade paper industry is using cotton hosiery and alternative ligno-cellulosic as raw material. The process consumes huge amount of water and goes as waste without any recovery. In the present day context, handmade paper units are also facing water shortage as the groundwater level is going down day by day and therefore minimization of water utilization and recycling of treated water using simple treatment methods is needed to conserve handmade paper making community. Therefore there is a need to make a detailed study and emphasize on recycling of water in handmade paper sector in order to make it eco-friendly.

Previously, the handmade paper industry was kept by the Central Pollution Control Board in green category and no objection certificate was issued to handmade paper units being classified under small scale sector. Now they have shifted handmade paper industry to orange category. As Sanganer is a cluster of handmade paper industries, it is essential for them to treat the effluent at affordable and easy to operate technology.

1.7 Objectives of the study

The broad objective of this research work is to closely examine the processes that generate effluent in a typical handmade paper industry and devise a suitable techno-managerial strategy for its safe disposal, which can be handled at small scale industry level. The specific objectives of the research work are:

- To devise a suitable strategy for waste minimization.
- Characterization of effluent streams from handmade paper industry and assessment of possible reduction in water consumption by way of recycling and reuse of partially/ completely treated effluents.

- Treatment of major effluent streams through low cost adsorption using fly ash, understanding the mechanism of sorption, and reuse of spent adsorbent for a possible close loop operation.
- Treatment of major effluent streams through biological/ chemical oxidation; mathematical modelling and simulation for developing kinetic parameters for the design of such systems; and utilization of sludge generated from the process.

1.8 Scope of work

The scope of the research work is as given below:

- Quantitative assessment, Characterization of different streams of effluent discharged from different operations of handmade paper making synthetic wastewater using conventional and alternative ligno-cellulosic raw material to minimize the waste emission.
- Feasibility studies following different treatment methods in sequence including adsorption, ozonation, bacteria, fungi etc. of effluent of conventional raw material and black liquor of different alternative ligno-cellulosic raw material.
- Trial to mix this with some organic solid waste to develop high energy briquettes/compost.
- Treatment kinetics for treatment of effluent.
- Development of mathematical model and model validation by experimental data.

1.9 Organization of the thesis

This thesis is organized in to ten chapters. Chapter 1 consists of introduction and objectives of the study. Chapter 2 compiles literature related to the waste water treatment methods for paper industry. The topics included in Chapter 3 describe details of the material and methods adopted for conducting studies while those included in Chapter 4 present the details of experimental setup for waste water treatment studies. The characterization studies are included in Chapter 5. The details of adsorption studies with fly ash as adsorbent are included in Chapter 6 and details of ozonation studies for treatment of waste water treatment are given in Chapter 7.

The Chapter 8 includes microbiological studies for black liquor and Chapter 9 consists of details of utilization of sludge of handmade paper industry to make energy briquettes. Chapter 10 includes the conclusion of this study.

CHAPTER 2 LITERATURE REVIEW

2.1 Introduction of paper making

In India, the history of papermaking dates back to the 3rd century BC. The handmade paper making has been practiced by a "Kagzis" for generations together (Saakshy et al. 2013). Even in the 14th century, during the rule of Feroze Shah Tughlaq, the royal family used handmade paper for official documents, miniature paintings, calligraphy to make copies of the Holy Quran and to maintain account books. In the 16th century, the ruler of Amber, Raja Man Singh brought the Kagzis to Sanganer (www.knhpi.org.in).

Approximately, 400 million metric tons per annum of paper and cardboard are produced globally. The China alone is responsible for around one quarter of the total production (Bajpai 2016; www.statistica.com). The United States, Japan, Germany, Canada, China, Finland, republic of Korea, Indonesia, Sweden and Brazil are the world's largest paper and paperboard producers. The largest pulp producers are United States, China, Canada, Brazil, Sweden, Finland, Japan, Russian Federation, Indonesia and Chile. These countries together were responsible for 81% and 73% of the world's pulp and paper and paperboard production in 2010 respectively (FAO 2014; Fracaro et al. 2012; www.fao.org/forestry/statistics;www.paperindustryworld.com;www.ibisworld.com/industry/global/global-paper-pulp-mills.html).

2.2 Raw Material

The raw material used in paper industry and handmade paper industry differ widely as low lignin raw material is used in the handmade paper industry.

2.2.1 Raw material used in Indian paper industry

The major raw material used in the Indian paper industry is broadly categorized as hardwoods, softwoods and recycled fiber.

The consumption of wood as raw material is on average 9 metric tons per annum. Wood consists of approximately 50-55% cellulose, 25-30% lignin and 20-25% hemicellulose. The hard wood species as raw material for paper industry include poplar, casuarina, subabul, eucalyptus etc. The three categories of non-wood fibers are used in paper industry viz. crops (hemp, kenaf, flax and jute), agricultural residues (wheat straw, rice straw, bagasse), wild plants (grasses, bamboo, seawood). The pre-consumer recycled fiber includes shaving, trimmings of paper machine such as printer rejects etc. The post-consumer recycled fiber include old waste paper collected from consumers such as newsprint, duplex board, Kraft paper etc. (Report 2014, Govt. of India).

2.2.2 Raw Material Used in Handmade Paper Making

More than 95% of handmade paper units in India utilize cotton ragas/hosiery waste, (botanical name-*Gossypium Herbaceum*) as a raw material. Cotton paper is made utilizing 100% cotton fibers (Figure 2.1) as raw material and has better strength and durability in comparison to mill made paper.

Figure 2.1 Cotton rags

The price of cotton rags is increasing by leaps and bounds. Keeping in view the scarce availability of cotton hosiery, the alternate and cost effective ligno-cellulosic raw materials available in different regions of India are being promoted for paper making. The locally available alternative ligno-cellulosic raw materials like Banana fiber, Jute fiber, Sunn hemp fiber, Ankara fiber, Bhimal fiber, Wheat straw, Rice straw etc. are suited for making specialty grade of handmade paper. These bast fibers extracted from bark have more lignin in comparison to cotton hosiery waste, which does not have any lignin content.

2.3 Composition of lignocellulosic raw material

The ligno-cellulosic raw material is a heterogeneous organic polymer with carbohydrates and lignin as main components. The carbohydrates are composed of cellulose and hemicelluloses bound together by lignin. Cellulose (Figure 2.2) is a homopolysaccharides composed of 10,000 D-glucopyranose units linked together by 1, 4- β -D- glucopyranoside units. It is the biggest component in both softwood and hardwood species. The only monomer present in cellulose is glucose. In chemical pulping and bleaching, the objective is to separate the wood fiber without seriously degrading the cellulose chain (Sjostrom. 1993).

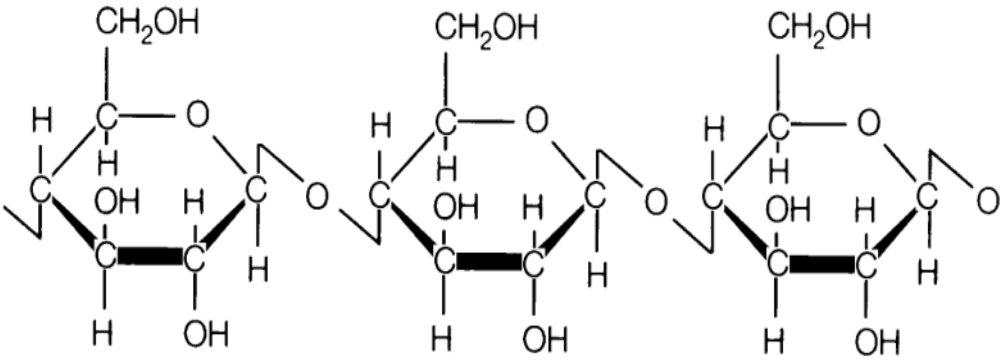

Figure 2.2 Cellulose structure

Hemicelluloses are heterogeneous polysaccharides and have a much shorter chain length. Hemicellulose can be easily hydrolyzed to their monomers comprising D Glucose, D galactose, D-mannose, D-xylose and L-rhamnose which are joined primarily by 1-4 glycoside bonds between monomer units.

Lignin is macromolecular compound consisting of phenyl propane units combined in a random formation. The three monolignols are p-coumarly, coniferyl and sinapyl alcohols (Figure 2.3). Softwood lignin is composed mainly of more than 90% gluaiacyl units derived from coniferyl alcohol. Both guaiacyl and syringyl units are present in significant amounts in hardwood and it is copolymer of coniferyl and sinapyl alcohols. The exact structure of lignin is not completely understood because of the random nature of the linkages between the phenyl propane units. Lignin content varies from 24-33% in softwoods and 19-28% in hardwoods.

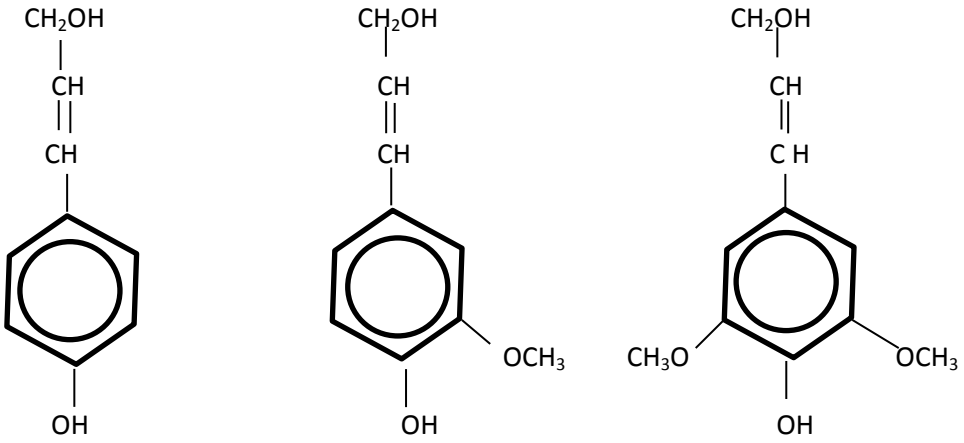

p-coumaryl alcohol coniferyl alcohol sinapyl alcohol

Figure 2.3 Lignin structure (Smook. 1992)

2.4 Manufacturing process of paper and handmade paper industry

The manufacturing process of paper industry and handmade paper industry differ on the basis of pulping and sheet making process.

2.4.1 Manufacturing process in paper industry

Raw Material preparation

The wood barks are debarked in debarker and chopped from 1 to 1.5 inches size in chopper.

Pulping process

The pulping process involves the separation of cellulosic fibers and removal of undesired impurities. The pulping is done by chemical pulping or Chemi-mechanical pulping method. In kraft process, the raw material is treated with sodium hydroxide and sodium sulphide at temperature of 165 -170 °C in pressurized digester to separate lignin and wood resins from the pulp. About 95% of the chemicals are recovered in the recovery system. The soda pulping process is employed for the pulping of agro-residues. In this process, the raw material is cooked with caustic soda at a temperature of 150-160 °C. The mild caustic soda is used to impregnate the wood chips to extract resin and lignin prior to refining and bleaching. The flow chart of the delignification process adopted in paper industry is given as Figure 2.4.

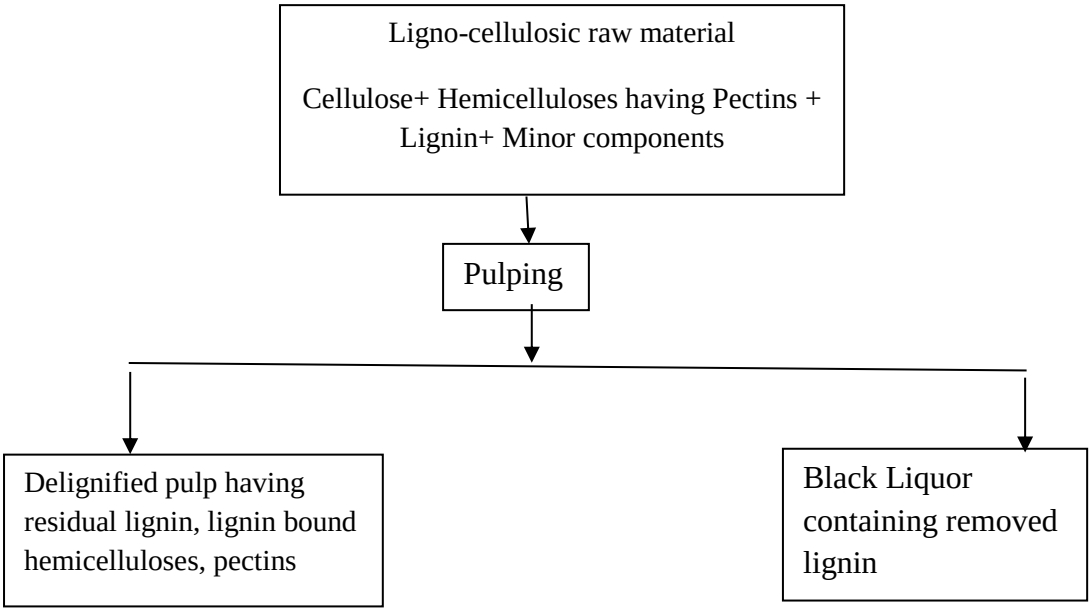

Figure 2.4 Flow chart of delignification

The pollutants emitted from handmade paper industry include cellulose, extractives, lignin, lignans, sugars, hemicelluloses.

Brown stock washing

This operation is used to separate pulp fibres from the black liquor containing spent cooking chemicals and dissolved raw materials. It has been observed that only few of the large wood and agro-based mills have upgraded their washing system to achieve minimum dilution factor and maximum washing efficiency with installation of efficient washing system mainly employing vacuum drum washers or belt washers or twin roll presses.

Bleaching

The chlorine dioxide or hypochlorite is used to bleach the pulp. The ECF (Elemental Chlorine Free) bleaching is being practiced in large paper mills where it uses oxygen delignification, chlorine dioxide and other chemicals. The conventional bleaching sequence is chlorine dioxide, caustic soda, oxygen delignification and hydrogen peroxide. The combination of ozone/oxygen delignification /peroxide leads to TCF (Total Chlorine Free) bleaching.

Sheet making

The sheet making in paper industry is with the help of heated rotary cylinders.

2.4.2 Manufacturing process in handmade paper industry

The raw material is vigorously shaken to remove the dust and dirt and then sorted manually to remove extraneous materials. The sorted material is chopped to 1 to 1.5 inches. The chopped raw material in case of cotton rags is fed in beater along with water and beaten in a Hollander beater. The handmade paper sheets are formed with diluted pulp slurry in a vat. The lifting mould is dipped into the vat, shaken vigorously and lifted out with the layer of entwined fibres on the mould. The sheets are made with the help of a cylinder mould vat machine and sanganeri vats. Then, wet paper is transferred onto a cotton cloth or felt. A hydraulic press or pneumatic press is used to remove the excess water from the sheets. The sheets are dried by hanging them in an covered area or under sunlight for drying. The dried sheets are placed between metallic plates and passed through heavy rollers in a calendaring machine for smoothening of paper sheets. The sheets are then cut to the desired size using a cutting machine or guillotine cutter.

2.5 Environmental issues

The environmental issues of paper industry and handmade paper industry are presented here.

2.5.1 Emission issues for paper industry

The pulp and paper industry is the third largest consumer of fresh water with consumption in the range 80-150 m^3/t of paper (GOI, 2014). Generally agro based mills consume much more water than Recycled Fiber based mills. The waste water discharged from paper industry contains various chemicals like thiols, sulphur dioxide, sulphite and sulphides, fibres and resins; bleaching agents and whitening agents. The effluent of paper industry constitutes of organic pollutants (starch, fibers, hemicellulose, and organic (acids). The composition of the black liquor depends on the raw material and the production process and varies considerably between different mills (Smook, 1992). The phenolic compounds present in black liquor pose powerful toxic effect on microorganisms.

Three kinds of lignin phenol oxidases produced are lignin peroxidase (Lip), manganese peroxidase (MnP) and laccase (Lac) (Hari Haran et al. 2013).

2.5.2 Emission issues for handmade paper industry

The effluent emitted by handmade paper industry utilizing cotton rags as raw material mainly consists of suspended solids and colour. If alternative ligno-cellulosic raw material likes banana fiber, jute fiber etc. is used, the black liquor, wash liquor mainly consists of lignin, which is recalcitrant in nature. However, only 5% of handmade paper units use alternative ligno-cellulosic raw material.

Process and type of effluent generated

The effluent generated from handmade paper units and their stages are given in Table 2.1

Table 2.1 Process and type of effluent generated (Saakshy et al 2008)

Process	Type of effluent
Potcher washer	Suspended solids having more fines
Agitator wash	Mainly having fiber as pulp locked in pockets of agitator
Paper making(Sanganeri vat or Auto vat)	Spillage having more fibers
Paper vat washing	Pulp having more fibers
Paper Lift Basin	Pulp fibers
Squeezing machine	Pulp fibers
Floor washing	Pulp fibers
Miscellaneous	Solid waste of sorting and chopping process. Discharge of dyes and chemicals, coloured threads, plastics along with other materials.

It has been found that the total suspended solids were high in effluent of vat wash discharge, paper lift basin wash and agitator wash.

2.6 Characterization of effluent of paper industry

The pulp and paper industry is one of the prominent pollution creating sectors. The effluent of handmade paper as well as paper industry has been characterized by various researchers as given in Table 2.2.

Table 2.2 Physico-chemical characteristics of paper industry

Source	Characteristics	Author, Year
Waste paper based paper mill	Raw waste water characteristics pH=6.8-7.1,Suspended solids =1160-1380 mg/l, Total dissolved solids=1043-1293 mg/l, BOD=268-387 mg/l, COD=1110-1272 mg/l	Kesalkar et al. 2012
Effluent of paper mills of Nilakotai Dindigul, Tamil Nadu	pH, Colour, odour, temperature, electrical conductivity, total dissolved solids, BOD, COD, Na, Ca and Mg from November 2010 to April 2011. All the parameters were found to exceed limits prescribed by WHO	Kuzhali et al. 2012
Physico-chemical characteristics of paper industry effluents-A case study of South India Paper Mill (SIPM)	BOD-203 mg/l; COD-1145 mg/l; Total dissolved solids-996 mg/l; Chloride -45 mg/l; Sulfate-8.5 mg/l	Devi et al.2011

An overview of certain physico-chemical parameters of paper mill effluent	pH-7.39, BOD-108 mg/l, COD-495 mg/l, Total dissolved solids-578 mg/l, Total solids-908 mg/l.	Dhanushree and Kousar. 2015
Physico – Chemical Analysis of Paper Industry Effluents in Jammu city (J&K)	pH-6.7 to 8.4, Turbidity- 289-309 NTU, Electrical conductivity-272.8 to 508.7 µs, Total dissolved solids-675 to 1423 mg/l, Total suspended solids-665 mg/l	Sharma & Ramotra. 2014

2.7 Legal aspects related to paper industry

The quality of water tolerance for the paper industry is shown in Table 2.3.

Table 2.3 Quality of water tolerance for paper industry (Source: IS 2724-1964)

Parameters	**Ground wood paper**	**Kraft paper bleached**	**Kraft paper unbleached and pulp unbleached**	**Soda and sulphite paper**	**High grade paper**
Colour, Hazen units	20	15	100	10	5
Turbidity, silica scale units, max.	50	25	100	15	10
Total dissolved solids, mg/l, max.	500	300	500	300	300

Total hardness as CaCo3, max.	200	100	200	100	100
Iron as Fe, mg/l, max.	1	0.25	1	0.25	0.25
Manganese as Mn, max	0.5	0.1	0.5	0.05	0.05
Total residual chloride, mg/l, max.	2	2	-	2	2
Suspended solids, mg/l, max.	25	25	25	25	10

The Indian handmade paper industry comes under the orange category as specified by the Central Pollution Control Board, Govt. Of India.

2.8 Treatment techniques of wastewater of paper industry

It was observed that in the majority of the paper mills, all raw effluents from various unit operations are mixed together and treated using conventional activated sludge process consisting of primary and secondary treatment. It is further treated in aerated lagoons prior to discharging into receiving water bodies. Few of the large paper mills have upgraded their Effluent Treatment Plants (ETPs) with installation of tertiary treatment systems for better effluent quality, particularly in terms of colour and suspended solids. Few of the medium sized agro-based paper mills have installed the non-conventional chemical recovery system, to incinerate the black liquor, which is one of the major causes of pollution, coupled with a system for tertiary treatment, involving the use of tube settler/ tertiary clarifier and pressure sand filter, to achieve better effluent quality. In India approximately 905.8 million cum of water is consumed and 695.7 of waste water is generated (Central Pollution Control Board, 2006).

The water consumption by agro industries making writing and printing paper, kraft paper mills is reported to consume 100 m^3/T and 75 m^3/T respectively. The recycled fiber based industry making writing and printing paper, duplex board, newsprint consume 50 m^3 /T while kraft paper mills consume 35 m^3/T of water.

2.8.1 Chemical precipitation

Studies have been conducted with aluminum chloride, ferric chloride, barium chloride and copper sulphate for chemical precipitation of paper industry effluent. The aluminum chloride dosage of 4 g/l showed 99.8% of colour removal at pH-5.0. The ferric chloride showed 99% colour removal at 4 pH and dosage of 2 g/l. The copper sulphate was quite effective at pH-10 removing colour up to 96%, phenols 94%, TSS 94%, at a dosage of 2.5 g/l. The barium chloride showed 96% colour removal at 9-12 pH (Swamy et al. 2016). A 5 g/l of dosage of aluminium chloride gave 86.30 % colour removal, copper sulphate as coagulant could remove 74% COD, polyaluminium chloride could give 82.85% COD removal and 91.81% colour removal in another study (Kumar et al. 2011).

Poly aluminium chloride dosage of 8 ml/L reduced COD and colour by 83% and 92% respectively at pH- 5.0. The 72% COD and 84% colour removal were observed with $AlCl_3$ dosage of 5 g/l at pH-4.0 (Chaudhary et al 2010).

2.8.2 Adsorption

The adsorption process for the treatment of paper effluent is generally physical in nature resulting from the effect of Van der Waals forces. On the other hand, chemisorption involves the exchange or sharing of electrons. The adsorbent should have large surface area and should be mechanically strong.

2.8.3 Ozonation

The ozonation treatment is known to be effective for decomposing organic chemicals containing C=C bonds, aromatic compounds, phenols, polycyclic aromatics, heterocyclics, C=N and C-H bonds. The ozone does not increase the volume of wastewater and sludge and can be applied in its gaseous state (Sundrarajan et al., 2007).

2.9 Adsorption isotherms

2.9.1 Langmuir Isotherms

The Langmuir adsorption isotherm assumes that adsorption occurs at specific homogeneous sites and occurs as monolayer adsorption. The Langmuir equation in linear form is given as equation 2.1:

$$\frac{C_e}{q_e} = \frac{1}{q_{\max} K_L} + \frac{C_e}{q_{\max}} \quad \textbf{.....(Eq. 2. 1)}$$

The values of q_{max} and K_L were computed from the slope and intercept of the graph between C_e/q_e with respect to C_e. The Langmuir isotherm can be given by separation or equilibrium parameter given by equation 2.2:

$$R_L = \frac{1}{1 + K_L C_0} \quad \textbf{..... (Eq. 2.2)}$$

R_L indicates the type of isotherms (Vijayaraghavan et al., 2006; Kundu and Gupta, 2006; Pérez-Marín et al., 2007; Webber and Chakravorti, 1974). The R_L values between zero and one confirms the favorable uptake of adsorbate on adsorbent.

2.9.2 Freundlich isotherm

Freundlich isotherm is based on non -uniform and non-ideal reversible adsorption over heterogeneous surfaces that are not limited to the formation of the monolayer adsorption (Bajeer et al., 2012; Freundlich, 1906; Adamson and Gast, 1997). A linear form of Freundlich expression is obtained by taking logarithm as shown in equation 2.3:

$$\ln q_e = \ln K_f + \frac{1}{n} \ln C_e \quad \textbf{.....(Eq. 2.3)}$$

The plot of ln q_e versus ln C_e gives the value of K_f and *1/n.* The graph between ln q_e with respect to ln C_e gives the value of 1/*n* and K_f.

2.9.3 Temkin isotherm

Temkin isotherm takes into the account of adsorbent–adsorbate interaction (Temkin and Pyzhev, 1940; Aharoni and Ungarish, 1977) is given by the equation 2.4:

$$q_e = B_T \ln A_T + B_T \ln C_e \quad \textbf{.....(Eq. 2.4)}$$

A plot of q_e versus ln C_e enables the determination of isotherm constants K_t and B_1.

2.10 Kinetic models of adsorption

The three models pseudo first order, pseudo second order rate equation and intra-particle diffusion model was studied.

2.10.1 Pseudo first order kinetic model

Lagergren equation is given to study pseudo first order kinetic model.

$$\log(q_e - q_t) = \log q_e - \frac{k_1 t}{2.303} \quad \textbf{.....(Eq. 2.5)}$$

The value of k_1 is evaluated by the slope of the graph between log (q_e-q_t) and time at different concentration. The values of k_1 and q_e are calculated from the slope and intercept of the graph.

2.10.2 Pseudo-Second order kinetic model

The second order kinetic model is given as:

$$\frac{t}{q} = \frac{1}{k_2 qe^{\overline{2}}} + \frac{t}{q_e} \quad \textbf{.....(Eq. 2.6)}$$

The initial adsorption rate is given as:

$$h = k_2 qe^2 \quad \textbf{.....(Eq. 2.7)}$$

The values of h (mg/g/ min) can be calculated from the slope and intercept of the plot t/q vs. t.

2.10.3 Intraparticle diffusion

In intraparticle diffusion, the uptake varies almost proportionately with the half-power of time (Ho and McKay, 1998). The intraparticle diffusion model proposed by Weber and Morris is given as equation 2.8:

$$q_t = k_{id} t^{0.5} + C \quad \text{.....(Eq. 2.8)}$$

2.11 Conventional adsorbent

Mari et al. 2006 (FPRDI) studied the treatment of wastewater from a HMP mill of Philippines. Specifically, the study assessed the potential of a charcoal-based treatment system in treating handmade paper mill wastewater.

The effluent was passed through settling ponds and the supernatant liquid was fed through two aerated charcoal bed (ACBs) for about 5 days each, which reduced biochemical oxygen demand (BOD) and total suspended solids (TSS) to acceptable limits (www.agris. fao.org) The study was conducted to remove colour from effluent of paper industry using waste sludge from ETP as an adsorbent (Chakradhar et al 2004). Activated carbon is the commonly used as an adsorbent, the major drawback being the high cost (Varma et al., 2013).

2.12 Low cost adsorbents

Coal currently caters around 42% of global electricity generation (International Energy Agency, 2010). The thermal power generation which accounts for 80-85% in India is expected to grow by 5% per annum. There are 88 thermal power stations based on coal/lignite for power generation having a total installed capacity of 80458 MW (Central Electricity Authority, 2015). The coal consumed by these power plants during 2010-12 was 407.61 MT with total ash generation of 131.09 MT. The generation of fly ash is expected to grow to 300-400 MT by 2016 (www.flyash2012missionenergy.org). The annual production of fly ash from coal power plants is 112 MT (Dhadse et al., 2008). In India, only 3% of fly ash produced is utilized while 80% of fly ash is reused in Germany (Senapati, 2011).

The Government of India focused efforts led by Fly Ash Mission (FAM), Technology Information, Forecasting & Assessment Council (TIFAC), along with other stakeholder agencies in 1994 for gainful utilization and safe disposal of fly ash.

The national thermal power corporation has also taken initiatives to make good quality of fly ash available to users. The major constituents of most of the fly ashes are Silica (SiO_2), alumina (Al_2O_3), ferric oxide (Fe_2O_3) and calcium oxide (CaO). The other minor constituents of the fly ash are MgO, NaO, K_2O, So_x, MnO, TiO_2 and un-burnt carbon (www.ntpc.co.in; Ash Utilization Division, NTPC). The physical and chemical properties of fly ash depend on the type of coal, boiler and collector set up. The ash from bituminous coal is finer than from lignite coal (Daniels et al., 2002).

The fly ash can be used as an adsorbent in various separation processes (Kao et al., 2000). The larger specific surface area, the higher carbon content and the fine particle size of the fly ash proves its good adsorption capacity. The specific surface areas of the fly ashes collected vary from about 250 m^2/g to 850 m^2/g (Chatterjee, 2010), , 400–700 m^2 /kg (Wesche, K., 1990), 276-792 m^2/kg (Leea et al., 2003). The fly ash can be used as adsorbent in various separation processes (Kao et al., 2000).

Studies have been conducted on the use of sugarcane bagasse fly ash in Thailand to adsorb BOD content of the combined wastewater having reactive dyes and adsorption was found to be between 46 to 95% (Lakdawala and Oza,2011; Rachakornkij et al., 2004). Table 2.4 presents the effects of different operational parameters on the efficiency of adsorption for paper industry effluent treated with fly ash and other adsorbents derived from various sources.

Table 2.4 Effect of various parameters on adsorption

Adsorbent	Name of dye	Initial concentration range, mg/l	% removal range	References
Effect of initial concentration				
Sawdust	Direct brown 2	600-850	99.6-99.1	Kannan and Sundaram, 2001
Bentonite	Acid Blue 193	100-250	-	Özcan et al. 2004
Fly ash	Congo red	5-30	99-84	Mall et al. 2006
Apricot seed	Astrazone Black	50-500	91-62	Kahraman et al. 2012
Sugarcane Bagasse	Basic Blue 9 Rhodamine B	250-500 100-500	94-55.5 99.1-87.1	Zhang et al. 2013
Effect of temperature				
Activated carbon	Methylene blue	308-333	97-100	Kavitha and Namasivayam. 2007
Kaolin & Na Bentonite	Congo red	279-333	< 90	Vimonses et al. 2009

Modified clay	Methylene blue	303-313	53-96	Auta and Hameed. 2012
Hydroxyl-terminated polybutadiene (HTPB)	Acid blue 92	298-318	88-96	Olya et al. 2013
Bottom ash	Eosin yellow	303-323	98	Mittal et al. 2013
		Effect of pH		
Activated carbon	Methylene blue	2-11	-	Kannan & Sundaram. 2001
		Effect of adsorbent dosage		
India rosewood sawdust	Methylene blue	2-10 g L-1	45-97	Garg et al. 2004
Fly ash	Methylene blue	8-20 g	45-96	Kumar et al. 2005
Bagasse fly ash	Orange G	0.05-0.2	23-89	Mall et al. 2006
Rice hull	Reactive orange 16	0.02-0.08	21.7-56.2	Ong et al. 2007
Tea waste	Basic yellow 2 Acid orange 7	2-20 g/l	19-60 90-99	Khosla et al. 2013

2.13 Ozonation

The ozone is one of the most effective chemical oxidation process for decolourization of wastewater having refractory organic matter which resist biodegradation (Dogruel et al. 2006).

2.13.1 Effect of pH

Ozone decomposes into its highly reactive species like HO•, HO_2• and HO_3• and occurs in an alkaline environment while at lower pH (acidic conditions) ozone exists in its molecular state and reacts with unsaturated chromophoric bonds of dye molecule through direct reactions (Carmen and Daniela; www.intechopen.com).

At ozone concentration of 2970 mg/l, the simulated reactive dye bath effluent at pH 7 showed remarkable decolourization while remained unchanged at pH 11 (Arslan et al. 2002). The decolourization of the Reactive Yellow 84 decreased as solution pH decreased from 6.1 to 3.2 (Koch et al, 2002). The 32% reduction in the dye decolourization time achieved as the pH of dye solution was changed from 2 to 12 (Konsowa et al. 2003). A remarkable decrease in liquor colour observed at pH 9 during ozonation (Beltran et al., 2006). The amount of reacted ozone and time of ozonation are lower for Reactive dye at the pH of 3 to 5 while in case of Direct Pink, the suitable pH was found to be between 7 to 10 (Guendy, et al. 2007). The decolourization of 40.6% was achieved for pH 3.0 and 67.5% for pH 9.1 (Somensi et al. 2010). The colour of a reactive dye was reduced to 69.69% at pH 12 with complete RO16 degradation within 8 minutes (Turhan et al. 2013).

2.13.2 Effect of concentration on ozonation treatment

At higher initial dye concentration of textile wastewater, more ozone consumption was observed (Lin et al., 1993, Sevimli and Sarikaya, 2002). A complete decolourization of exhaustive reactive dye wastewater was achieved at ozone consumption of 76.5 mg/l after ozonation for 40 minutes (Sundrarajan et al. 2007).

2.13.3 Effect of ozonation on biodegradability

A study by Tarragona et al., 2015 indicated that the toxicity effects of 2,4-DCP decreased due to ozonation. The lag phase was remarkably reduced and the maximal SOUR increased with increase in ozone reaction time. An increase of the biodegradable COD fraction was also observed (Aken et al 2015). The ozonation pre-treatment enhanced the biodegradability of distillery wastewater in an anaerobic digester treatment (Ordono et al 2012). The biodegradability index of textile wastewater increased by 1.6 times at ozonation dosage of 300 mg/dm^3 (Sevimli and Sarikaya, 2002). The less toxicity and remarkable biodegradability improvement was found in ozonated wastewater of textile dyes (Arslan Alaton, 2003). The simulated reactive dye and reactive yellow 84 biodegradability reached to 80 times (Koch *et al.*, 2002).

2.13.4 Effect of ozonation time

The pulp and paper mill effluent having initial COD of 360 mg/l showed complete decolourization after 60 minutes of ozonation time at ozone of 3g/h (He et al. 2016). The 97% colour removal achieved with 20 mg/min of ozone dosage (Solmaz et al , 2006). The 99% colour removal was observed in 10 minutes with 6.0, 7.5 and 9.0 dm^3/min ozone dosages (Ciardelli and Ranieri. 2000). The complete colour removal is achieved within 20-60 minutes (Selçuk. 2005). The industrial sample having reactive black 5 dye completely decolourized within 10 minutes (Colindres*et al*, 2010). The colour removal was 60% after 5 minutes, 80% after 10 minutes, 85% after 12.5 minutes and 90% after 20 minutes (Meriç*et al.* , 2005).

2.14 Biological treatment methods

The black liquor study conducted with anaerobic baffled reactor showed the maximum COD reduction of about 60% at an organic loading rate of 5 kg/ m^3/d at a hydraulic retention time of 2 days, pH of 8.0 and temperature of 35 °C (Grover et al. 1999). The COD removal of 84.3% and biogas production of 21.2 l/d were observed at hydraulic retention time of 23 hours and temperature of 35 °C (Sridhar et al 2015). The UASB reactor has found to be effective for the anaerobic digestion of pulp & paper mill wastes (Kamali et al. 2016).

The anaerobic digestion of black liquor of cereal straw pulping mill in batch UASB reactor showed up to 60% COD removal efficiency at organic loading rates of 5-10 kg COD /m^3/day (Dangcong et al. 1993). The decolourization of 70-80% and COD removal of 60% was achieved with white rot fungus *Trametes versicolor* treatment of black liquor of soda pulping mill (Font et al. 2003). The lignolytic fungus *Phanerochaete chrysosporium* showed decolourization, COD removal and BOD removal of 86.4%, 78.8% and 70.5%, respectively (Jaganathan et al. 2009). The black liquor and bleach effluent from Kraft pulping processes showed 63% COD removal with mixture of six strains of bacteria i.e. *Agrobacterium sp. ,Bacillus sp., E. Cloacae, Gordonia sp., P. stutzeri* and *P. Putida* (Chen et al. 2010). The COD removal ranged from 35-98% and TSS removal ranged from 12-89% was found with black liquor effluent, when treated with *Diplodia oryzae* and *Phaerochaete chrysosporium* (Helmy et al, 2003).

The effluent of pulping liquors was treated with sulphate reducing bacteria isolated from sediments from sediments from pulp and paper mills in Vietnam. The treatment reduced 70-75% COD after 3 weeks, which could further increased to 88% by further aerobic treatment after 48 hours (Hoa and Man. 2006). The effluent from the treatment with $AlCl_3$ at pH-5 was further processed with *P. putida* at pH 7 for 48 hours, leading to marginal further reductions in colour, phenols, TSS, and COD. The sequential treatment of chemical precipitation and *putida* resulted in better quality water than chemical precipitation alone (Swamy et al 2016). A potential lignin-degrading fungal strain, identified as *Aspergillus flavus strain F10* reduced colour up to 31–51 % and lignin content 39–61%in ten days of incubation when used as a free form, while in immobilized condition it reduced more colour and lignin content within 6 day of treatment. The toxicity of paper and pulp effluent was measured in the term of phytotoxicity. A high germination index of treated samples indicates that the treatment reduced pollution load in effluent to low levels, which were not toxic to plants (Barapatre and Jha, 2016). The maximum decolourization of 83% was achieved when 1% sucrose ($C_{12}H_{22}O_{11}$) and 1% NH_4Cl was added the effluent containing immobilized cells of *P. Chrysosporium* (Gomathi et al 2012).

2.15 Modelling

Modelling helps in deeper understanding of the reality of physical processes and helps in designing of system from laboratory scale to pilot plant or field scale. The modelling also finds its application in waste water treatment techniques including adsorption and ozonation treatment. The bubble diffuser contacting system is simpler with better ozone transfer rates and less energy requirement (Langlais et al. 1991). The process during ozonation include convection, back mixing process of the liquid and gas phases in contacting chamber, ozone gas mass transfer, ozone auto-decomposition, and reaction of dissolved ozone with the wastewater (El-Din et al. 2003).

2.15.1 Modelling of ozone treatment

The oxidation efficiency of ozone can be calculated by determination of utilized ozone, ozone absorption rate and the overall mass transfer coefficient (k_{La}). Ozone for pulp mill effluent follows the fast or instantaneous kinetics (Mohamed Gabal El-Din et al, 2001). Table 2.5 summarizes the literature on ozone modelling of wastewater.

Table 2.5 Ozone modelling

Authors, Year	Wastewater/ Component	Parameters	Remarks
Beltrán et al. 2000	Atrazine	Outlet atrazine concentration, Dissolved ozone, hydrogen peroxide	Continuous bubble contactors with kinetic modelling. Non-ideal flow, dispersion model. Non-steady state and steady state regimes.

Bin et al. 2001	Tap water	Axial dispersion and ozone mass transfer coefficients in the liquid phase.	8-60 g/m^3 O_3
Kuosa et al. 2006	Water	Ozone self-decomposition kinetics in a semi batch bubble column reactor	Axial dispersion model. The model parameters were determined by parameter estimation using a nonlinear optimization method.
Gong et al. 2007	Water	Euler–Lagrange method, Finite difference method, Lagrangian approach..	The ozone transfer process from bubbles to liquid is computed by modelling the mass transfer rate of individual bubbles.
Tiwari. 2007	Water	Gas phase is considered to be plug flow.	Mass transfer is as per Lewis–Whitman two film theory
Dhaouadi et al. 2008	-	Dynamic model	Gas liquid volumetric mass transfer coefficient for different superficial gas velocity.

Erol et. al. 2009	Aqueous dye solutions	Residence time distribution, Peclet number and axial dispersion coefficient.	Reactor was modelled as two CSTRs in Series.
Konsowa et al. 2010	Industrial waste water	Semi-batch bubble column reactor	-
Beltrán et al. 2010	Aqueous diclofenac photocatalytic ozonation	Kinetic model	Total organic carbon (TOC), ozone and hydrogen peroxide concentrations as output variables.
Kimmermann et al. 2011	Secondary wastewater effluent	The kinetics of oxidation and disinfection processes.	The R_{ct} value was identified as a major contribution.
Zhang et al. 2014	Water of City of Tampa	Combining computational fluid dynamics (CFD) modelling	The finite volume method to discretize the governing flow and scalar transport equations.
Zheng et al. 2015	Wastewater of acrylic fibre manufacturing industry.	COD, NH_3 -N, and UV_{254} of the wastewater.	Microbubble-ozonation in comparison to macro bubble-ozonation.

Marce et al. 2016	Primary urban effluent of WWTP, Spain	Mass transfer coefficient, ozone decomposition rate, Total ozone demand and Immediate ozone demand.	Semi batch reactor.
Rhim et al. 2004	-	The overall mass transfer coefficient k_{La}	Measurement of the equilibrium dissolved ozone, overall decomposition rate constant, and overall Henry's law constant.

2.15.2 Modelling of adsorption treatment

The Bed Depth Service Time model (BDST) was applied to the experimental data to represent the breakthrough curve. The calculated adsorption capacity (N_0) and the rate constant (K) were 55.2 µg/cm^3 and 12.2 cm^3/µg/h, respectively As(III) on column studies (Negea et al. 2011). The details of studies conducted on adsorption modellling by other researchers is given in Table 2.6.

Table 2.6 Adsorption modeling

Authors, Year	Adsorbent	Adsorbate	Conditions	Remarks
Nouri Hanen et al. 2013	Granular Activated carbon	Phenol	Flow rate=2.2 to 8.4 ml/min Bed depth=5, 10, 15, 20 cm	Well predicted by Clark model Yoon Nelson model
Sotelo J L et al. 2012	Granular Activated carbon	-	Well predicted by Thomas model, Yoon Nelson model	-
Nwabanne et al. 2012	Activated carbon prepared from nipa palm nut	Lead (II) and Copper (II)	Thomas model, Yoon & Nelson model	-
Han et al. 2008	Rice husk	Congo red	1.2 cm internal diameter, height-50 cm, Bed depth-12, 20, 30 cm, flow rate-5.6 ml/min	BDST model. Thomas model fitted the data
Hasan and Srivastava. 2011	Immobilized Arthrobacter sp.	Cd(II)	Glass column of 2 cm internal diameter, height-30cm. Bed depth-7,10,13,16,19 cm, flow rate-1ml/min to 5 ml/min.	BDST model applied, Yoon Nelson model fitted.
Taty-Costodes et al. 2005	Pinus sylvestris saw dust	Lead(II) ions	Flow rate-5 ml/min, Bed depth-6.5, 8.5, 13 cm, Internal diameter-1.5 cm	BDST model
Nwabanne. 2012	Activated carbon from oil palm fiber	Lead (II)	Flow rate-5 to 10 ml/min, Column height-30 cm, internal diamtere-3 cm, Bed depth -5, 10, 15 cm	Yoon and Nelson model

The breakthrough curve in fixed bed studies for removal of atenolol from aqueous solutions aqueous solutions by activated carbon were predicted through Bohart-Adams, Thomas and Yoon-Nelson models (Sotelo et al. 2012). The mass transfer coefficient of the model was estimated. A simplified form of the dual rate model was used to predict the column performance in terms of treatment efficiency, consumption of carbon, and organic removal. The mass transfer coefficients of the model were determined based on micro column experimental data. The lower performance of the GAC column system was attributed to a possible low efficiency in terms of carbon usage in the micro column experiment (Zheng Zing et al 2000).

CHAPTER 3 MATERIALS AND METHODOLOGY

This chapter presents the material and methods adopted for preparation of raw material and black liquor, isolation of lignin, characterization of effluent, black liquor, briquettes, lignin and dyes used in handmade paper industry. The chapter includes the material and methods adopted for ozonation, adsorption, fungi and bacteria treatment of black liquor.

3.1 Raw material preparation

The banana and jute fibers were collected from handmade paper unit and were chopped to the size range of 1.0 to 1.5 inches manually.

Figure 3.1 Banana Fiber

Figure 3.2 Jute Fiber

3.2 Preparation of black liquor

Black liquor was prepared by alkaline peroxide pulping process for banana fiber and alkaline sulphite pulping process for jute fiber. The chopped raw material was fed in the digester along with chemical solution (Table 3.1) maintaining a specific material to liquor ratio. The pulping process has been conducted as per standard pulping process (James P Casey, 1980).

Table 3.1 Conditions of pulping process

Particulars	Alkaline Peroxide Pulping	Alkaline Sulphite Pulping
Amount of chopped fiber, kg	1	1
Chemicals	Sodium Hydroxide-8% of raw material Hydrogen peroxide-2% of raw material	Sodium Hydroxide-5.6% of raw material Sodium Sulphite-2.4% of raw material
Material :Liquor	1:8	1:8
Temperature, °C	120	120
Time at 120 °C, hrs	3	3

The banana fiber was cooked at 120 °C for 3 hours. After digestion, black liquor was collected from bottom of digester after degassing of digester. The collected black liquor was collected in 2 liters reagent bottles and preserved at 4 °C for further analysis.

3.3 Isolation of Lignin:

The concentrated sulphuric acid in dosage of 0.5% was added to black liquor and then stirred at 150 rpm for 10 minutes and 50 rpm for 30 minutes and then allowed to settle overnight. The settled lignin was filtered with the help of Whatman grade 42 filter paper kept on Buchner funnel and washed with hot distilled water and vacuum dried over P_2O_5 (Lin and Dence, 1992).

3.4 Characterization of Black liquor:

The various parameters of black liquor including residual active alkali, conductivity, total solids and TGA of lignin were analyzed.

3.4.1 Residual Active Alkali

20 ml of black liquor was taken in Erlenmeyer flask and 0.1 N HCl was added drop wise until pH of the solution reached 8.3. The burette reading was noted and residual active alkali determined by the equation 3.1.

$$RAA,\ gpl = \frac{Molecular\ \ wt.\ of\ \ NaOH\ \ X\ \ Normality\ of\ \ HCl\ \ X\ \ B.R}{Amount\ of\ \ black\ \ liquor} \text{ ……....(Eq. 3.1)}$$

3.4.2 Conductivity

Conductivity was determined with the help of conductivity meter (Hanna Instruments) after calibration of conductivity meter with potassium chloride.

3.4.3 Total solids

Total solids was determined by taking black liquor & wash liquor in petri dish and kept in oven at 105 °C for 24 hours until the weight was constant after drying. After complete drying, total solids were determined by using the formula as given as equation 3.2.

$$Total\ solids\ ,\% = \frac{Wt.\ of\ black\ liquor\ after\ drying\ in\ oven \times 100}{Wt.\ of\ black\ liquor} \quad \textbf{……(Eq. 3.2)}$$

3.4.4 TGA Analysis of lignin

TGA is an analytical technique used to determine thermal stability of material by monitoring the weight change that occurs as a specimen is heated. The objective of thermal analysis is to identify temperature regimes where major weight losses (and phase transformations) occur and decide upon the minimum sintering temperature. TGA analysis was conducted with the help of STA 6000 (Perkin Elmeris) as per ASTM E1131, ISO 11358.

Appropriate environment was maintained with the help of inert (usually N_2) and oxidative (O_2) gas flow rates. About 15 mg of test material was placed in the specimen holder and the temperature of the furnace was raised in steps. The initial weight reading was set to 100%, and the heating program was initiated. The gas environment is preselected for either a thermal decomposition (inert-nitrogen gas), an oxidative decomposition (air or oxygen), or a thermal-oxidative combination. The sealed DSC scans were performed at a heating rate of 5 °C/min from 30 to 400 °C under nitrogen environment. Loss of weight at every step of temperature rise was automatically recorded.

3.5 Characterization of raw water and effluent of handmade paper industry

The raw water was characterized for total hardness and chloride content.

Total Hardness It was measured using Ethylene Di amine Tetra Acetic Acid as titrant with few drops of ammonium hydroxide buffer solution and Erichrome Black T as indicator.

Chloride content It was determined by Mohr's method using silver nitrate as titrant and potassium chromate solution as indicator.

The effluent of handmade paper industry was characterized for parameters like BOD, COD, and colour as per standard testing method of Standard Methods of Examination of Water & Waste water (APHA, 20^{th} edition 1998). The sample was centrifuged at 10,000 g to remove the suspended matter. The pH of the supernatant was adjusted to 7.6 and absorbance was measured at 465 nm as per Canadian Pulp & Paper Association (1974). The A_{465} values were transformed into colour units (CU) according to the formula where A_1 is the absorbance of 500 CU platinum–cobalt standard solution (A_{465}=0.132) and A_2 is the absorbance of the wastewater sample (CPPA, 1974; Barapatre and Jha. 2016). The colour can be determined as given in equation 3.3.

Color, $PCU = 500\,\frac{A_1}{A_2}$ **……..(Eq. 3.3)**

Where,

A_1=Absorbance of sample

A_2=Absorbance of 500 units of Platinum Cobalt standard

3.6 Characterization of dyes used in handmade paper industry

The dyes being used in handmade paper industry was characterized for pollution parameters like BOD, COD, and colour as per standard testing method of Standard Methods of Examination of Water & Waste water (APHA 1998).

3.6.1 Determination of maxima

The black dye of 50 mg/l concentration was scanned in the range of 200–1100 nm with the help of double beam UV-Vis. spectrophotometer (Shimadzu UV 1800), Shimadzu for determination of wavelength corresponding to maximum absorbance.

3.7 Adsorption treatment

3.7.1 Preparation of Fly Ash

Fly ash was received from Thermal Power Plant, Yamuna Nagar. 500 g of fly ash was washed with distilled water and dried in oven at 103 ºC for 3 hours. The dried fly ash was passed through several sieves of ASTM No. 50, 80, 100, 170, 200, 270, 300 and 325 to get fly ash of various particle sizes and collected in polythene bags for further study.

3.7.2 Preparation of dye solution

Commercial grade Indosol Black dye of Clariant make, Mumbai which is widely used in handmade paper industry, was taken for the study. The direct black dye samples of various concentrations i.e. 30, 40, 50, 100, 150 and 200 mg/l were prepared by dilution of the stock dye solution for further studies.

3.7.3 Simulation of effluent of handmade paper industry

A stock of a mixture of commercial dyes, i.e., Direct Orange 26, Direct Navy Blue 6 and Direct Violet 66 was simulated in the laboratory in a specific ratio to simulate actual composition of the effluent from handmade paper industry and treated as a stock solution of 1000 mg/l. The ratio of Direct Navy Blue: Direct Orange: Direct Violet is 1: 0.2:2. The stock solution was preserved and used for further studies by dilution of stock solution.

3.7.4 Characterization of fly ash

The characterization of fly ash included measurement of surface area, particle size distribution and analysis of other morphological and elemental parameters using SEM, XRD and FTIR.

3.7.4.1 Surface area measurement

The specific surface area of fly ash was determined using methylene blue adsorption test (MBT) method. The surface area covered by one methylene blue molecule is typically assumed to be 130 $Å^2$ (1 Å = 0.1 nm) (Santamarina et al. 2002). 1 g of fly ash was dissolved in 300 ml of methylene blue solution of different concentration i.e. 3, 6, 9, 12 and 15 mg/l. Stirring of methylene blue solution with fly ash was carried out for 2 hours and then it was kept for 24 hours to reach equilibrium. The samples were collected and centrifuged at 13500 RPM for spectrophotometric studies. The specific surface area was calculated from the amount of adsorbed methylene blue.

$$S_{MB} = 10^{-20} q_m a_{MB} N_A / M_{MB} \quad \textbf{.....(Eq. 3.4)}$$

A stock solution of 1000 mg/l was prepared by dissolving 1.127g Methylene blue, dried at 110°c for 2 hours before use, in 1000 ml distilled water (Omomnhenle et al., 2006). The stock solution was diluted to make solution of 3, 6, 9, 12 and 15 mg/l. The absorbance of each concentration of methylene Blue was determined at 630nm with the help of UV – Visible spectrophotometer (Chongrak et al. 1998).

3.7.4.2 Particle size distribution of fly ash

100 g of fly ash was fed to an ash sieve shaker in which sieves of ASTM no. 50, 80, 100, 170, 200, 270, 300, and 325 were stacked from top to bottom. The fly ash in different screens was collected and weighed for determination of particle size distribution.

3.7.4.3 Details of microstructure by SEM studies

The surface morphology of raw and adsorbed fly ash samples was characterized by Scanning Electron Microscope (Nova Nano FE-SEM 450 FET) with accelerating voltage of 5 kV and magnification of x500 to x5000 and field emission gun SEM at Malaviya National Institute of Technology Jaipur. The FESEM is coupled to EDX detector for measuring the elemental composition of nano- materials. Particles were slightly carbon coated before analysis to make their surface more conductive. X ray analysis was done in spot mode at 25 kV.

3.7.4.4 X- Ray Diffraction Studies

The X- Ray Diffraction studies of original fly ash and adsorbed fly ash were conducted with the help of X-Ray Diffractometer (Panalytical X Pert Pro) with CuKα radiation at wavelength of 1.540 A° and scans were carried out with 0.03° step and 1 second. The identification of compounds was done by High score plus software.

3.7.4.5 Infrared Spectroscopy studies

The Fourier Transform Infrared Spectroscopy (FTIR) was carried out at room temperature using Perkin Elmer version 10.4 Spectrophotometer in the spectral range of 4000 to 400 cm^{-1} with a resolution of 4 cm^{-1} with KBr disc method. The KBr disks of samples were prepared by mixing 1 to 1.5 mg of sample finely grounded with approximately 200 mg of KBr (FTIR grade) in vibratory ball mixer for 20 s. The KBr disks were prepared under vacuum in standard device.

3.7.4.6 Addition of fly ash as filler in paper making

The adsorbed fly ash was dried at 60 °C and vacuum dried over P_2O_5 and further stored in polythene bags for its utilization as filler in handmade paper making. The cotton pulp beaten up to 400 ml freeness level, collected from the pilot plant of the Kumarappa National Handmade Paper Institute was used to conduct the studies. The stock solution of retention aid of 1000 mg/l was prepared to study increase in retention of fly ash on cotton fiber after addition of retention aid to the pulp slurry. The adsorbed fly ash was added in dosages of 2.5 & 5 % (w/w) and retention aid, 1,2-Ethanediamine, polymer with chloromethyloxirane and N-methyl methanamine (Catiofast of BASF India Limited) in dosage of 0.15% (w/w) on the basis of oven dry weight of cotton pulp was added to the cotton pulp for the studies.

3.8 Ozonation treatment

3.8.1 Preparation of dye solution and black liquor for Ozonation treatment

Commercial grade Indosol Direct Red and Indosol Blue GLL p of Clarian make, which is widely used in handmade paper industry, was taken for the study. Stock solutions of 1000 mg/l concentration of both direct red and direct blue dyes were prepared by dissolving dry powdered dye in 1000 ml of distilled water. The stock solution was diluted to prepare dye solutions of various concentrations.

3.8.2 Determination of Dissolved ozone

The dissolved ozone in collected samples were measured by indigo method by analyzing absorbance at 600 nm with the help of double beam UV-Vis spectrophotometer as per standard testing method no. ASTM D7677-11.

$$Dissolved\ ozone = 100\left(\frac{\Delta A}{fbV}\right) \text{……..……...(Eq. 3.5)}$$

Where, f = 0.42.

3.8.3 Determination of residual ozone

The measured amount of 2% KI solution is taken in gas bottle and the residual ozone is passed into it for a specific time. The sample was drawn and 1 ml of 4N sulphuric acid was added instantly and titrated against 0.1N sodium thiosulphate.

$$residual\ ozone = \frac{Burette\ \ reading\ X\ 24\ X\ 0.1N}{ml\ \ sasmple\ \ taken}\ X\ \ Dilution\ \ Factor \text{ …….(Eq. 3.6)}$$

3.9 Microbiological treatment

3.9.1 Simulation of black liquor

Jute fibers were cut into small pieces and fed in rotatory digester of 2.5 kg capacity. 8% sodium hydroxide was added along with water to maintain bath ratio of 1:6 and was heated at 95 °C for 3 hours. After 3 hours the digester was switched off and degassed. The black liquor was collected from bottom drain valve. The extracted black liquor is shown in Figure 3.3. The remaining jute fibers were washed with distilled water to extract the washed liquor. The black liquor and wash liquor was then stored at 4°C for further use.

Figure 3.3 Black liquor of Jute Fiber

3.9.2 Procurement of fungal cultures

The fungal cultures were procured from Microbial Type Culture and Collection, IMTECH, Chandigarh as given in Table 3.2

Table 3.2 List of fungal cultures with MTCC No.

MTCC No.	Fungus
787	*Phanerochaete Chrysosporium*
164	*Trichoderma reesie*
872	*Aspergillus niger*
1806	*Pleurotus Sajor Caju*
4954	*Pleurotus Ostreatus*
138	*C. Versicolour*

870	*Aspergillus fumigatus*
1434	*Bacillus sp.(Isolated from paper mill)*

The cultures were stored in refrigerator below 4 °C for further studies.

3.9.3 Subculturing of fungus

The fungus was subcultured in respective media as mentioned in catalogue of MTCC. The fungus with their respective media is shown in Table 3.3

Table 3.3 Fungal culture with respective media

Name of fungus	Media	Enzyme
Phanerochaete Chrysosporium	Malt extract agar (Blakeless formula) Malt extract 20 g+ Glucose 20 g + Peptone 1 g + Agar 20 g + Distilled water 1L	Ligninase Peroxidase (LiP) Xylanase Dehydrogenase
Trichoderma reesie	Malt extract agar Malt extract 20 g + Agar 20 g + Water 1L(Adjust pH to 6.5)	-
Aspergillus niger	Yeast extract agar (Czapeck formula) Czapeck concentrate* 10 ml + K_2HPO_4 1 g+ Yeast extract 5 g + Sucrose 30 g +Agar 15 g +Distilled water 1 L (*Czapeck concentrate-$NaNO_3$ 30 g + KCL 5 g +$MgSO_4.7H_2O$ 5 g +$FeSO_4$. 7 H_2O 0.1 g + Distilled water 100 ml)	-
Pleurotus Sajor Caju	Potato Dextrose Agar	Lignolytic enzymes

Pleurotus Ostreatus	Yeast extract 5 g + Glucose 10 g + Agar 15 g + Distilled water 1 L (Adjust pH to 5.8)	Extracellular peroxidase Lignin Peroxidase
Coriolus Versicolour	Yeast extract 5 g + Glucose 10 g + Agar 15 g + Distilled water 1 L (Adjust pH to 5.8)	Laccase
Aspergillus fumigatus	Czapeck Yeast extract agar Czapek concentrate* 10 ml + K_2HPO_4 1 g+ Yeast extract 5 g + Sucrose 30 g +Agar 15 g +Distilled water 1 L (*Czapek concentrate-$NaNO_3$ 30 g + KCL 5 g +$MgSO_4.7H_2O$ 5 g +$FeSO_4$. 7 H_2O 0.1 g + Distilled water 100 ml)	-
Bacillus sp.	Nutrient agar	Levan Peroxidases

The media prepared was autoclaved at 121 °C and 15 psi for 15 minutes and was poured in sterilized disposable petri plates and was kept overnight to solidify. The sub-culturing of fugus was done next day.

The media was employed for isolation of fungi by spread plate method using serial dilution technique. All the plates of Phanerochaete Chrysosporium, Trichoderma reesie, Pleurotus Sajor Caju were incubated at 25 °C for 7 days aerobically, Pleurotus Ostreatus at 25 °C for 5 days, C. Versicolour at 25 C for 10 days; aspergillus niger, aspergillus fumigatus was incubated at 30 °C for 3 days and bacillus sp. at 37 °C for 2-3 days.

3.9.4 Isolation of bacteria

The bacteria were inoculated from sludge of handmade paper industry by serial dilution method. The morphological distinct bacteria were purified by plate streak method on agar plates containing lignin-0.2 gpl, D-glucose- 10 gpl (carbon source), peptone-5 gpl (nitrogen source), Na_2HPO_4-2.4 gpl, K_2HPO_4-2 gpl, NH_4NO_3-0.1 gpl, $MgSO_4$-0.01 gpl, $CaCl_2$-0.01 gpl (Chandra et al. 2007) and added in black liquor and wash liquor with 30 times dilution under aseptic conditions. The batch experiments were performed at optimized conditions in 250 ml flasks containing 100 ml black liquor. The samples were tested for colour and reducing sugars.

3.9.5 Treatment of effluent in batch reactor

The lignolytic fungi *Phanerochaete Chrysosporium, Trichoderma reesie* and *Aspergillus Niger* were used to treat final effluent in batch reactor in 250 ml conical flask. 2 g/l of glucose was added to the effluent inoculated with 5-6 g of *Phanerochaete Chrysosporium, Trichoderma reesie* and *Aspergillus Niger*. The initial pH of the effluent was maintained at 5.4 to 5.6 and incubated at 25 °C at 125 rpm. The samples were withdrawn after 0, 2, 4, 5, 7, 9, 11, 14 days and analyzed for colour, reducing sugars, pH and lignin content. The pH of the samples was adjusted to pH-5.5 with the help of 0.1 N sulphuric acid prior to addition of fungi and to pH-8.0 prior to addition of inoculated bacteria.

3.10 Utilization of sludge for making briquettes

The sludge of handmade paper industry was collected from handmade paper units accumulated as waste due to fibre loss in the effluent. The collected sludge was stored in polythene bags and kept at 4 °C for further studies. The sludge of the handmade paper industry was mixed with black liquor with the help of domestic electric blender. The briquettes were formed with the help of press mould after proper mixing of the mixture and dried at room temperature for 24 hours. Then it is further dried at 60 °C for 24 hours. The briquettes were then kept in sealed polythene bags to avoid moisture.

3.10.1 Determination of calorific value

The gross calorific value of briquettes was determined as per standard testing method no. ASTM D 5865.

3.11 Statistical analysis

All the samples were assayed in triplicate and the mean along with standard deviation has been reported in the results. The mean values of these parameters obtained for different test solutions were compared with that of control sample using students ‘t’ test analysis at 95 % confidence level.

CHAPTER 4 EXPERIMENTAL SET UP

This chapter presents the experimental set up required for batch and fixed bed adsorption studies of fly ash with direct black dye and mixture of dyes used in handmade paper industry. The chapter includes the experimental set up of ozonation bubble column for treatment of wastewater of handmade paper industry.

4.1 Adsorption Experimental set up

4.1.1 Batch study

Fly ash samples of size ranges (150–300 microns), (90–150 microns) and (75–90 microns) were taken for the decolourization studies. The effect of pH was studied with black dye of 50 mg/l concentration at pH 4, 6, 8 and 10 pH was maintained with the help of 1 N NaOH mg/l and 1N HCl. The effect of initial concentration of black dye varying from 30 to 200 mg/l was studied at optimized pH and dosage. Batch studies were conducted in thermostatically controlled cabinet at 200 rpm in Erlenmeyer conical flask of 250 ml capacity. The percentage removal of dye or decolourization and amount adsorbed was calculated by the following equation (Kumar et al., 2013).

Decolourization, % = $100\frac{(C_0 - C_e)}{C_0}$ **……...(Eq. 4.1)**

Amount adsorbed q_e **(**$mg\ g^{-1}$**) =** $\frac{(C_0 - C_e)V}{M}$ **……...(Eq. 4.2)**

4.1.2 Column study

A borosilicate column of 1cm internal diameter and 15 cm length was taken for the column studies. A fine mesh was introduced at the bottom of column over which a layer of sand was spread to prevent escape of fly ash. The beds of fly ash of several bed lengths 1.2 cm, 1.8 cm and 2.4 cm were prepared. The dye solution was fed from top to the bed of fly ash in down flow mode. A sample of treated solution was collected at regular intervals and analyzed with the help of double beam UV-Vis spectrophotometer. The samples were drawn at regular interval till the concentration of effluent reached 99% of initial concentration signifying breakthrough or the exhaustion of fixed bed.

The effect of initial pH at 4, 6, 8, and 10 has been studied on decolourization of black dye of 50 mg/l concentration and fly ash dosage varying from 0.4 to 5 g/l in the column. The effect of several initial concentrations of dye ranging from 30 to 200 mg/l on decolourization of black dye was studied.

4.2 Ozonation experimental set up

4.2.1 Ozone Generation

The ozonation system consists of oxygen concentrator, ozone generator and ozone-water reaction system. The ozone generator L 15 G of Faraday Make based on concentrated oxygen as feed gas was used for ozonation studies. The Oxygen Concentrator OX5-02, Faraday make of oxygen concentration: 1-5 LPM, operating temperature of 41 °F to 105 °F was used to make concentrated oxygen from air as feed gas. The concentrated oxygen of 90% ± 3% purity was fed to ozone generator of capacity 15 g/h. Ozone generator of 15 g/h capacity was used for the ozonation studies using coronal discharge technology for ozone generation. The ozonation set up is shown in Figure 4.1.

Figure 4.1 Ozonation set up

4.2.2 Semi batch studies

The ozone was fed to gas washing bottle of 500 ml capacity by adjusting flow rate of ozone with the help of rotameter and output weight % of ozone generator. The concentration of fed ozone was determined with the help of online ozone meter ANSEROS Germany OZOMATGM Type GM-6000-OEM, 230 YAC/50 Hz, 0-20 mA, 0-200 g O_3/m^3. The schematic of the experimental set up is shown in Figure 4.2.

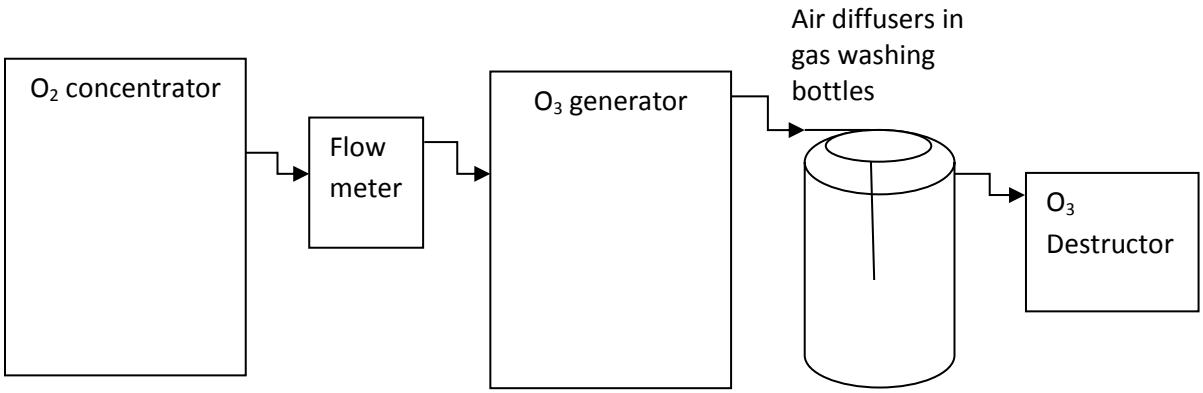

Figure 4.2 Scheme of experimental set up for ozonation semi-batch studies

The ozonation studies were conducted at various affecting parameters including pH ranging from 4 to 10, temperature from 313 to 333 K and initial concentration of dye solution varying from 50 to 1000 mg/l. The ozone of concentration 15 mg/l flow rate of 2 LPM was fed to 300 ml of dye solution. The treated samples after a specific interval of time were collected for further analysis. The concentration of ozone at the feed was analyzed using an ozone analyzer of Hanna make. The initial pH of the dye solution was varied from 4 to 10 with the help of 1 N HCl and 1 N NaOH. The decolourization efficiency was expressed as percentage decrease in absorbance at maxima of dye solutions as shown in equation 4.3.

$$Decolorization,\% = \frac{Absorbance_{initial} - Absorbance_{final}}{Absorbance_{initial}} X100 \quad \textbf{.....(Eq. 4.3)}$$

4.2.3Bubble column experimental set up

The bubble column reactor was made up of a glass column of 3.2 cm internal diameter and 100 cm height with fine bubble diffuser at the bottom. The ozone was fed from the bottom of the column. The ozone dosage could be readily adjusted by varying ozone weight percentage and gas flow rate. The schematic of the experimental setup is shown in Figure 4.3. The ozone feed concentration was determined with the help of ozone meter. The reactor used for this study includes a porous diffuser that produces fine bubbles. During ozonation tests, water samples were withdrawn from five sampling points at every 20 cm interval along the column height.

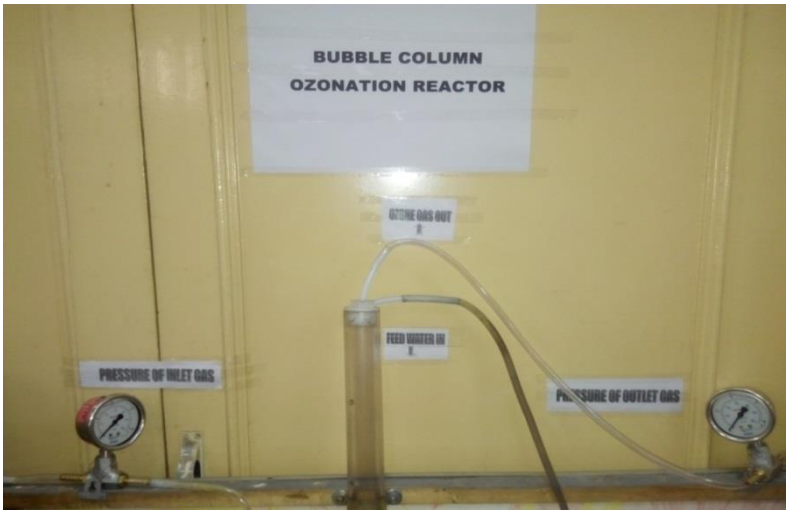

(a) Top of bubble column

(b) Bottom of bubble column

Figure 4.3 Scheme of process for decolourization of dye solution with ozonation bubble column as shown in (a) Top of bubble column and (b) Bottom of bubble column

CHAPTER 5 –CHARACTERIZATION

The characterization studies include characterization of raw water, wastewater, quantification of water consumption and waste water generation. The black liquor of various raw materials at various pulping processes has been analyzed.

5.1 Characterization of raw water used in handmade paper units

The technical visits have been made to 30 handmade paper units of Sanganer region and the raw water being used was tested for pH, Hardness and Chloride content which are given as Table 5.1.

Table-5.1 Characterization of raw water used in handmade paper units

	pH	Hardness, mg/l	Chloride, mg/l
Range	7.52-7.60	382-646	175-290
Mean	7.57	495	220

The higher hardness in some of the handmade paper units may be due to the presence of many textile units in the vicinity, which are in the process of bleaching and printing the textiles. Handmade paper unit in village Chaksu, which is 20 km from the Institute, has shown quite low hardness of 220 mg/l as there in no textile mills near this handmade paper industry. It has been found that the quality of raw water depends on the presence of units, creating pollution in the surrounding area and depth of boring. As per IS No. 2724-1964 (64 Reaffirmed 1983) tolerance of various parameters have been standardized. The tolerance limit of hardness of raw water used for making high-grade paper is 100 mg/l while it is 200 mg/l for ground wood paper and kraft paper unbleached and pulp unbleached.

5.2 Quantification of water consumption and waste water generation

The study of 30 handmade paper units of Sanganer showed the following results of water consumption and waste water discharge as given in Table-5.2.

Table-5.2 Quantification of water consumption and waste water discharge

Particulars	Sanganeri vat	Cylinder Mould vat machine
Water consumption, L/kg	32-95	35-62
Waste water generation, L/kg	29-72	30-59

No data are available for water consumption in handmade paper industries. The ministry of Environment & Forests, Govt. of India vide notification no. 422 dated 19th May, 1993 had envisaged the limits of effluent discharge for small pulp & paper industries as 150 m^3/T of paper produced for industries using agro-residues as raw material and 50 m^3/T of paper produced for industries using waste paper as raw material (www.envfor.nic.in). It has been observed that the water consumption in handmade paper units is beyond the range of standards set for paper industry using waste paper (50-150 m^3/ton). Paper industry on an average consumes about 125 - 300 m^3/t of water (Report by CPPRI, 2004).

5.3 Analysis of effluent discharged from handmade paper units

The effluent collected from 30 handmade paper units of Sanganer and analyzed for various parameters like pH, Total suspended solids, BOD, COD, Total dissolved solids and Color. The analysis of effluent collected from handmade paper units showed the following results as in Table-5.3.

Table-5.3 Analysis of effluent discharged from handmade paper units

Parameter	Range	Mean	Std. Deviation	CPCB standards for discharge in inland
pH	6.9-7.9	7.2	0.30	5.5-9.0
Suspended solids, mg/l	120-640	312	172	100
Total dissolved solids, mg/l	550-1750	1133	339	2100 max.
BOD, mg/l	55-610	308	188	30
BOD, kg/T	6.9 -49.6	17.3	14.25	-
COD, mg/l	350-1810	1182	450	250
COD, kg/T	21-109.8	68	46	-
Color, Pt.-CU Unit	55-1000	364	372	Absent

Number of samples=30

The results showed that some parameters exceed their prescribed limits. The suspended solids of some of the handmade paper units is quite high whereas Biochemical oxygen demand is slightly above the limit. The chemical oxygen demand also showed the exceeded value. The color of effluent varied as per the color and quality of dye used for dyeing the pulp. The handmade paper makes various colored handmade paper with different shades. The color of the effluent of the paper mill was 6285 PCU, total dissolved solids 1046 mg/l, total suspended solids 3263 mg/l, COD 4306 mg/l (Swamy et al. 2016). The effluent of recycled paper industry of Nagpur showed suspended solids of 1160-1380 mg/l, total dissolved solids of 1043-1293 mg/l, COD 1110- 1272 mg/l and BOD of 268-387 mg/l (Kesalkar et al. 2012). The waste water from South India Paper Mill of Karnataka using recycled waste paper as raw material showed pH 5.5 to 6.8, total dissolved solids of 1010-1015 mg/l, COD of 1120-110 mg/l and BOD of 200-210 mg/l. (Devi et al. 2011); COD of 4957 mg/l, BOD of 312 mg/l, TDS of 1280 mg/l (Alluri et al 2016)

5.4 Analysis of Fiber Loss

The fiber loss of handmade paper units has been evaluated, the results of which are given as Table-5.4.

Table-5.4 Analysis of fiber losses

Particulars	Range	Mean
Fiber Loss, %	0.41-4.75	2.31

The handmade paper units analyzed for suspended solids and with the help of flow rate of effluent generated showed the fiber loss vary from 0.4% to 4.75% The fiber losses of most of the paper units range from 0.30 to 0.70% while proposed norm is 0.25 to 0.30 % (Report by CPPRI 2004).

5.5 Characterization at each stage of handmade paper making

The characterization of effluent at each stage of handmade paper making process was carried out and the results are tabulated in Table 5.5.

Table 5.5 Analysis of effluent at each stage of handmade paper making process

Characteristics	Plant wash	Vat	Beater wash	Agitator wash	Pressing
pH	7.4 ±0.15	7.4 ±0.11	7.4 ±0.07	8.10 ±0.11	7.3 ±0.05
Total Suspended Solids, mg/l	771 ±48.3	242 ±5.86	200 ±5	497 ±6.25	10 ±1.03
Total Dissolved Solids, mg/l	750 ±9.42	1000 ±64.63	1125 ±14.14	1285 ±13.94	750 ±11.54
COD, mg/l	370 ±11.83	480 ±10.54	170 ±6.66	75 ±5.27	40 ±6.32
BOD, mg/l	45 ±5.27	65 ±5.0	20 ±0	15 ±2.23	10 ±0
Color, Pt.-CU	669 ±5.67	717 ±3.52	742 ±5.86	726 ±4.59	680 ±9.69
Flow rate, L/H	3199 ±13.49	1096 ±4.43	2256 ±8.03	14223 ±12	6599 ±49.31

Higher percentage of suspended solids was found to be present in the effluent from beater, paper making spillage and agitator wash.

5.6 Characterization of various dyes used in handmade paper industry

The direct dyes used in handmade paper industry have been characterized for various parameters including pH, solubility, λ_{max}, COD, BOD and color.

5.6.1 Characterization of dyes for various parameters

The dyes were characterized for various parameters as given in Table 5.6 and the structure of dyes is given in Table 5.7

Table 5.6 Characteristics of various dyes

Name of dye	pH	Solubility, %	$\lambda_{max,}$ nm	COD of 1000 mg/L dye solution, mg/l	Retention on pulp, %	BOD of 1000 mg/l dye solution, mg/l	Color, Pt.-CU
Orange	7.86	95	238 304 491	2600	970	75	103
Easy Brown	7.65	94	245 307 410	640	950	45	80
Sheet Pink	7.54	96	236.5 310 527	960	194	64	66
Navy blue	7.34	91	312.5 569.5	900	1292	56	52
Lemon Yellow	7.55	95	365	2590	2640	65	97
Green	7.76	97	375 622	1020	1280	50	121
Khaki	7.34	93.4	242.5 309 407	1000	394	35	120
Turquoise Blue	7.79	93	262 335 621.5	1080	292	142	118
Sky Blue	7.23	94.5	208.5 234 320 601.5	930	187	41	138
Black	7.88	92.5	318.5 509.5	3450	920	49	45
Red	7.7	98	530	2400	970	140	52

It has been observed that the dye solution of 1000 mg/l concentration is highly polluted.

Table 5.7 Chemical structure and molecular formula of dyes

Name of dye	Chemical structure	Molecular Formula
Orange	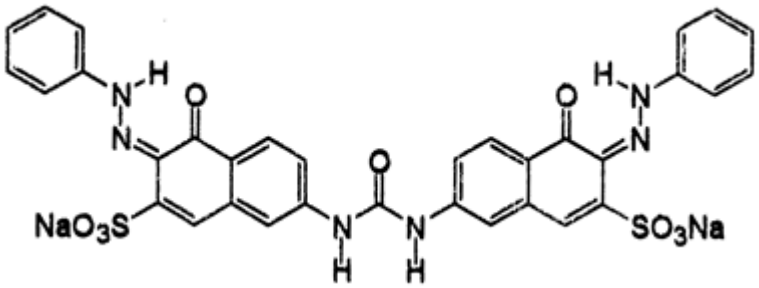	$C_{33}H_{22}N_6Na_2O_9S_2$
Brown	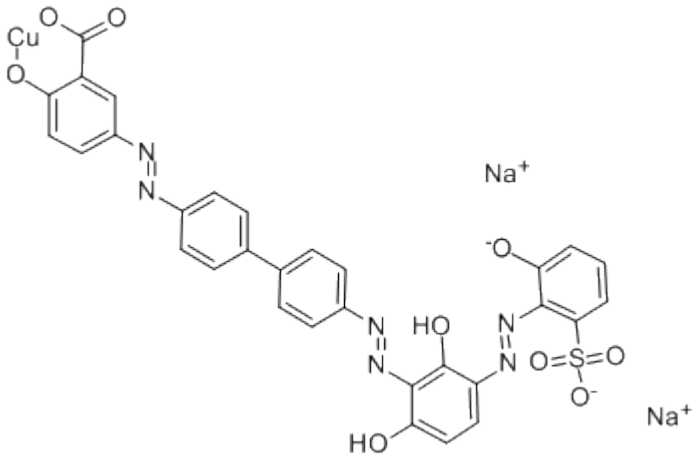	$C_{31}H_{18}CuN_6O_9S.2Na$
Navy blue	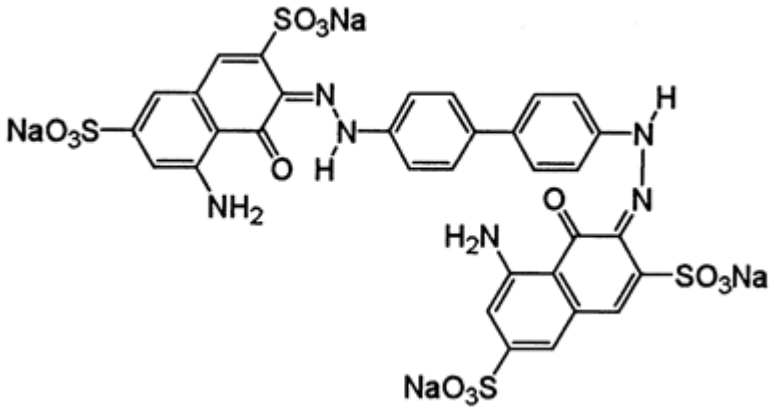	$C_{32}H_{20}N_6Na_4O_{14}S_4$

Lemon Yellow	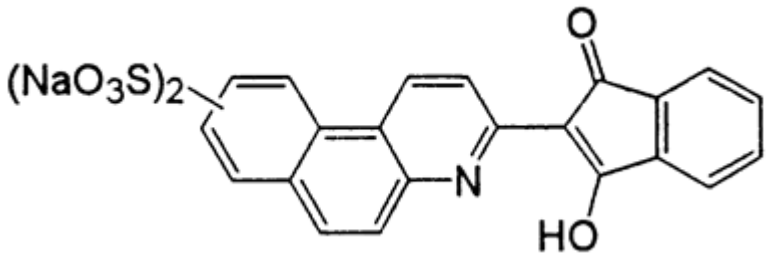	$C_{22}H_{11}NNa_2O_8S_2$
Green	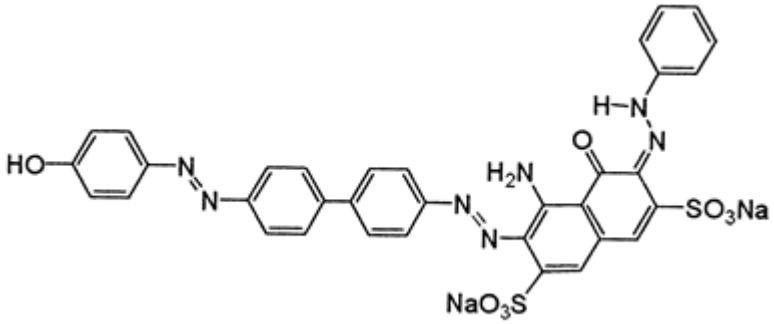	$C_{34}H_{23}N_7Na_2O_8S_2$
Turquoise Blue	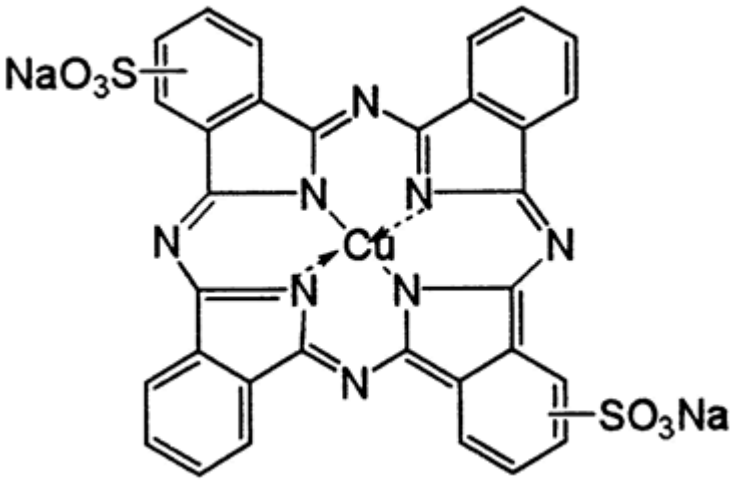	$C_{32}H_{14}CuN_8Na_2O_6S_2$
Black	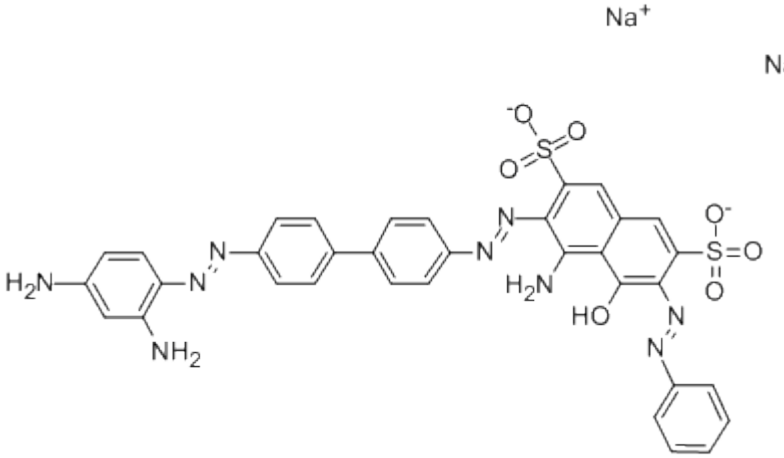	$C_{34}H_{25}N_9Na_2O_7S_2$

Red	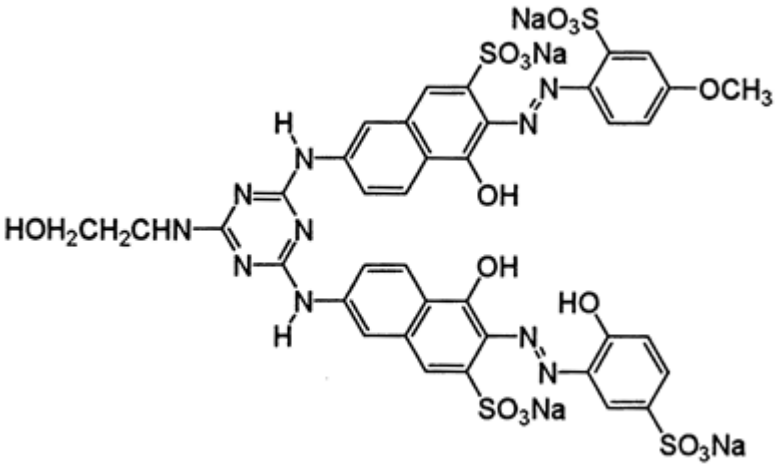	$C_{38}H_{28}N_{10}Na_4O_{17}S_4$

5.6.2 Maxima of direct dyes

The maxima of direct dyes used in handmade paper industry are shown in Figure 5.1 and Table 5.8 respectively.

Khaki 250 mg/l, pH-7.34

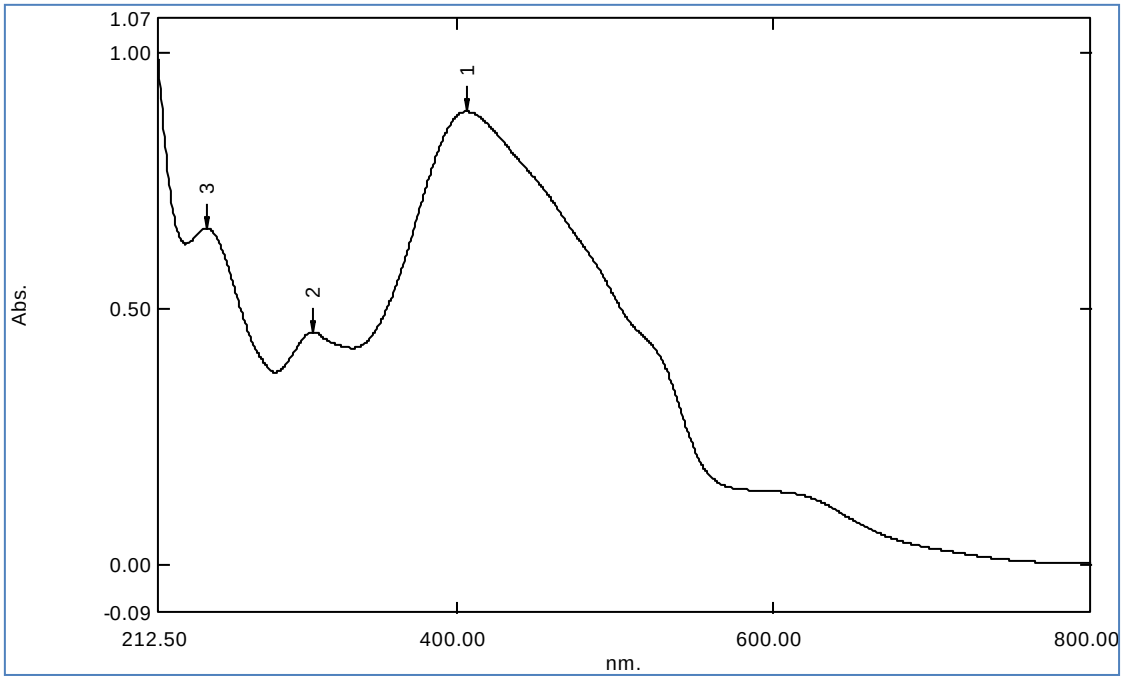

Lemon Yellow 100 mg/l, pH-7.55

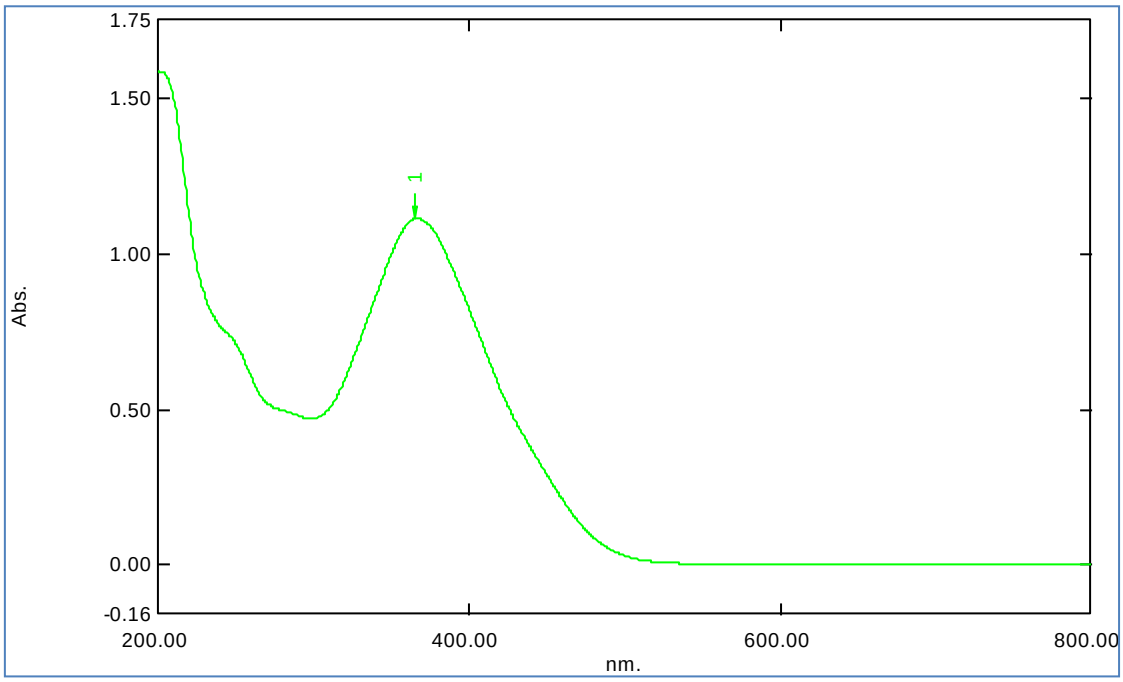

Orange 50 mg/l, pH-7.86

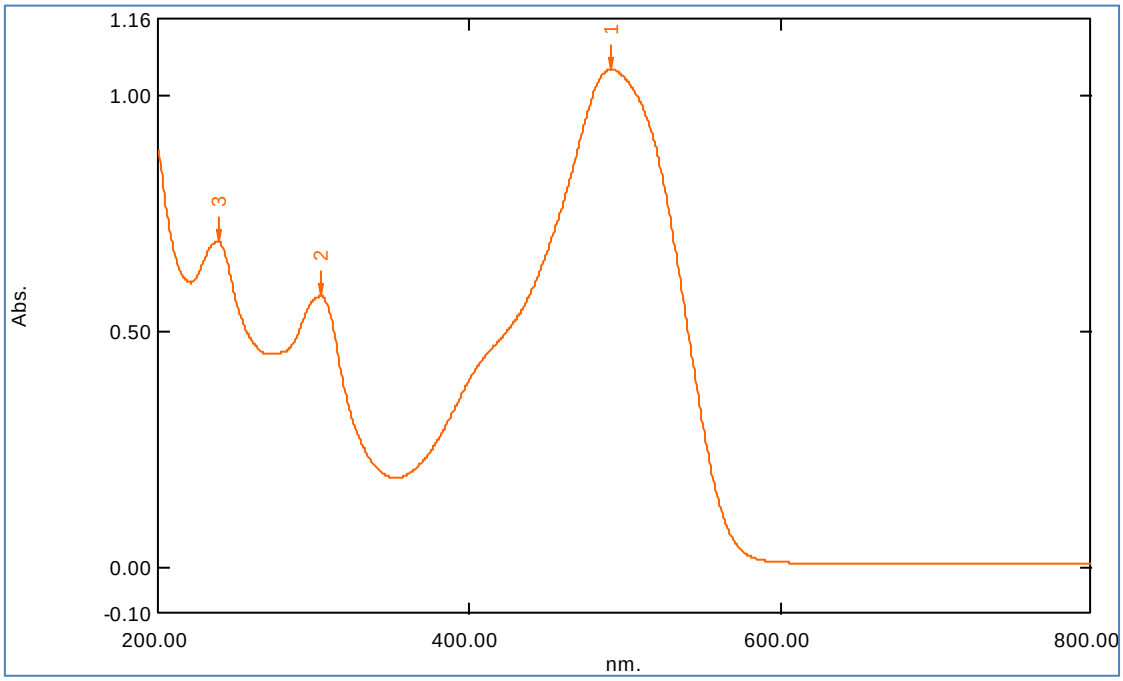

Black 100 mg/l , pH-7.88

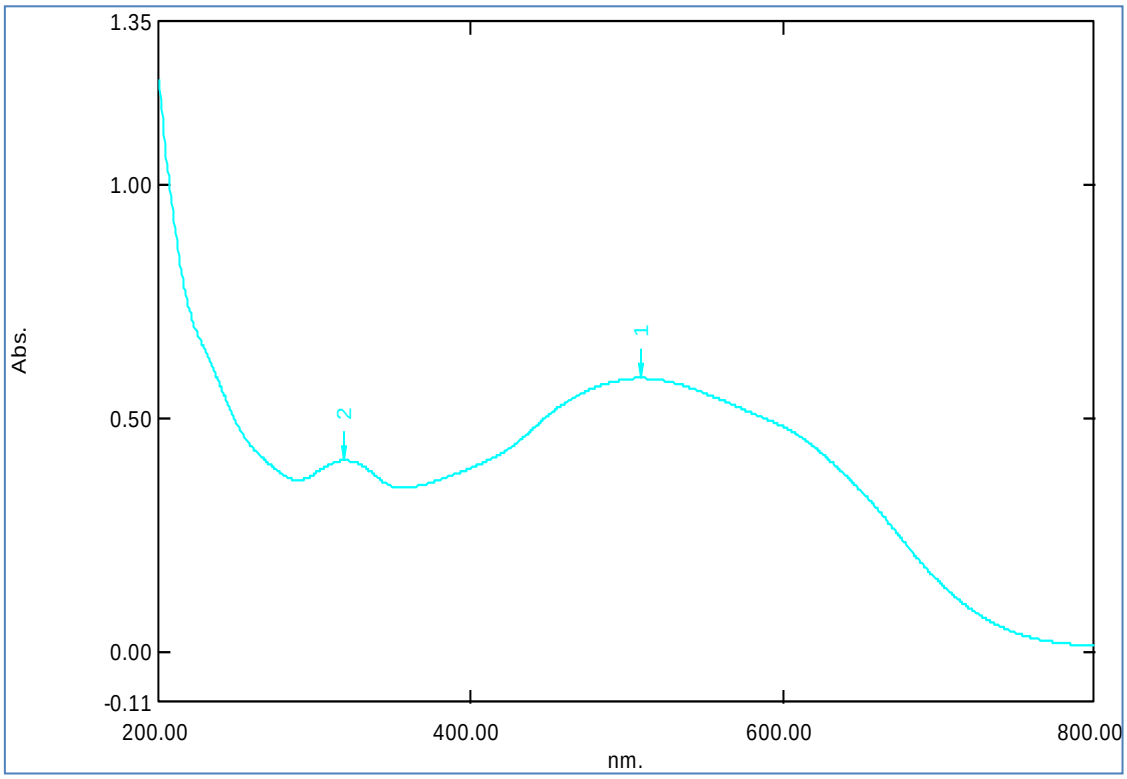

Easy Brown 100 mg/l, pH-7.65

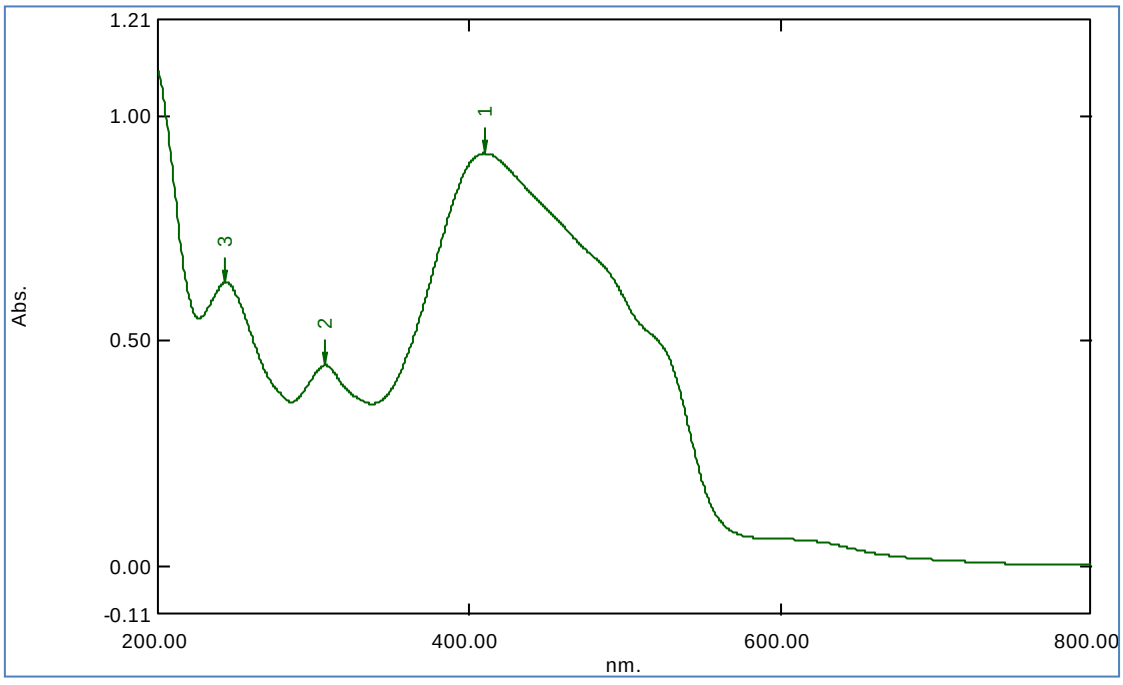

Sheet pink 100 mg/l, pH-7.54

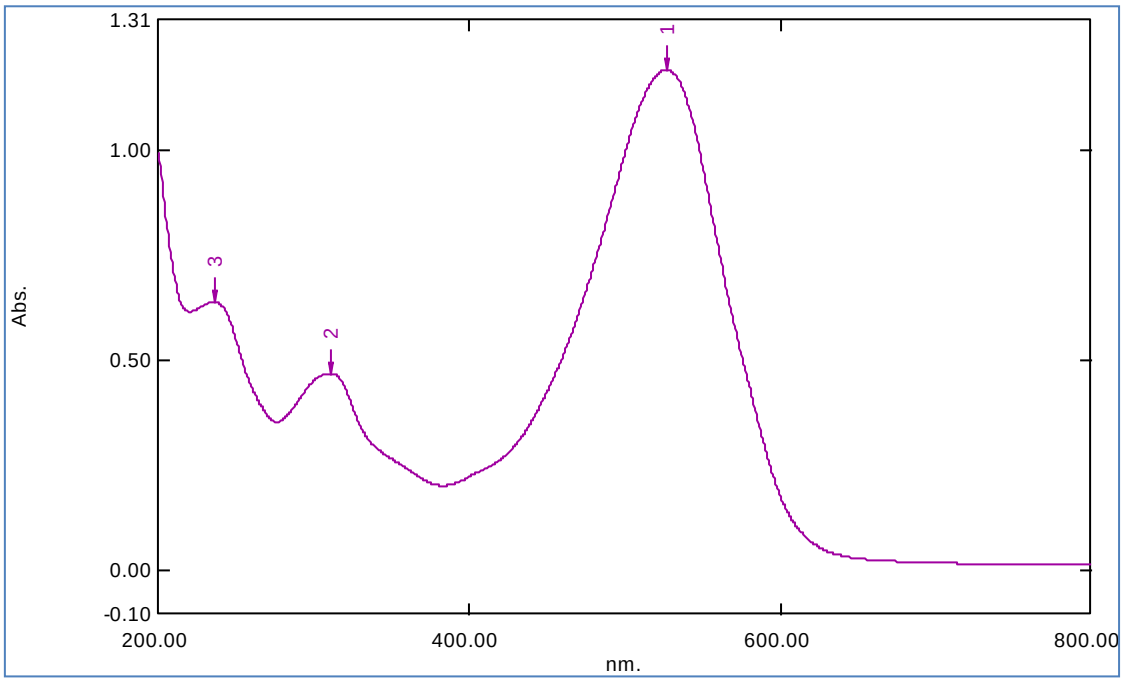

Turquoise blue 50 mg/l, pH-7.79

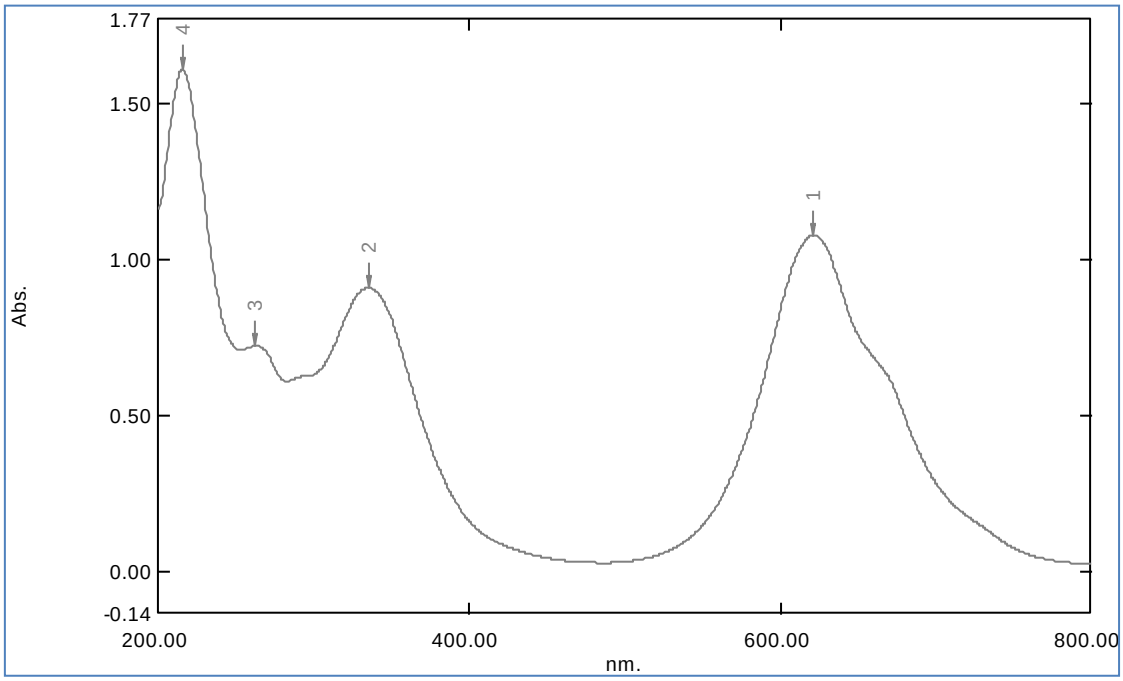

Green 100 mg/l, pH-7.76

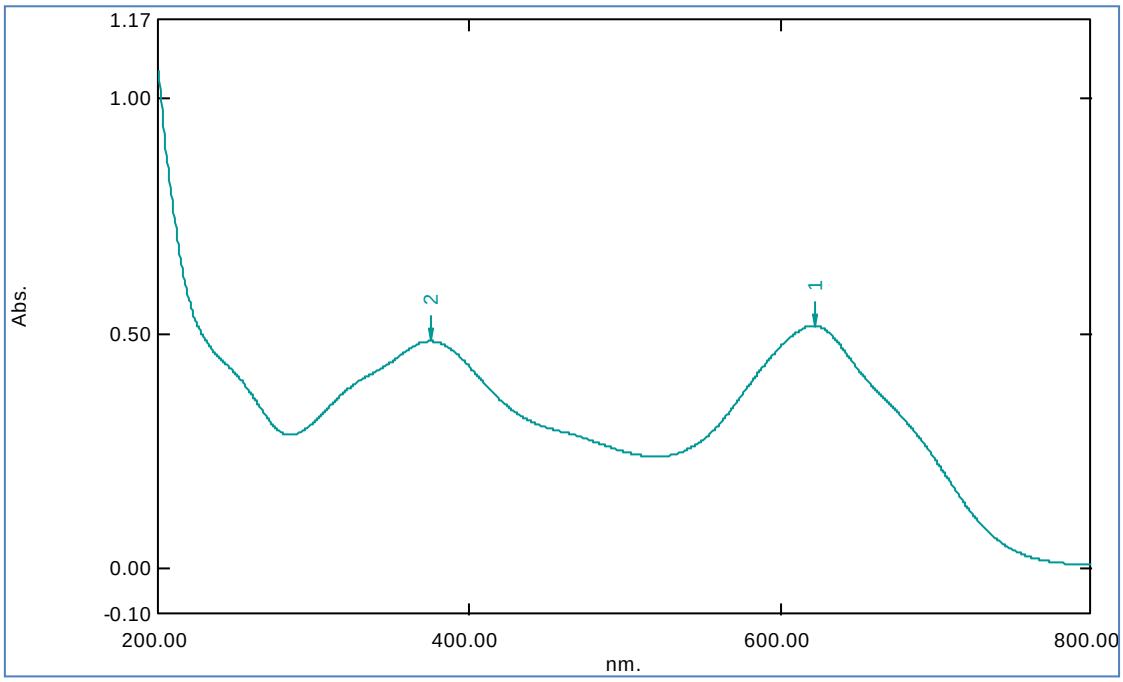

Sky blue-50 mg/l, pH-7.23

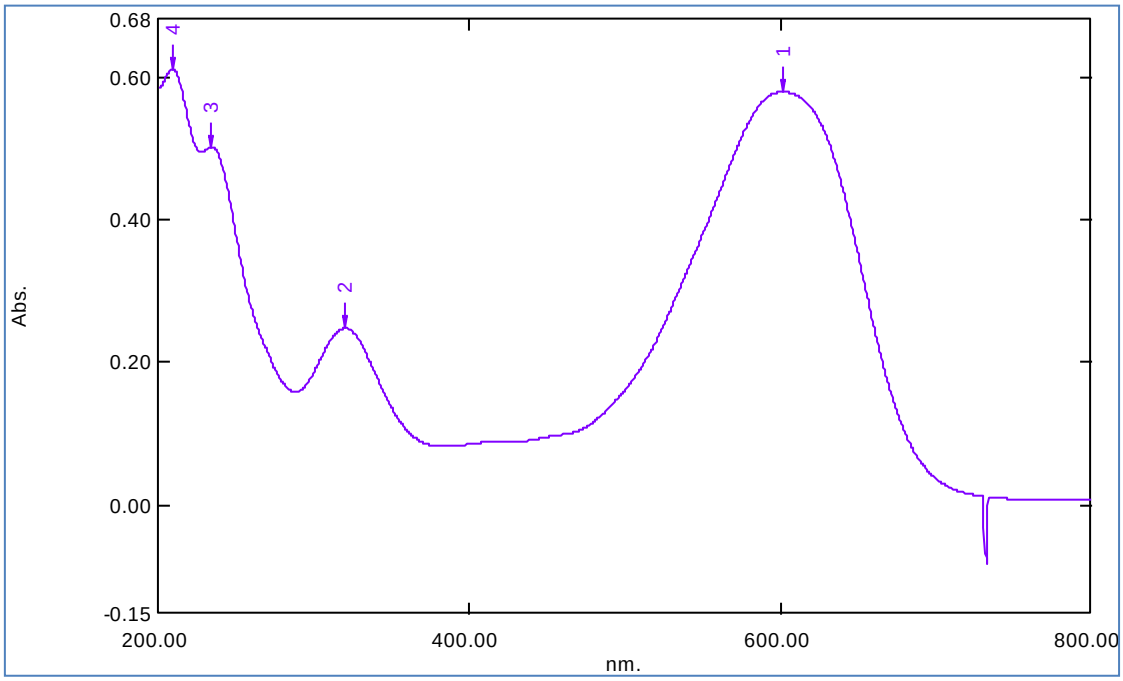

Navy blue -100 mg/l, pH-7.34

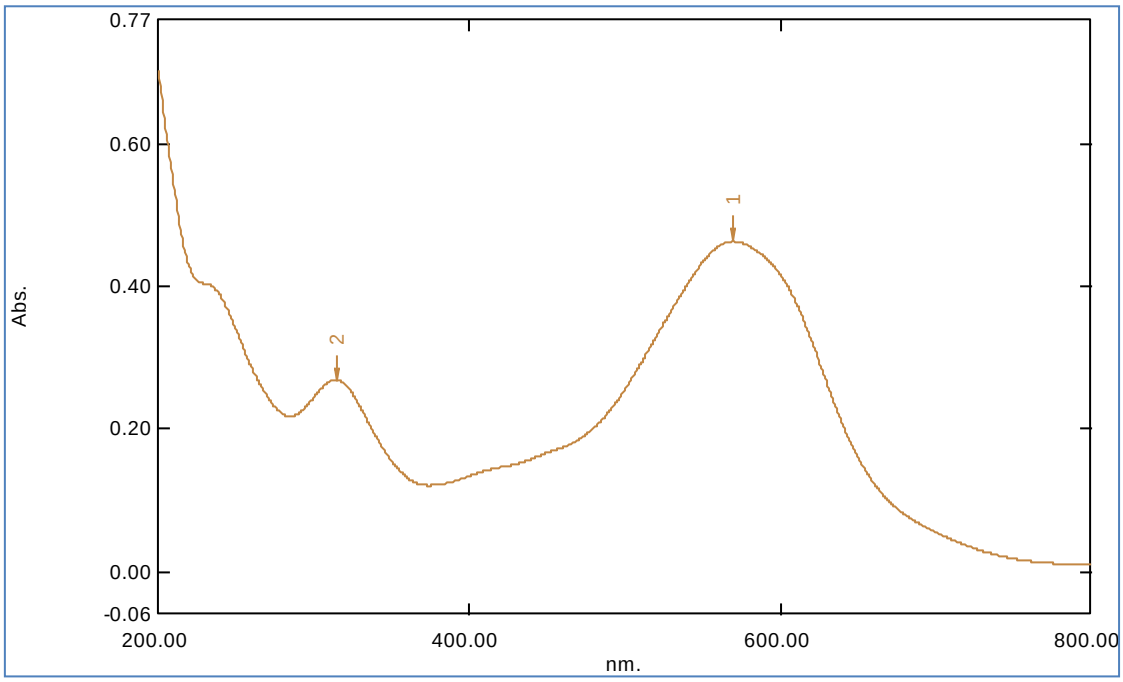

Figure 5.1 Maxima of direct dyes

Table 5.8 Maxima of direct dyes

Name of dye	Maxima	Absorbance
Khaki	407, 309, 242.5	0.89, 0.46, 0.66
Lemon yellow	365	1.11
Orange	491, 304, 238	1.06, 0.58, 0.69
Black	509.5, 318.5	0.59, 0.41
Easy Brown	410, 307, 245	0.92, 0.45, 0.63
Sheet pink	527, 310, 236.5	1.19, 0.47,0.64
Turqouise blue	621.5, 335, 262, 215.5	1.08, 0.91, 0.72, 1.61
Green	622, 375	0.52, 0.48
Sky Blue	601.5, 320, 234, 208.5	0.58, 0.25, 0.50, 0.61
Navy Blue	569.5, 312.5	0.41, 0.24

5.7 Characterization of spent liquor of each dye from handmade paper unit

The spent dye was characterized for various parameters as shown in Table 5.9.

Table 5.9 Characteristics of spent dye

Name of dye	pH	COD, mg/l	BOD, mg/l	Color, Pt.-CU
Orange	7.65	260	75	103
Easy Brown	7.50	120	45	80
Sheet Pink	7.50	152	64	66
Navy blue	7.45	90	36	52
Lemon Yellow	7.57	259	53	97
Green	7.66	102	49	121
Khaki	7.48	100	33	120
Turquoise Blue	7.60	148	72	118
Sky Blue	7.49	93	41	138
Black	7.56	345	49	45
Red	7.54	178	71	51

It has been observed that the spent dye solution has COD and BOD above limit. The color of the spent dye solution showed high value. No previous studies have been conducted for characterization of spent dye solution of handmade paper industry.

5.8 Characterization of various direct dyed handmade paper

The strength properties of various direct dyed handmade paper is given in Table 5.10.

Table 5.10 Characterization of various direct dyed handmade paper

Particulars	Tensile Index, Nm/g	Tear Index, mN.m2/g	Burst Index, kPa.m2/g	Double Fold, No.
Cotton control	30.56	10.36	1.74	267
Lemon Yellow	33.75	9.77	1.96	155
Sky Blue	30.20	10.17	1.93	142
Navy Blue	32.28	10.62	2.03	196
Turquoise Blue	27.79	10.42	2.06	184
Black	29.93	11.21	1.86	179
Green	39.31	10.10	1.95	272
Sheet Pink	27.38	10.23	1.88	131
Easy Brown	32.31	10.69	1.67	261
Khaki	31.47	10.09	2.05	351
Orange	30.54	10.54	1.86	295

It is observed from Table 5.9 that the tensile index, tear index, burst index and double fold of cotton pulp and after addition of dye increases or decreases according to the type of dye.

5.9 Characterization of black liquor

The black liquor of alternative ligno-cellulosic raw material with various pulping processes have been analyzed for various parameters. The results are given as Table-5.11.

Table 5.11 Analysis of Black Liquor

	pH	Total solids, mg/l	COD, mg/l	BOD, mg/l	λ_{max}, nm	Color, Pt.-CU	Lignin, mg/l
Jute (Urea pulping)	8.6	0.123	86500	21000	220	15654	17680
Jute (Soda)	10.2	0.156	203400	22400	220	17100	4000
Banana (APP)	9.5	0.108	185700	12000	280	14094	6780
Banana (Soda)	9.8	0.112	25640	19400	280	16100	2100
Sunn Hemp (15% urea commercial)	8.4	0.133	16740	14000	220	13800	2300
Bhimal, (8% APP)	9.2	0.117	20310	18700	222	14050	9800
Bagasse, (8% APP)	9.0	0.120	22450	19000	230	18100	3500
Jute (Alkaline sulphite)	9.3	0.119	156780	16570	239	19580	8000

The COD of black liquor of M/s Package Paper Mill, Lahore is 28270 mg/l and color of 1640 Pt.-CU (Irfan et al. 2013). The raw black liquor showed initial COD of 7150 mg/l and initial color of 18750 PCU (Rastegarfar et al. 2015).The initial COD and lignin content in black liquor of pine (92700 mg/l & 23.7 g/l) and bamboo (67000 mg/l & 19.6 g/l) respectively (Wen-bo et al. 2003).

5.10 FTIR spectra of black liquor

The FTIR spectra of black liquor of alternative ligno-cellulosic raw material at various pulping process is given in Figure 5.2 & Table 5.12.

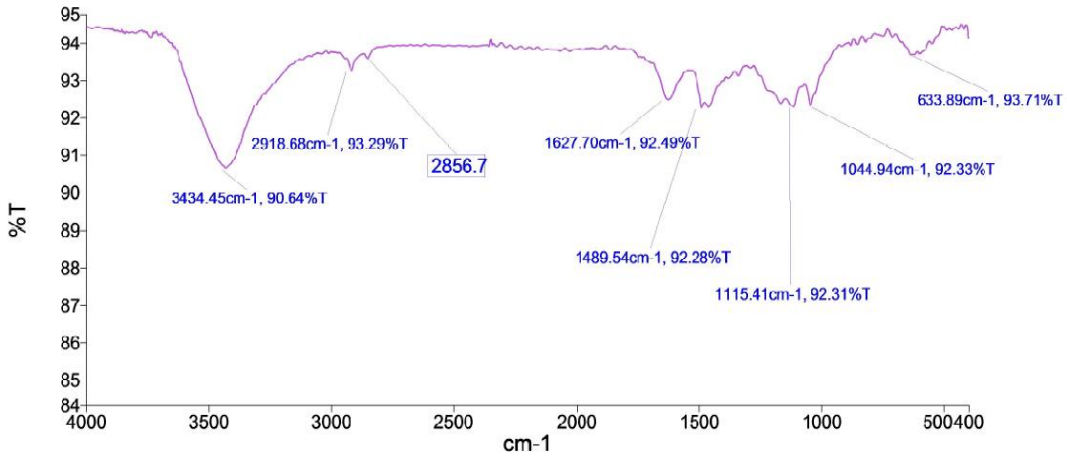

(a) Jute fiber at urea pulping

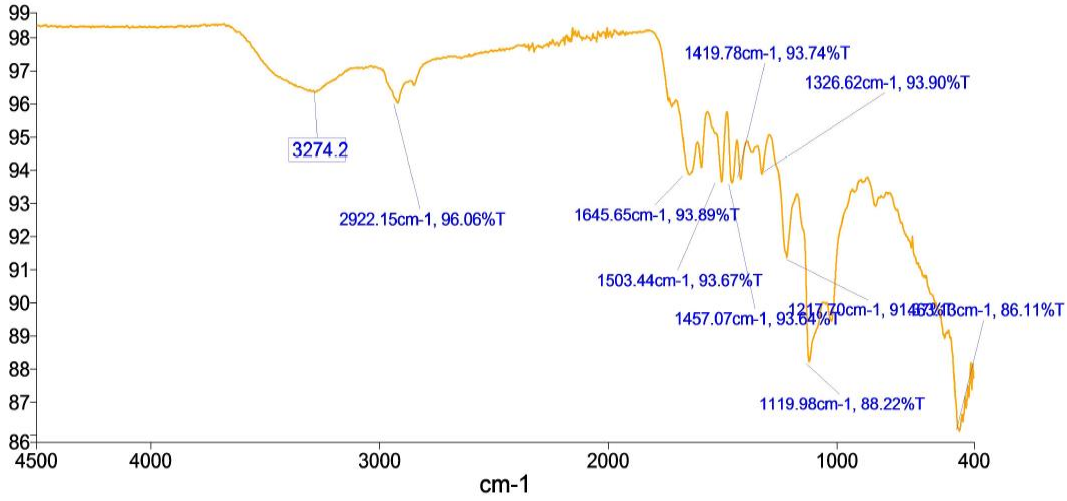

(b) Jute fiber at soda pulping

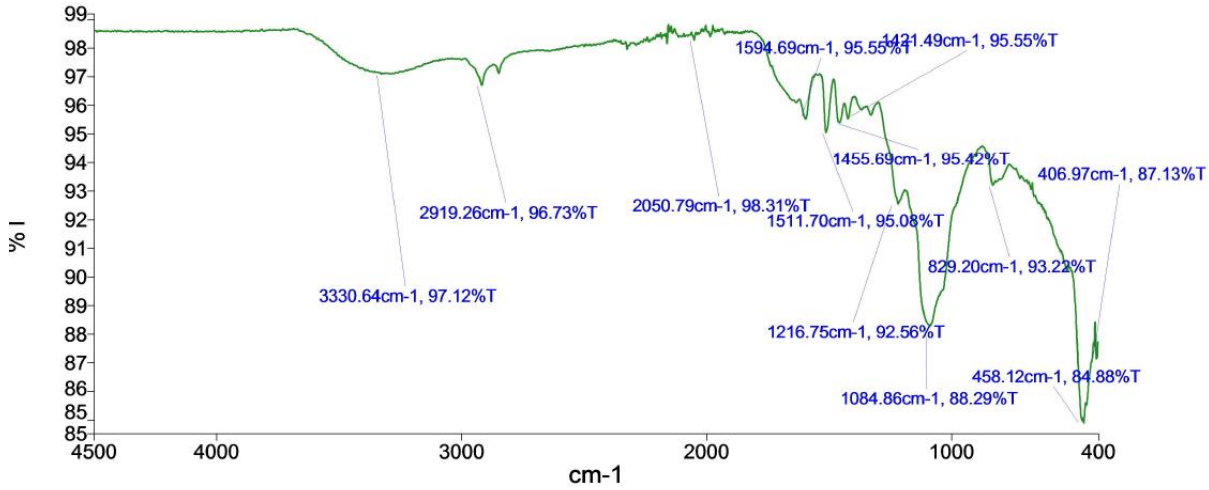

(c) Banana fiber at alkaline peroxide pulping process

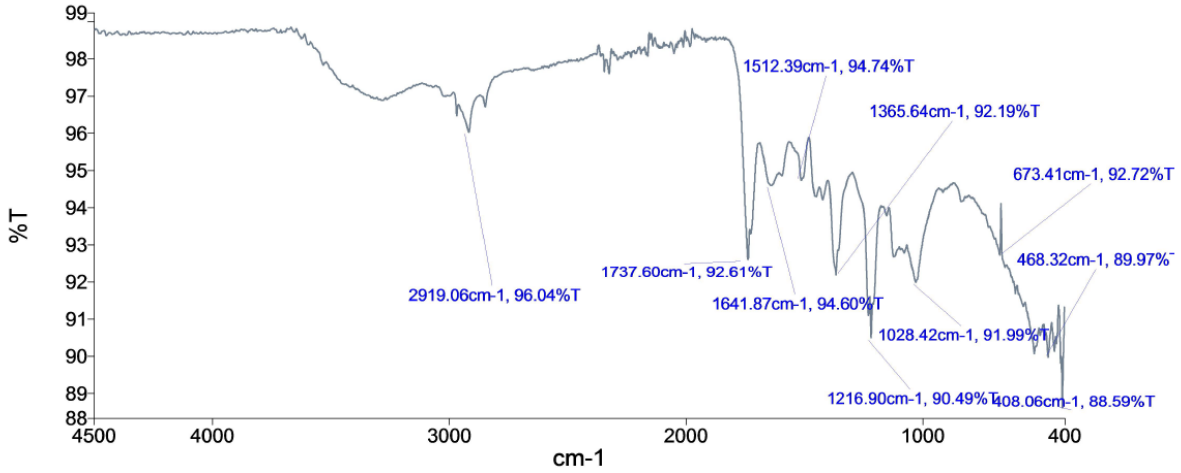

(d) Banana fiber at soda pulping

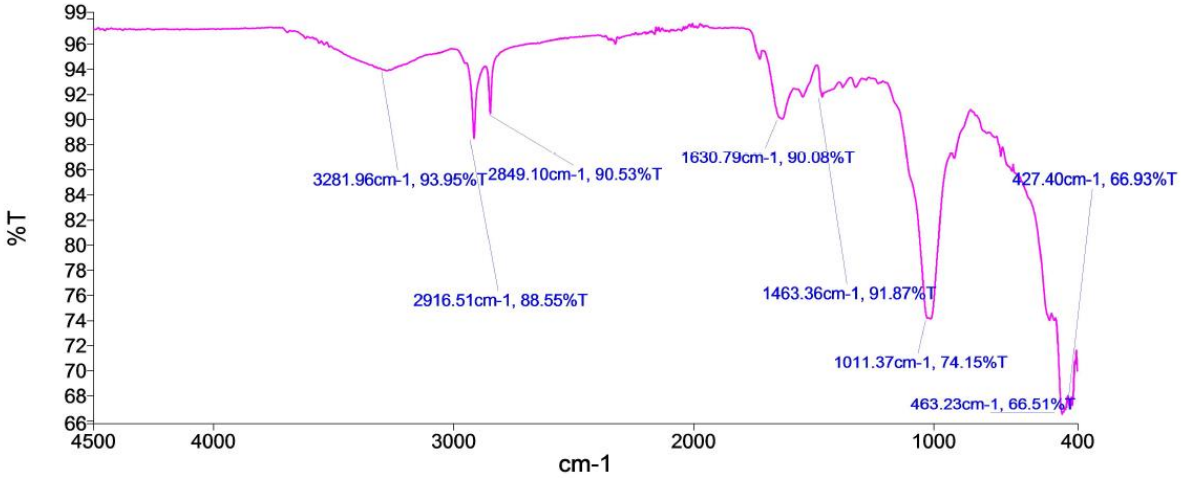

(e) Sunn Hemp fiber at urea pulping

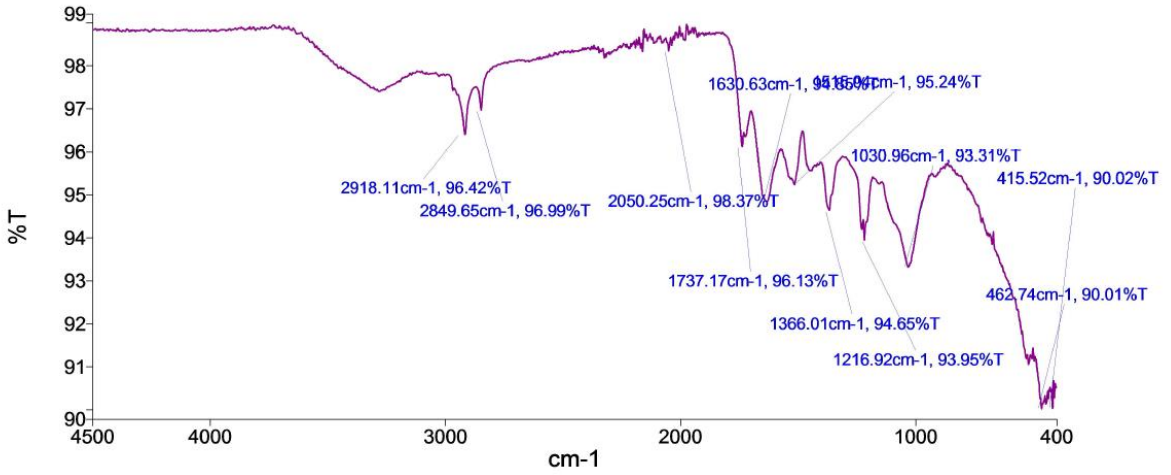

(f) Bhimal fiber at alkaline peroxide pulping

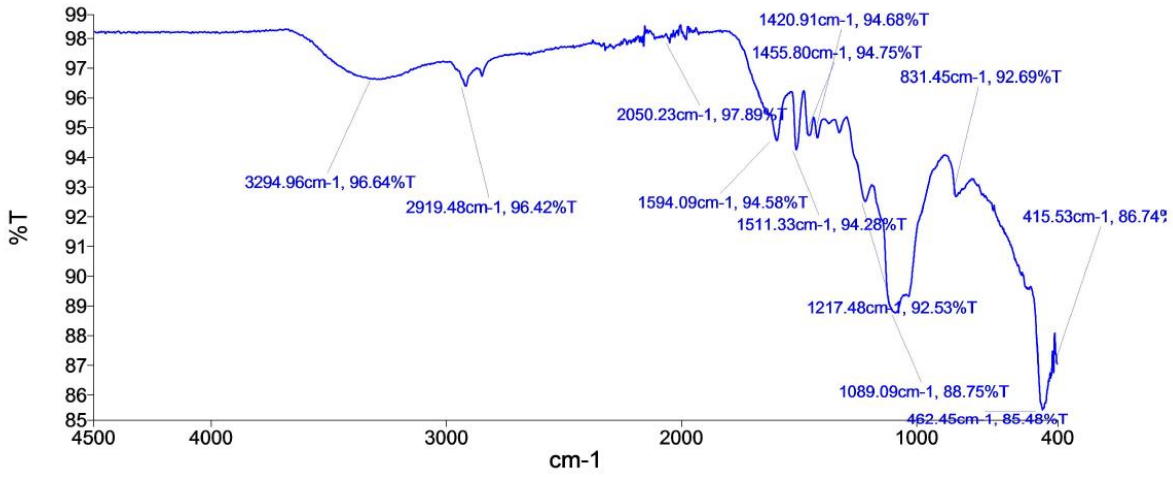

(g) Bagasse at alkaline peroxide pulping

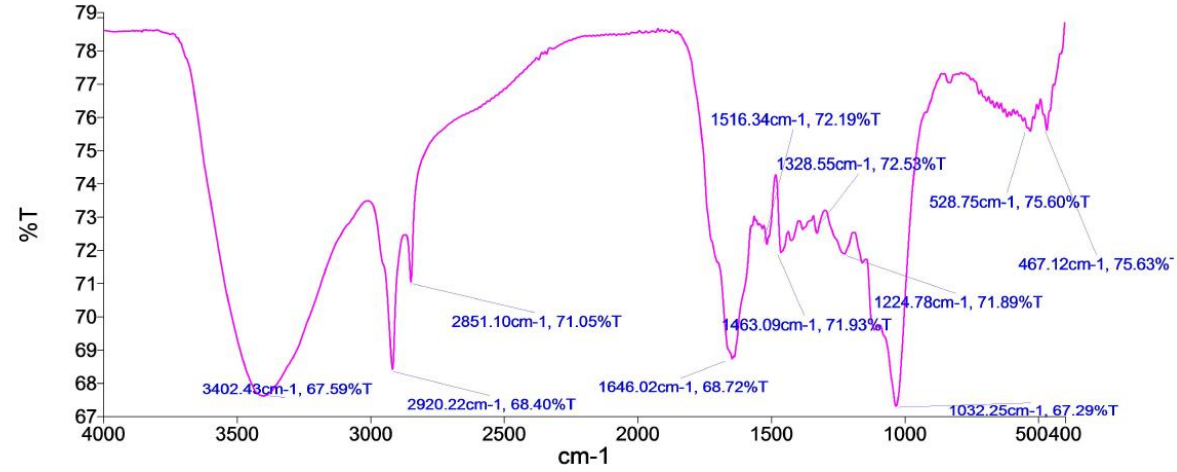

(h) Banana Open Digestion

Figure 5.2 FTIR spectra of lignin extracted (a) Jute urea pulping (b) Jute soda pulping (c) Banana APP (d) Banana soda pulping (e) Sunn Hemp urea pulping (f) Bhimal APP (g) Bagasse APP (h) Jute Alkaline Sulphite

Table 5.12 Analysis of FTIR Spectra of various lignin

Raw material and pulping processes	Peaks
Jute Urea Pulping	3434.45, 2918.68, 1627.70, 1489.54, 1044.94, 1115.41, 633.89
Jute Soda Pulping	3274.2, 2922.15, 1645.65, 1503.44, 1457.09, 1419.78, 1326.62, 1119.98, 1217.70, 463
Banana Alkaline Peroxide Pulping	3330.64, 2919.26, 1511.70, 1594.69, 1455.69, 1421.49, 1216.75, 1084.86, 829.2, 458.12, 406.97
Banana Soda Pulping	2919.06, 1737.60, 1641.87, 1512.39, 1365.64, 1216.90, 1028.42, 673.41, 468.32, 406.06
Sunn Hemp Urea Pulping	3281.96, 2916.51, 2849.10, 1630.79, 1463.36, 1011.37, 463.23, 427.40
Bhimal Alkaline Peroxide Pulping	2918.11, 2849.65, 1737.17, 1630.63, 1366.01, 1216.92, 1030.96, 462.74, 415.52
Bagasse, APP	3294.96, 2919.48, 1594.09, 1511.33, 1455.80, 1420.91, 1217.48, 1089.09, 831.45, 462.45, 415.53
Jute, Alkaline Sulphite puping	3402.43, 2920.22, 2851.10, 1646.02, 1463.09, 1516.34, 1328.55, 1224.78, 1032.25, 528.75, 467.12

The peak at 3402.43, 3281.96 cm^{-1} attributed to the hydroxyl groups in phenolic and aliphatic structures in Jute Alkaline Sulphite and Sunn Hemp Urea pulping. The peaks at 3330 cm^{-1} showed OH stretching in Banana APP. The bands centered around 2918.68, 2922.15, 2920.22, 2851.10, 2919.48, 2918.11 and 2849.65, 2919.26, 2916.51 and 2849.10, 2919.06, 2916.51 and 2849.10 cm^{-1} showed presence of CH stretching in aromatic methoxyl groups and in methyl and methylene groups of side chains in Jute Urea pulping, Jute soda pulping, Jute Alkaline Sulphite pulping, Bagasse APP, Bhimal APP, Banana APP, Sunn Hemp Urea pulping, Banana soda pulping and Sunn Hemp Urea pulping (Boeriu et al. 2004).

The ester and unconjugated carbonyl stretching absorption at 1737.17, 1737.60 cm^{-1} was found in Bhimal APP and Banana soda pulping (Sammons et al. 2013).

The peak at 1511.33, 1594.09, 1503.44, 1516.34, 1512.39, 1511.70 and 1594.69 cm^{-1} are characteristics of aromatic compounds (phenolic hydroxyl groups) and are attributed to aromatic skeleton vibrations in Bagasse APP, Jute soda, Jute Alkaline Sulphite pulping, Banana soda, Banana APP and Jute soda pulping. The peak at 1489.54, 1463.09, 1455.80, 1457.09, 1463.36, 1455.69 cm^{-1} indicates the presence of C-H deformation methyl and methylene in Jute Urea pulping, Jute Alkaline Sulphite, Bagasse APP, Jute soda, Banana APP and Sunn Hemp Urea pulping. The peak at 1419.78, 1420.91, 1421.49 cm^{-1} indicates the presence of aromatic ring stretching with in plane C-H deformation in Jute soda, Bagasse APP and Banana APP.

The peak at 1328.55, 1366.01, 1365.64, 1326.62 cm^{-1} indicates the presence of C-O stretch of syringyl in lignin structure in Jute Alkaline Sulphite, Bhimal APP, Banana soda and Jute soda pulping process. The peak at 1224.78, 1217.48, 1216.92, 1216.9, 1216.75, 1217.70 cm^{-1} indicates presence of C-O stretch of guaiacyl lignin can be associated with C–C plus C–O plus C=O stretching in Jute Alkaline Sulphite, Bagasse APP, Bhimal APP, Banana soda, Banana APP and Jute soda pulping. The band at 1200 cm^{-1} range indicates presence of guaiacyl lignin found in all except Jute Urea pulping and Sunn Hemp Urea pulping. The bands at 1300 cm^{-1} (syringyl) and 1200 cm^{-1} (guaiacyl) indicate the presence of both syringyl and guaiacyl in lignin's chemical structure (Watkins et al. 2015). The peak at 1115.41, 1119.98 cm^{-1} indicates the presence of aromatic C-H deformation of S units in Jute urea and Jute soda pulping. The peak at 1089.09, 1084.86 cm^{-1} shows the presence of C-O stretch of secondary alcohols and aliphatic esters in Bagasse APP and Banana APP.

The peak at 1044.94, 1032.25, 1030.96, 1011.37, 1028.42 cm^{-1} indicates the presence of C-O, primary alcohols in Jute Urea, Jute sulphite, Bhimal APP, Sunn Hemp urea and Banana soda pulping. The peak at 831.45, 829.29 cm^{-1} indicates C-H bending of S units in Bagasse APP and Banana APP. The peak at 633.89, 673.41 cm^{-1} indicates the presence of C-OH out of plane bending in Jute urea and Banana soda pulping.

5.11 TGA analysis of lignin

Thermal analysis TGA of lignin under N_2 atmosphere and DTG curves are presented in Figure 5.3 and 5.4 respectively and thermal analysis of lignin is given in Table 5.13.

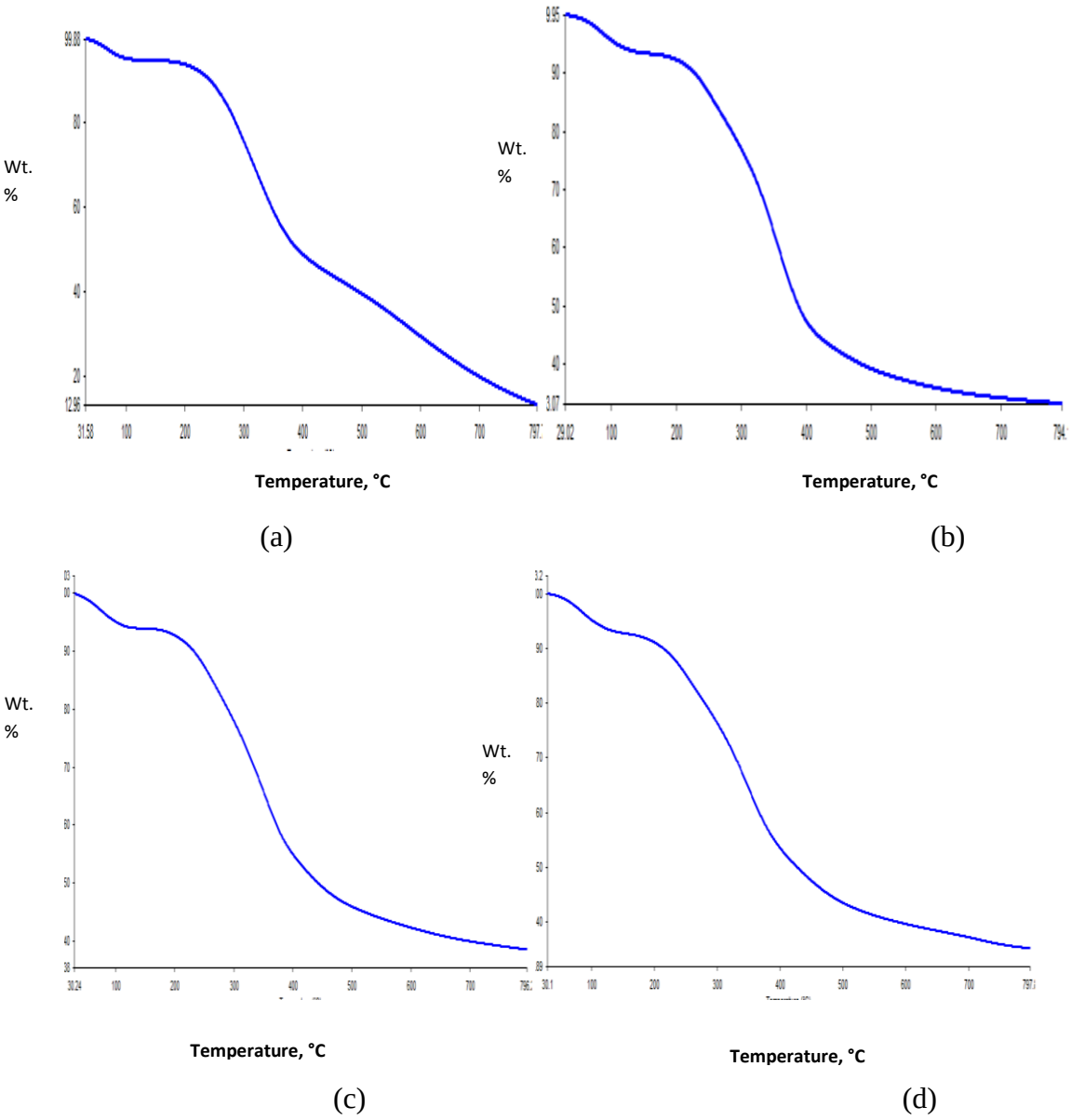

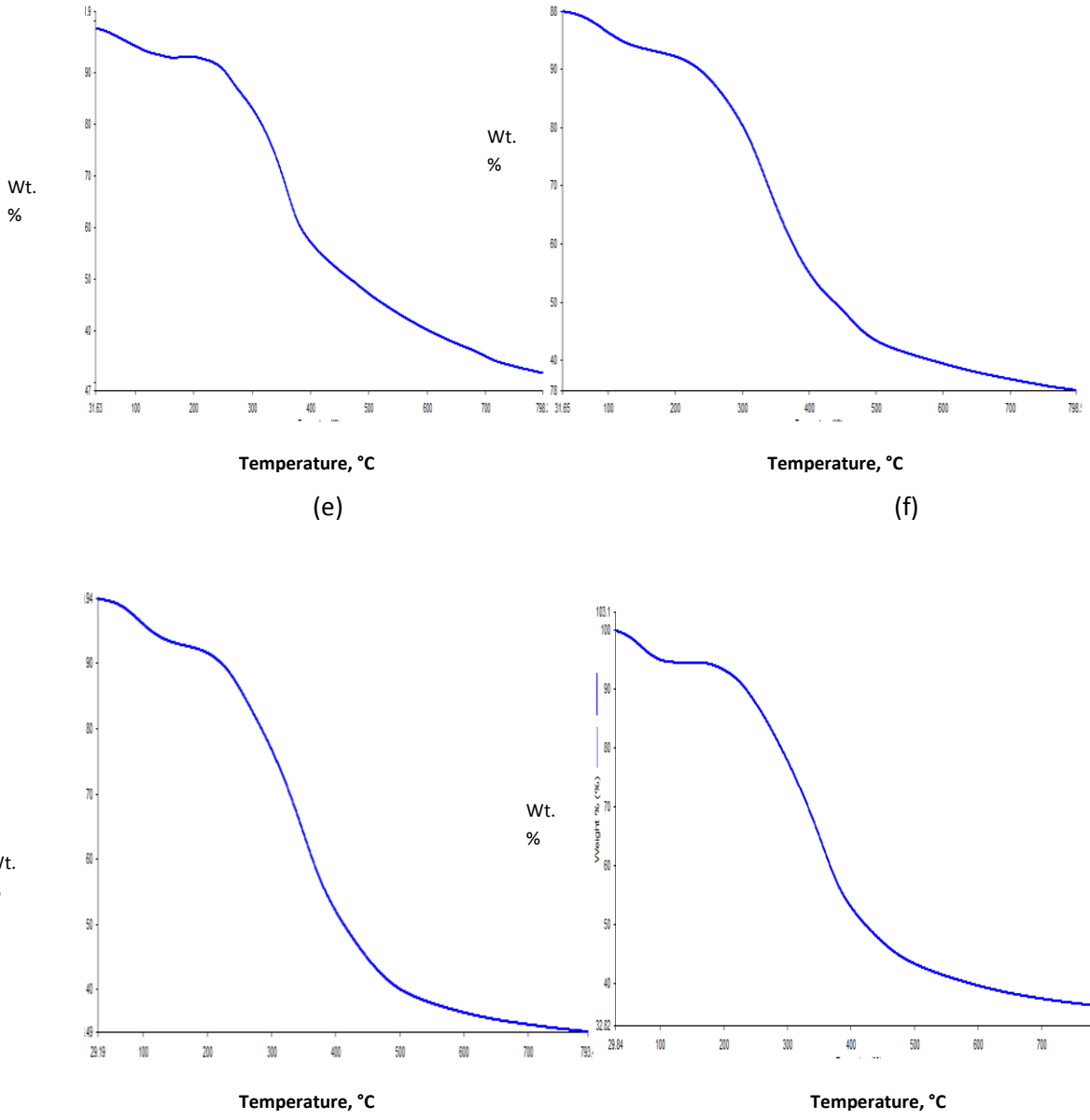

Figure 5.3 TGA Thermal plot of lignin at 5°C/min (a) Jute Urea pulping (b) Jute Soda pulping (c) Banana APP (d) Banana Soda pulping (e) Sunn Hemp Urea pulping (f) Bhimal APP (g) Bagasse APP (h) Jute Alkaline Sulphite pulping

It has been observed that thermal decomposition started at about 200 °C. A major weight loss occurred between 200 and 400 °C (Yang and Wu, 2009). However, over 400-500 °C, slow mass loss up to the final temperature has been observed. The loss of weight at 100°C can be attributed to the loss of moisture from lignin. The thermal decomposition has been observed up to almost 750-800 °C.

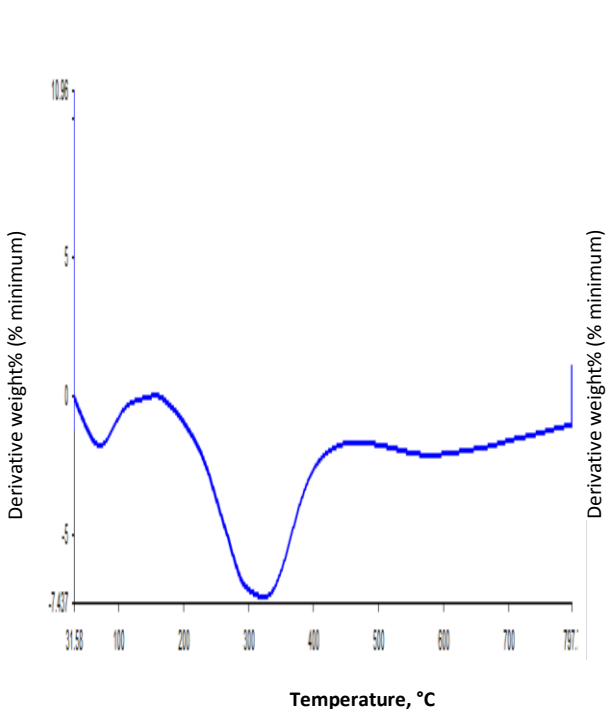
Derivative weight% (% minimum)
Temperature, °C

(a)

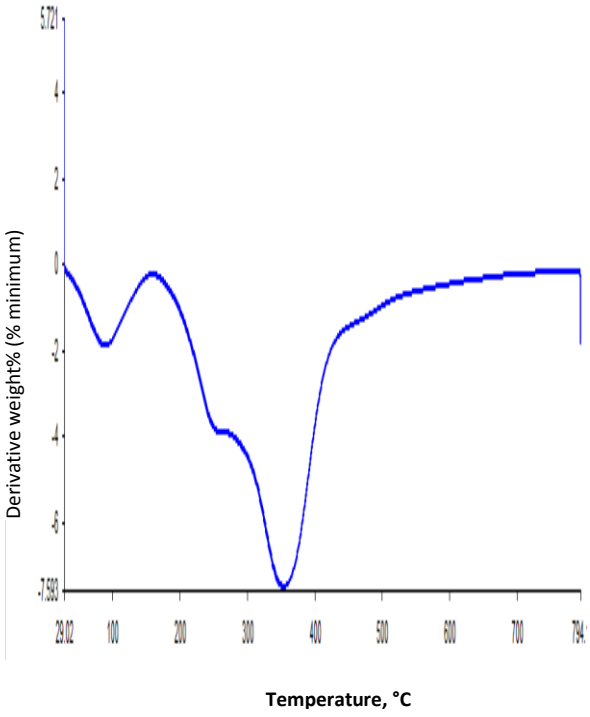
Derivative weight% (% minimum)
Temperature, °C

(b)

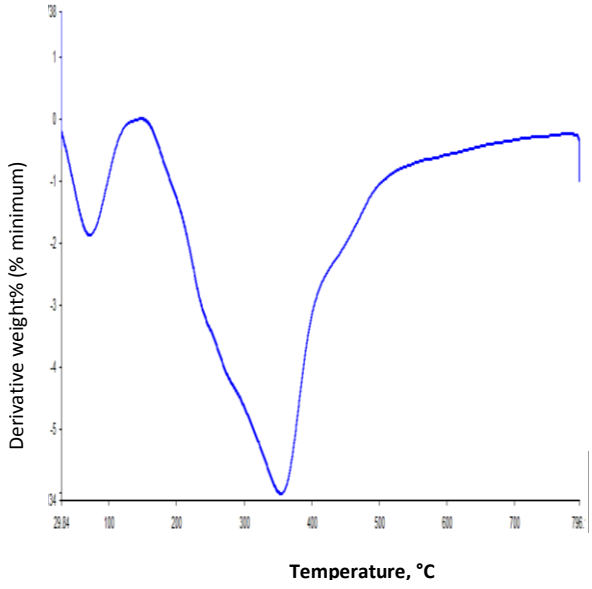
Derivative weight% (% minimum)
Temperature, °C

(C)

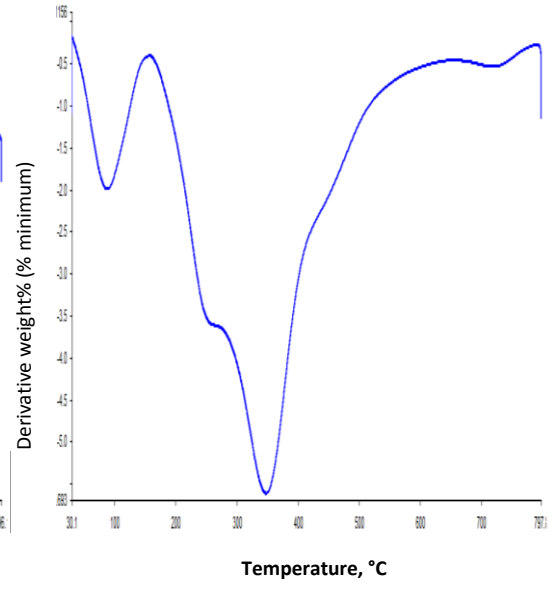
Derivative weight% (% minimum)
Temperature, °C

(d)

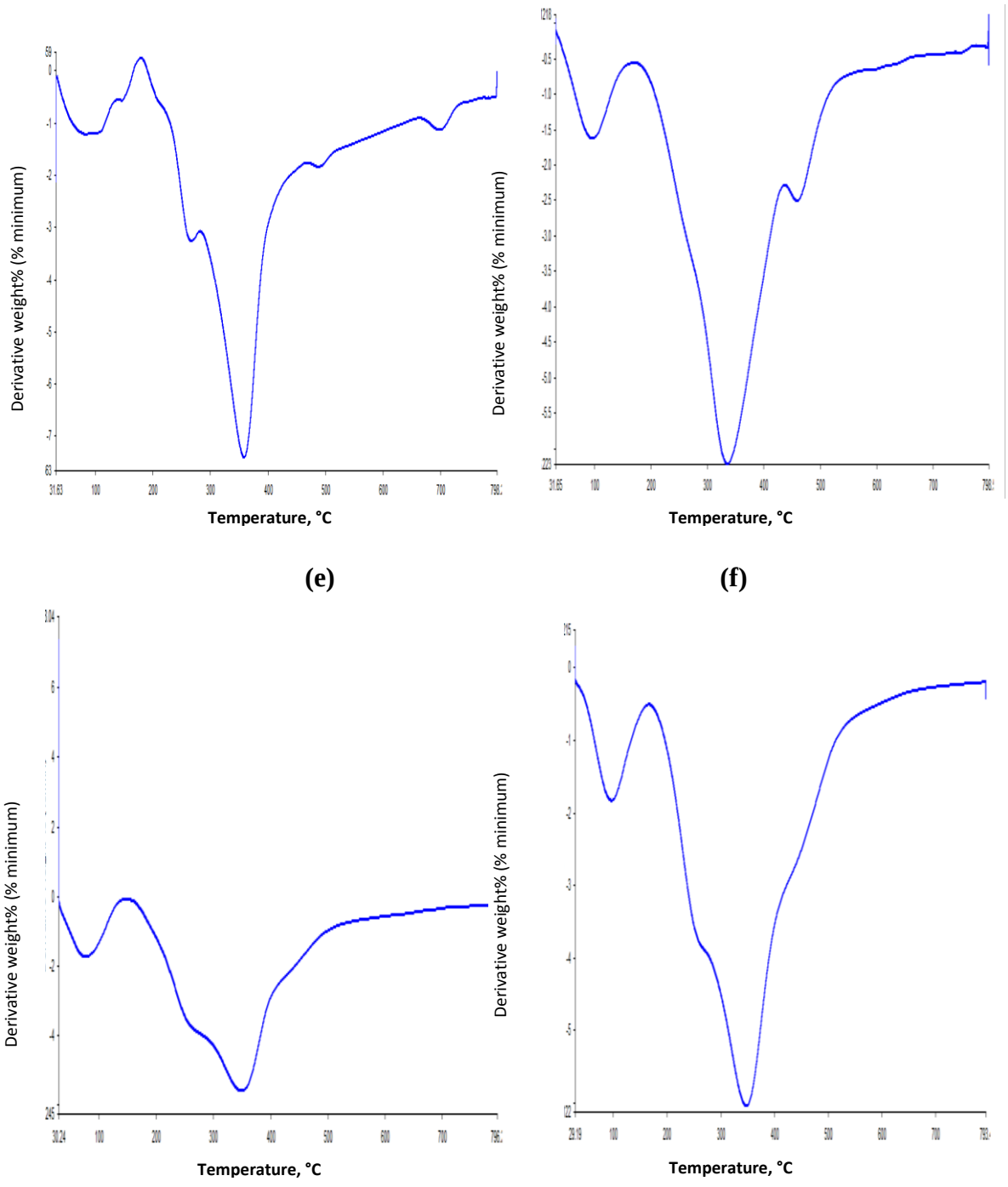

Figure 5.4 Derivative TGA curves of lignin at 5°C/min (a) Jute Urea pulping (b) Jute Soda pulping (c) Banana APP (d) Banana Soda pulping (e) Sunn Hemp Urea pulping (f) Bhimal APP (g) Bagasse APP (h) Jute Alkaline sulphite pulping

The DTG range between 300 to 400 ° C for all lignin in the study from Figure 5.4.

Table 5.13 Thermal Analysis of Lignin

Particulars	Temp. to 5% weight loss, °C	T_{onset}, °C	Wt. loss, % at T_{onset}	Fast degradation	Slow degradation	Residue at <700°C ,%
Jute Urea pulping	106	180	4	180-385	385-796	32.82
Jute Soda pulping	107.8	190	7.5	190-427 C Wt. Loss%=44%	427-785	33.07 at 785° C
Banana APP	110	200	4	195-400	400-796	12.96
Banana Soda pulping	120	200	7	200-470	470-793	33.49
Sunn Hemp, Urea pulping	120	380	8	120-380	380-800	28.47
Bhimal APP	140	280	10	280-420	420-798	34.78
Bagasse APP	120	215	8	215-370	370-795	35.38
Jute Alkaline Sulphite pulping	115	210	5	210-380	380-795	31.89

CHAPTER 6 ADSORPTION

This chapter presents the characterization of fly ash, adsorption studies have been conducted with low cost adsorbent fly ash with direct black dye and mixture of dyes used in handmade paper industry

6.1 Characterization of fly ash

Fly Ash was obtained from Kota Super Thermal Power Station and was tested for different physical and chemical characteristics as detailed in the subsequent sections.

6.1.1 Surface area measurement

The surface area of fly ash was determined to be 240 m^2/g using methylene blue method described by Santamarina et al. (2002). The result is well in agreement with the studies conducted by other researchers (Ramezanianpour et al 2014; Maroto-Valer et al 2001; Papachristou-Kolovea 1982).

6.1.2 Particle size distribution of fly ash

The particle size distribution of fly ash was determined using standard sieves and is shown in Table 6.1, which clearly indicates that 48.14% of fly ash particles are less than 53 microns size.

Table 6.1 Differential particle size of fly ash

Different particle size, µ	% Weight
-300	1.10
-300+180	10.06
-180+150	5.67
-150+90.9	9.11
-90.9+75	10.47
-75+53	13.91
-53	48.14

The (–) sign indicate the size of fly ash retained on the the screen while (+) indicate the size of fly ash that passed through the screen. Thus, -300+180 means the fly ash of 300 µ and smaller and 180 µ and bigger retention on the screen.

6.1.3 Chemical composition of fly ash

The chemical composition of fly Ash was supplied by Kota Super Thermal Power Station and is shown in Table 6.2. It is a class F fly ash with less than 10 % of lime CaO as major component. The fly ash mainly contained SiO_2 andAl_2O_3.

Table 6.2 Chemical composition of fly ash (Report of Kota Thermal Station)

S.N.	Particulars	Result
1	pH	8.56
2	Moisture %	7.96
3	Ash %	2.30
4	Bulk density, kg/m^3	750
5	Fixed carbon %	25
6	Na_2O %	0.89
7	MgO %	1.74
8	Alumina % Al_2O_3	23.7
9	Silica % SiO_2	51.96
10	P_2O_5 %	1.11
11	Fe_2O_3, %	6.66
12	TiO_2, %	1.86
13	CaO,%	5.86
14	Surface area, m^2/g	240.08

The sum of the major components (SiO_2+Al_2O_3+Fe_2O_3) is greater than 70% in fly ash, and according to ASTM C-618, it falls under F class category, which does not aggregate in long contact with water.

6.2 Batch Studies

Batch studies were conducted with fly ash at various pHs, dosage of fly ash, initial concentration and temperature of adsorbate, the details of which are described below.

6.2.1 Effect of pH

The adsorption is highly dependent on pH of the adsorbate. The study has been carried out with fly ash of dosage 5 g/l on black dye of 50 mg/l initial concentration maintained at various pH values of 4, 6, 8 and 10. The percentage uptake of black dye by fly ash at different pH is shown in Figure 6.1.

The effect of decolourization efficiency of fly ash(40 g/l dosage and 45–75 µm particle size) with mixture of dye solution of178.6 mg/l initial concentration at various pH 4, 6,8, 10 at 298 K is shown in Figure 6.2.

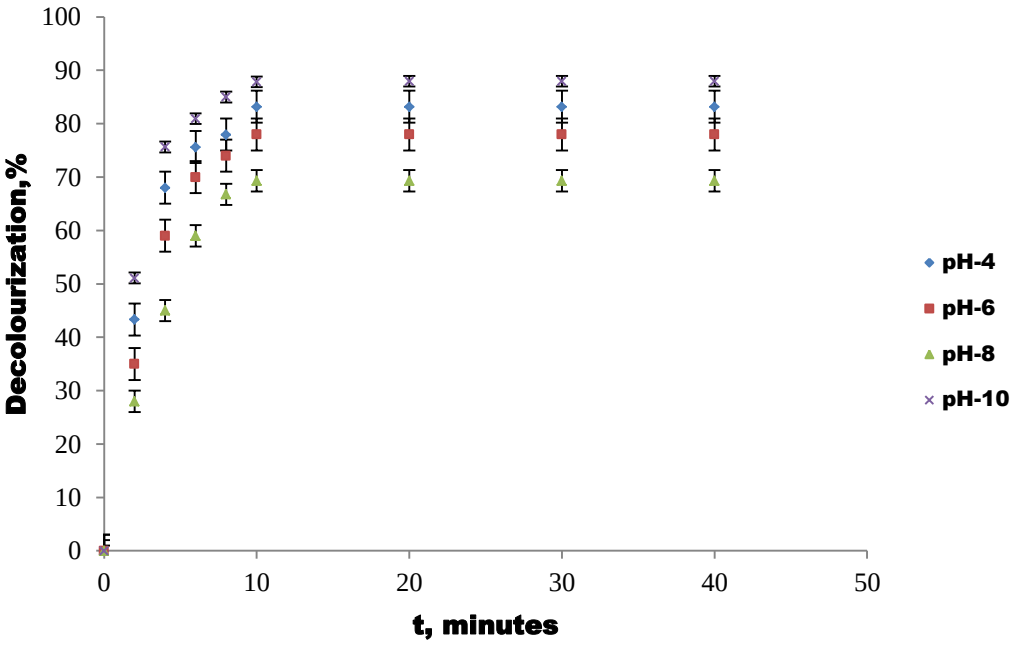

Figure 6.1 Effect of pH for Direct Black dye
[Black dye-50 mg/l, Fly ash dosage- 5g/l, Temperature-298 K, Stirring speed-125 rpm, Particle size-53 to 75µm]

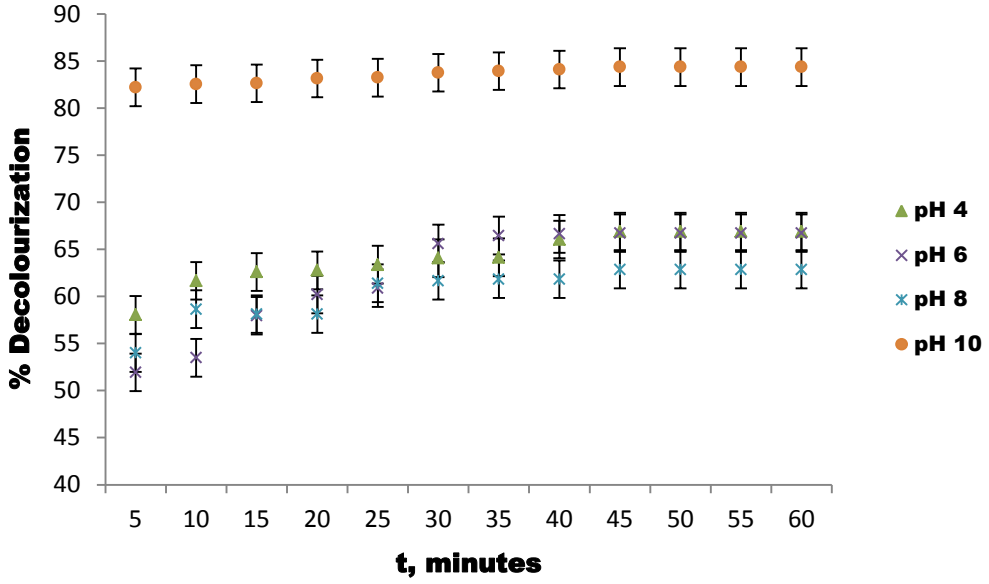

Figure 6.2 Effect of pH for mixture of dyes
[Initial concentration of dye- 178.6 mg/l, Fly ash dosage- 40g/l, Particle size- 45-75 µm, Temperature-298 K]

It can be observed from Figure 6.1 & 6.2 that fly ash showed best rate of adsorption at pH of 10. At high pH, the surface of adsorbent gets negatively charged and shows increased adsorption for positively charged adsorbate (Khan et al., 2004).The final pH of the dyed water after fly ash treatment of initial pH-4, 6, 8 & 10 is 4.8, 6.7, 8.2 and 9.5 respectively.

6.2.2 Effect of fly ash dosage

The effect of dosage of fly ash of 180-300 µm particle size varying from 0.4 g/l to 5 g/l was studied on adsorption of black dye of 50 mg/l concentration maintained at pH 4. The black dye uptake at various dosages of fly ash is shown in Figure 6.3. The effect of fly ash dosage on decolourization of mixture of dyes of initial concentration 178.6 mg/l maintained at 298 K and pH 7.5 was also studied the results of which are shown in Figure 6.4.

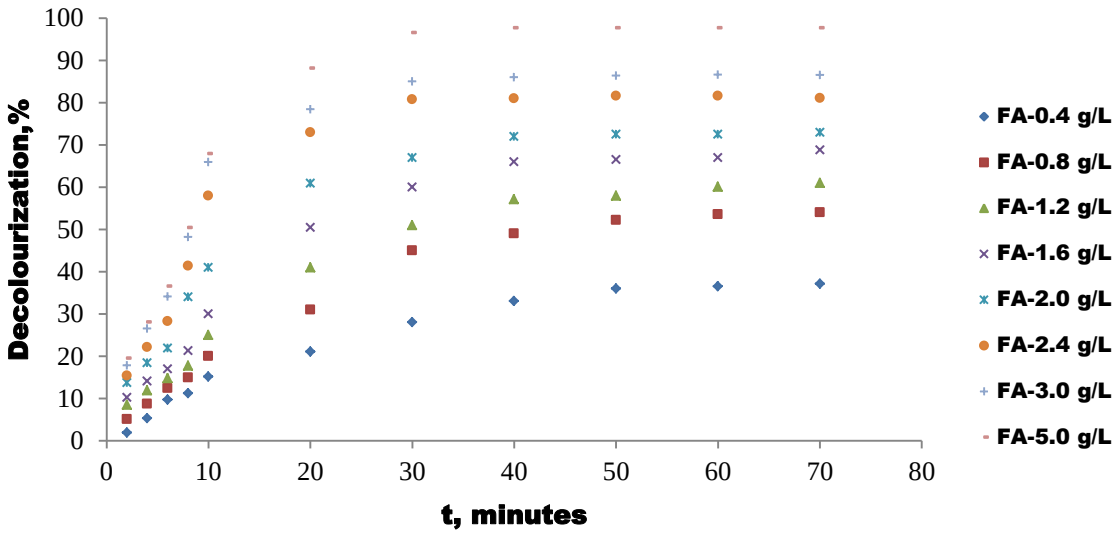

Figure 6.3 Effect of dosage of fly ash for Direct Black dye [pH-10, Black dye-50 mg/l, Temperature-298 K, Stirring speed-125 rpm, Particle size-53 to 75µm]

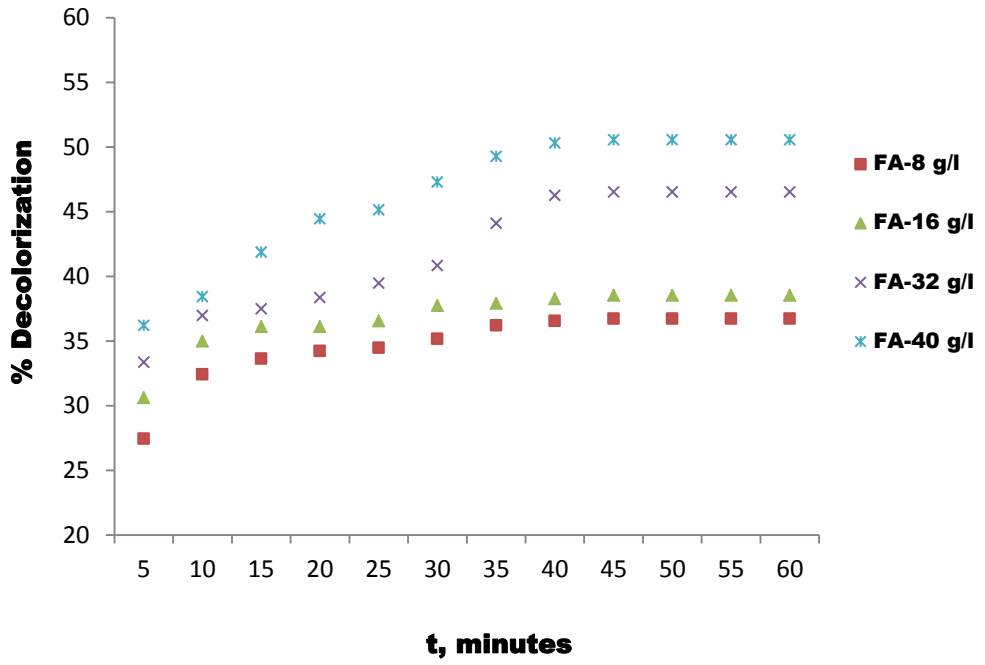

Figure 6.4 Effect of adsorbent dosage for mixture of dyes
[Initial concentration of dye- 178.6 mg/l, pH-10, Temperature-298 K]

It has been observed from Figure 6.3 that there is maximum adsorption of black dye at fly ash dose of 5 g/l while Figure 6.4 shows that decolourization of mixture of dye solution obtained by 8, 16, 32, and 40 g/l dosage of fly ash at 45 minutes was 36.7, 38.5, 46.5, and 50.6%, respectively. The increase in percent removal efficiency with increase in dosage was due to the fact that with the increase in the adsorbent dosage, the number of active sites available for adsorption of dye increases. Similar results have been reported previously by Mall et al 2006.

6.2.3 Effect of initial concentration and stirring time

The percentage removal of dye by fly ash for various initial concentrations of direct black dye in the range of 30-200 mg/l at pH 4 is shown in Figure 6.5. The effect of initial concentration of mixture of dyes at various concentrations 44.65, 89.3, 119.06, 127.57, and 178.6 mg/l on the decolourization efficiency of fly ash of particle size 45–75 μm and 40 g/l dosage is shown in Figure 6.6.

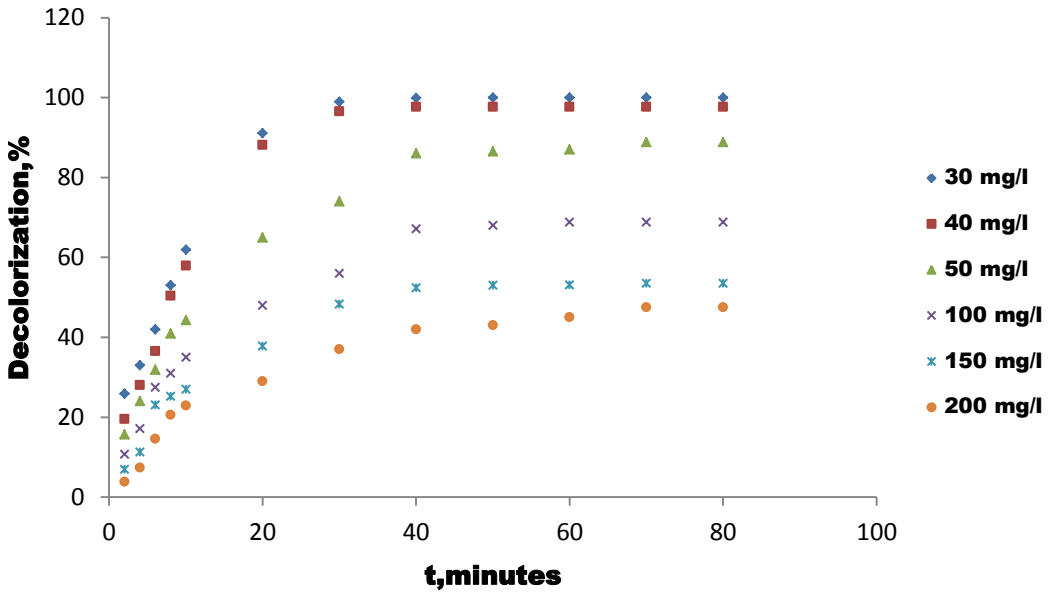

Figure 6.5 Effect of initial dye concentration on adsorption of Direct Black dye [pH-10, Fly ash -5 g/l, Stirring speed- 125 rpm, Temperature-298 K, and Particle size-53 to 75µm]

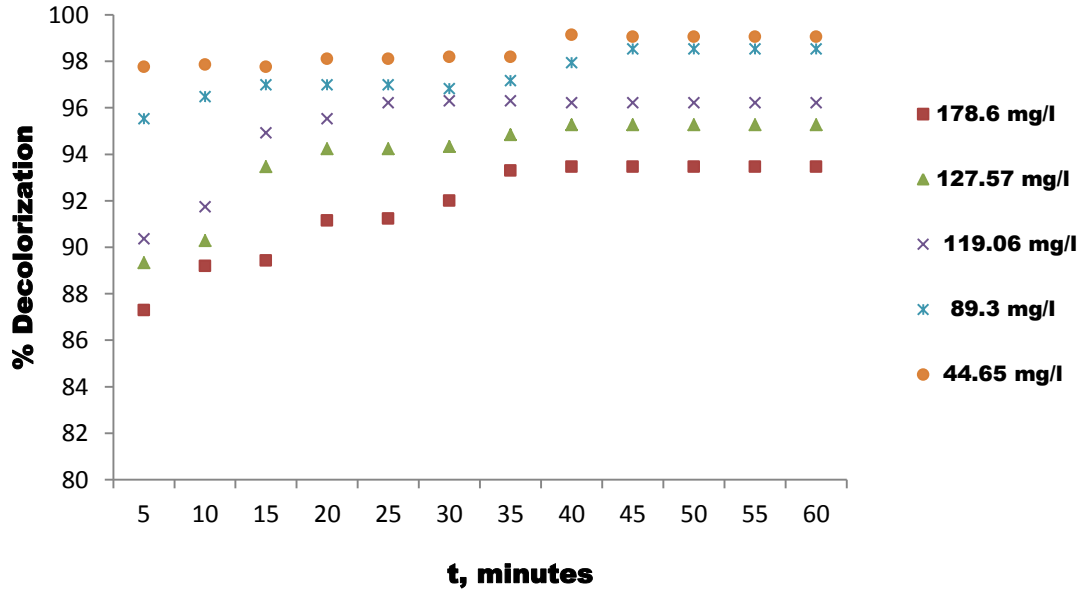

Figure 6.6 Effect of initial concentration on adsorption of mixture of dyes [Fly ash dosage- 40g/l, Particle size- 45-75 µ, pH- 10, Temperature-298 K]

From Figure 6.5, it has been observed that maximum decolourization of 47.5% and 100% was achieved at 200 mg/l and 30 mg/l initial concentration of black dye, which is in line of the results obtained by other researchers that adsorption increases with increase in initial concentration of dye (Yamada et al., 2003).

The percentage reduction in colour of mixture of dyes having initial concentrations 44.6, 89.3, 119, 127.5, and 178.6 mg/l was 99, 98.5, 96.2, 95.3 and 93.5%, respectively, at 45 minutes as shown in Figure 6.6. The results show that the adsorption efficiency of fly ash is dependent on initial concentration of dye solution. At low concentration, the number of adsorbate molecules was less, while at high concentration; the number of adsorbate molecules was more as compared to the active sites on the adsorbent. Thus, with the increase in the concentration of the dye, the competition for active sites of adsorbent increases, and as a result, complete removal of dye takes longer time at higher concentrations than at lower concentrations of the dye (Yadav et al 2014). Thus, at high concentrations, the amount of dye adsorbed is less, and as a result, percentage removal is also low.

6.2.4 Effect of particle size

The fly ash of particle size 180-300, 90-150and 53-75 µm size was added to black dye of 50 mg/l concentration as shown in Figure 6.7. The effect of decolourization efficiency of fly ash dosage of 40 g/l and 45–75, 75-150, 150-180 and 180-300 µ particle size with mixture of dye solution of178.6 mg/l initial concentration at pH 10 at 298 K is shown in Figure 6.8.

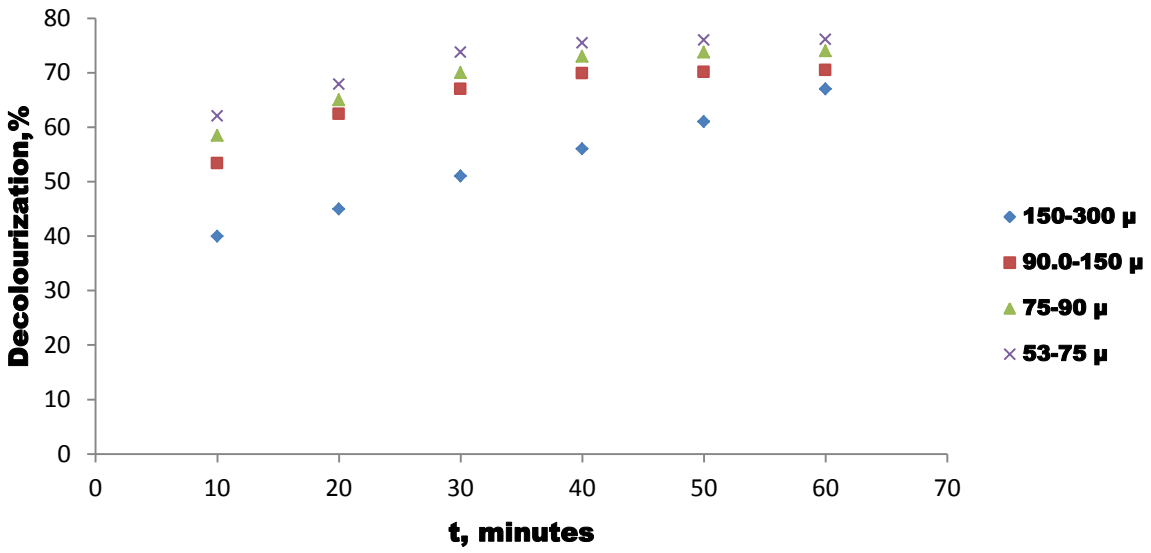

Figure 6.7 Effect of particle size on adsorption of black dye
[Black dye- 50 mg/l, pH-10, Temperature-298 K,
Stirring speed 125 rpm, and Fly ash dosage-2.0 g/l]

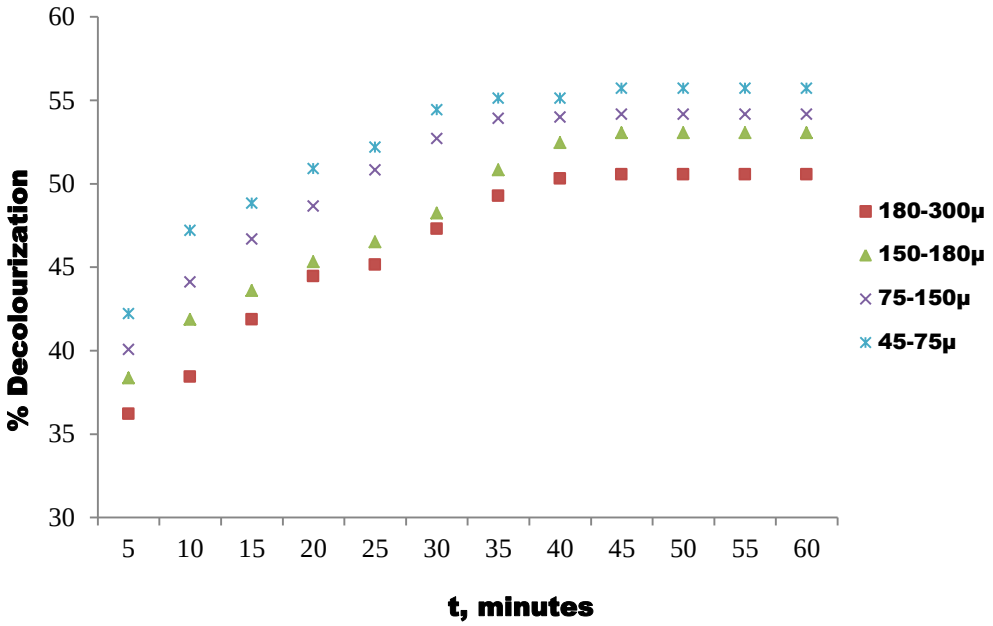

Figure 6.8 Effect of particle size of adsorbent
[Initial concentration of dye-178.6 mg/l,
Fly ash dosage-40g/l, pH- 7.5, Temperature-298 K]

It is observed from Figure 6.7 & 6.8 that maximum adsorption rate of black dye was achieved with fly ash of smallest size 53-75 µ with percentage reduction of 76% while maximum percentage reduction in colour of mixture of dyes obtained by fly ash of particle size 45–75 µ was 55.7% at 45 minutes. The decolourization of dye solution increased with the decrease in the particle size of fly ash because smaller particles have relatively larger surface area and therefore offer more adsorption sites. Similar results have been reported by Kara et al., Gupta et al., 1988. The presence of more than one dye showed less reduction in comparison to single dye i.e. black dye. It may be due to competitive adsorption onto adsorption sites. The attraction of dye to the interfaces of adsorbent is different for each dye and therefore, the presence of mixture of dyes enhances competitive adsorption (Regti et al. 2016).

6.2.5 Effect of temperature

The effect of various temperature of dye solution, i.e. 20, 25, 30, 35 and 40°C on decolourization efficiency of black dye solution of initial concentration of 178.6 mg/L maintained at pH 4is shown in Figure 6.9.

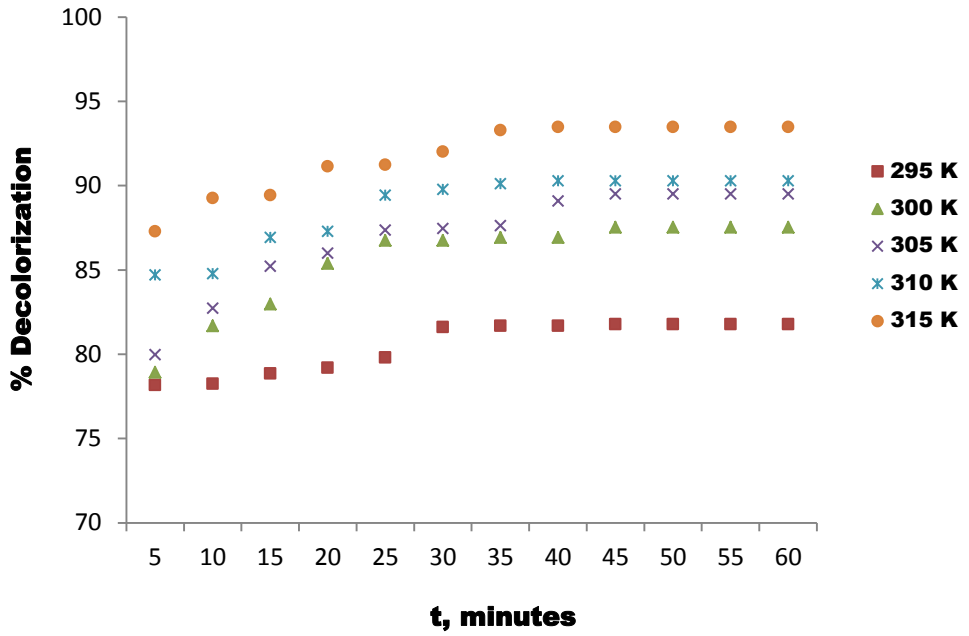

Figure 6.9 Effect of temperature on mixture of dyes
[Initial concentration of dye: 178.6 mg/l,
Fly ash dosage: 40g/l, Particle size: 45-75 µm, pH-10]

It has been found that the decolourization efficiency of fly ash increased with the increase in temperature of dye solution. The percentage reduction in colour, obtained by treating effluent at temperature 20, 25, 30, 35, and 40°C was 81.8, 87.5, 89.5, 90.3, and 93.5%, respectively, at 45 minutes. The increase in adsorption efficiency of fly ash with increase in temperature may be attributed to increase in mobility of the dye molecules with increase in temperature thereby facilitating better interaction between the dye molecules and the active sites of the adsorbent (Sonar et al. 2014). At high temperature, the internal structure of fly ash gets swollen, which increase the pore size and consequently adsorption (Acemioglu et al. 2004).

6.3 Adsorption equilibrium

Equilibrium data are important for designing an adsorption system. The equilibrium data were analysed using Langmuir, Freundlich, Temkin, Dubinin–Radushkevich isotherms. (Shah et al., 2013; Mittal and Lishakurup, 2007; Chavan and Paul, 2013) as explained below.

6.3.1 Isotherms of adsorption of Black dye

Langmuir Isotherm

The values of q_{max} and K_L were computed from the slope and intercept of the graph between C_e/q_e with respect to C_e as seen in Figure 6.10.

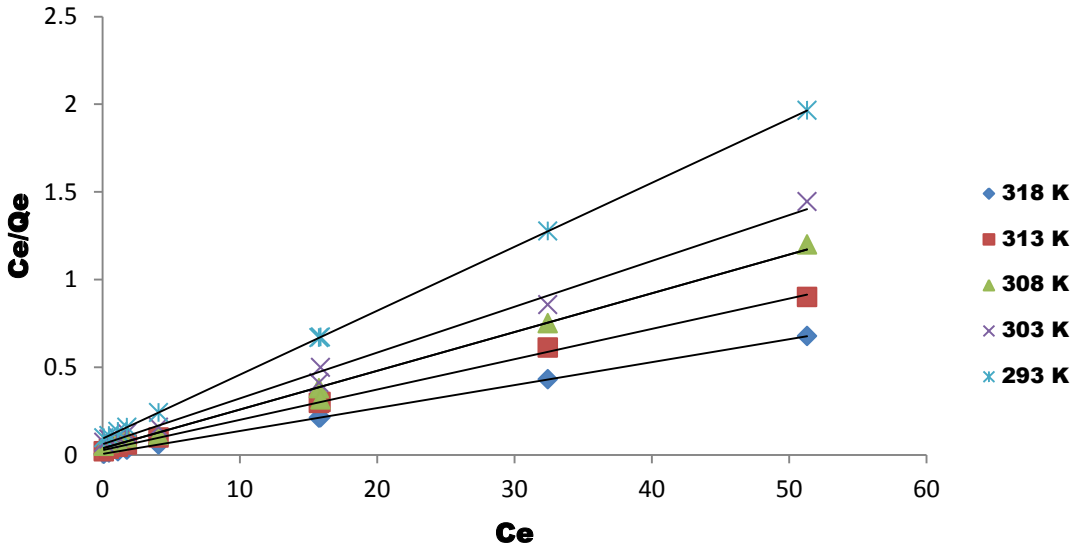

Figure 6.10 Langmuir isotherm of Direct Black dye with fly ash

Freundlich Isotherms

The graph between ln q_e with respect to ln C_e gives the value of $1/n$ and K_f as tabulated in Table 6.3. The value of K_f is 59.65 with R^2 value less than 0.98 showing marginally lesser fitting of the Freundlich isotherm to the adsorption data.

Temkin isotherm

A plot of q_e versus ln C_e enables the determination of isotherm constants A_t and B and tabulated in Table 6.3.

Table 6.3 Isotherm Prediction

	Langmuir Isotherm				Freundlich Isotherm			Temkin Isotherm		
Temp, K	**Q_{max} (mg g^{-1})**	**K_L L mg^{-1}**	**R^2**	**R_L**	**1/n**	**K_f (mgmg^{-1})(Lmg^{-1})$^{1/n}$**	**R^2**	**A_T (Lmg^{-1})**	**B**	**R^2**
293	27.39	0.396	1	0.077	0.291	9.615	0.923	7.82	4.81	0.968
303	38.16	0.439	0.994	0.071	0.312	13.03	0.863	4.62	7.64	0.964
308	45.24	0.592	0.994	0.0533	0.479	10.61	0.880	3.95	10.82	0.940
313	57.80	0.645	0.999	0.049	0.210	27.28	0.916	23.6	8.40	0.948
318	76.33	2.42	1	0.014	0.070	59.65	0.886	28.6	4.74	0.902

The R_L values between zero and one confirms the favorable uptake of black dye on fly ash. The maximum monolayer coverage capacity of fly ash q_{max} from Langmuir isotherm was determined to be 76.33 mg/g. Langmuir isotherm constant of 2.42 L/mg with R^2 value greater than 0.98 from Table 6.3 proves that the Langmuir isotherm fitted well to the adsorption data.

6.3.2 Isotherm of mixture of dyes

Langmuir Isotherms

The values of q_{max} and K_L were computed from the slope and intercept of the graph between C_e/q_e with respect to C_e as seen in Figure 6.11.

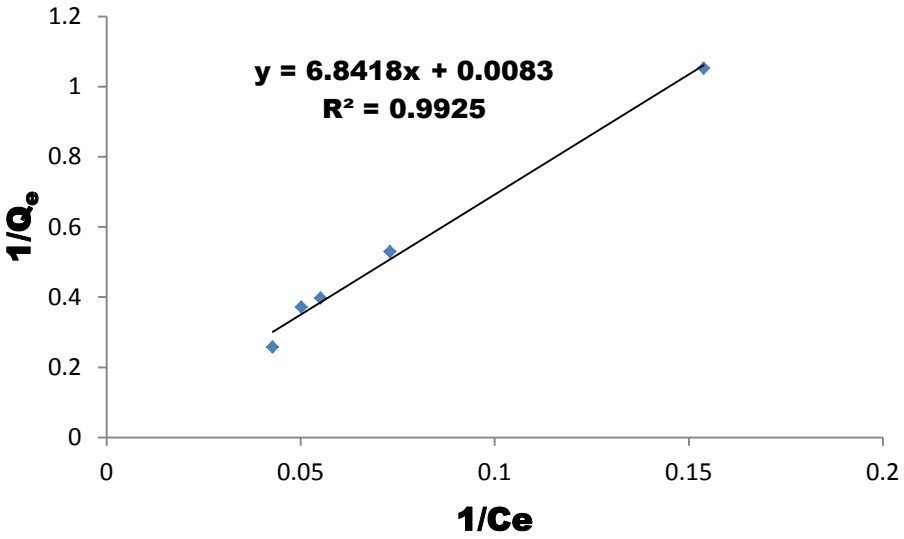

Figure 6.11 Langmuir adsorption isotherms for adsorption of mixture of dyes [Temperature-313 K; pH-4; Fly ash dosage- 40 g/l; Time- 45 min]

Freundlich Isotherms

The graph between ln q_e with respect to ln C_e as shown in Figure 6.12 gives the value of 1/*n* and K_f as tabulated in Table 6.4.

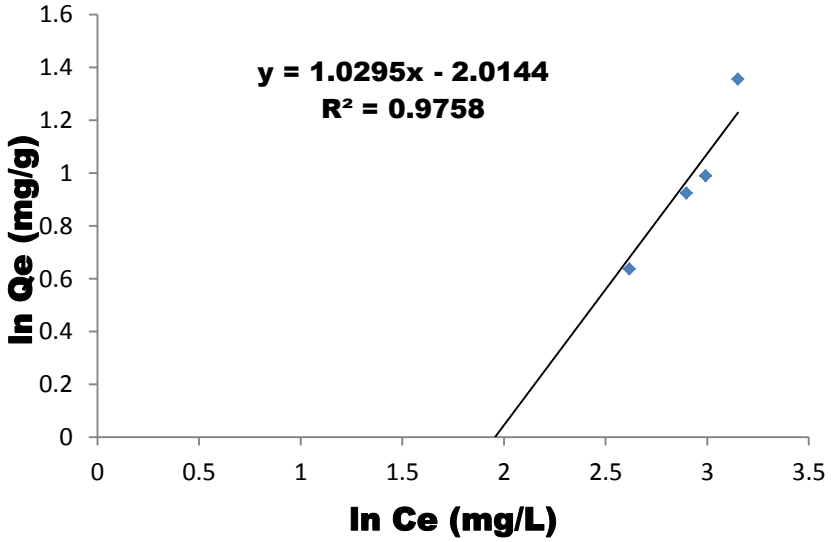

Figure 6.12 Freundlich adsorption isotherms for adsorption of mixture of dyes [Temperature-313 K; pH-4; Fly ash dosage- 40 g/l; Time-45 min]

The value of K_f is 59.65 with R^2 value less than 0.98 show marginally inferior fitting of the Freundlich isotherm to the adsorption data.

Temkin isotherm

A plot of q_e versus ln C_e enables the determination of isotherm constants K_t and B_1 and tabulated in Table 6.4.

Table 6.4 Isotherm constants for adsorption of mixture of dyes on to fly ash at pH-4 and 40°C

Langmuir isotherm	Freundlich isotherm	Temkin isotherm	Dubinin-Radushkevich isotherm
Q_{max}= 120.482 mg/g	K_F ((mg/g)/(mg/L)$^{1/n}$ =0.1334	A_T (L/ mg)=20	E (kJ/mol)=0.707
K_L(L/mg)= 1.213	1/n = 0.971	B_T=0.068	q_s (mg/g)=3.508
R^2= 0.993	R^2=0.976	R^2=0.970	R^2=0.927

It was observed that the equilibrium data fitted better with a Langmuir model for adsorption of mixture of direct dyes on fly ash with higher correlation coefficient value of 0.993. This exemplifies monolayer coverage of dye mixture of fly ash particles. The value of R_L is 0.8219. Since the value of R_L lies between 0and 1, adsorption using coal fly ash is favoured. The values of K_F and n were calculated from the intercept and slope of the plot of ln q_e vs ln C_e and the values of Q_{max} and K_L were calculated from the intercept and slope of the plot of $1/q_e$ vs. $1/C_e$. From Table 6.4, it can be seen that the maximum sorption capacity Q_{max} (mg/g) of fly ash for the mixture of dyes was 120.482 mg/g. The E value of 0.7 kJ/mol from Dubinin-Radushkevich model indicates adsorption of a mixture of dyes on fly ash as physisorption process (Olalekan et al, 2012).

6.4 Kinetic models

The three models pseudo first order, pseudo second order rate equation and intra-particle diffusion model were studied.

6.4.1 Kinetics of adsorption of black dye

Pseudo first order kinetic model

The value of k_1 is evaluated by slope of graph between ln (q_e-q_t) and time, t at different concentration as shown in Figure 6.13. The values of k_1 and q_e are calculated from the slope and intercept of the graph and tabulated in Table 6.5.

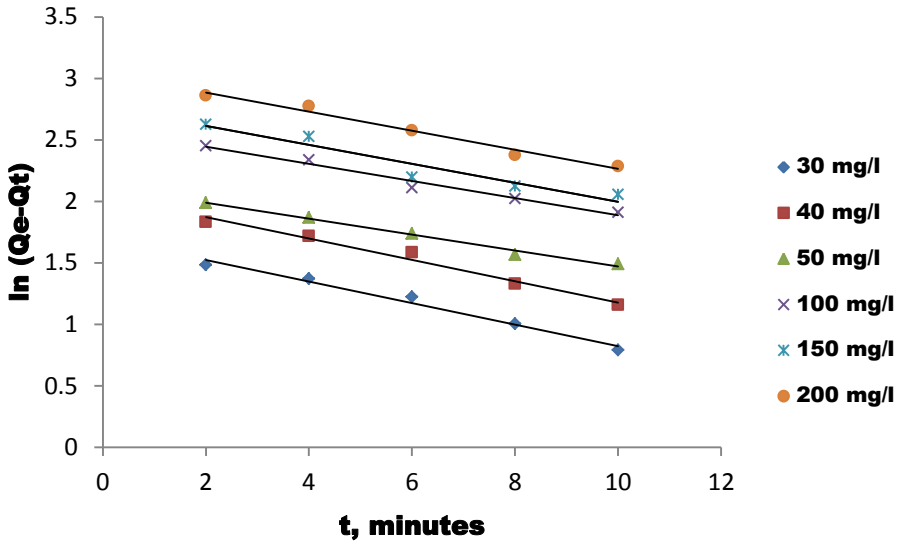

Figure 6.13 Pseudo first order kinetics for Direct Black dye on fly ash

Pseudo-Second order kinetic model

The second order kinetic model is given as

$$\frac{t}{q} = \frac{1}{k_2 qe^2} + \frac{t}{qe} \quad \text{.....(Eq. 6.1)}$$

The initial adsorption rate is given as

$$h = k_2 qe^2 \quad \text{.....(Eq. 6.2)}$$

The values of h (mgg^{-1} min^{-1}) has been calculated and given in Table 6.5 from the slope and intercept of the plot t/q vs. t.

Intraparticle diffusion

The intraparticle diffusion model proposed by Weber and Morris is given as equation 6.3.

$$q_t = k_{id} t^{0.5} + C \quad \text{.....(Eq. 6.3)}$$

A plot of q_t versus $t^{1/2}$ gives slope k_{id} and intercept C at different concentration and gives the value of intercept C and k_{id} and tabulated in Table 6.5.

Table 6.5 Kinetics of adsorption of black dye on fly ash

	Ist order kinetics				**IInd order kinetics**				**Intraparticle diffusion**	
C_0, mg/l	**q_e, mg/g (exp.)**	**q_e, mg/g (calc.)**	**$k_{1,\ 1/min}$**	**R^2**	**q_e, mg/g (calc)**	**$k_{2,g/mg\ min}$**	**h mg/g min**	**R^2**	**$K_{id,\ mg/g\ min^{0.5}}$**	**R^2**
30	5.92	5.47	0.201	0.981	8.305	0.0101	0.696	0.971	1.17	0.978
40	7.81	7.74	0.200	0.978	12.07	0.0051	0.742	0.967	1.403	0.948
50	8.88	8.33	0.149	0.989	17.09	0.0024	0.700	0.949	1.311	0.978
100	13.7	13.27	0.160	0.976	19.26	0.0030	1.112	0.966	1.934	0.948
150	15.9	15.94	0.177	0.919	23.52	0.0022	1.217	0.914	2.40	0.913
200	19.0	20.90	0.178	0.979	26.80	0.0017	1.221	0.986	2.414	0.952

It has been found that the intra-particle rate constant values (K_{id}) increased with increase in initial concentration of black dye solution. This may be due to the fact that at increased concentration of dye solution, a higher concentration gradient promoted more pore diffusion in fly ash resulting in larger number of dye particles diffusing in to the pores of fly ash. The presence of intraparticle diffusion as the rate determining step has been indicated by the high correlation coefficient value (Abechiet al., 2011). The kinetic models were compared and his comparison is shown in Table-6.5.

6.4.2 Kinetics of adsorption of mixture of dyes with fly ash

Pse udo first order kinetic model

The values of $k_1$and q are evaluated from the slope and intercept of graph between log (q_e-q_t) and time at different concentrations and tabulated in Table 6.6.

Pseudo-Second order kinetic model

The values of h (mgg^{-1} min^{-1}) have been calculated and given in Table 6.6 from the slope and intercept of the plot t/q vs. t as shown in Figure 6.14.

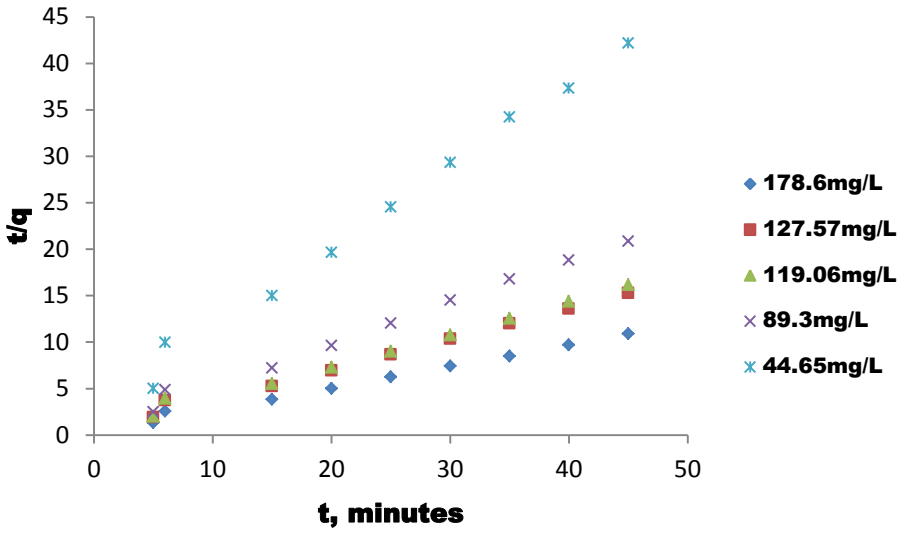

Figure 6.14 Pseudo second order plot for adsorption of mixture of dyes [Temperature 40°C; pH 2.0; dose 40 g/L; time 45 min]

Intraparticle diffusion

A plot of q_t versus $t^{1/2}$ gives slope k_{id} and intercept C at different concentration and gives the value of intercept C and k_{id} and tabulated in Table 6.6.

Table 6.6 Adsorption rate constants for adsorption for mixture of dyes

	Pseudo- first order kinetics			Pseudo second order kinetics			Intraparticle diffusion	
C_O(mg/L)	q_e, mg/g	k_1(1/min)	R^2	k_2 (g/mg min)	h (mg/g min)	R^2	$k_{id, (mg/g\ min^{0.5})}$	R^2
44.65	0.078	0.228	0.954	0.395	0.40	0.999	0.013	0.613
89.3	0.160	0.045	0.621	0.116	3.13	0.999	0.022	0.771
119.06	0.344	0.310	0.976	0.054	5.67	0.999	0.079	0.836
127.57	0.436	0.197	0.914	0.410	2.44	0.999	0.078	0.886
178.6	0.763	0.221	0.763	0.312	4.84	0.999	0.078	0.972

The high correlation coefficient indicates the presence of intra-particle diffusion as the rate determining step.

6.4.3 Comparison of experimental and predicted value

The comparison of experimental and predicted value of qe for adsorption of black dye and mixture of dyes is shown as Figure 6.15 & 6.16 respectively.

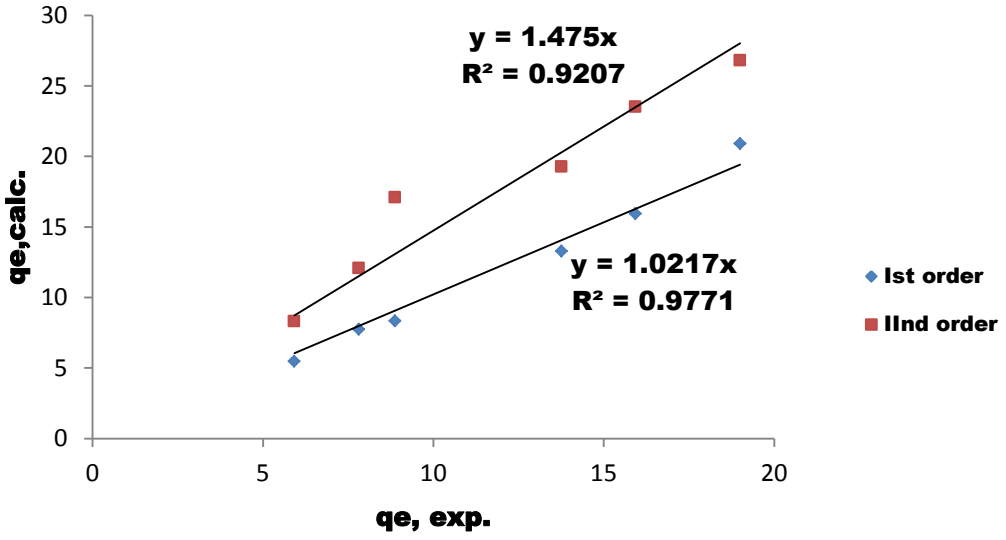

Figure 6.15 Comparison of experimental and predicted value of qe for Direct Black dye

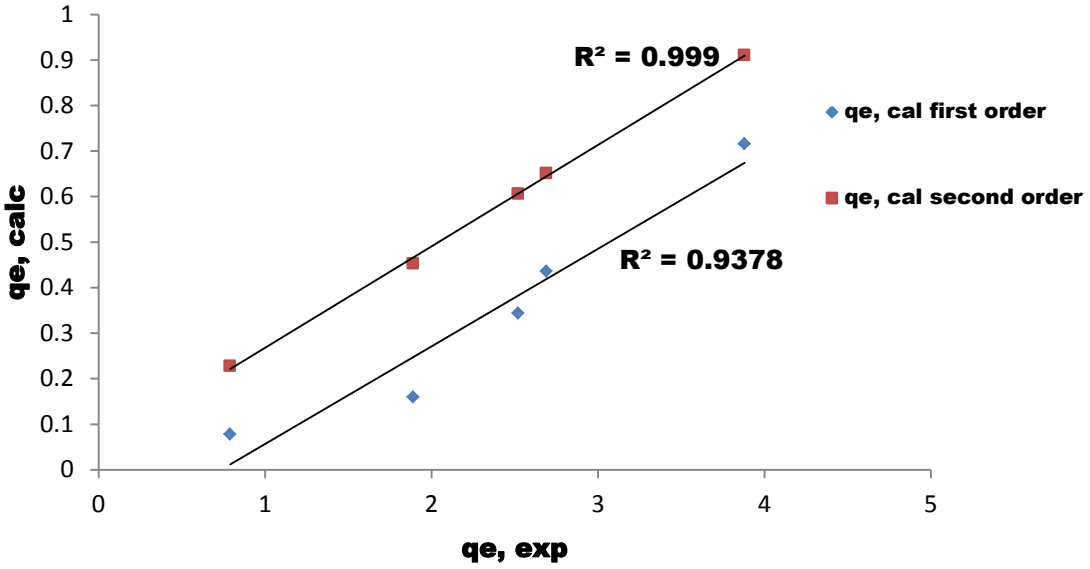

Figure 6.16 Comparison of experimental and predicted value of qe for Mixture of dyes

The R^2 values from Figure 6.15 & 6.16 showed better fitting of I^{st} order kinetics for adsorption of black dye and mixture of dyes on fly ash.

6.5 Thermodynamics

The thermodynamic properties such as enthalpy, free energy and entropy change can be estimated from the following equations:

$$\Delta G_0 = -RT \ln K_c \quad \text{.....(Eq. 6.4)}$$

According to Van't Hoff equation

$$\log_{10} K_c = \frac{\Delta S_0}{2.303R} - \frac{\Delta H_0}{2.303RT} \quad \text{.....(Eq. 6.5)}$$

$$Kc = \frac{Qe}{Ce} \quad \text{.....(Eq. 6.6)}$$

The graph has been plotted between log Q_e/C_e vs. 1/T as Figure 6.17 and the values ΔH° and ΔS° can be estimated from the slopes and intercepts of the graph.

6.5.1 Thermodynamics of black dye

The graph plotted between log Q_e/C_e versus 1/T as shown in Figure 6.17 gives the value of **ΔG**, **ΔH** and **ΔS** as tabulated in Table 6.7.

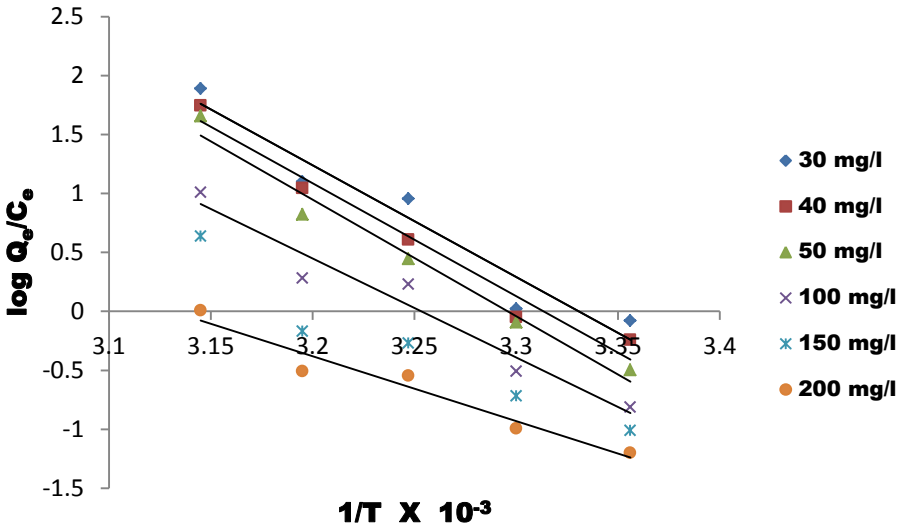

Figure 6.17 Effect of temperature on adsorption of Direct Black dye

Table 6.7 Thermodynamic parameters of adsorption of direct black dye

Co, mg/L	Temperature, K	ΔG, MJ/mol	ΔH, kJ/mol	ΔS, kJ/mol/K
30	298	-180.13	181.68	605.08
	303	-183.15		
	308	-186.18		
	313	-189.20		
	318	-192.33		
40	298	-180.99	183.48	607.99
	303	-184.03		
	308	-187.07		
	313	-190.11		
	318	-193.15		
50	298	-185.76	189.33	624.02
	303	-188.88		
	308	-192		

	313	-195.12		
	318	-198.24		
100	298	-47.41	160.86	523.36
	303	-155.8		
	308	-161.1		
	313	-163.65		
	318	-166.26		
150	298	-132.97	60.45	446.43
	303	-135.20		
	308	-137.43		
	313	-139.67		
	318	-141.9		
200	298	-98.42	105.3	329.69
	303	-99.79		
	308	-101.43		
	313	-93.16		
	318	-104.73		

The negative values of ΔG° and positive values of ΔH° shown in Table 6.7 indicate that the black dye adsorption process by fly ash is a spontaneous and endothermic. The positive value of ΔS° suggests increased randomness at the solid/solution interface occur in the internal structure of the adsorption of black dye onto fly ash (Rahchamani et al. 2011; Han et al. 2013; Hameed et al. 2007).

6.5.2 Thermodynamics of mixture of dyes

The graph plotted between log Kc versus 1/T as shown in Figure 6.18 gives the value of ΔG, ΔH and ΔS as tabulated in Table 6.8.

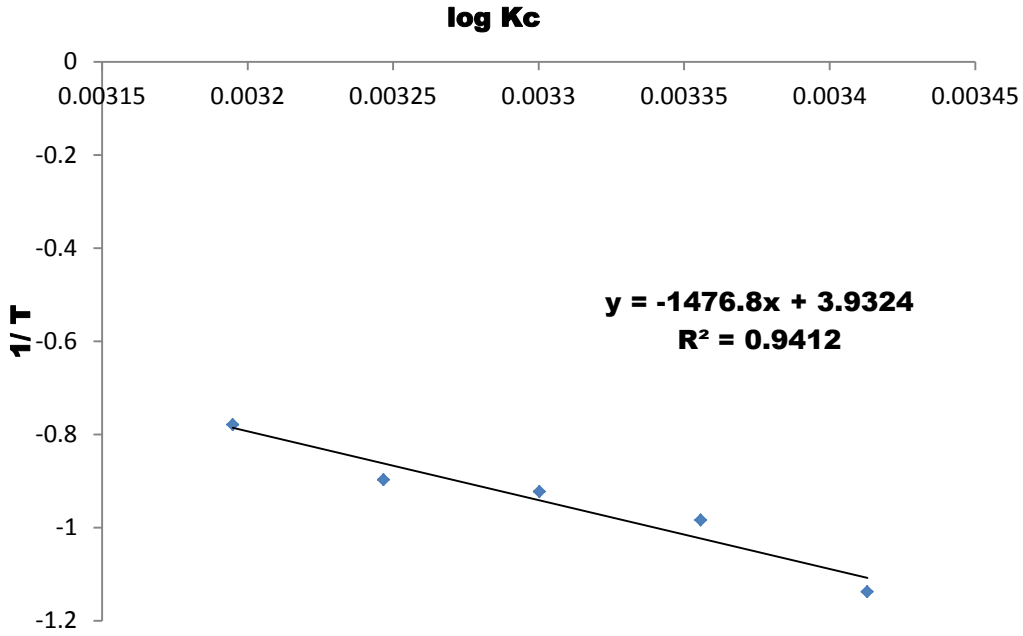

Figure 6.18 Van't Hoff plot of log K versus 1/T for adsorption of mixture of dyes

Table 6.8 Thermodynamic parameters for the adsorption of mixture of dyes

Temperature(K)	K(L/g)	ΔG^o (kJ/mol)	ΔH^o (kJ/mol)	ΔS^o (J/mol K)
293	0.0728	-6.3825	28.2765	75.2942
298	0.1038	-5.5128		
303	0.1195	-5.3520		
308	0.1267	-5.2895		
313	0.1661	-4.6710		

A straight line plot was obtained with a regression coefficient of 0.941 as shown in Figure 6.18 and the thermodynamic parameters for adsorption of a mixture of dyes on fly ash are given in Table 6.8. The positive value of ΔH° indicates that the process is endothermic in nature and the positive value of ΔS° indicates the increased randomness at the solid/solution interface during the adsorption of the dye onto fly ash. While, the negative values of ΔG° indicate the feasibility of the process and the spontaneous nature of the adsorption (Pengthamkeerati et al. 2010; Agarwal et al. 2016).

6.6 Column Studies

The column studies were conducted with fly ash for adsorption of effluent having black dye. The decolonization efficiency of fly ash was studied at various affecting parameters viz. pH, particle size of fly ash, initial concentration of black dye, bed depth of fly ash.

6.6.1 Effect of particle Size on dye removal efficiency

The effect of different particle size of fly ash on dye removal efficiency in column was studied with black dye of 50 mg/l concentration. Fly ash of different size ranges (300-150 µm), (150-90 µm) and (90-75 µm) was taken for the dye removal studies. The black dye of 50 mg/l initial concentration was fed from the top of the column of 12 g of fly ash of different sizes. The breakthrough curve of different particle size is shown as Figure 6.19.

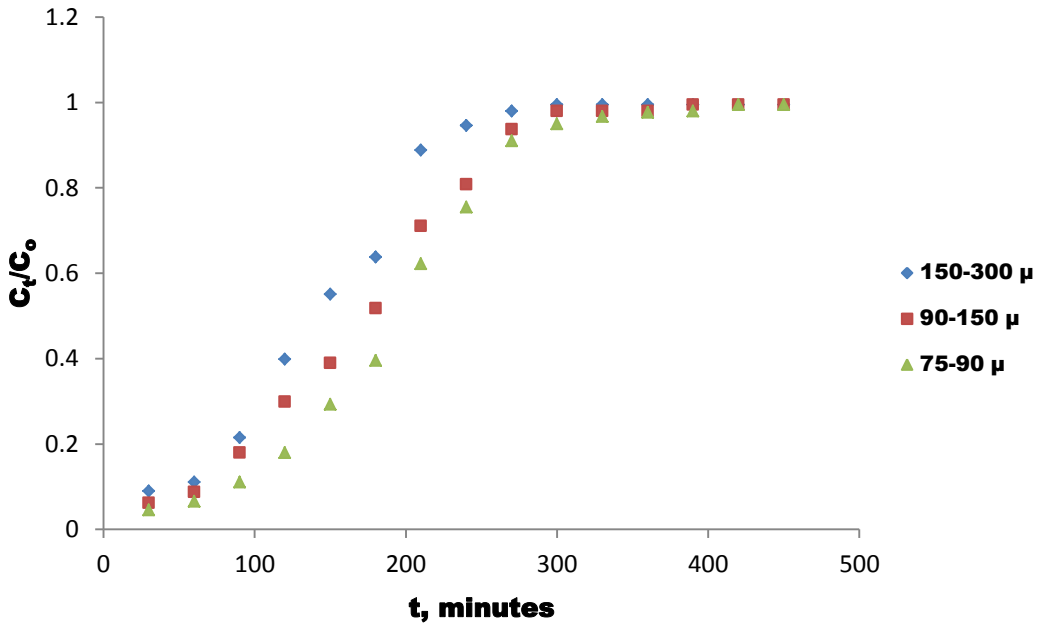

Figure 6.19 Breakthrough curves at different particle size

It has been observed that the rate of removal of black dye is high at 75-90 microns size due to increased surface area for adsorption at lesser particle size.

6.6.2 Effect of pH

50 mg/l of black dye maintained at different pH was fed from the top of the column to 12 g of fly ash of particle size (150-300 microns). The effect of pH on dye removal is shown as Figure 6.20.

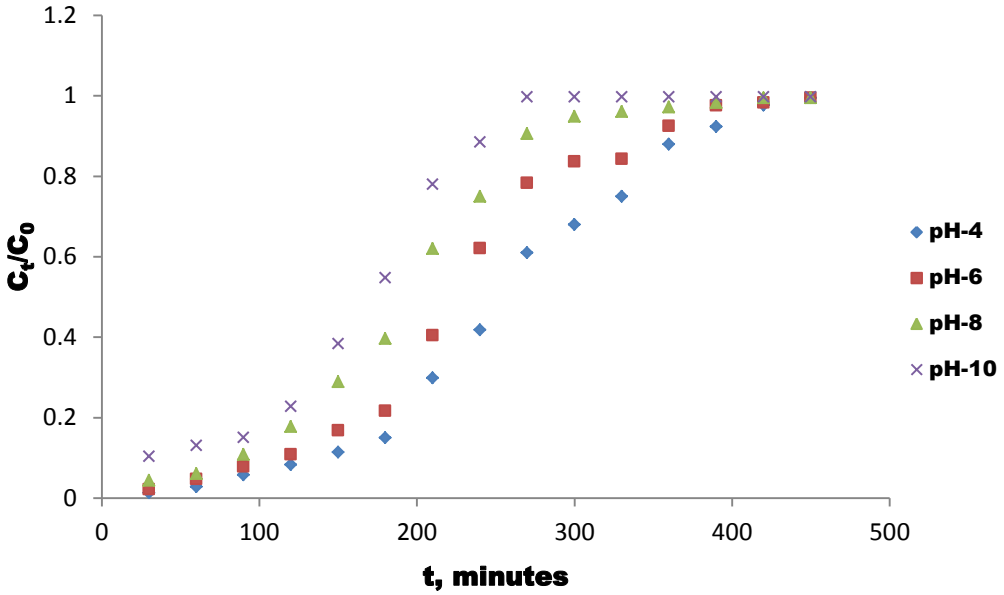

Figure 6.20 Breakthrough curves at different pH

It has been observed that the rate of removal of black dye is high at pH-4 in comparison to pH-6, 8 & 10.

6.6.3 Effect of Bed Depth

The percentage removal of dye is dependent on bed depth at fixed flow rate and initial concentration of dye. The bed depth was varied for black dye of 50 mg/l initial concentration at pH-4. The breakthrough curves of adsorption of black dye with different bed depth of fly ash are shown in Figure 6.21.

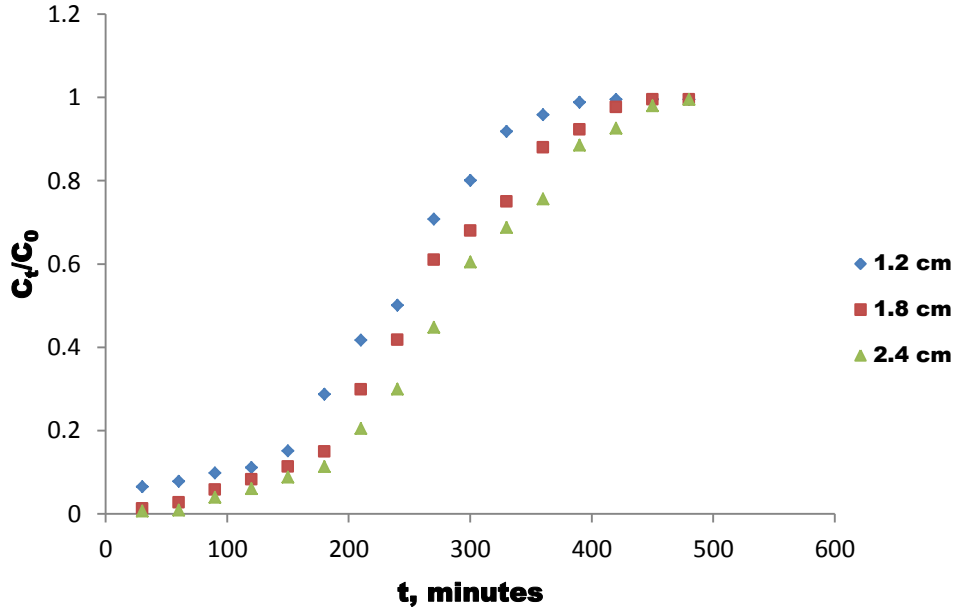

Figure 6.21 Breakthrough curves at different Bed depth

The curves followed S shaped profile. The exhaustion time corresponding to an effluent concentration of 90% of C_0 was found to increase with increase in bed depth. The exhaust time and break through time increased with increasing bed depth as more binding sites are available for sorption. (Negrea et al., 2015)

6.6.4 Effect of initial concentration

The black dye of various initial concentrations (50, 100, 150 mg/l) was fed to 8 g of fly ash of 150-300 µm particle size. The results are shown in Figure 6.22.

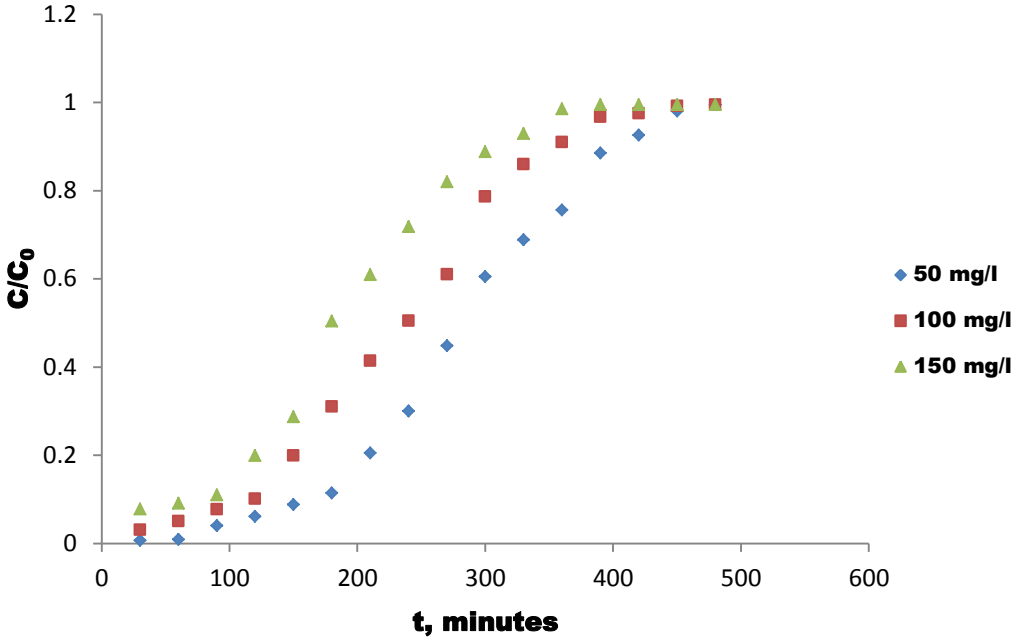

Figure 6.22 Breakthrough curve at different initial concentration

It has been observed that removal of black dye decreases as we increase the initial concentration of dye at the same bed depth. It may be due to increase in adsorbate to adsorbent ratio for the same amount of fly ash. The higher inlet concentration showed steeper slope of breakthrough curve due to increase of driving force and decrease in adsorption zone length. The similar results were obtained for removal of lead II from synthetic and real effluents using immobilized Pinus sylvestris sawdust (Taty et al., 2005), removal of nickel from aqueous solution using crab shell particles (Vijayaraghavan et al., 2006)

6.7 Breakthrough curve modeling

Bohart and Adams model, Yoon Nelson model and Thomas model were used to fit the experimental data in the column and to describe the fixed bed column behavior and to scale it up for industrial applications (Han et al. 2008).

6.7.1 Bohart and Adams model

The Bohart and Adams model describes a fundamental relationship between the normalized concentration (C_t/C_0) and the bed depth (Z) described by the equation 6.7:

$$\ln \frac{C}{C_0} = k_{AB} C_0 t - k_{AB} N_0 \frac{Z}{L} \quad \text{.....(Eq. 6.7)}$$

A linear plot of ln (C_t/C_o) against time (t) was drawn for different initial concentration of black dye and values of k_{AB} and N_o were determined from the slope and interception point of the plot and tabulated in Table 6.9. As for the R^2, the values show distribution between 0.730 and 0.901 which indicate that the data does not fit into the model perfectly.

6.7.2 Yoon-Nelson model

The Yoon-Nelson model is based on the assumption that the rate of decrease in the probability of adsorption for each adsorbate molecule is proportional to the probability of adsorbate adsorption and the probability of adsorbate breakthrough on the adsorbent. The linearized form of the Yoon-Nelson model for a single component system is expressed as equation 6.8: (Hasan and Srivastava. 2011)

$$\boldsymbol{ln \frac{C_t}{C_0 - C_t} = k_{YN} t - \tau k_{YN}} \quad \textbf{.....(Eq. 6.8)}$$

The graph of ln (C_t/C_0-C_t) with respect to time has been plotted for different amount of fly ash in Figure 6.23 to determine the rate velocity constant (k_{YN}) and time required to achieve 50% breakthrough (τ). The values of k_{YN} at different initial concentration and bed depth are given in Table 6.9. . The 50% breakthrough time (τ) was increased with increasing feed concentration (C_0) and bed depth (Z) .

The results indicate that the τ value increased from 207 to 273.9 min when the bed depth was increased from 1.2 cm to 2.4 cm at 50 mg/l initial concentration while τ value decreased from 273.9 to 181.4 min when the initial concentration of dye solution was increased from 50 to 150 mg/l at 2.4 cm bed depth The linear coefficient (R^2) value more than 0.97 indicates close fitting of model to adsorption data.

6.7.3 Thomas Model

Thomas in 1944 developed a model for adsorption processes in which external and internal diffusion limitations are not present. The linearized form of the Thomas model can be expressed as in Equation 6.9 (Ahmad and Hameed. 2010):

$$\ln\left(\frac{C_0}{C_t} - 1\right) = \frac{k_{TH}\ qe\ W}{Q} - k_{TH}\ C_0\ t \quad \textbf{.....(Eq. 6.9)}$$

The value of C_o/C_t is the ratio of inlet to outlet concentration of black dye. A linear plot of ln $((C_o/C_t) - 1)$ against time (t) was drawn to determine the values of q_e and k_{TH} from the interception point and slope of the plot in Figure 6.24. The values of k_{TH} at different initial concentration and bed depth are given in Table 6.9. It has been observed that when initial concentration of dye solution was increased from 50 mg/l to 150 mg/l, the value of k_{TH} decreased from 0.408 to 0.134 mL min^{-1} $mg^{-1}$and Q_e increased from 1.369 to 2.721 mg g^{-1}. This may be due to increased driving force due to high inlet concentration of dye solution. The R^2value range from 0.95 to 0.97 and thus validates the Thomas model to predict maximum adsorption capacity of bed.

Table 6.9 Values of constants for different models in column study

			Bohart and Adams model			Yoon-Nelson model			Thomas model		
Initial conc., C_o	Bed depth, Z (cm)	Q (ml/min)	k_{AB} (mlmin^{-1} mg^{-1})	N_0 (mg/L)	R^2	k_{YN} (ml/min)	$\tau(min^{-1})$	R^2	k_{TH} (ml/min. mg)	Qe (mg/g)	R^2
50	2.4	1.60	0.118	1327	0.81	0.020	274	0.98	0.408	1.37	0.98
100	2.4	1.60	0.077	2708	0.86	0.019	225	0.99	0.183	2.30	0.95
150	2.4	1.60	0.072	4188	0.88	0.020	181	0.97	0.134	2.72	0.97
50	1.2	2.10	0.138	3567	0.89	0.021	207	0.97	0.410	2.72	0.97
50	1.8	1.86	0.186	2119	0.88	0.021	246	0.98	0.414	1.92	0.98

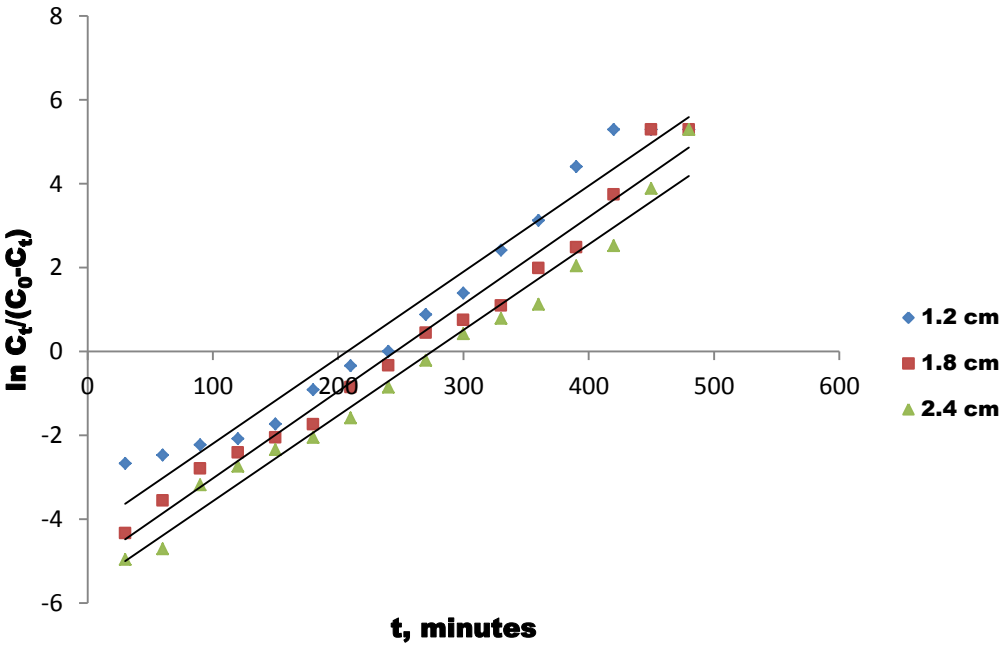

(a)

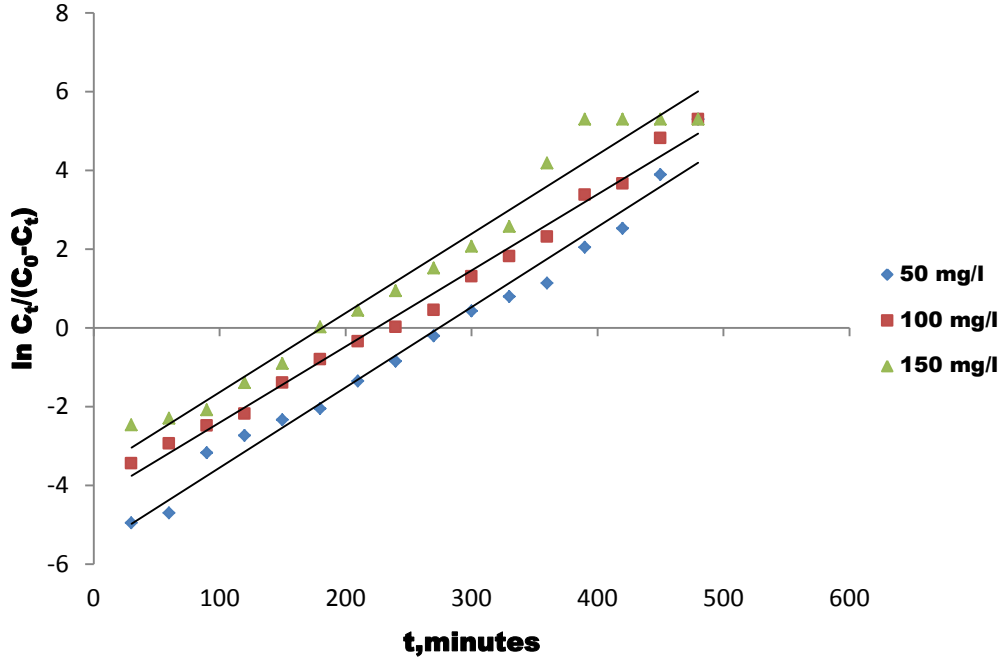

(b)

Figure 6.23 Fitting of Yoon Nelson Model for (a) Different Bed depths (b) Different Initial concentrations

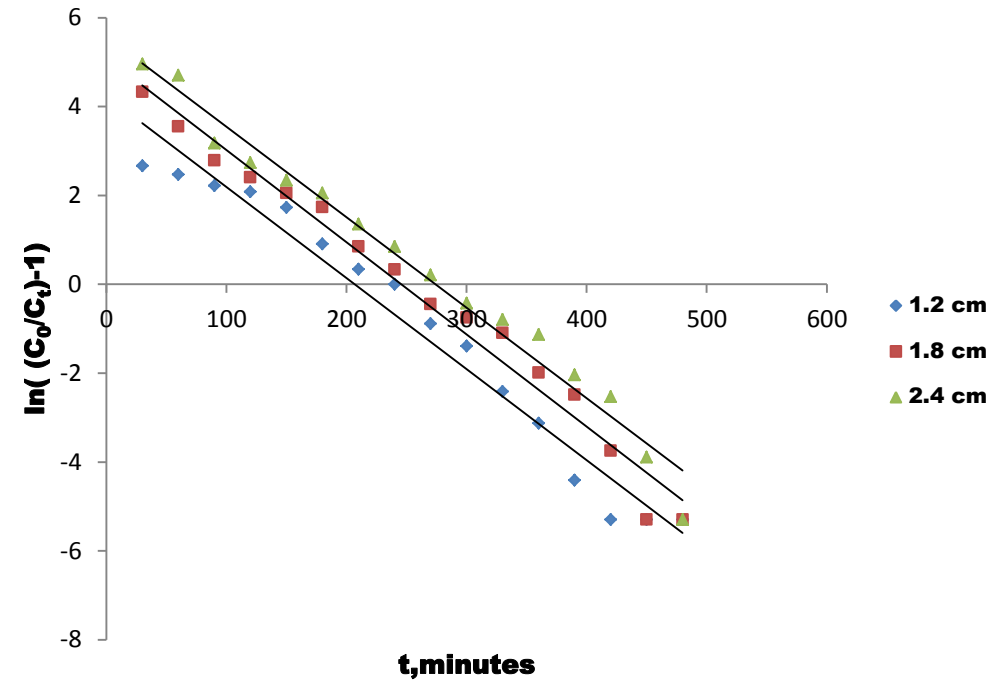

(a)

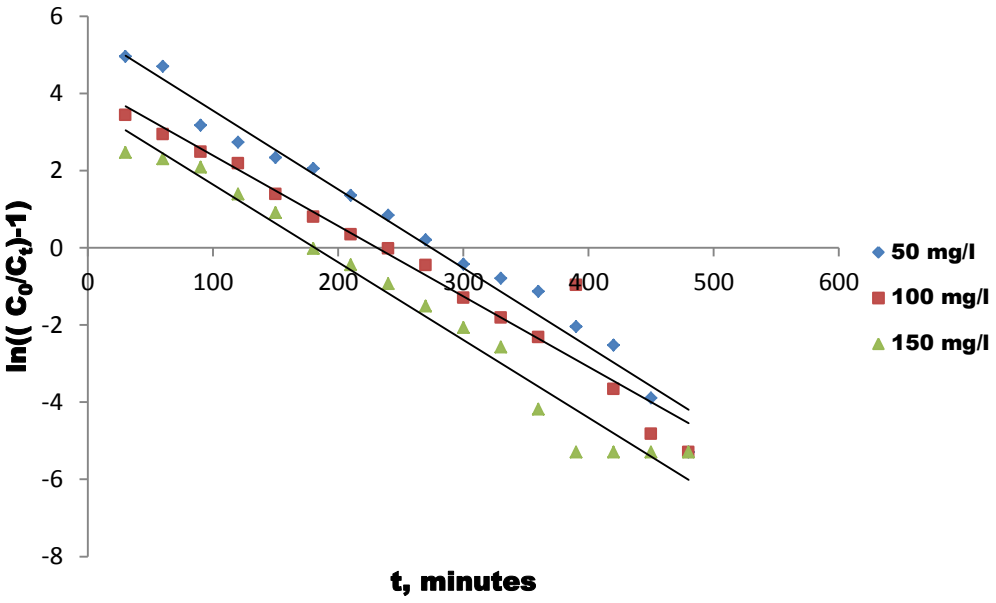

(b)

Figure 6.24 Fitting of Thomas Model for (a) Different Bed depths (b) Different initial concentration

,

The removal of atenolol, a pharmaceutical pollutant and a pesticide isoproturon from aqueous solutions by adsorption on fixed beds of granular activated carbon has been studied. The maximum adsorption capacity by activated carbon is 112.7, 187.4 and 171.5 mg/g at bed depth of 8, 10 and 12 cm. The breakthrough time as depicted by Yoon Nelson model is 99.6, 156.2 and 171.5 hours. (Sotelo et al).

6.8 Scanning Electron Microscopic Studies

The fly ash particles were analyzed by means of Scanning Electron Microscopy (SEM) equipped with Energy Dispersive X-ray (EDX) to study the shape and structure of fly ash particles along with chemical composition. The physical morphology of fly ash before and after adsorption through SEM image, SEM-EDX and distribution of different elements at 1,00,000 X magnification is given as Figure 6.25, 6.26 and 6.27 respectively.

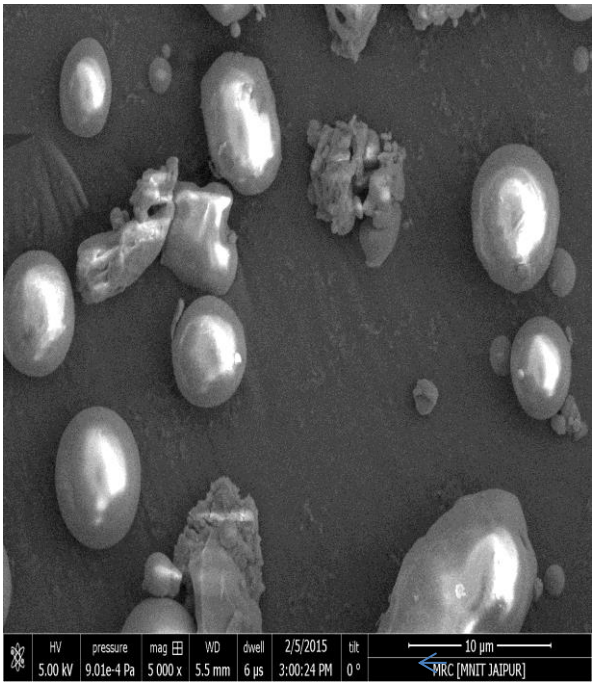

(a) Raw fly ash

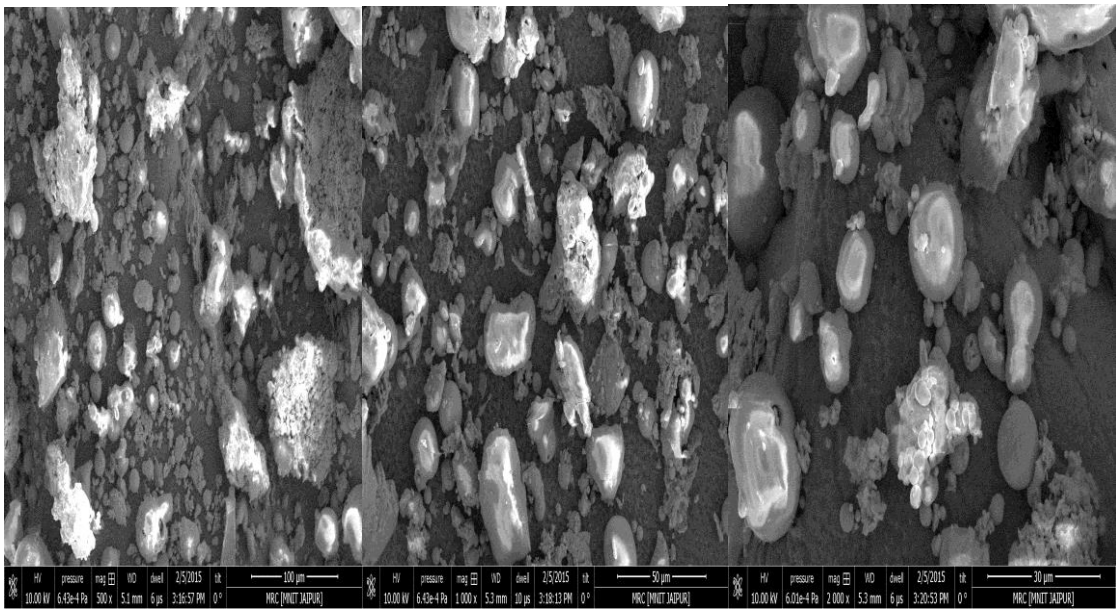

(b)

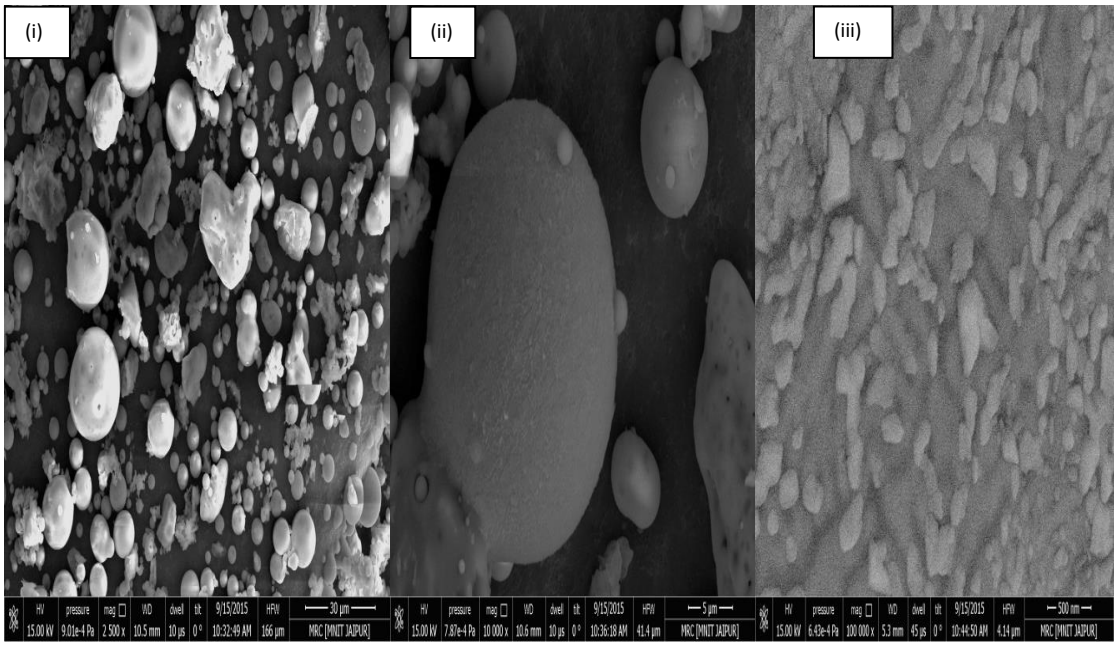

(c)

Figure 6.25 SEM images of (a) Raw fly ash (b) Fly ash after adsorption of Direct Black dye (c) Fly ash after adsorption of mixture of dyes

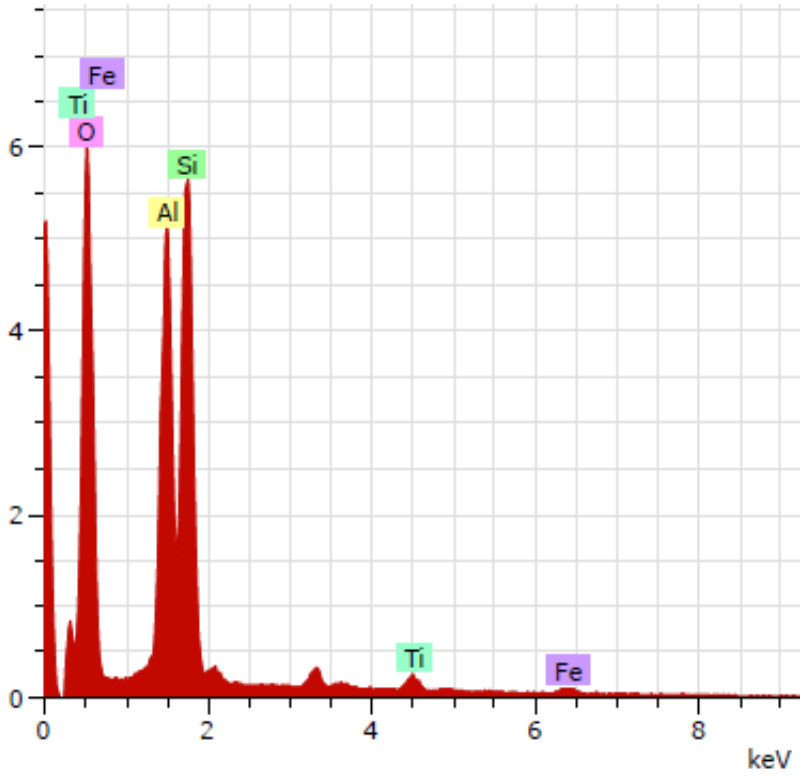
Fe
Ti
O
Si
Al
Ti
Fe
6
4
2
0
0
2
4
6
8
keV

(a)

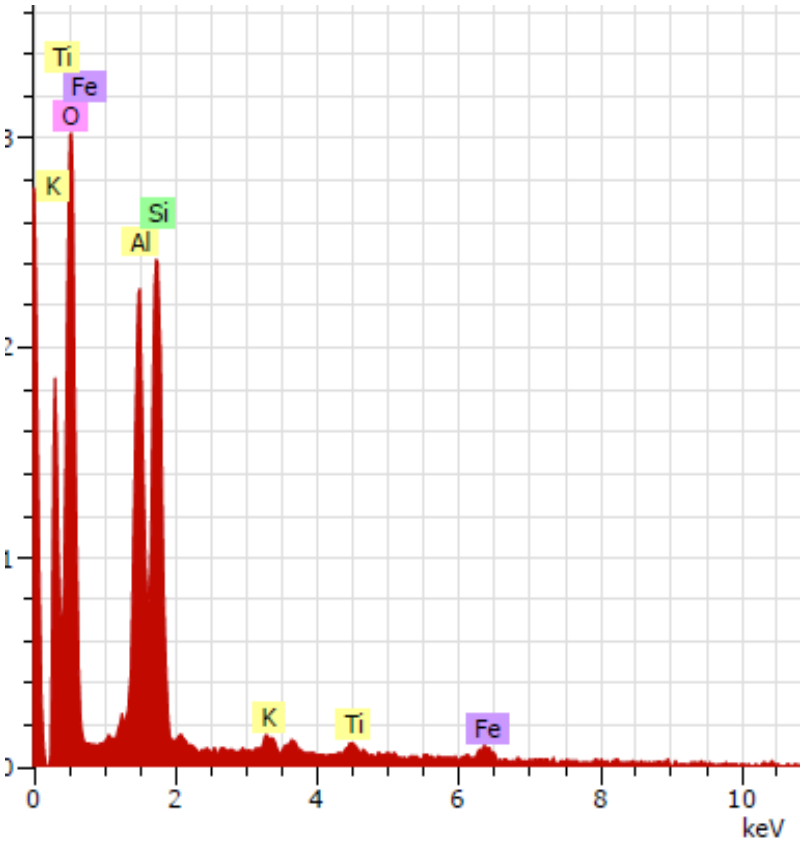
Ti
Fe
O
K
Si
Al
K
Ti
Fe
0
2
4
6
8
10
keV

(b)

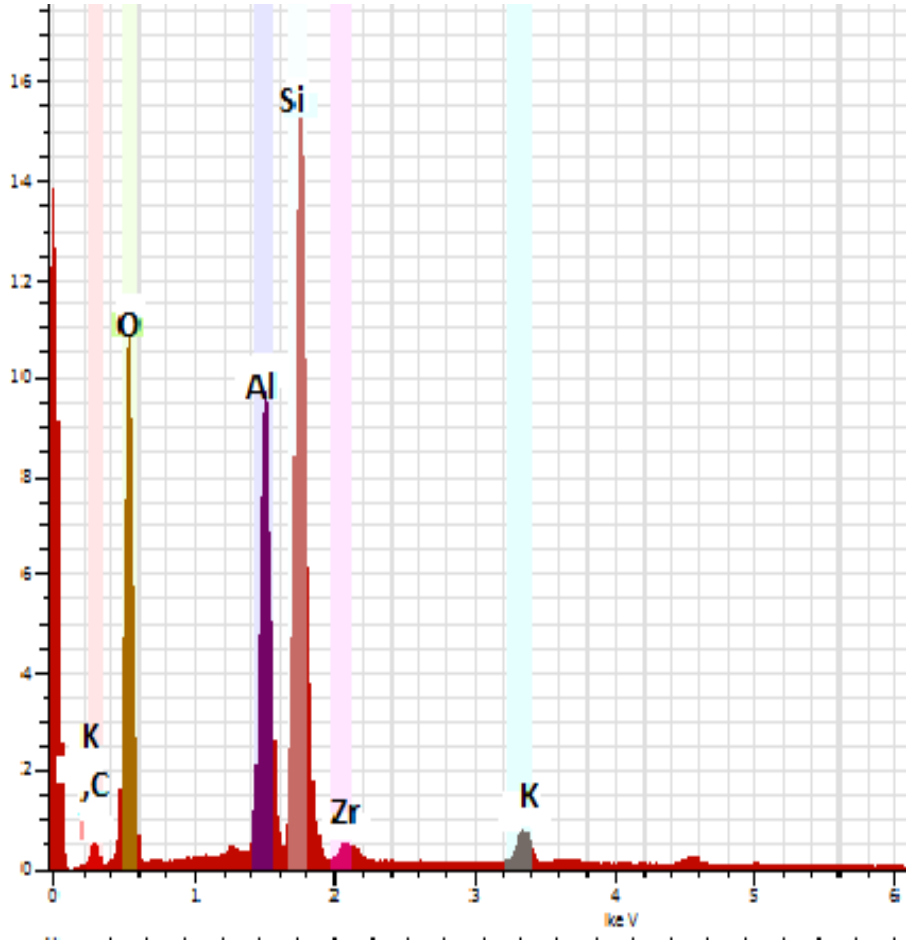

(c)

Figure 6.26 SEM-EDX of (a) Original fly ash (b) EDX of adsorbed fly ash with Direct Black dye (c) EDX of adsorbed fly ash with mixture of dyes

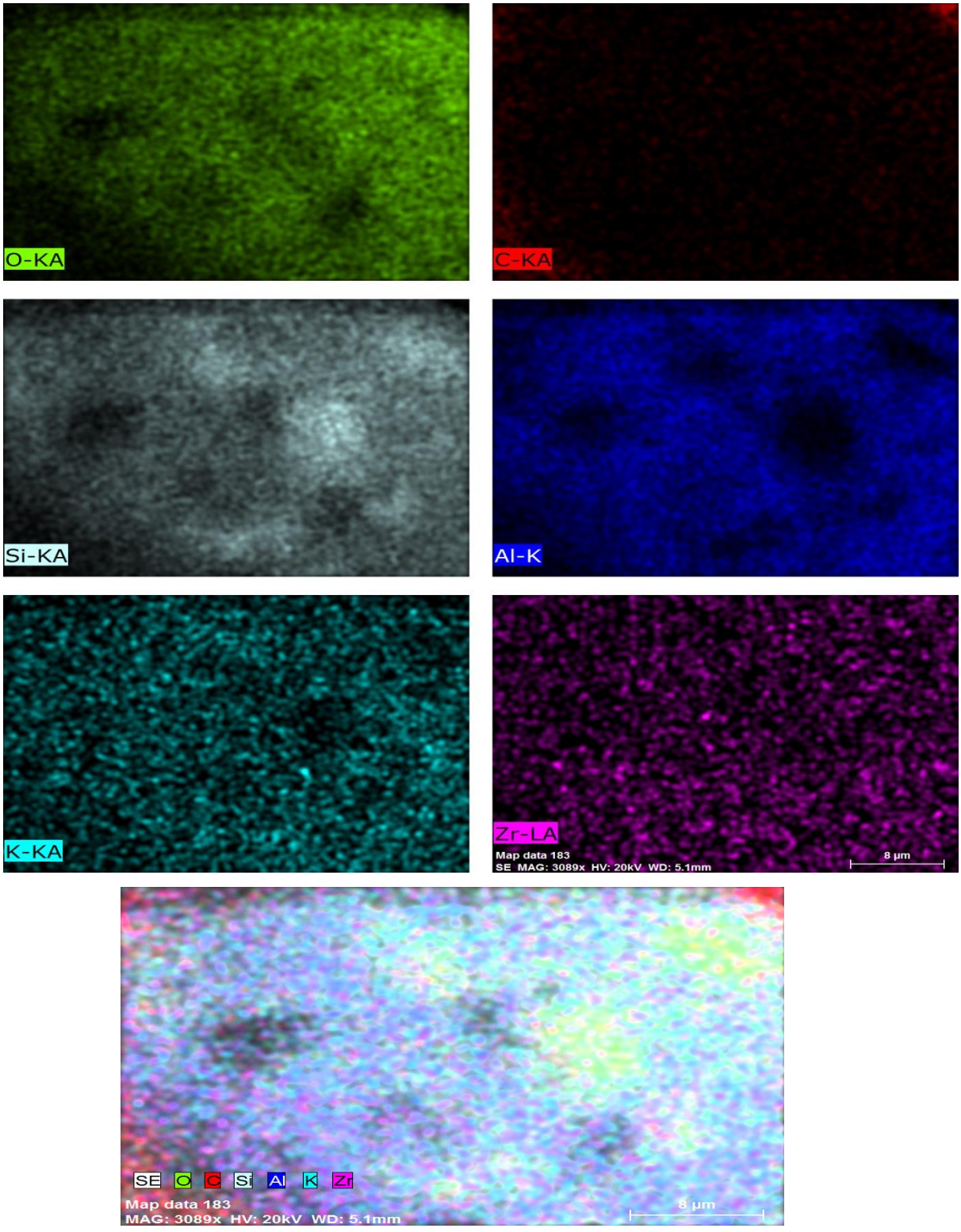

Figure 6.27 Different elements (O, C, Si, Al, K & Zr) in adsorbed fly ash with mixture of dyes at 1, 00,000X magnification

Table 6.10 Energy Dispersive X Ray analysis of fly ash before and after adsorption with black dye

Element	Unn. C (Wt. %)	Norm. C (wt. %)	Atom. C (at. %)	Sigma (wt. %)	Unn. C (wt. %)	Norm. C (wt. %)	Atom. C (at. %)	Sigma (Wt. %)
	Original fly ash				Adsorbed fly ash with direct black dye			
O	43.91	54.9	68.50	5.23	41.3	56.1	69.76	6.02
Si	19.06	23.8	16.94	0.82	16.4	22.3	15.82	0.76
Al	14.36	17.9	13.28	0.70	12.5	16.9	12.52	0.65
Fe	1.24	1.54	0.55	0.09	1.59	2.16	0.77	0.14
Ti	1.39	1.74	0.73	0.08	0.98	1.33	0.55	0.10
K	-	-	-		0.83	1.13	0.57	0.08
Total	79.96	100	100		73.7	100	100	

Table 6.11 Energy Dispersive X Ray analysis of fly ash before and after adsorption with mixture of dyes

Element	Unn. C (wt. %)	Norm. C (wt. %)	Atom. C (at. %)	Sigma (wt. %)	Unn. C (wt. %)	Norm. C (wt. %)	Atom. C (at. %)	Sigma (wt. %)
	Original fly ash				Adsorbed fly ash with direct black dye			
O	43.91	54.92	68.50	5.23	44.79	53.85	63.04	5.22
Si	19.06	23.83	16.94	0.82	7.34	20.84	13.90	0.77
Al	14.36	17.96	13.28	0.70	11.44	13.76	9.55	0.57
Fe	1.24	1.54	0.55	0.09	1.79	2.15	0.44	0.10
Ti	1.39	1.74	0.73	0.08				
K	-	-	-		1.23	1.48	0.71	0.07
Total	79.96	100	100		83.18	100	100	

The morphology of fly ash showed that raw fly ash consists of small and spherical particles. The spheres of different sizes and surfaces are either found loose or embedded in a larger matrix like structure (White and Case, 1990). The fly ash contains TiO_2, Fe_2O_3, Al_2O_3, and MnO_2. The elemental composition of fly ash before adsorption and after adsorption of black dye and mixture of dyes is seen in Table 6.10 & 6.11 respectively which shows the presence of Ti, Zr, Fe, Al, Si, O in raw fly ash and additional K element in adsorbed fly ash with black dye and K & C elements in fly ash adsorbed with mixture of dyes. The raw fly ash mainly comprised of amorphous alumino-silicate spheres and small amount of iron rich spheres. The iron rich spheres consist of iron oxide and amorphous alumino-silicate.

6.9 XRD studies

The graph of XRD of original fly ash and adsorbed fly ash with black dye and mixture of dyes is given in Figure 6.28.

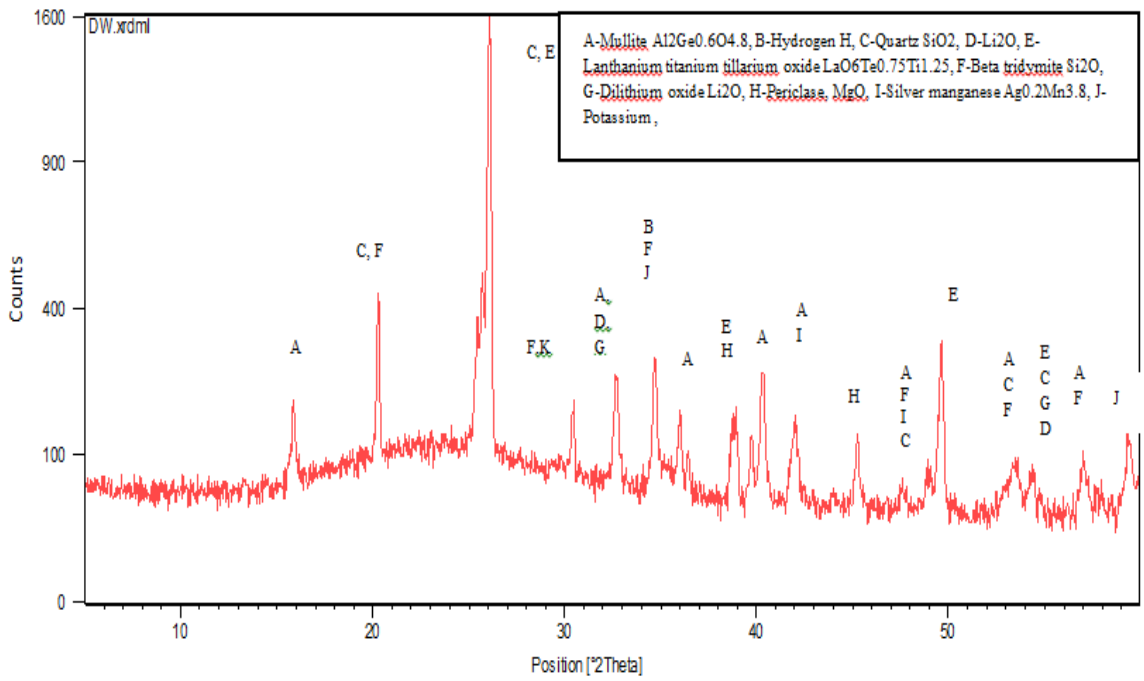

(a)

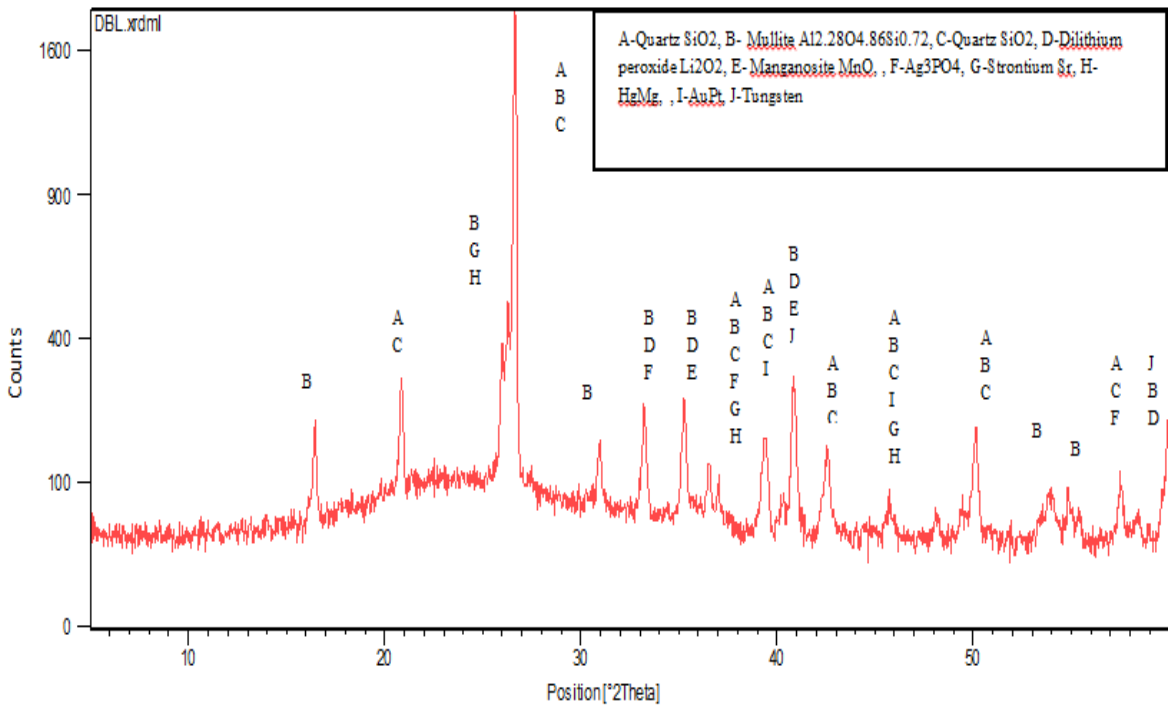

(b)

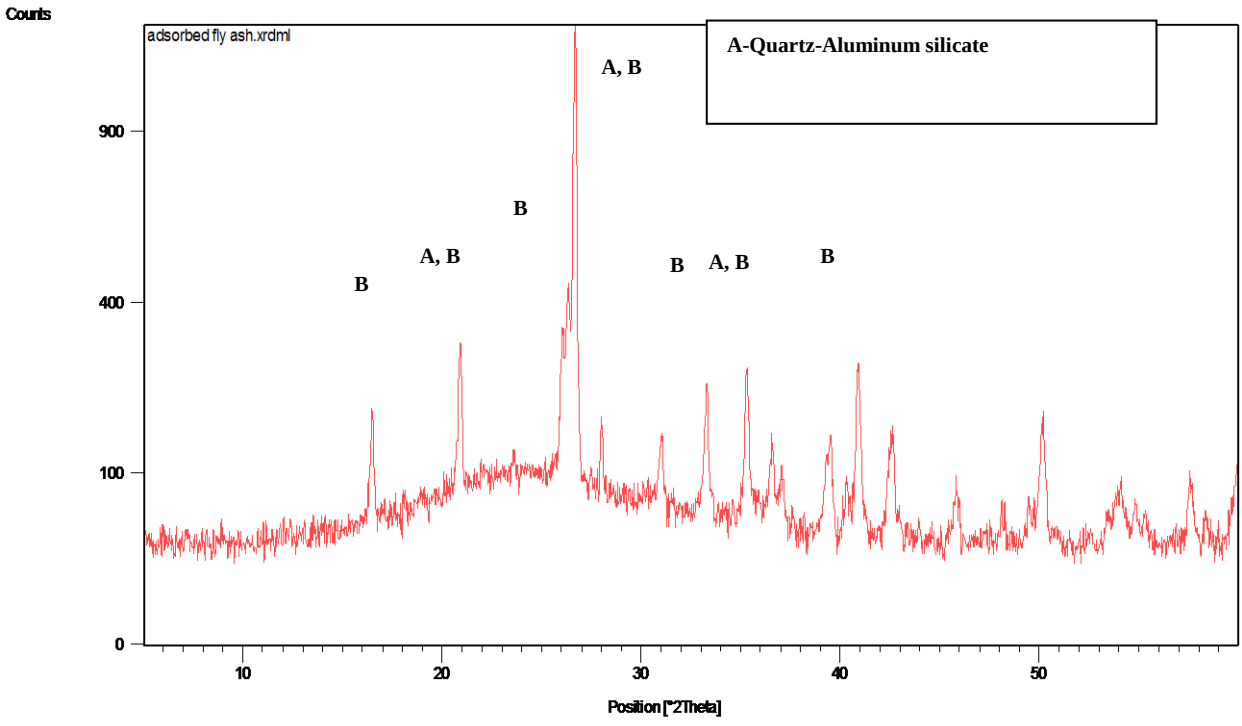

Figure 6.28 X-Ray Pattern Diffraction of (a) Raw fly ash (b) Fly ash adsorbed with Direct Black dye (c) Fly ash adsorbed with mixture of dyes

The diffraction pattern showed that the predominant phase is crystalline and the major components in fly ash include silicon oxide (SiO_2), Sodium aluminum oxide, alumina (Al_2O_3), and hematite (Fe_2O_3). The adsorbed fly ash consisted of crystalline quartz (SiO_2) and new crystalline phase of aluminum silicate. The presence of quartz and mullite has also been observed in fly ash in previous studies (Ismail et al. 2007).

6.10 Fourier Transform Infra- Red studies

The FTIR studies of raw fly ash, fly ash adsorbed with black dye and fly ash adsorbed with mixture of dyes is given as Figure 6.29.

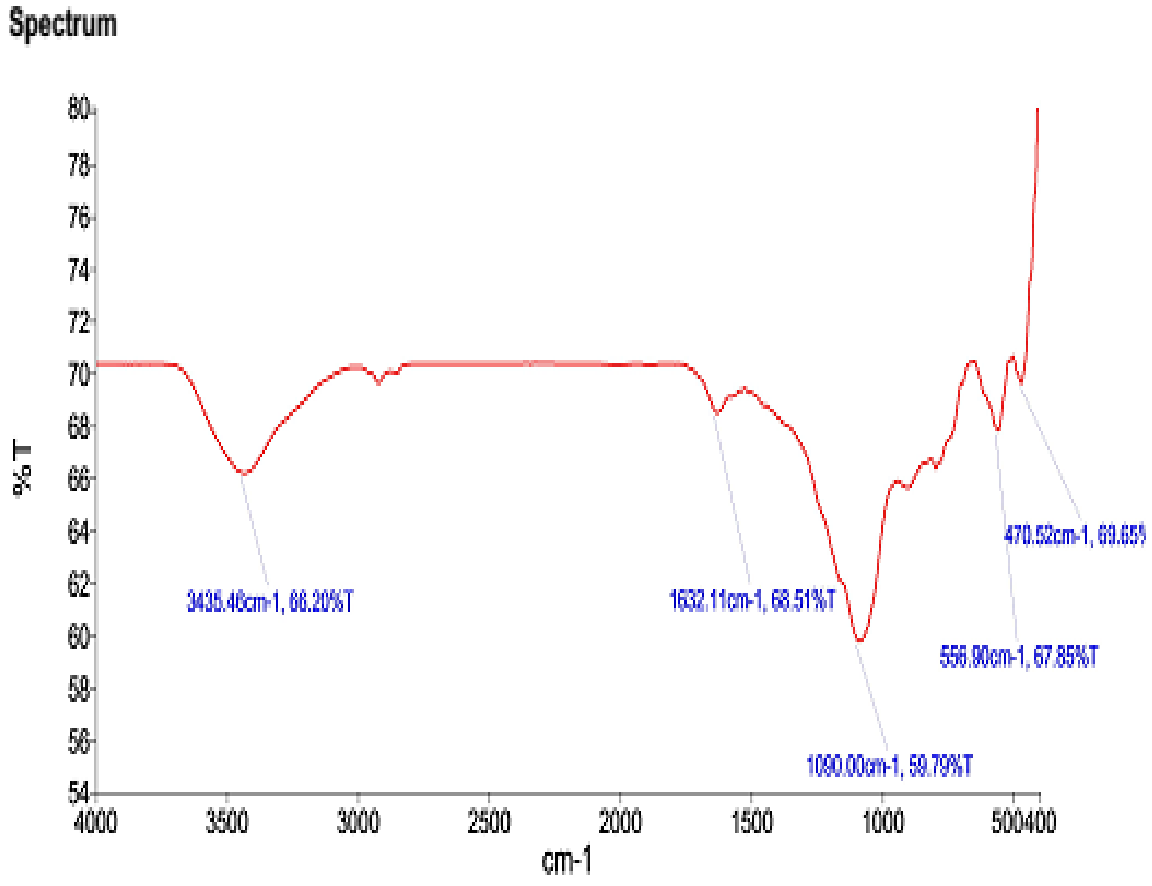

(a)

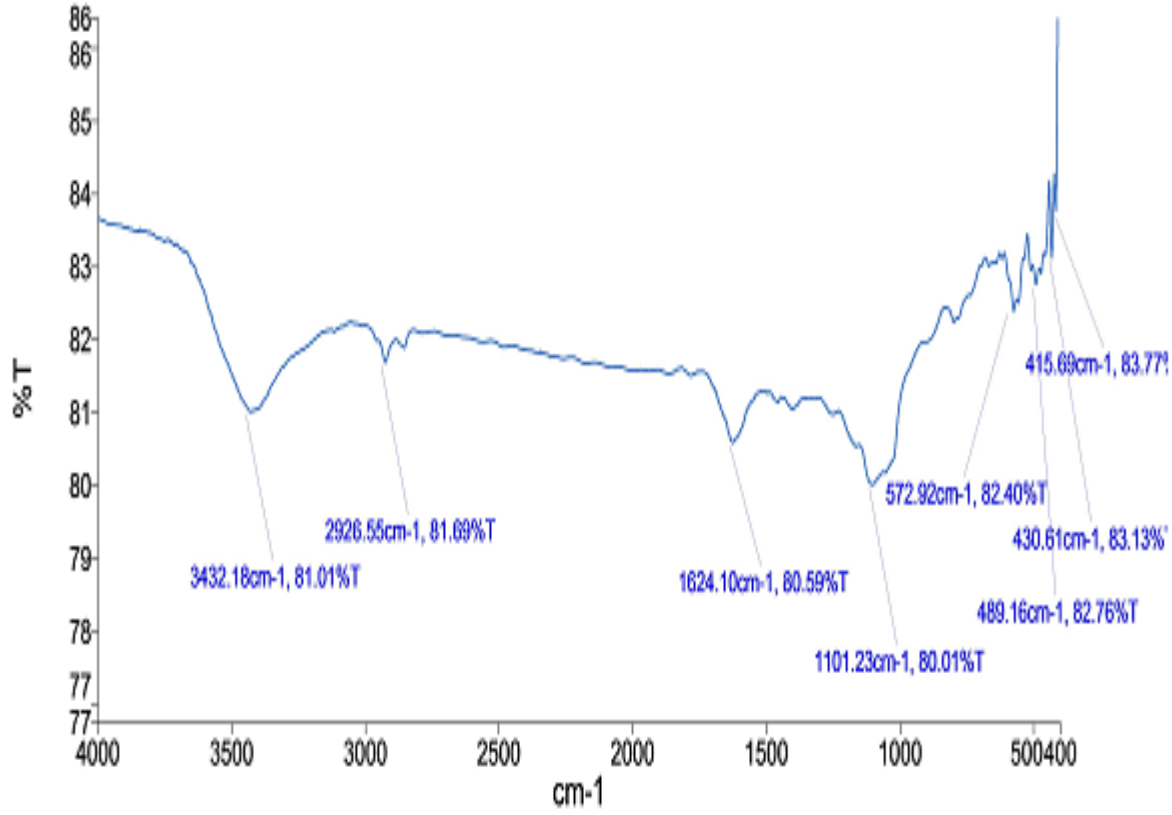

(b)

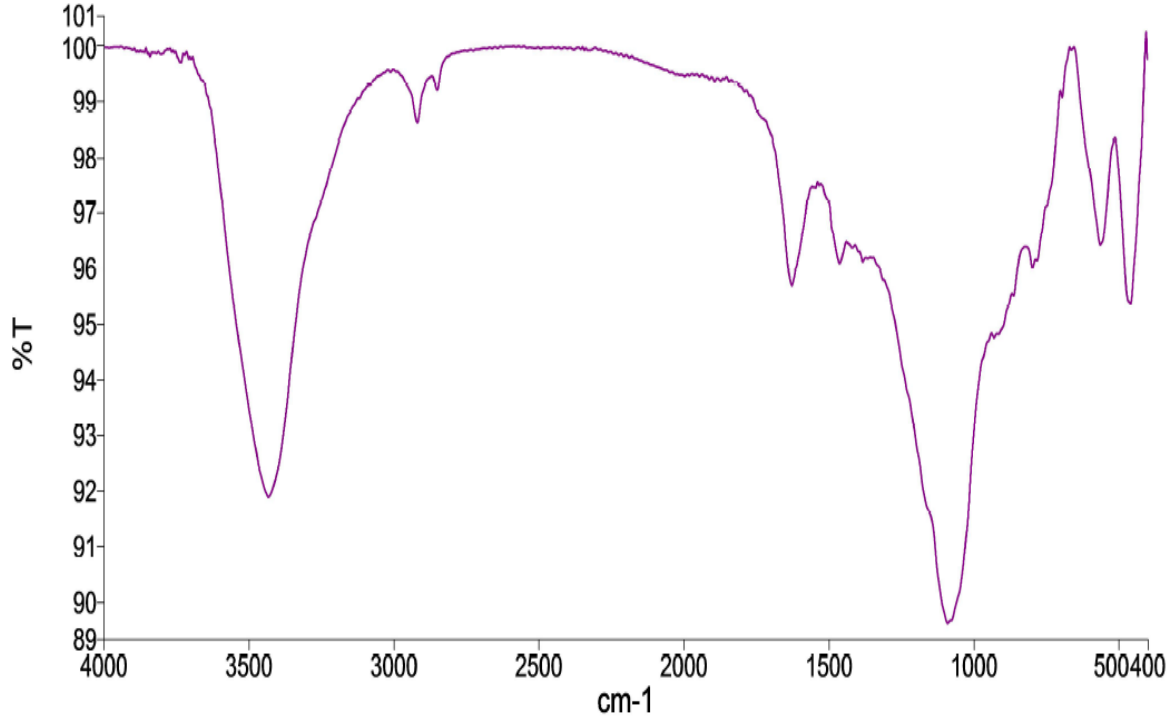

(c)

Figure 6.29 FTIR Spectra of (a) Raw fly ash (b) Adsorbed fly ash with Direct Black dye (c) Adsorbed fly ash with mixture of dyes

The broadband between 3100 and 3700 cm^{-1} in Figure 6.29 (b) may be due to presence of hydroxyl group on the surface of adsorbed fly ash with black dye. The primary aliphatic amines of band from 3250-3450 cm^{-1} has been observed in adsorbed fly ash with black dye may be due to adsorption of aliphatic amines of black dye on fly ash. The FTIR spectra of spectra of fly ash indicated strong broadband in the region of 1600-1800 cm^{-1} due to C=O group stretching bands from aldehydes and ketones in dye adsorbed fly ash. The fundamental bending of H_2O molecule corresponds to a sharp peak at 1646 cm^{-1}. The bond at 1646 cm^{-1} may be due to the conjugated hydrocarbon bonded carbonyl groups. The intense vibration at 600 to 400 cm^{-1} attributed to silicate minerals. The C-N stretching absorption of aliphatic amines occurs in the region 1090 to 1020 cm^{-1} to higher frequency in adsorbed fly ash while stretching of 1101 cm^{-1} due to interaction of nitrogen from amino group of black dye. The C-H stretching can be found in adsorbed fly ash between 2541 and 2973 cm^{-1} due to aliphatic hydrocarbon. The C-C stretching of 1579-1652cm^{-1} was found in both raw and adsorbed fly ash (Devi and Gayathri. 2010; Giri et al. 2011).

The FTIR study from Figure 6.29 (c) showed primary aliphatic amines of band from 3250 to 3450 cm^{-1} in adsorbed fly ash due to adsorption of aliphatic amines of mixture of dyes on fly ash. The FTIR spectra of adsorbed fly ash indicated strong broadband in the region of 1,600–1,800cm^{-1} due to C=O group stretching bands from aldehydes and ketones in dye-adsorbed fly ash. The intense vibration at600–400 cm^{-1} attributes to silicate minerals in raw and adsorbed fly ash. The C–N stretching absorption of aliphatic amines occurs in the region 1,090–1,020 $cm^{-1}$to higher frequency in adsorbed fly ash. The C–H stretching can be found in adsorbed fly ash between 2,541 and 2,973 cm^{-1} due to aliphatic hydrocarbon. The C–C stretching of 1,579–1,652cm^{-1} was found in both raw and adsorbed fly ash. The stretching of Si–O quartz is attributed to 1,079.77 cm^{-1} in original fly ash and 1,089, 796.08 cm^{-1} in adsorbed fly ash. The stretching of Si–O–Al is attributed to 558.38 cm^{-1}in original fly ash and 561.70 cm^{-1} to adsorbed fly ash.

6.11 Dye fixation

The black dye was added to cotton pulp for paper making and the spent liquor was collected for analysis of black dye concentration. The dye fixation on cotton pulp was 95%.

6.12 Characterization of effluent after treatment with fly ash

The effluent of handmade paper industry using black dye and mixture of dyes for colouring handmade paper and the treated effluent with fly ash has been analyzed for its various parameters. The results are given as Table 6.12 & 6.13 respectively.

Table 6.12 Characterization of effluent of direct black dye

Particulars	Before treatment	After treatment
pH	7.6	6.5
Chemical oxygen demand, mg/l	850	206
Biochemical oxygen demand, mg/l	200	44
Colour, PCU	250	10

Table 6.13 Characterization of effluent of mixture of dyes

Particulars	Before treatment	After treatment
pH	7.41	6.9
Chemical oxygen demand, mg/l	1023	243
Biochemical oxygen demand, mg/l	231	66
Colour, PCU	342	25

6.13 Utilization of adsorbed fly ash in paper making

The strength properties of cotton pulp after addition of fly ash is tabulated in Table 6.14.

Table 6.14 Effect of addition of adsorbed fly ash on strength properties

Particulars	**Control**	**Fly ash-2. 5%**	**Fly ash-5%**	**Fly ash-2.5% With retention aid**	**Fly ash-5% With retention aid**
Tensile Index, Nm/g	2.56 ±S.D 0.15	2.61 ±S.D 0.14	2.43 ±S.D 0.12	2.71 ±S.D 0.13	2.51 ±S.D 0.15
Tear Index, $mN.m^2/g$	18.79 ±S.D 0.56	19.76 ±S.D 0.55	17.78 ±S.D 0.54	19.99 ±S.D 0.54	17.85 ±S.D 0.56
Burst Index, $kPa.m^2/g$	1.76 ±S.D 0.07	1.85 ±S.D 0.09	1.67 ±S.D 0.07	1.91 ±S.D 0.08	1.73 ±S.D 0.09
Double Fold, No.	789 ±S.D 3.02	850 ±S.D 2.99	721 ±S.D 2.76	865 ±S.D 3.11	750 ±S.D 2.85

S.D-Standard Deviation

It has been found that only a marginal effect on strength properties of pulp was observed after addition of 5% of adsorbed fly ash along with retention aid. Therefore, the adsorbed fly ash can be used as filler in handmade paper making. Further, increase in dosage increases the dusting tendency of paper.

6.14 Cost economic analysis of utilization of fly ash

The fly is available free of cost from thermal power plants and only transportation cost is incurred as cost of raw material while powdered activated carbon is approximately Rs. 500/- per kg. The cost analysis of fly ash in comparison with traditional adsorbent is given in Table 6.15.

Table 6.15 Comparative cost of traditional adsorbent and fly ash

	Adsorption capacity, mg g^{-1}	**Cost of adsorbent, Rs./- per kg**	**Costing of removal of 1gm dye, Rs./-**
Fly ash	75(This study) 129 mg g^{-1} for Remazol Red dye (Kare et al., 2007)	2 (transportation cost from Jaipur to Delhi)	2.66
Powdered activated carbon	135.2 for Direct Blue 53 dye (Prola et al.,2013)	500	37
	151.52 for crystal violet dye (Nagda and Ghole, 2008)		33

6.15 Mathematical modeling

The mathematical model for adsorption has been developed to predict the behavior of adsorption in column studies.

6.15.1 Development of model

Assumptions

1) The adsorption column operates under isothermal conditions.

2) The equilibrium of adsorption is described by Langmuir isotherm.

3) Mass transfer across the boundary layer surrounding the adsorbent particles is characterized by the external-film mass transfer coefficient, k_f.

4) The linear velocity of the bulk phase remains constant along the fixed-bed column.

5) The adsorbent particles are spherical and homogeneous in size and density.

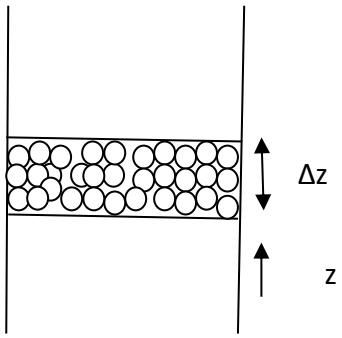

(a) Fixed bed column

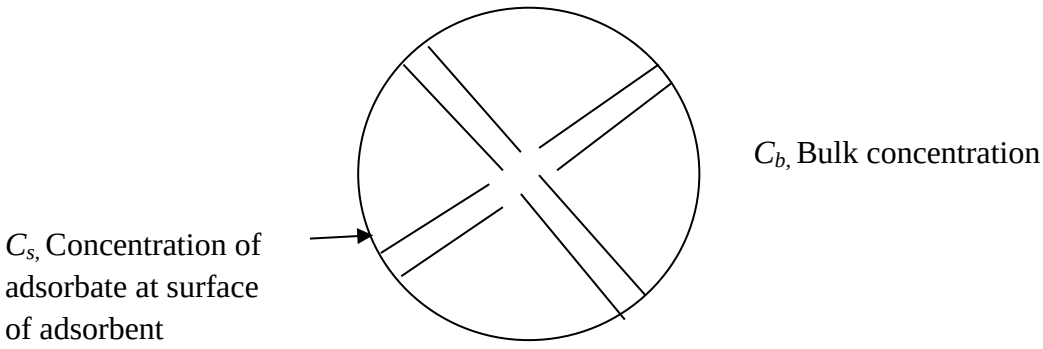

(b) Adsorbent particle

Figure 6.30 (a) Fixed Bed Column (b) Adsorbent particle

Based on the above assumptions, the net rate of accumulation or depletion is given by equation-

$$\varepsilon\, S v_s\, c_b\big|_z - \varepsilon\, S v_s\, c_b\big|_{z+\Delta z} + \left(-D_L\, S\varepsilon \frac{\partial C_b}{\partial z}\right)\Big|_z - \left(-D_L\, S\varepsilon \frac{\partial C_b}{\partial z}\right)\Big|_{z+\Delta z} = \frac{\partial}{\partial t}\left(\varepsilon\, S\, \Delta z\, c_b + (1-\varepsilon) S\, \Delta z\, q + (1-\varepsilon)\varepsilon_p S \Delta z c_p\right) \quad \text{.....(Eq. 6.10)}$$

On Dividing by $\varepsilon\, S\Delta z$,

$$-\frac{\partial (v c_b)}{\partial z} + D_L \frac{\partial^2 c_b}{\partial z^2} = \frac{\partial}{\partial t}\left[C_b + \frac{(1-\varepsilon)}{\varepsilon} q + \frac{(1-\varepsilon)}{\varepsilon}\varepsilon_p C_p\right] \quad \text{.....(Eq. 6.11)}$$

Assuming that v is independent of z, we get

$$D_L \frac{\partial^2 C_b}{\partial z^2} - v \frac{\partial C_b}{\partial z} = \frac{\partial C_b}{\partial t} + \frac{(1-\varepsilon)}{\varepsilon}\frac{\partial (q)}{\partial t} \quad \text{.....(Eq. 6.12)}$$

$$4\pi R^2 k_f (C_b - C_s) = \frac{\partial (q)}{\partial t}\frac{4\pi R^3}{3}$$

where,

$$\frac{\partial q}{\partial t} = \frac{3k_f}{R_p \rho_p}(C_b - C_s)$$

$$C_s = \frac{q}{K(q_m - q)}$$

Initial and boundary conditions are,

at $t = 0$, $C_b = 0$

at $z = 0$, $C_{in} = C_b - \frac{D_L}{v}\frac{\partial C_b}{\partial z}$

at $z = L$, $\frac{\partial C_b}{\partial z} = 0$

Applying finite difference method (Choosing N finite difference points from z=0 to z=L),

At z=0,

$$C_{in} = C_{b1} - \frac{D_L}{v}\left(\frac{C_{b2} - C_{b0}}{2\Delta z}\right) \quad \text{(Eq. 6.13)}$$

or,

$$C_{b0} = \frac{(C_{in} - C_{b1})v\,2\Delta z}{D_L} + C_{b2} \quad \text{(Eq. 6.14)}$$

At i=1

$$\frac{\partial C_b}{\partial z} = (C_{b1} - C_{in})\frac{v}{D_L} \quad \text{(Eq. 6.15)}$$

or, $$\frac{C_{b2} - C_{b0}}{2\Delta z} = (C_{b1} - C_{in})\frac{v}{D_L} \quad \text{(Eq. 6.16)}$$

or, $$C_{b0} = C_{b2} - \frac{2\Delta z\, v(C_{b1} - C_{bin})}{D_L} \quad \text{(Eq. 6.17)}$$

Second order derivative becomes,

$$\frac{\partial^2 C_b}{\partial z^2} = \frac{C_{b2} - 2C_{b1} + C_{b0}}{\Delta z^2} \quad \text{(Eq. 6.18)}$$

Therefore,

$$\frac{\partial^2 C_b}{\partial z^2} = \frac{C_{b2} - 2C_{b1} + \left(C_{b2} - \frac{2\Delta z\, v(C_{b1} - C_{bin})}{D_L}\right)}{\Delta z^2} \quad \text{(Eq. 6.19)}$$

or, $$\frac{\partial^2 C_b}{\partial z^2} = \frac{C_{b2} - 2C_{b1} + C_{b2} - \frac{2\Delta z\, v}{D_L}C_{b1} - \frac{2\Delta z\, v}{D_L}C_{bin}}{\Delta z^2} \quad \text{(Eq. 6.20)}$$

or,

$$\frac{\partial^2 C_b}{\partial z^2} = \frac{2C_{b2} - 2C_{b1}\left(1 + \frac{\Delta z\, v}{D_L}\right) - \frac{2\Delta z\, v}{D_L}C_{bin}}{\Delta z^2} \quad \text{(Eq. 6.21)}$$

At *i*=*N*

$$\frac{\partial^2 C_b}{\partial z^2} = \frac{C_{b_{N+1}} - 2C_{b_N} + C_{b_{N-1}}}{\Delta z^2} \quad \text{.....(Eq. 6.22)}$$

$$\frac{\partial C_b}{\partial z} = 0, \Rightarrow \frac{C_{b\,N+1} - C_{b\,N-1}}{2(\Delta z)} = 0 \quad \text{.....(Eq. 6.23)}$$

or,

$$C_{b_{N+1}} = C_{b_{N-1}}$$

Therefore,

$$\frac{\partial^2 C_b}{\partial z^2} = \frac{2(C_{b_{N+1}} - 2C_{b_N})}{\Delta z^2} \quad \text{.....(Eq. 6.24)}$$

6.15.2 Determination of external mass transfer coefficient

According to McKay plot of kinetic curves (Yesim Sag et al 2000), the equation of determination of external mass transfer coefficient is given by:

$$\ln\left(\frac{C}{C_0} - \frac{1}{1+mK}\right) = \ln\left(\frac{mK}{1+mK}\right) - \left(\frac{1+mK}{mK}\, k_f S_s t\right) \quad \text{.....(Eq. 6.25)}$$

Where,

$$S_s = \frac{6m}{d_p\ \rho_p\ (1-\varepsilon_p)}$$

6.15.3 Determination of axial dispersion coefficient

As per Ruthven (1984), the equation of determination of axial dispersion coefficient is given by

$$\frac{D_L}{u_0 d_p} = \frac{20}{\varepsilon}\left(\frac{D_m}{u_0 d_p}\right) + \frac{1}{2} \quad \text{..... (Eq. 6.26)}$$

Where,

u_0= superficial velocity, m/s

d_p=particle diameter, m

D_m=molecular diffusivity of dye in water, m^2/s

6.16 Simulation studies

The model parameter values for simulation are given in Table-6.16.

Table 6.16 Model parameters for simulation of fixed bed adsorption

Parameter	Value
Bed porosity, ε (-)	0.514
Particle density, kg/m^3	750
Liquid density, kg/m^3	1.013 X 10^3
D_L, Axial dispersion coefficient, m^2/s	56.5 X 10^{-5}
Q_m, Maximum adsorption capacity, mg/g	27.39 mg/g
b, Langmuir isotherm constant, ml/mg	0.396
k_f, External mass transfer coefficient, m/s	7.08 × 10^{-8}
D, bed diameter, m	0.034
Bed depth, cm	1.2, 1.8, 2.4
Initial concentrations of dye, mg/l	50, 100, 150

The model of dye adsorption on fly ash in column studies was simulated in MATLAB using finite difference method.

6.16.1 Effect of bed depth on breakthrough curve

The effect of bed depth on breakthrough curve is shown in Figure 6.31.

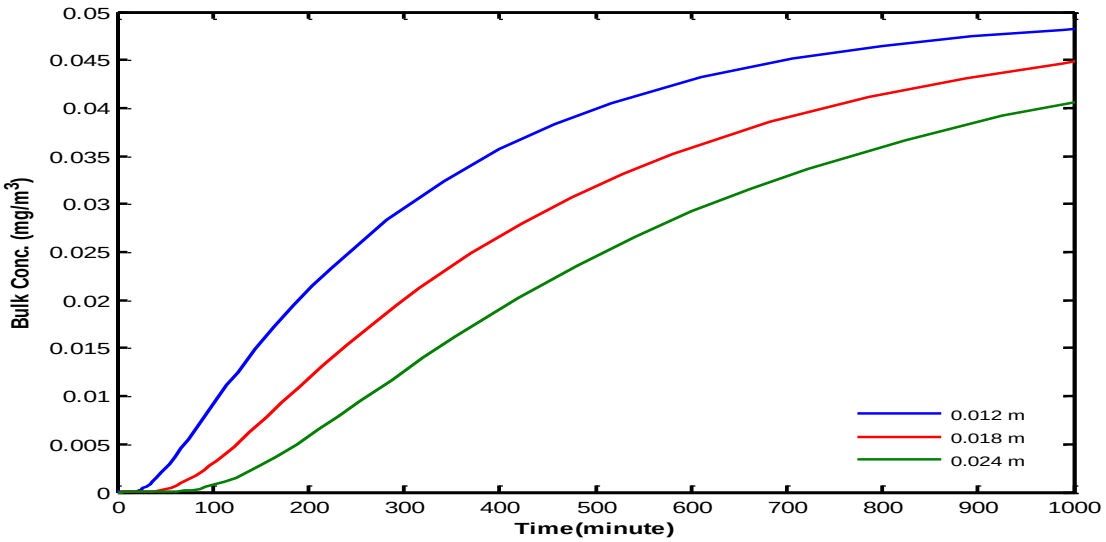

Figure 6.31 Effect of bed depth on breakthrough curve: Simulation results [Bed depth-1.2cm, 1.8 cm, 2.4 cm, velocity-0.5505×10^{-4}m/s, Initial concentration of dye=50 mg/l]

The Figure 6.31 confirmed that breakthrough curve is dependent on bed depth. The breakthrough time increased with increase in bed depth showing better efficiency of fly ash at 2.4 cm bed depth.

6.16.2 Effect of flow rate on breakthrough curve

The effect of bed depth on breakthrough curve is shown in Figure 6.32.

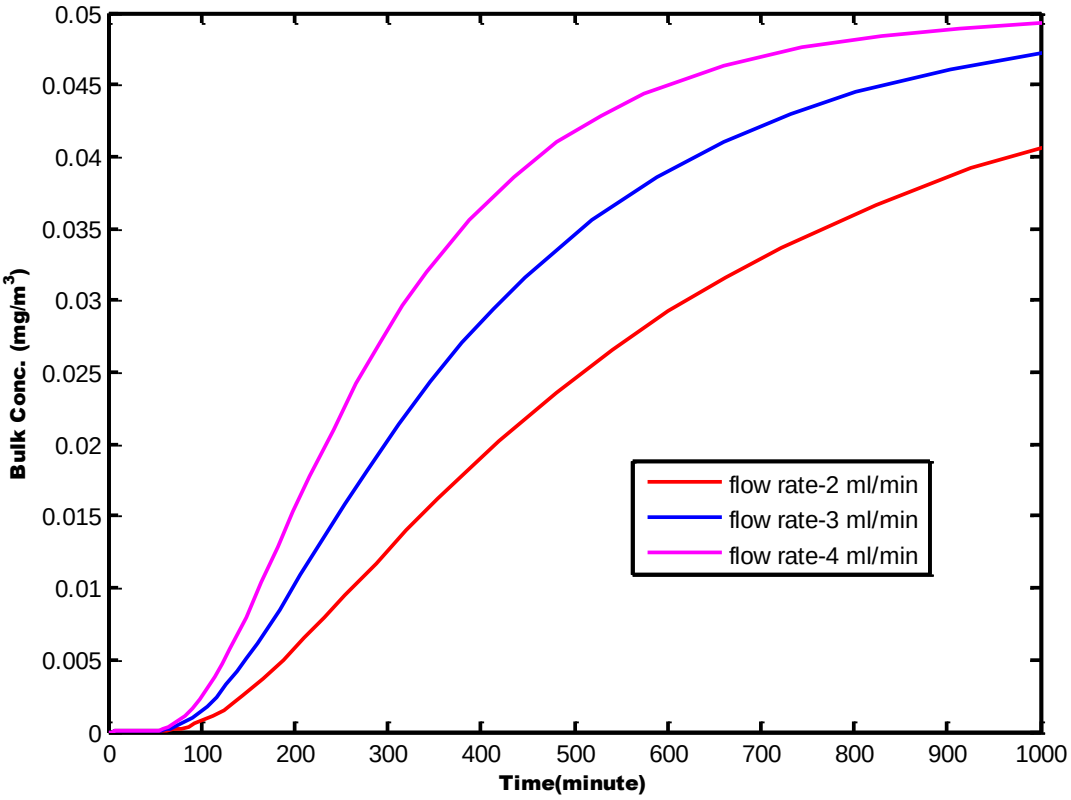

Figure 6.32 Effect of flow rate
[Flow rate- 2, 3, 4 ml/min, Bed height-2.4 cm,
Initial concentration of dye- 50 mg/l]

The better efficiency of fly ash has been achieved at flow rate of 2 ml/min in comparison to 4 ml/min as shown in Figure 6.32.

6.16.3 Effect of inlet concentration in breakthrough curve

The effect of bed depth on breakthrough curve is shown in Figure 6.33.

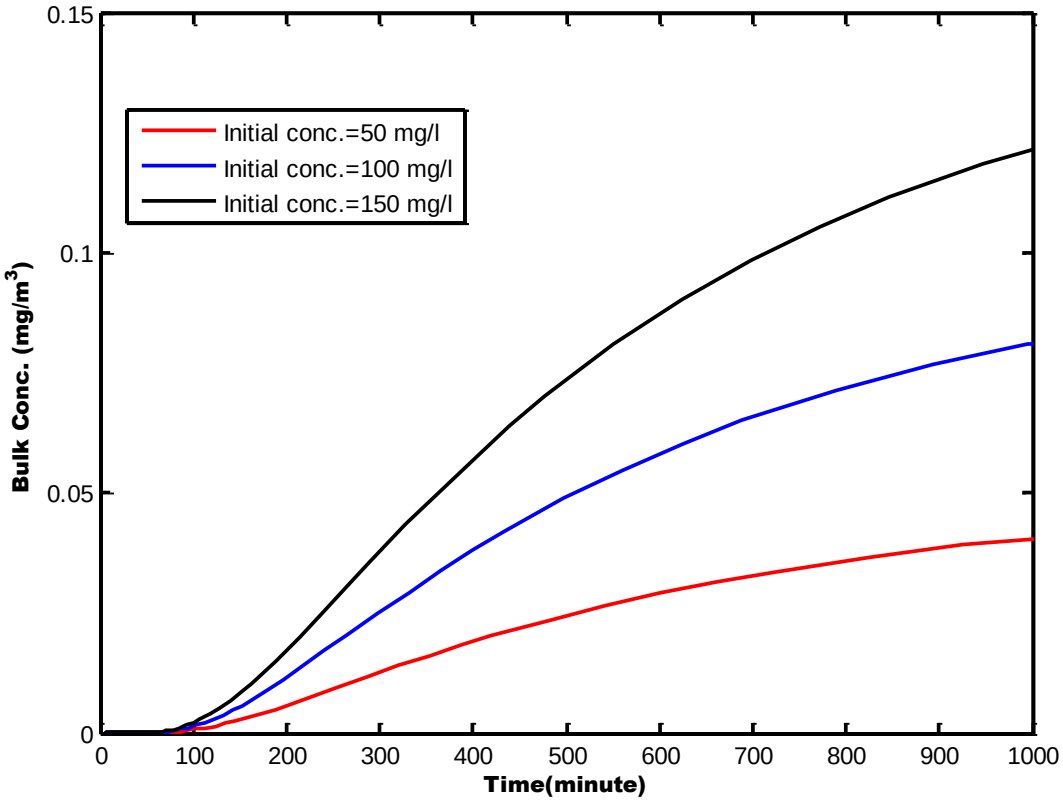

Figure 6.33 Effect of initial concentration

[Initial concentration-50, 100, 150 mg/l, Bed height-2.4 cm, Velocity-0.367X10^{-4} m/s]

The better efficiency of fly ash has been achieved at 50 mg/l initial concentration at bed depth of 2.4 cm and flow rate of 2 ml/min as shown in Figure 6.33.

6.17 Comparison between experimental and predicted value of concentration of dye

The predicted values were compared with experimental values at various initial concentration and bed depths is shown in Figure 6.34 & 6.35 respectively.

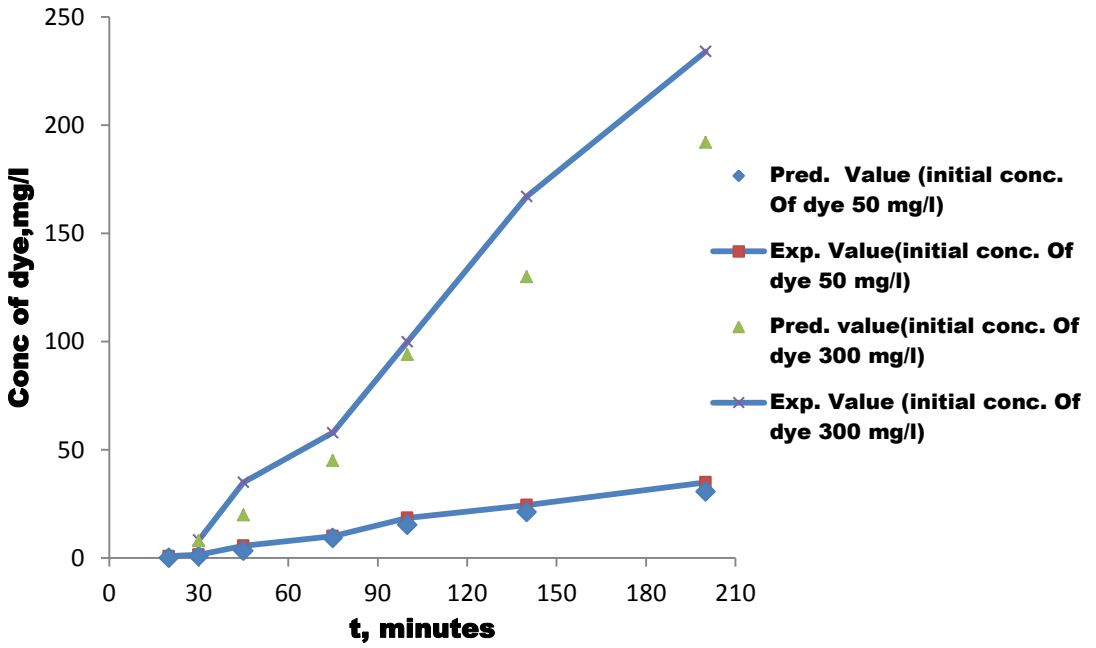

Figure 6.34 Experimental vs. Predicted value for various initial concentration

[Bed depth-1.2 cm, Flow rate-2ml/min]

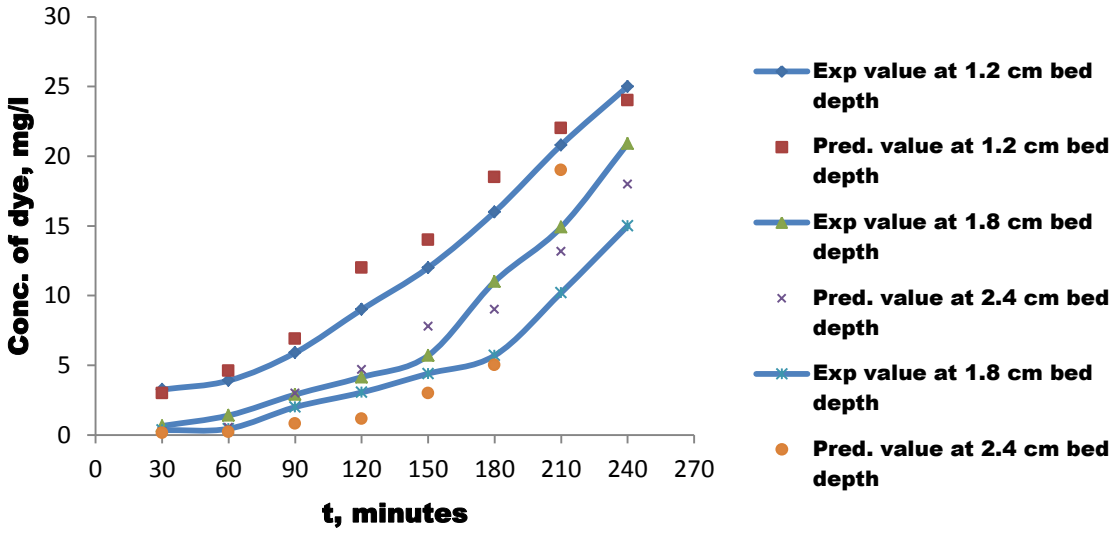

Figure 6.35 Experimental vs. Predicted value for various bed depths

[Initial conc.-50 mg/l, Flow rate-2ml/min]

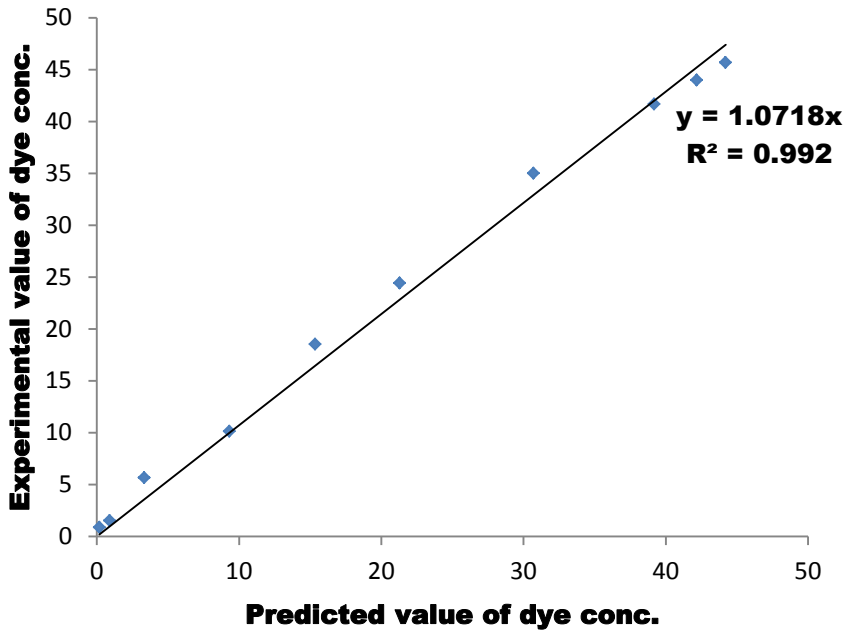

Figure 6.36 Experimental vs. Predicted value of dye concentration for initial concentration-50 mg/l [Initial conc.-50 mg/l, Bed depth-1.2 cm, Flow rate-2ml/min]

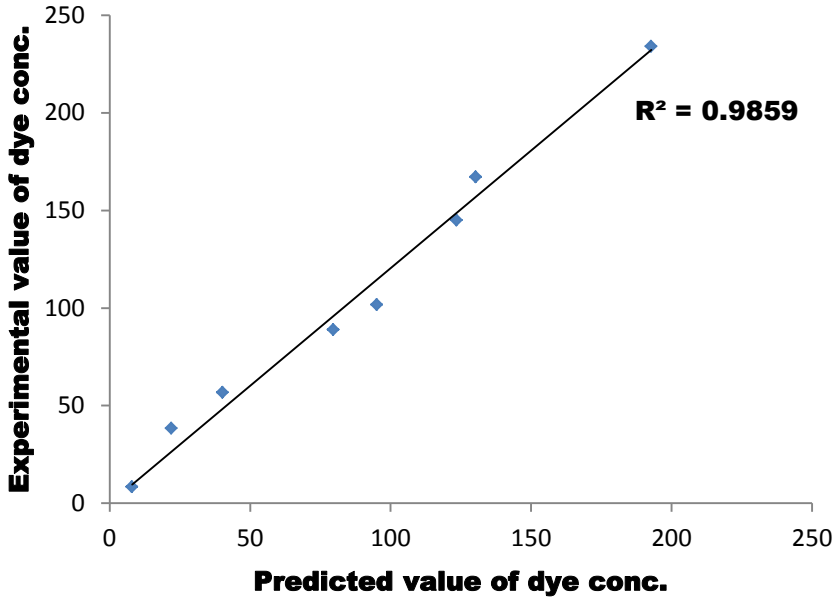

Figure 6.37 Experimental Vs. Predicted value for initial concentration-300 mg/l [Initial conc.-300 mg/l, Bed depth-1.2 cm, Flow rate-2ml/min]

To validate the model of fixed bed adsorption, the simulation results of outlet dye concentration from the bed were compared with experimental results. The value of R^2 obtained in Figure 6.36 & 6.37 is more than 0.98, thus confirming the predicted values with experimental values.

CHAPTER 7 OZONATION

The ozonation studies were carried in semi batch mode with the help of gas bottles, and in continuous mode with the help of bubble column with direct red and direct blue dyes as well as black liquor of banana fiber at 8% Alkaline peroxide pulping and Alkaline Sulphite pulping processes. The detailed results of these experiments along with their mathematical modeling are contained in this chapter.

7.1 Semi-batch studies on ozonation treatment

The effect of initial concentration, pH and temperature of dye solution was studied on decolourization efficiency of ozonation treatment of direct red and direct blue dye used commonly in handmade paper industry.

7.1.1 Effect of initial concentration and time on colour removal

The effect of initial concentration of dye solution on the decolourization efficiency of ozone was studied with direct red and direct blue dye. The results are shown in Figures 7.1 & 7.2 respectively.

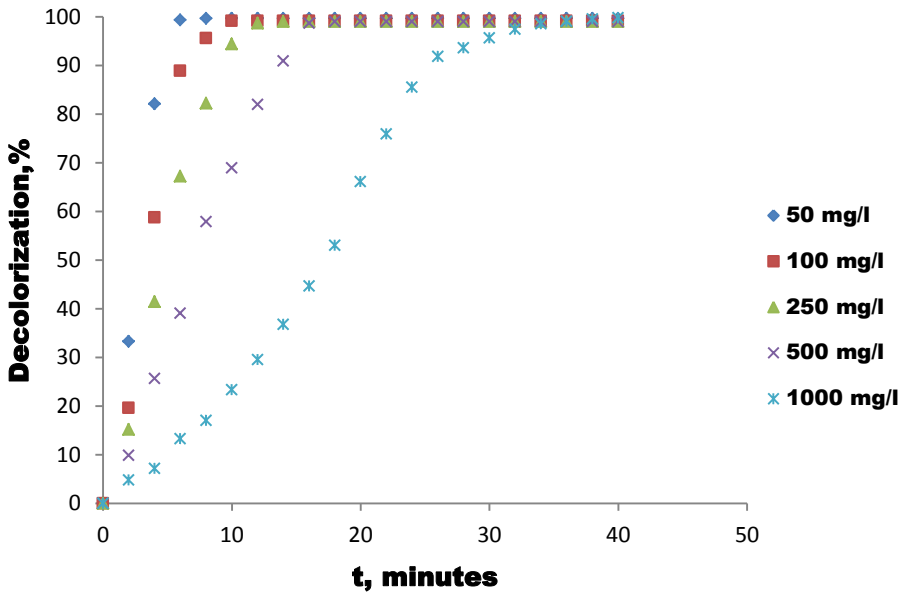

Figure 7.1 Effect of ozonation on decolourization of Direct Red dye [Ozone dosage-27.5 mg/l, Ozone flow rate-2 LPM, pH-7.5]

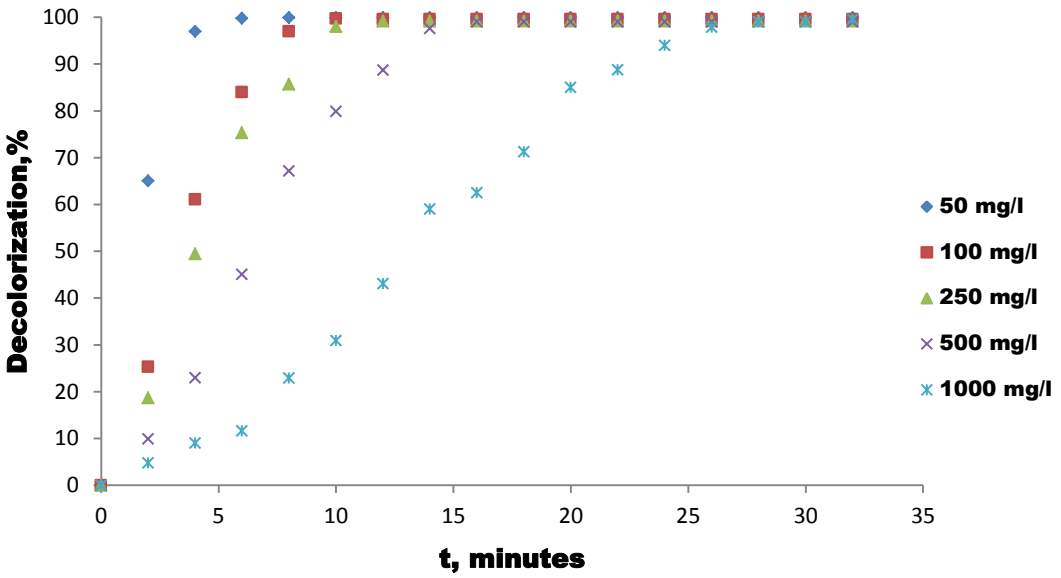

Figure 7.2 Effect of initial concentration on decolourization of Direct Blue dye [Ozone dosage-27.5 mg/l, Ozone flow rate- 2 LPM, pH-7.5]

The increase in the initial concentration of red and blue dye solution decreases the decolourization efficiency of ozone as shown in these figures. The results show that the decolourization efficiency of ozone treatment is dependent on the initial concentration of dye solution. The time required for complete colour removal increases with an increase in the initial dye concentration. For initial dye concentration of 50, 500, and 1000 mg/l, the time required for complete colour removal is 5, 15, and 30 minutes respectively for both direct red and direct blue dyes. The results are well in agreement with those of other researchers (Zhou et al. 2002, Mehmet et al. 2002, Konsowa et al. 2003, Selcuk et al. 2005, Meric et al. 2005).

7.1.2 Effect of temperature on colour removal

The temperature of waste water discharged from the handmade paper industry is higher than the normal temperature of water due to the heat released during processing of the product and hence, this study was designed to cover a temperature range of313 to 333 K, usually observed in such streams.The decolourization trends of direct red and direct blue dye at 313, 318, 323, 328 & 333 K are shown in Figures 7.3 & 7.4 respectively.

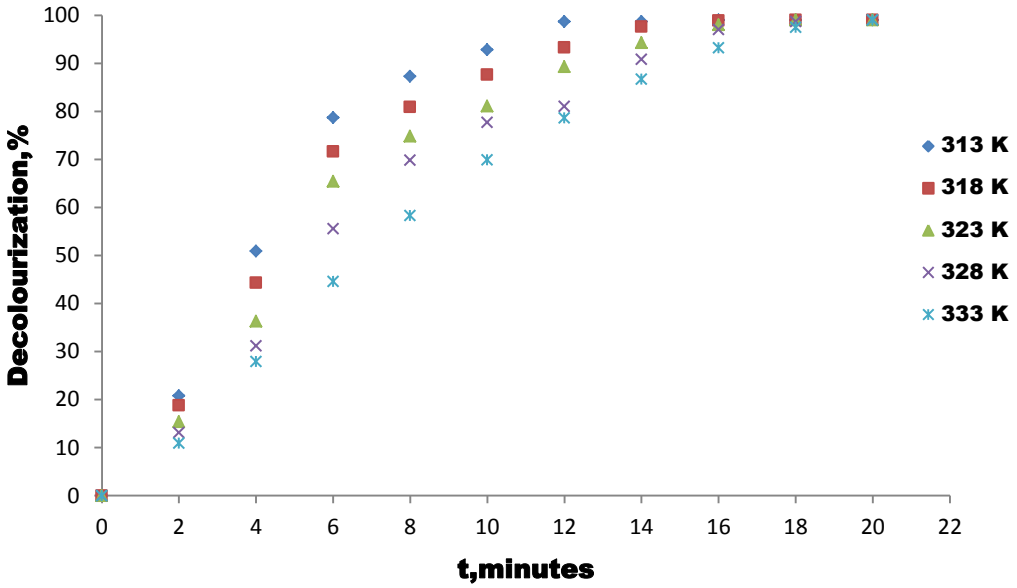

Figure 7.3 Effect of temperature on decolourization of Direct Red dye [Ozone dosage-27.5 mg/l, Ozone flow rate- 2 LPM, Initial concentration-50 mg/l, pH-7.5]

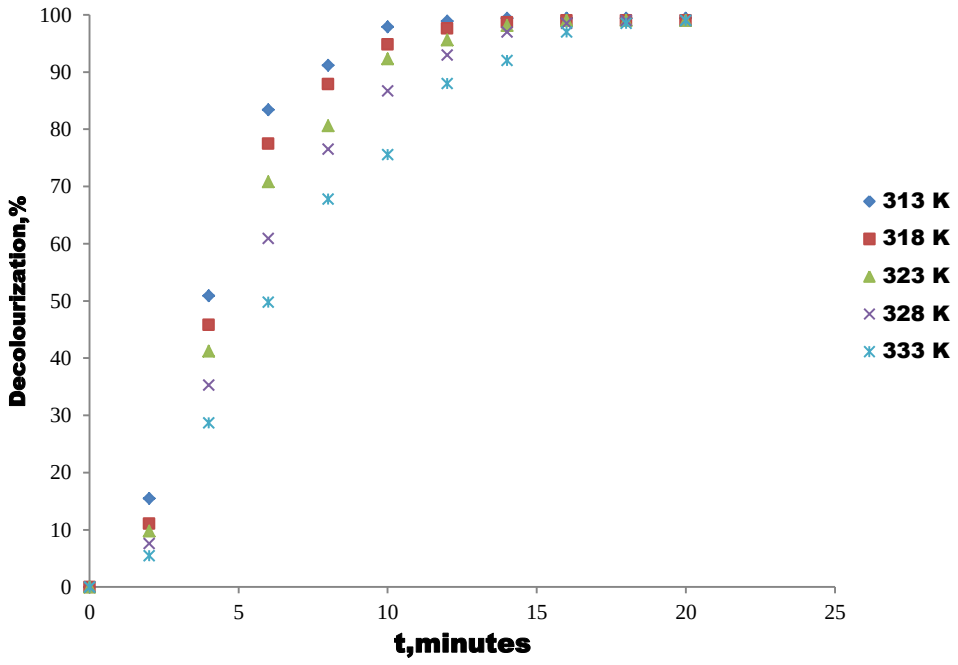

Figure 7.4 Effect of temperature on decolourization of Direct Blue dye [Ozone dosage-27.5 mg/l, Ozone flow rate- 2 LPM, Initial concentration-50 mg/l, pH-7.5]

The results showed the best decolourization efficiency of ozone at the lowest temperature studied, i.e.313 K, for both direct red and direct blue dye waste streams. At high temperature, there is less solubility of ozone, therefore, resulting in less quantity of ozone available for the reaction (Wu et al. 2001; Yong et al. 2005) attributed the difference in solubility to the inhibition of reactions between ozone and organics. Temperature has a notable effect on the decolourization efficiency of ozone. The rate constant of reaction rate and variation of ozone solubility with temperature increases with increase in temperature.

7.1.3 Effect of pH on colour removal

The influence of pH (4, 6, 8 & 10) on efficiency of ozonation treatment was studied for maximum decolourization of direct red and direct blue dye as shown in Figures 7.5 &7.6 respectively.

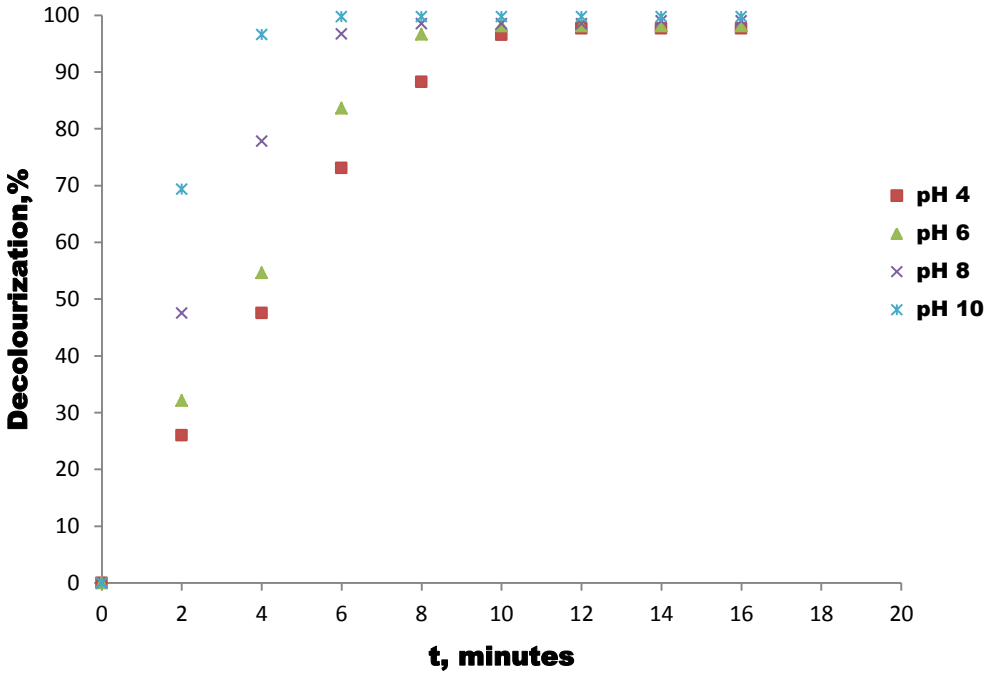

Figure 7.5 Effect of initial pH on decolourization of Direct red dye [Ozone dosage-27.5 mg/l, Ozone flow rate- 2 LPM, Temperature-333 K, Initial conc. =50 mg/l]

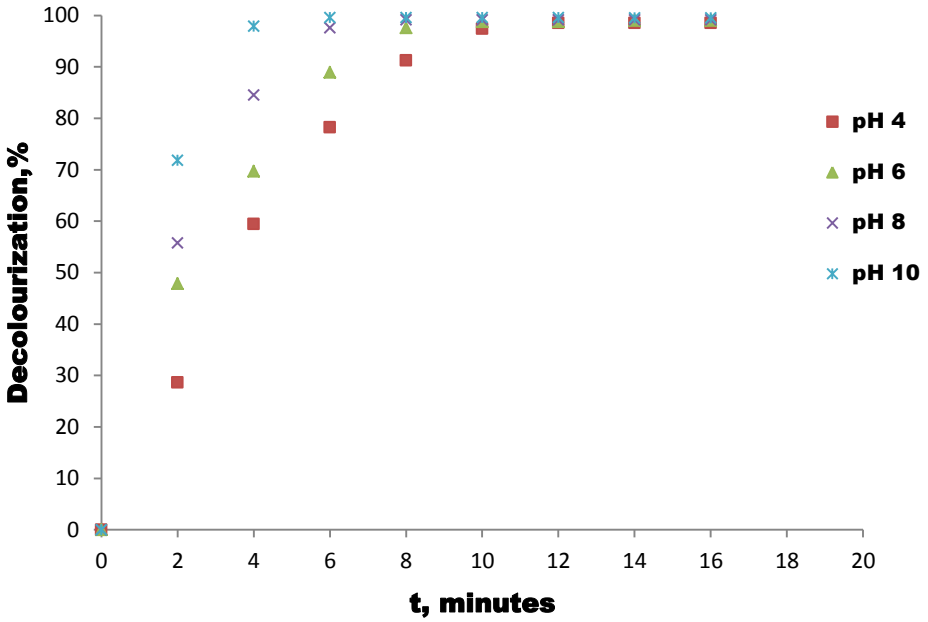

Figure 7.6 Effect of initial pH on decolourization of direct blue dye [Ozone dosage-27.5 mg/l, Ozone flow rate-2 LPM, Temperature-333 K, Initial conc. =50 mg/l]

Figure 7.5 and 7.6 show that the best decolourization efficiency was observed at pH of 10 for both the dyes, which is well in agreement with the studies conducted by other researchers (Yasar et al. 2007; Hoigne et al. 1983; Fanchiang et al. 2009) .This can be explained by the fact that under acidic conditions, ozone, mainly decomposes to hydroxyl (OH) radicals, which react with the target pollutant and are more effective in carrying out the oxidation reactions.

7.1.4 UV-Vis spectra during Ozonation treatment

The samples were scanned from 200 to 1100 nm to study the spectra during ozonation treatment. The UV-Vis spectra of direct red and direct blue dye are shown in Figures 7.7 & 7.8 respectively.

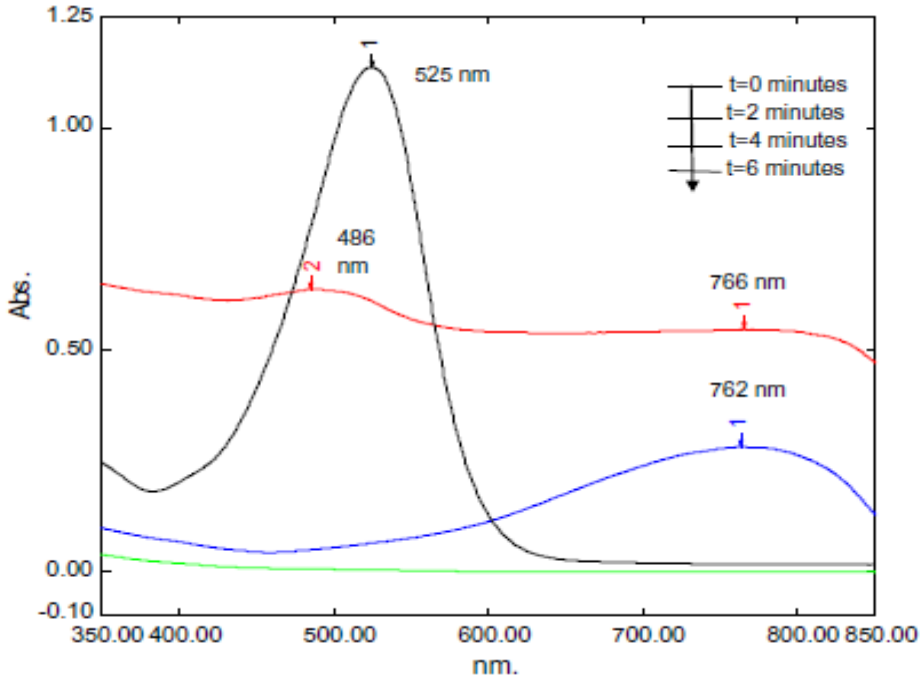

Figure 7.7 UV-Vis Spectral changes of direct red dye at 50 mg/l [Ozone dose-27.5 mg/l, Ozone flow rate- 2 LPM, pH-10]

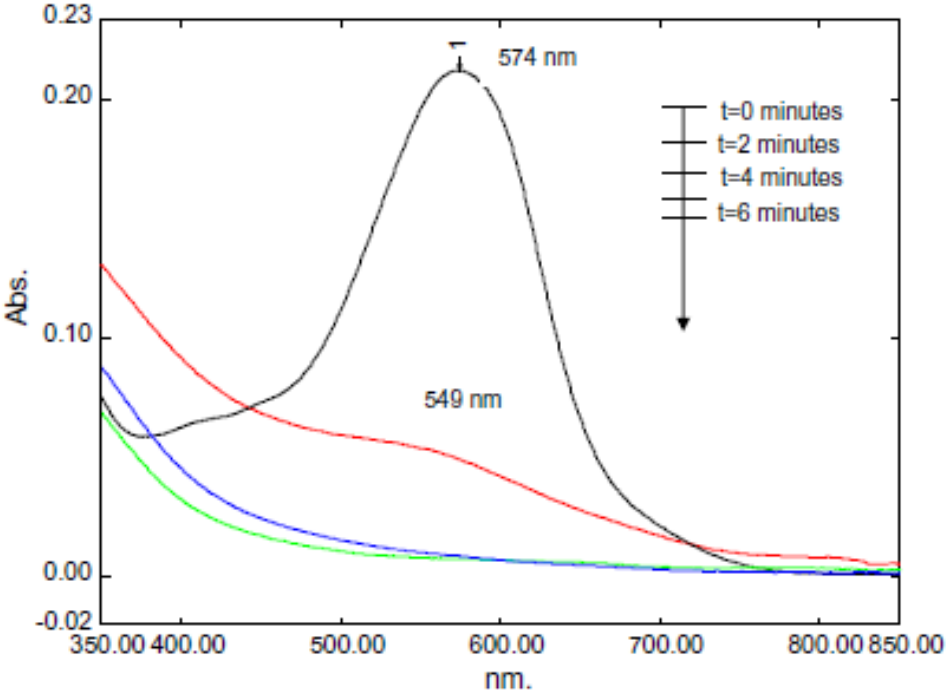

Figure 7.8 UV-Vis spectral changes of direct blue dye at 50 mg/l [Ozone dosage-27.5 mg/l, Ozone flow rate-2 LPM, pH-10]

Figure 7.7 shows a bimodal development in absorbance giving one peak corresponding to the original wavelength and another with a considerable shift at about 760 nm in direct red dye. The reason might be the rapid destruction of dye chromophore structure (–N=N–) by ozone. Another possibility is that this commercially available dye has two hues with the one at 525 nm masking the other. It may be due to breaking up of original dye in to some other molecule giving a different hue.

It has been observed from Figure 7.8 that there is no shift in wavelength corresponding to the maximum absorbance showing that ozonation of direct blue dye solution finally yields a colourless solution. The indicators of another peak leading to the UV range may correspond to the intermediate organic products of ozonation reactions.

Other researchers have also reported the peak absorbance for this dye in the vicinity of what we observed (Kozakova et al. 2010; Saroj et al. 2014) where this wavelength should not correspond to red colour. After initial ozone reactions, the red coloured dye is perhaps first released showing the second peak at 760 nm, and then get oxidized further. The ozonation results well agree with those of other investigators (Paprocki et al. 2010; Lu et al. 2009; Tehrani Bagha et al. 2010; Faria et al. 2009), but the intermediate reaction products need to be analysed to confirm our hypothesis.

7.1.5 Kinetic studies

An attempt was made to develop an analytical model to represent the reaction kinetics the details of which are presented below.

The reaction of ozone with solute A may be described as equation 7.1.

$$A + O_3 \rightarrow A_{oxid} \quad \textbf{.....(Eq. 7.1)}$$

Assuming the reaction to be first order with respect to ozone and solute A which can be formulated as equation 7.2.

$$\frac{d[A]}{dt} = k_A [O_3][A] \quad \textbf{.....(Eq. 7.2)}$$

Where, k_A is the rate constant for decolourization of dye solution by ozone.

The oxidation with ozone comes from either molecular ozone or hydroxyl free radicals. Equation 7.2 can be rewritten as equation 7.3.

$$d[A] = kO_3[A][O_3] + k_{OH}[A][OH^o] \text{ ……..……..……(Eq. 7.3)}$$

Where, (A) is the concentration of dye in the solution. (O) and (OH^-) are the concentrations of ozone and hydroxyl radicals, k_O and k_{OH} are the corresponding rate constants.

The concentration of ozone and hydroxyl free radicals is assumed to be constant i.e. the concentration of ozone and hydroxyl free radicals to be constant. Equation 7.4 can be arranged as equation 7.4.

$$d[A] = kO_3[A][O_3] + k_{OH}[A][OH^o] = -k[A] \text{ ……..(Eq. 7.4)}$$

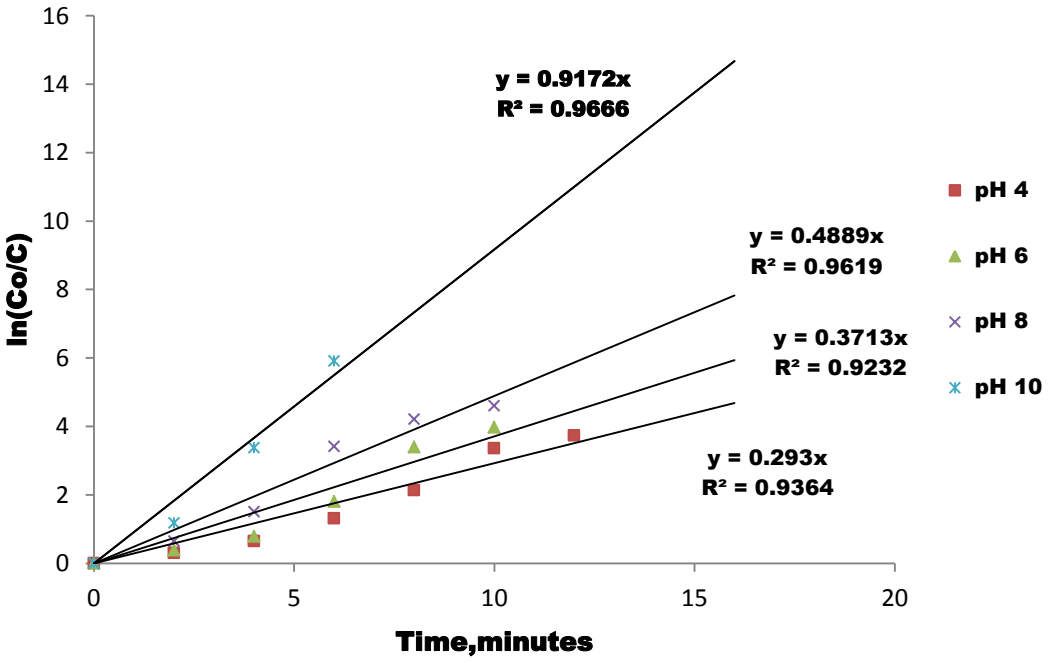

Figure 7. 9 Rate of degradation of direct red dye by ozone [Ozone dosage-27.5 mg/l, Ozone flow rate-2 LPM]

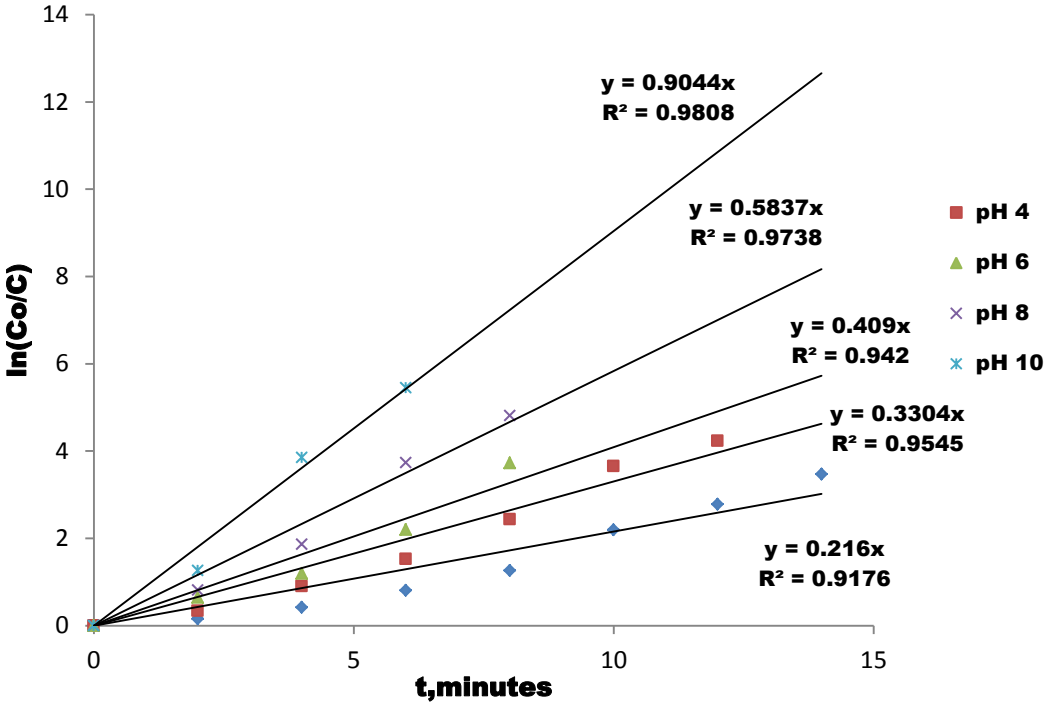

Figure 7.10 Rate of degradation of direct blue dye by ozone

[Ozone dosage-27.5 mg/l, Ozone flow rate-2 LPM]

Table 7.1 Pseudo first order constant for decolourization of direct red dye

Ozone dosage, mg/l	Initial concentration of dye, mg/l	pH	Pseudo first order constant k, min^{-1}	R^2
27.5	50	4	0.293	0.936
		6	0.371	0.923
		8	0.488	0.961
		10	0.917	0.966

Table 7.2 Pseudo first order constant for decolourization of direct blue dye

Ozone dosage, mg/l	Initial Conc. of dye, mg/l	pH	Pseudo first order constant k, min^{-1}	R^2
27.5	50	4	0.330	0.954
		6	0.365	0.955
		8	0.583	0.973
		10	0.904	0.980

The decolourization rate at different pH for direct red and direct blue dye is shown in Figure 7.9 & 7.10 respectively. The pseudo first order constants at various pH is given in Table 7.1 & 7.2 for direct red and direct blue dye respectively. The applicability of pseudo first order model to the decolourization of direct red and direct blue dye with respect of various pH of the dye solution has been confirmed by high value of regression coefficient. The similar studies were conducted by other researchers who also found these reactions to be of the first order (Usharani et al. 2012; Khan et al. 2010; Shawaqfaha et al. 2012; Lafi et al. 2006).

7.1.6 Chemical Oxygen Demand Reduction

The chemical oxygen demand variations of direct red and direct blue dye with time for various initial concentrations of dye are given in Figs. 7.11 and 7.12 respectively.

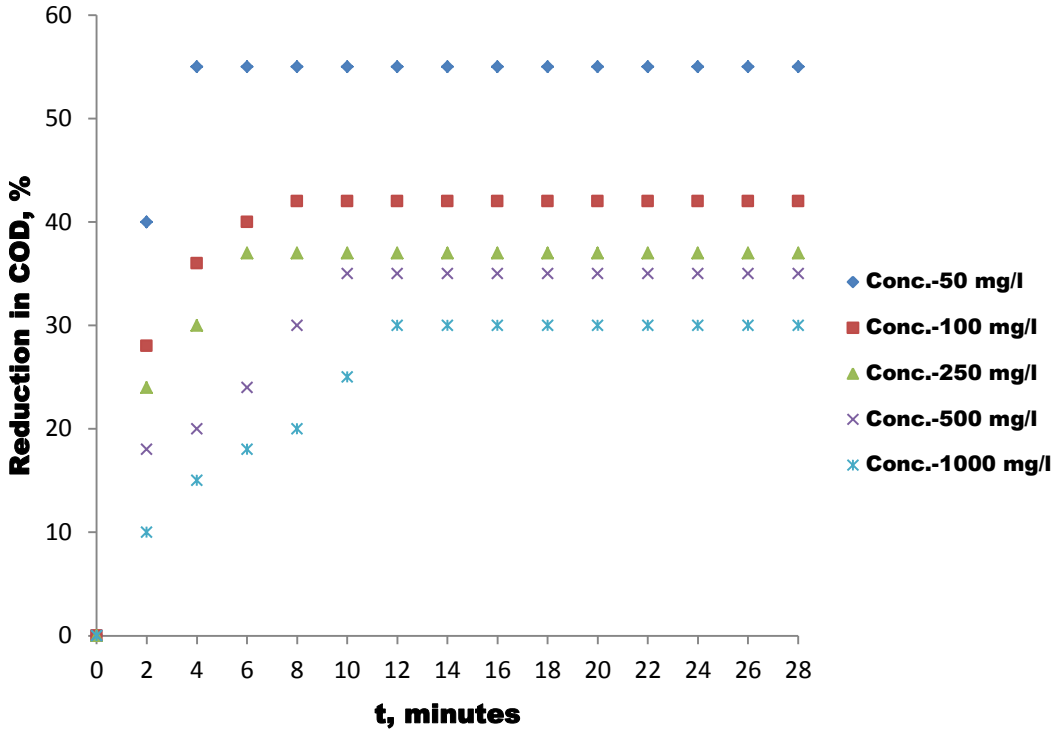

Figure 7. 11 Reduction in COD of direct red dye

[Ozone dosage-27.5 mg/l, Ozone flow rate-2 LPM]

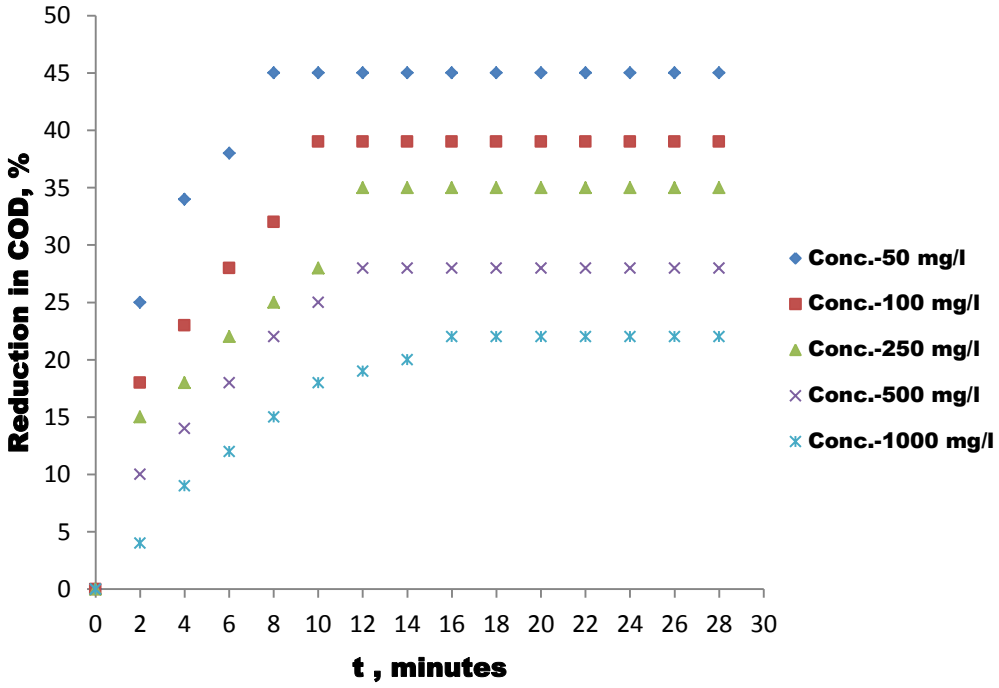

Figure 7.12 Reduction in COD of Direct Blue dye

[Ozone dosage-27.5 mg/l, Ozone flow rate-2 LPM]

The maximum COD reduction for direct red dye solution is 54% while it is 45% for direct blue dye. The studies conducted by other researcher showed maximum 68% reduction of COD with Congo red dye (Tapalad et al. 2008; Choi et al. 2004). The formation of nonreactive intermediates of the reaction is probably not allowing COD to reduce further, which is a cause of concern and has to be studied in details. It has been observed that the ozonation efficiency is less for highly concentrated dyes in comparison to diluted dye solutions.

The chemical oxygen demand of direct red and direct blue dye at various ozone dosage is shown in Table 7.3. The chemical oxygen demand of direct red and direct blue at various ozone consumption is shown in Figure 7.13 and 7.14 respectively.

Table 7.3 COD of direct red and direct blue dye at various ozone dosage

Direct red dye				**Direct blue dye**			
O_3 fed, mg	O_3 cons., mg	O_3 cons., %	COD, mg	O_3 fed, mg	O_3 cons, mg	O_3 cons, %	COD, mg
0	0	0	255	0	0	0	300
60	59	98.33	153	60	58	98.33	225
120	115	95.83	140	120	118	96.66	198
180	165	91.66	114	180	150	83.33	185
240	190	79.16	114	240	200	83.33	166

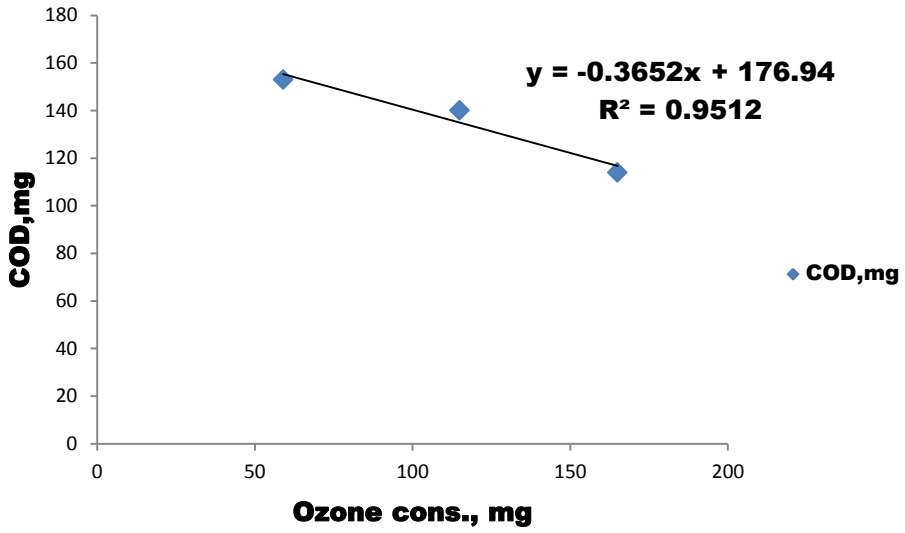

Figure 7.13 COD at various ozone consumption for Direct Red dye

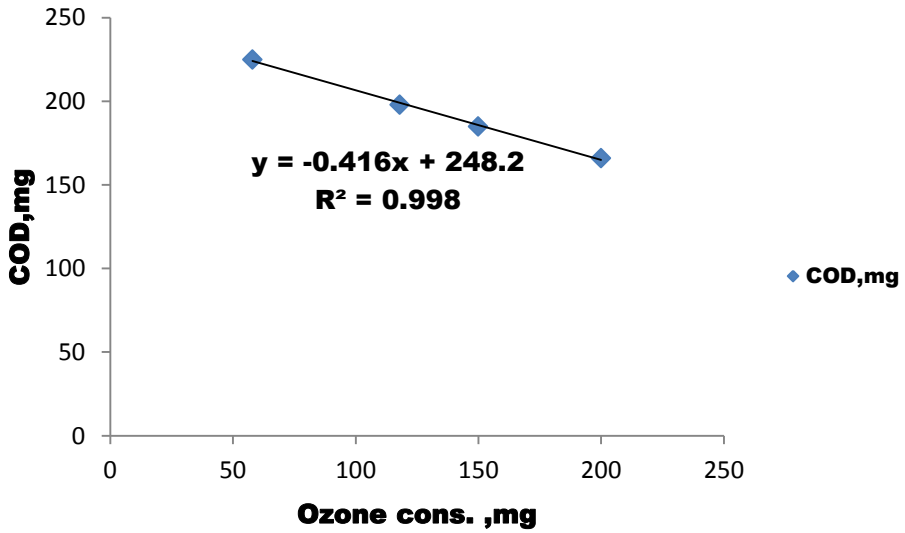

Figure 7.14 COD at various ozone consumption for Direct Blue dye

It has been observed from Figure 7.14 that 0.15 g O_3 /litre was consumed for 20% COD reduction. As per the studies conducted by Patricia A Terry, 2010, 0.318 g O_3/min/litre was consumed for 14.8% COD reduction having initial COD of 5244 mg/l. Tuin et al. 2004 found requirement of about 3 kg O_3 per m^3 for about 80-90% COD removal.

7.2 Semi batch studies on ozonation treatment of black liquor of Banana

7.2.1 Effect of pH of black liquor during ozonation

The black liquor of banana fiber obtained after alkaline peroxide pulping (8% APP) was diluted to 3.5% for further studies. The ozone dosage was 15 mg/l and flow rate of ozone gas was maintained at 2 LPM by setting the flow rate of concentrated oxygen. The samples were collected after every 10 minutes. The reduction in lignin and decolourization of black liquor with time is shown as Figures 7.15 & 7.16.

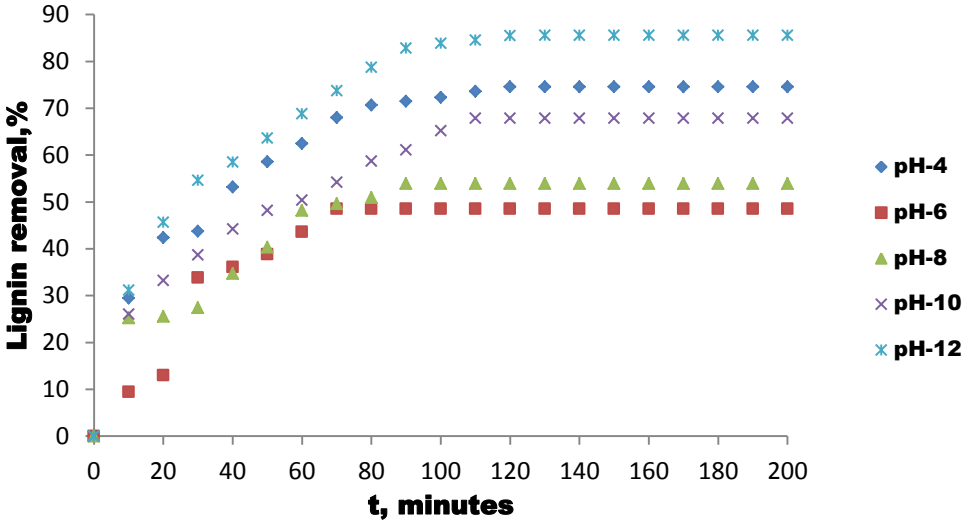

Figure 7.15 Lignin removal of black liquor of banana fiber at various pH and time

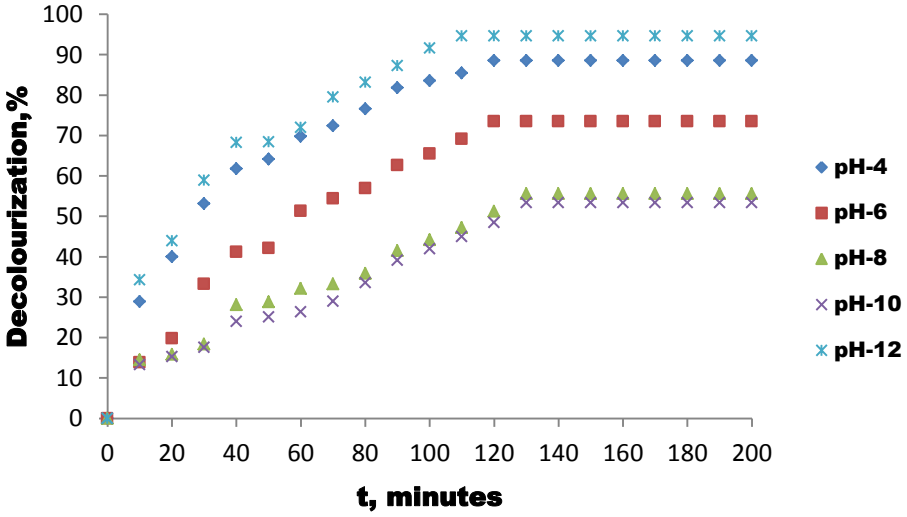

Figure 7.16 Decolourization of black liquor of banana fiber at various pH

The ozonation efficiency was found to be higher at pH of 12, which is in agreement with the studies conducted by other researchers (Meza et al., 2010). This is due to the increase in the number of hydroxyl radicals at high pH (Mandavgane and Yenkie. 2011). These radicals exhibit a much higher reaction rate than molecular ozone (Gomes et al. 2012).

7.2.2 Effect of pH on Ozone consumption

The ozone consumption at various pH values ranging from 4, 6, 8, 10, and 12 is given in Table 7.4 and Figure 7.17.

Table 7.4 Effect of pH on ozonation

		Ozone consumed, mg				
Time, minutes	**Feed Ozone, mg**	**pH-4**	**pH-6**	**pH-8**	**pH-10**	**pH-12**
10	57.6	24.53	20.25	18.27	17.25	30.05
20	115.2	98.45	75.29	50.45	44.58	99.48
30	172.8	159.21	100.78	88.65	75.39	160.08
40	230.4	211.82	149.81	101.24	92.78	215.78
50	288	273.95	200.18	154.97	101.79	273.99
60	345.6	337.66	258.65	199.78	197.85	338.44
70	403.2	382.36	299.48	257.19	209.79	388.78
80	460.8	396.89	321.58	287.49	250.68	425.81
90	518.4	435.29	398.54	305.79	275.81	475.49
100	576	505.26	438.47	389.74	321.87	548.76
110	633.6	530.28	497.48	411.56	394.84	612.84
120	691.2	580.26	500.99	490.72	458.76	659.18
130	748.8	659.56	546.27	538.35	511.99	728.09
140	806.4	729.87	621.32	600.79	575.18	779.84
150	864	809.45	721.42	658.38	600.47	849.84
160	921.6	899.26	798.51	711.82	666.84	900.57

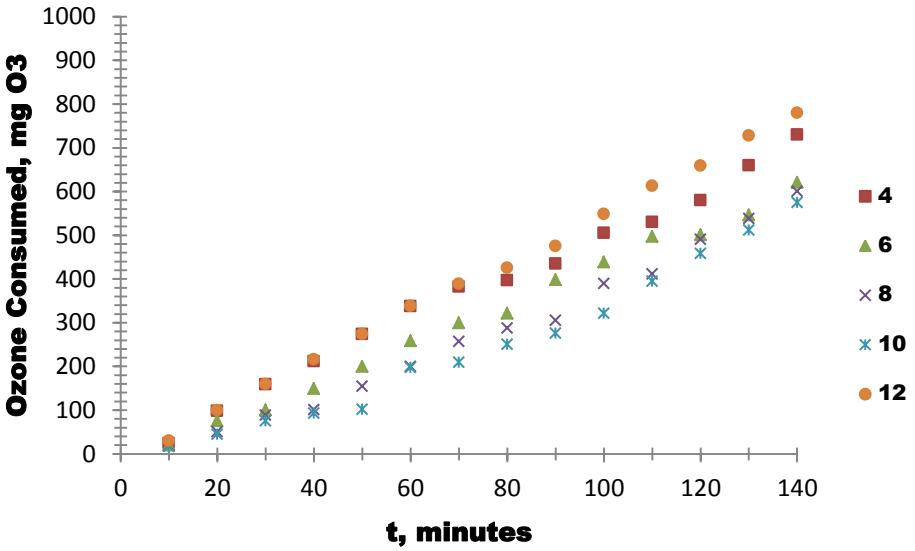

Figure 7.17 Ozone consumption by black liquor of banana fibre

The maximum ozone consumption was observed at pH-12 which is well in agreement with the maximum decolourization efficiency of ozone at pH-12.

7.2.3 Effect of dilution of black liquor during ozonation

The black liquor was diluted to different volume for the studies. The ozone dosage was 15 mg/l and flow rate of ozone gas was maintained at 2 LPM by setting the flow rate of concentrated oxygen. Samples were collected after every 10 minutes. The reduction in lignin and decolourization of black liquor during ozonation treatment is shown in Figures 7.18 &7.19 respectively.

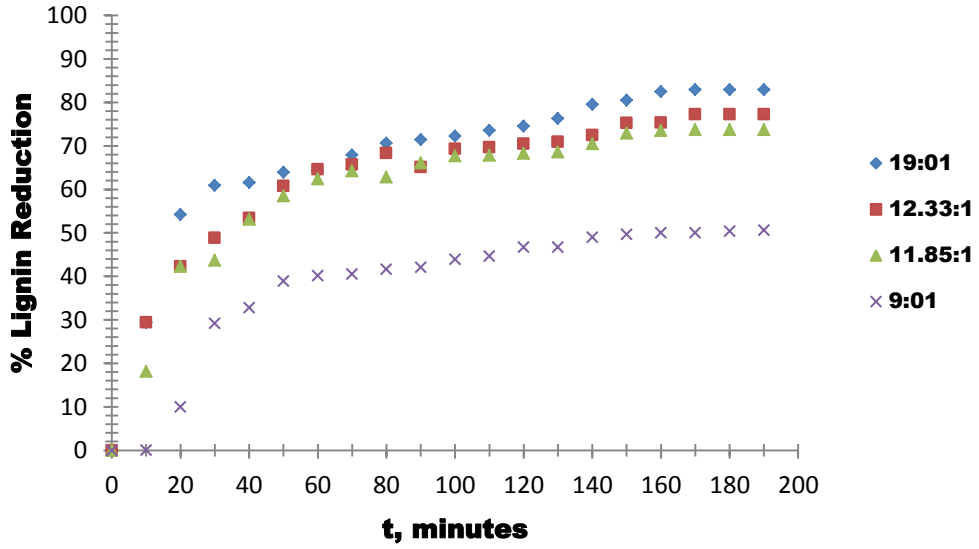

Figure 7.18 Reduction of lignin of black liquor at various dilutions

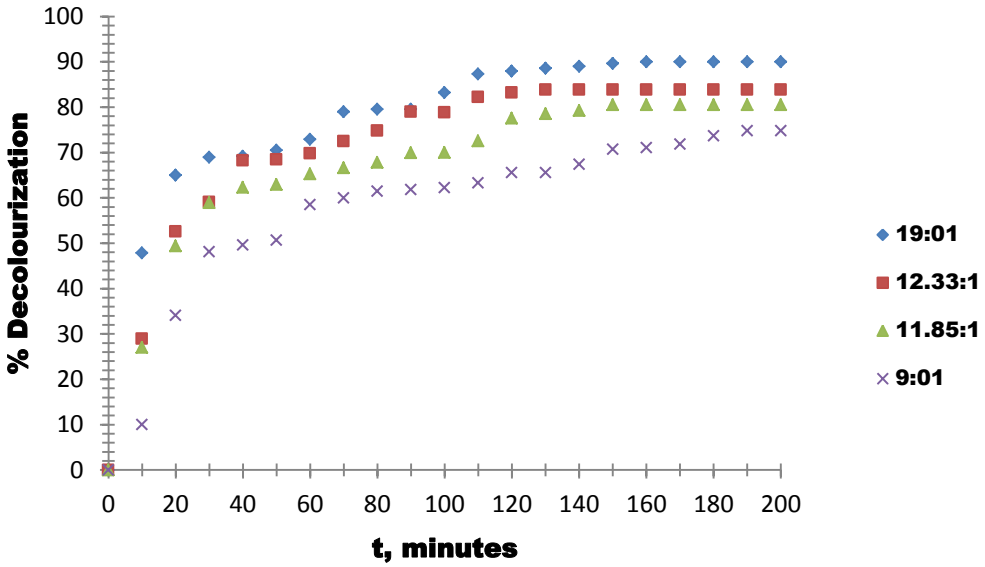

Figure 7.19 Decolourization of banana black liquor at various dilutions

It has been observed that there is no significant reduction in lignin and colour after 11 times dilution. The relationship between ozone consumption and chemical oxygen demand of black liquor at 11 times dilution is shown in Figure 7.20.

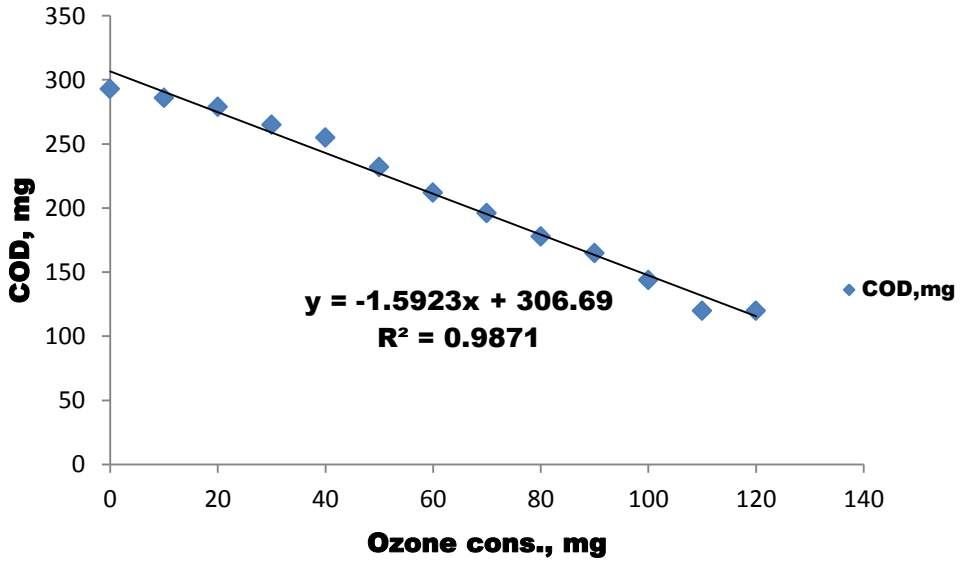

Figure 7.20 Ozone consumption vs. COD of banana black liquor

It has been observed from Figures 7.19 & 7.20 that there is a significant reduction in lignin and colour after 11 times dilution. So, it is advisable to dilute the black liquor prior to ozonation treatment for higher decolourization and lignin removal of black liquor.

7.3 Bubble Column studies

The effect of parameters including the ratio of flow rate of water and ozone, and height of the column has been studied for bubble column studies.

7.3.1 Effect of Ratio of flow rate of water and ozone

The studies have been conducted at various flow rate of wastewater varying from 0.1 to 0.5 LPM at fixed dosage of ozone i.e. 1 LPM. The graph is shown as Figure 7.21.

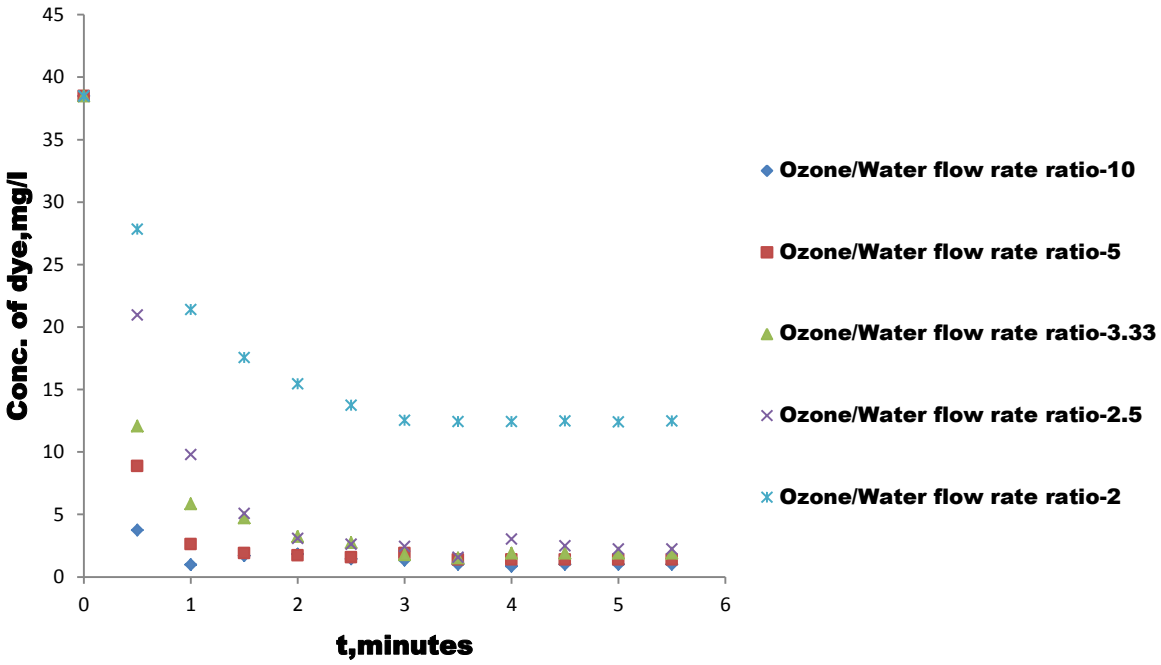

Figure 7.21 Effect of ratio of ozone and wastewater on ozonation efficiency

From Figure 7.21, it can be seen that a decrease in concentration of dye has been observed at ozone to water flow ratio of 10. However, there is only marginal difference in this ratio of flow rate of ozone to liquid from 10 to 2.5. But, beyond this value, the decrease in concentration was found to be quite low.

7.3.2 Effect of height of column

The effect of height of bubble column on the decolourization efficiency of ozone was studied and the results are shown in Figure 7.22.

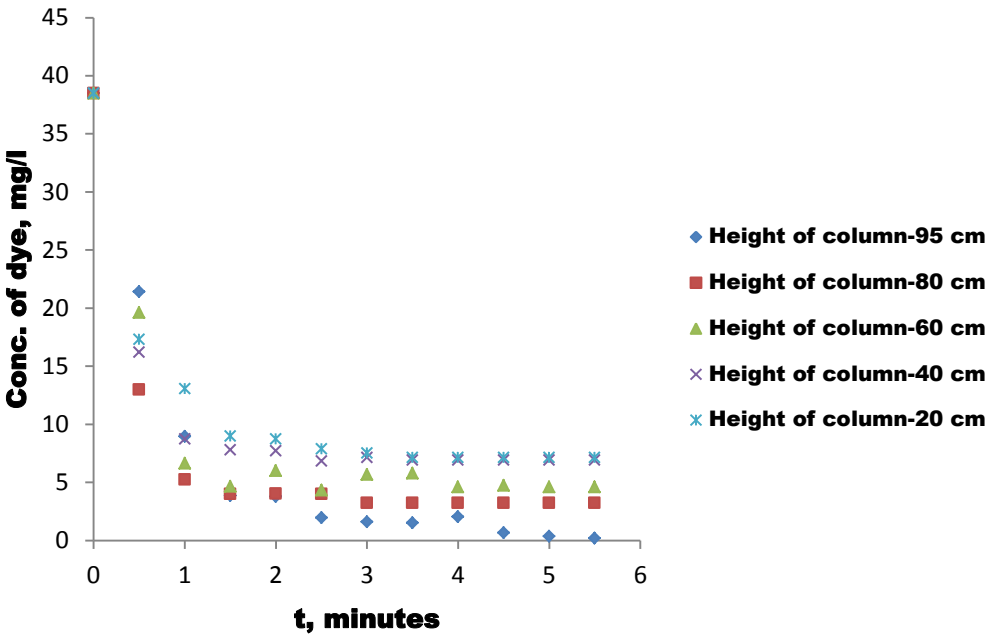

Figure 7.22 Effect of height of column on decolourization of dye

From Figure 7.22, it is observed that maximum decolourization efficiency of ozone is at height of 95 cm. However, as the height of column decreases, the decolourization efficiency of ozone also decreases.

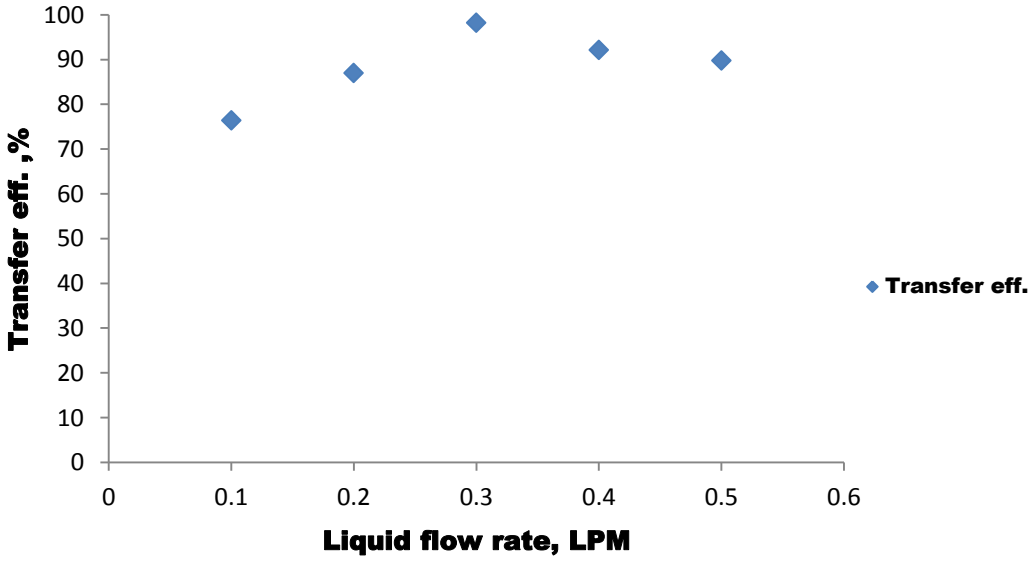

Figure 7.23 Ozone consumption at various height of column

It has been observed from Figure 7.23 that the maximum ozone transfer efficiency is achieved at the liquid flow rate of 0.3 LPM keeping constant flow rate of ozone-1LPM.

7.4 Response surface methodology

The response surface methodology was adopted to optimize the parameters of the bubble column study. The experimental ranges and levels of independent test variables are given as Table 7.5.

Table 7.5 Experimental ranges and levels of the independent test variables

Independent variables	Ranges and levels				
	-α	**-1**	**0**	**+1**	**+α**
Ratio of flow rate of O_3/H_2O	10	5	3.33	2.5	2
O_3 dosage, mg/L	5	10	15	20	27.5
Height of column, m	0.20	0.40	0.60	0.80	0.95

7.4.1 Experimental design

In this study, a Central Composite Design (CCD) based on response surface methodology (RSM) was used to obtain an appropriate mathematical model for prediction of the behavior of the process. The variables such as waste water flow rate, ozone dosage, height of column were selected as independent variables. As shown in Table 7.6, the ozone concentration ranged from 5.0 to 27.5 mg/L, water flow rate ranged from 0.1 to 0.5 LPM and height of column ranged from 0.20 cm to 0.95 m. The analysis of variance is given as Table 7.7.

Table 7.6 Experimental design matrix with coded values and observed responses

Runs	Ratio of flow rate of O_3/H_2O	O_3 dosage, mg/l	Height of point of injection of O_3 dosage	Exp. Decol. %	Pred. Decol. %
		Coded values			
1	-1	-1	-1	73.34	72.46
2	1	-1	-1	64.45	63.54
3	-1	1	-1	75.76	73.65
4	1	1	-1	65.54	68.98

5	-1	-1	1	72.81	70.65
6	1	-1	1	70.41	72.76
7	-1	1	1	89.51	87.54
8	1	1	1	80.89	78.98
9	-1.682	0	0	75.76	79.67
10	1.682	0	0	60.37	63.21
11	0	-1.682	0	71.56	73.21
12	0	1.682	0	91.54	88.09
13	0	0	-1.682	72	69
14	0	0	1.682	90.5	88.98
15	0	0	0	64.45	68
16	0	0	0	64.45	68
17	0	0	0	64.45	68
18	0	0	0	64.45	68
19	0	0	0	64.45	68
20	0	0	0	64.45	68

Table 7.7 Analysis of variance

Source	Sum of squares	DF	Mean Square	F Value Calculate	p- value Prob.>F
Model	1659.23	9	184.36	30.80	< 0.0001
A	35.60	1	35.60	5.95	0.0349
B	47.43	1	47.43	7.93	0.0183
C	2.62	1	2.62	0.44	0.5229
AB	7.13	1	7.13	1.19	0.3008
AC	8.18	1	8.18	1.37	0.2695
BC	70.03	1	70.03	11.70	0.0065
A^2	8.23	1	8.23	1.38	0.2680
B^2	406.17	1	406.17	67.86	< 0.0001
C^2	390.23	1	390.23	65.20	< 0.0001
Residual	59.85	10	5.99		
Lack of fit	59.85	5	11.97		

Pure error	0.000	5	0.000		
Cor Total	1719.08	19			
Std. Dev.	2.45			**R-Squared**	0.9652
Mean	72.06			**Adj. R-Squared**	0.9338
C.V. %	3.40			**Pred R-Squared**	0.7402
PRESS	446.63			**Adeq. Precision**	18.9204

The model F-value of 30.80 implies the model is significant. There is only a 0.01% chance that an F-value this large could occur due to noise. The values of "Prob > F" less than 0.05 indicate model terms are significant. In this case A, B, BC, B^2, C^2 are significant model terms. The values greater than 0.10 indicate the model terms are not significant. The "Pred. R-Squared" of 0.7402 is in agreement with the "Adj. R-Squared" of 0.9338. The parameters at which maximum decolourization was achieved is given in Table 7.8.

Table 7.8 Maximized process parameters

Water flow rate, LPM	Height , m	Ozone dosage, mg/l	Decolourization, %
0.102	0.887	27.5	92.95

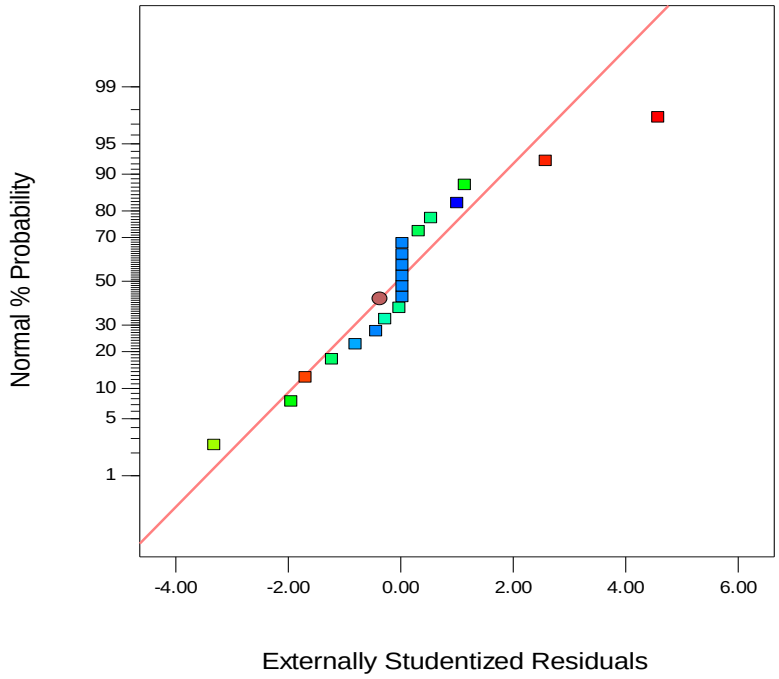

Figure 7.24 Normal probability plot of residuals

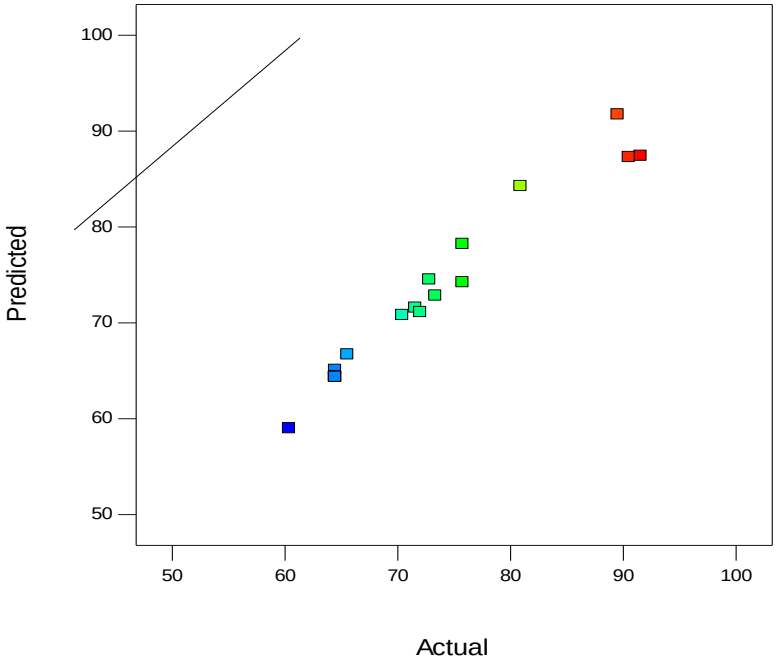

Figure 7.25 Plot of Residuals vs. Predicted response

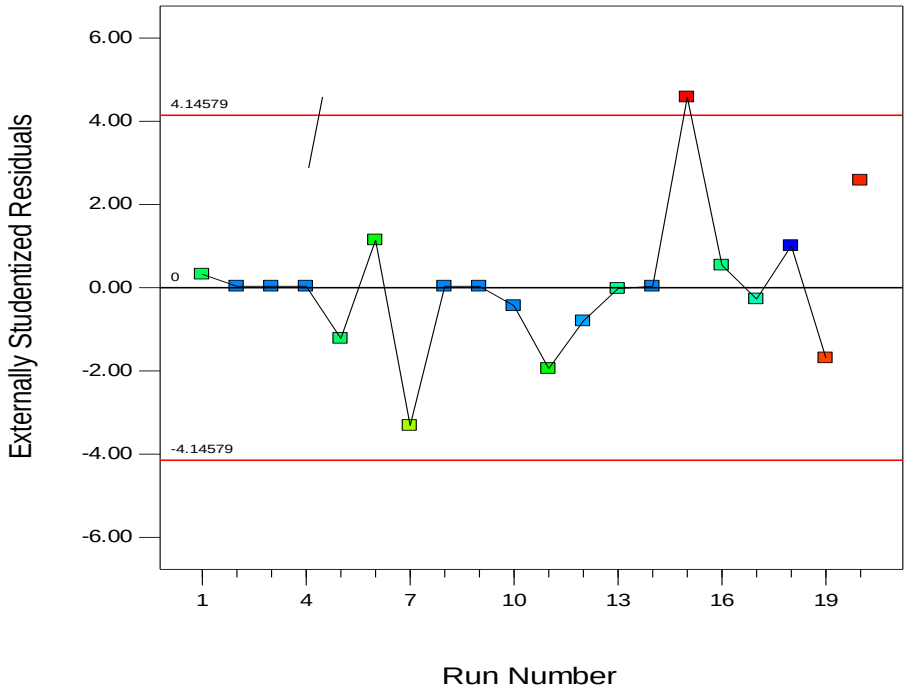

Figure 7.26 Residual vs. Run

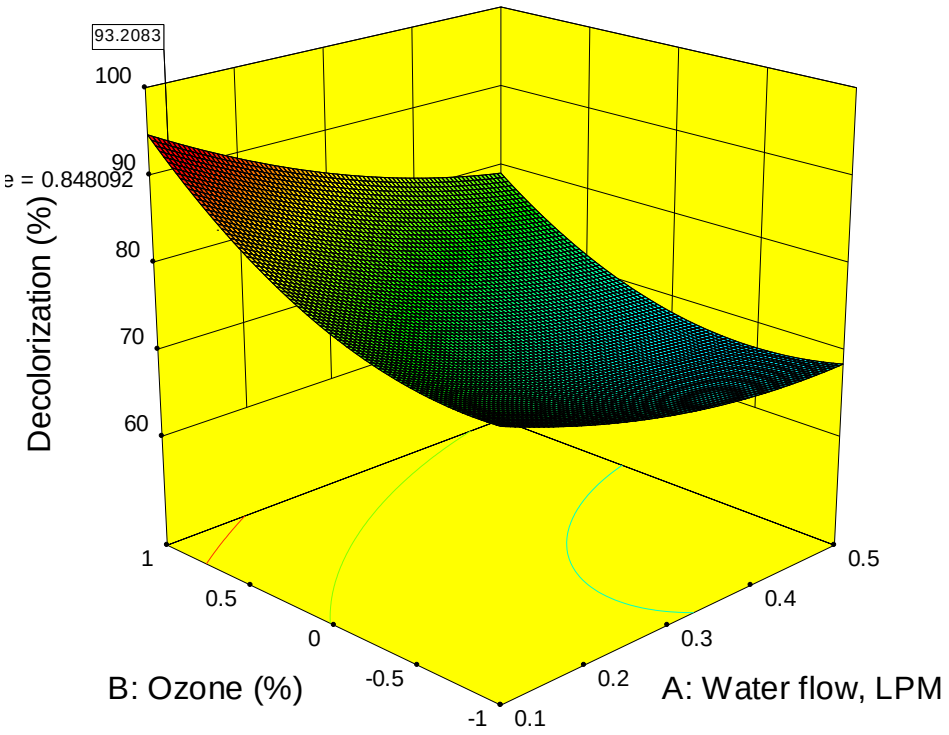

Figure 7.27 Decolourization of dye with ozone dose and water flow

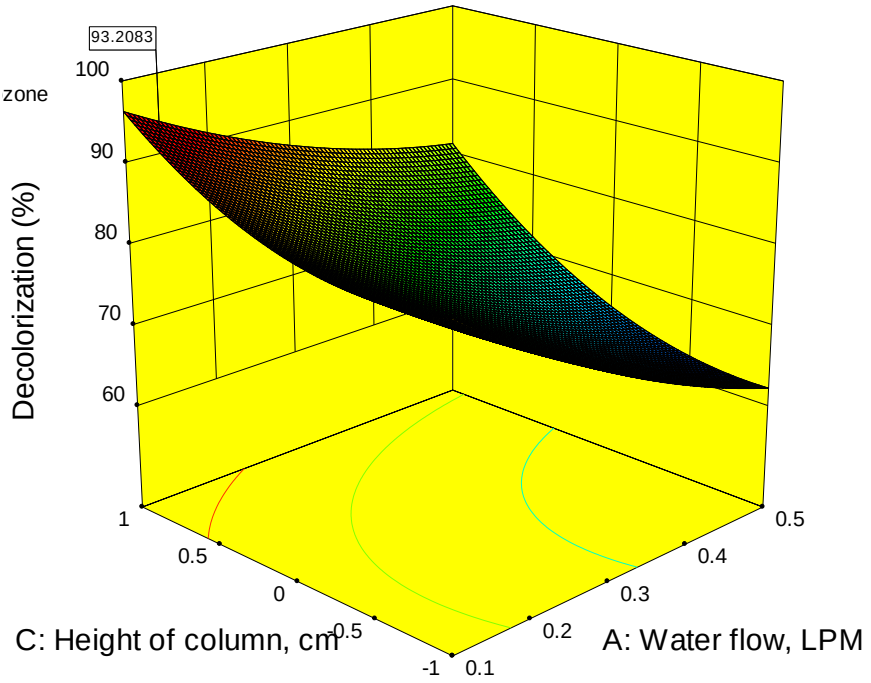

Figure 7.28 Decolourization of dye with height of column and water flow

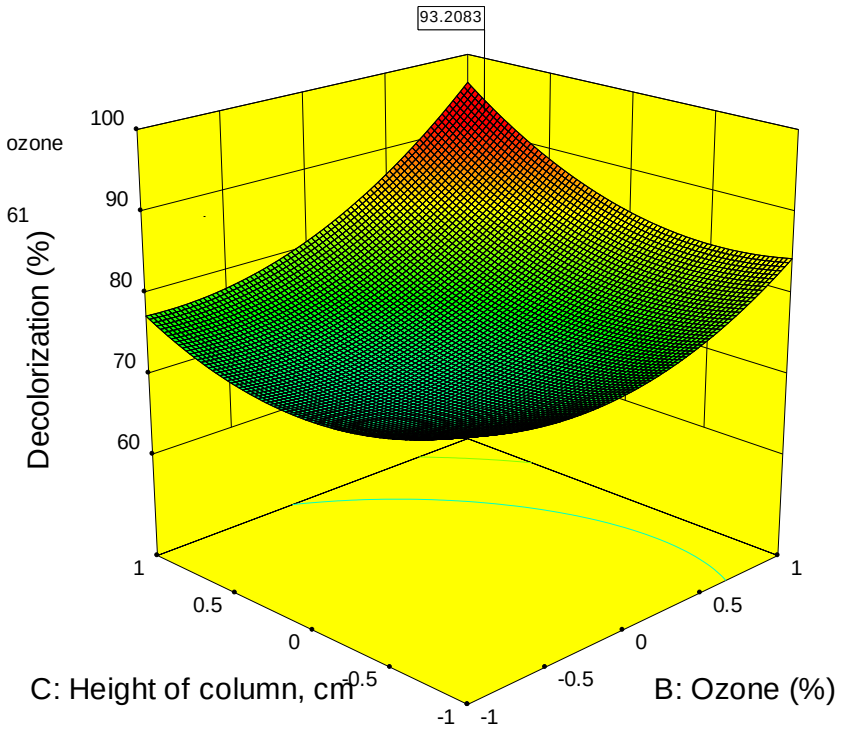

Figure 7.29 Decolourization of dye at various height of column and ozone dosage

From Figures 7.26, 7.27 & 7.29, depict decolourization at various ozone dosage and water flow; water flow and height of column; height of column and ozone dosage. The maximum values of decolourization have been achieved at parameters given in Table 7.9.

Table 7.9 Optimized process parameters

Parameters	Maximum value	Std. error	Desirability
Water flow, LPM	0.103	3.076	1.0
Ozone dosage, mg/l	22.17		
Height of column, m	0.999		
Decolourization,%	91.51		

The optimum value of parameters for maximum decolourization is given in Table 7.9. The relationship between decolourization and affecting parameters is given as equation-7.5.

Decolourization, % = + 80.86 - 71.89*Water flow, LPM + 7.54*Ozone dose, mg/L + 1.77*Height of column - 9.44*Water flow, LPM * Ozone dosage + 10.11* Water flow, LPM * Height of Column + 2.96 * Ozone dosage * Height of column + 56.36* Water flow, LPM^2 + 5.35*$Ozone^2$ + 5.25*Height of $column^2$..... ……(Eq. 7.5)

7.5 Bubble diffusion contactor

The bubble diffusion contactor for ozonation treatment is shown in Figure 7.30. The gas is fed with the help of sparger at bottom and liquid is fed through top.

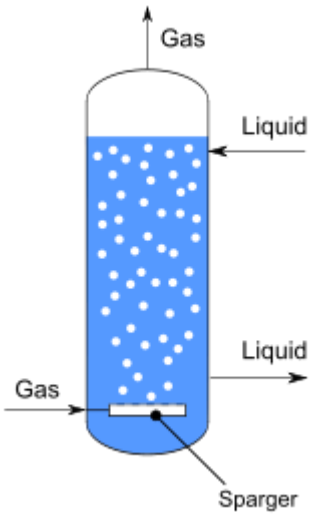

Figure 7.30 Countercurrent bubble ozonation column

Process

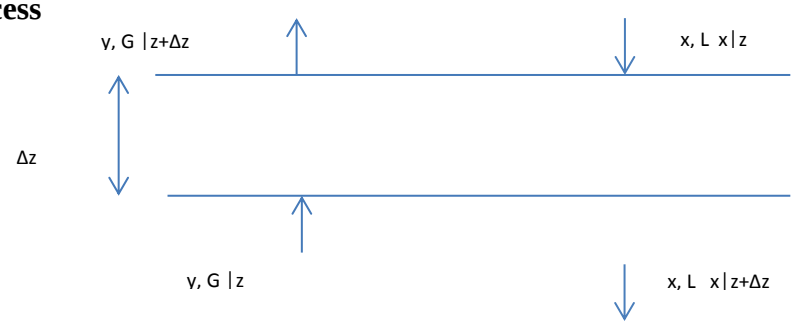

Figure 7.31 Process diagram of gas and liquid flow in bubble column

The factors for ozonation model include system hydrodynamic behavior; Gas liquid mass transfer; Ozonation reaction kinetics & Ozone self-decomposition kinetics.

7.6 Development of mathematical model for ozonation

The mathematical model for ozonation was developed with following assumptions:

Assumptions

- Gas flow rate and liquid flow rate in the column is considered constant throughout the column.
- Interfacial area and gas holdup are constant along the height of the column.
- Henry's law applies.

  Ozone decay rate is pseudo-first-order in the liquid phase.
- The experiments are performed under isothermal conditions.
- Mixed flow conditions considered for ozone gas. The liquid phase considered perfectly mixed.
- The concentration of ozone considered constant throughout the column.

7.6.1 Model Equations

The model equations for ozone in gas phase, ozone in liquid phase and ozone in dye solution is given as equation 7.6, 7.7 & 7.8.

For Ozone in gas phase

$$\frac{\partial C_G}{\partial t} = \frac{U_G}{\varepsilon_G}\frac{\partial C_G}{\partial z} - \frac{k_{La}}{\varepsilon_G}(C_L^{\,*} - C_L) \quad \text{.....(Eq. 7.6)}$$

For Ozone in Liquid phase

$$\frac{\partial C_L}{\partial t} = \frac{U_L}{(1-\varepsilon_G)}\frac{\partial C_L}{\partial z} + \frac{k_{La}(C_L^{\ *} - C_L)}{(1-\varepsilon_G)} + D_L\frac{\partial^2 C_L}{\partial z^2} + rO_3 \quad \textbf{.....(Eq. 7.7)}$$

For Dye in solution

$$\frac{\partial C_d}{\partial t} = \frac{U_L}{(1-\varepsilon_G)}\frac{\partial C_d}{\partial z} + D_d\frac{\partial^2 C_d}{\partial z^2} + r_d \quad \textbf{.....(Eq. 7.8)}$$

Where,

r_d- dye reaction rate, mg/L/s

C_L* is the equilibrium concentration of ozone in liquid phase, which is in equilibrium with the gas phase

Initial conditions

At t=0, 0<z<L

$C_d=C_{din,}$ $C_L=0$, $C_G=0$

Boundary conditions

At z=0, t>0

$$U_L C_{Lin} = -(1-\varepsilon_G)E_L\frac{\partial C_L}{\partial z} + U_L C_L$$

$$U_G C_{Gin} = -\varepsilon_G E_G\frac{\partial C_G}{\partial z} + U_G C_G$$

$$U_L C_{din} = -(1-\varepsilon_G)E_d\frac{\partial C_d}{\partial z} + U_L C_d$$

$$\text{at } z = L, \frac{\partial C_L}{\partial z} = 0$$

$$\frac{\partial C_G}{\partial z} = 0$$

$$\frac{\partial C_d}{\partial z} = 0$$

7.7 Determination of Reaction rate of degradation reaction of the dye when ozone is in excess and dye is limited

The reaction rate of degradation of dye was determined in semi-batch mode when ozone is in excess and dye is limited. The studies were conducted with dye of initial concentration of 40 mg/l and inlet ozone concentration was 9.5 mg/l with ozone flow rate of 1 LPM.

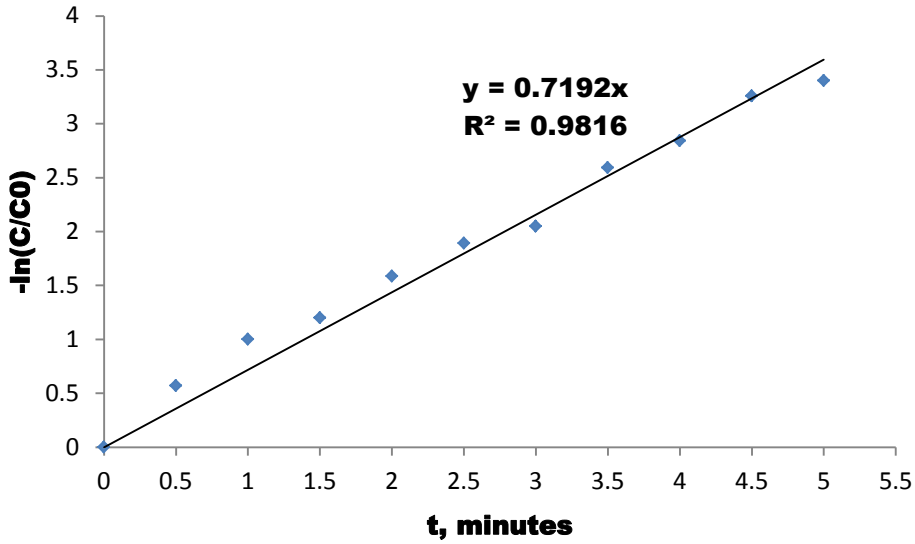

Figure 7.32 Kinetics of dye degradation by ozone
[Inlet ozone=9.5 mg/l, Ozone flow rate= 1LPM, Inlet conc. of dye=40 mg/l]

From Figure 7.32, the kinetics of dye degradation is 0.7192 min^{-1}, when ozone is in excess.

7.8 Reaction rate of decomposition of ozone when the dye is in excess

The reaction rate of decomposition of ozone was determined in batch mode when the dye is in excess. The studies were conducted with dye of initial concentration of 40 mg/l, inlet ozone concentration was 27.5 mg/l, ozone flow rate of 1 LPM, Injecting time of ozone-10 second, amount of ozone injected of 4.583 g.

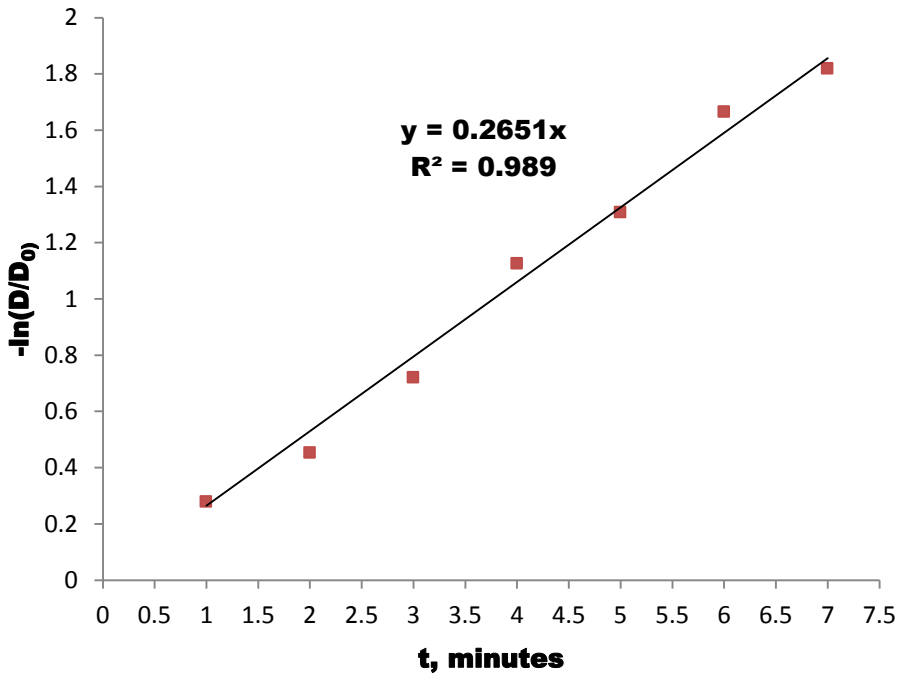

Figure 7.33 Kinetics of decomposition of ozone

[Inlet ozone-27.5 mg/l, Ozone flow rate- 1LPM, Injecting time of ozone-10 sec, Amount of ozone injected-4.583 g, Inlet conc. of dye-40 mg/l, Equilibrium dye conc.-22 mg/l]

From Figure 7.33, the kinetics of ozone decomposition is 0.2651 min^{-1}, when dye is in excess

7.9 First order kinetics at various molar concentration of turquoise blue dye

The first order relationship between first order constant of the kinetics of dye degradation at various initial moles of dye is shown in Figure 7.34.

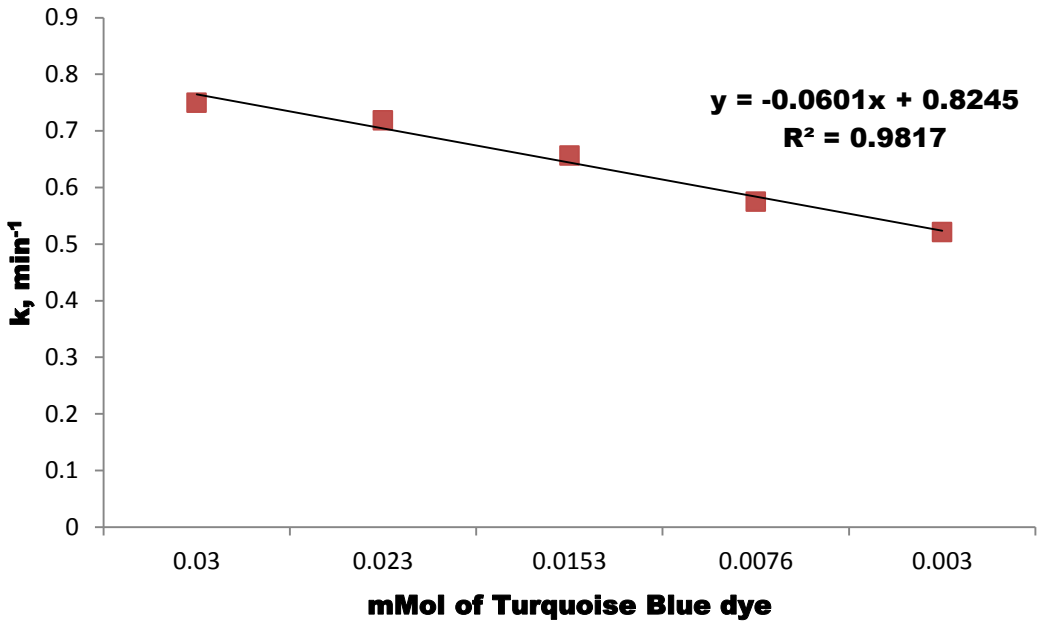

Figure 7.34 Kinetics of decomposition of ozone

The relationship between the various initial molar concentrations of dye with reaction rate constant of dye degradation is shown as Figure 7.34.

7.10 Total reaction rate with respect to ozone consumption

The relationship between total reaction rate and ozone consumption is shown in Figure 7.35.

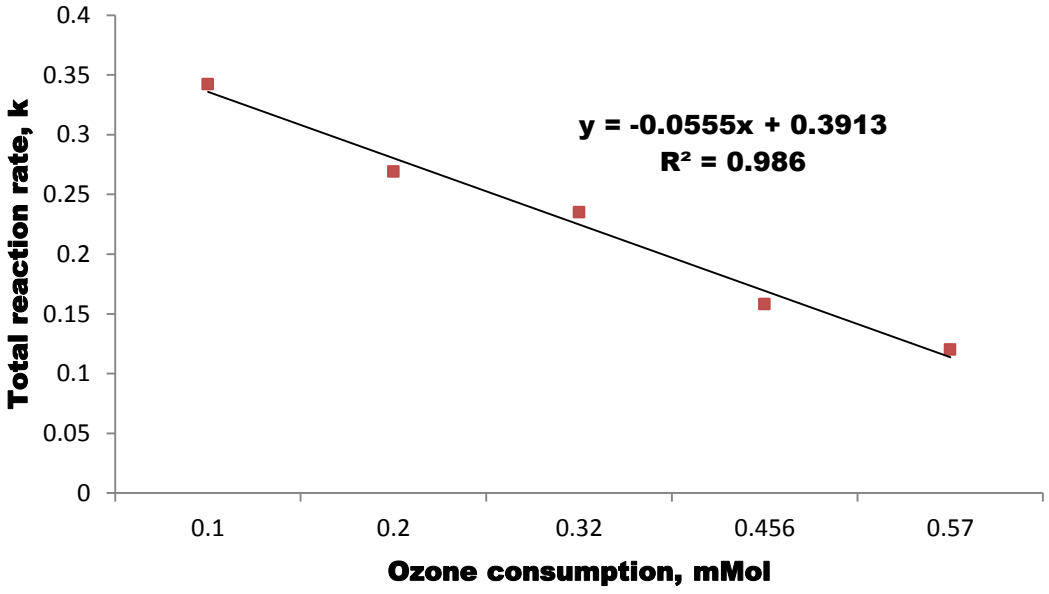

Figure 7.35 Total reaction vs. Ozone consumption

It has been observed from Figure 7.35 that the total reaction rate increases with the increase in ozone consumption.

7.11Stoichiometry ratio between ozone and dye

The stoichiometric ratio of ozone-dye decolourization reaction was determined in batch at an initial concentration of with limited ozone and dye in excess and is reported in Figure 7.36 at various initial concentration of dye. The reaction was stopped when the ratio of the decolourization of dyes reached over 95% and the ozone consumption was calculated after determination of residual ozone in dye.

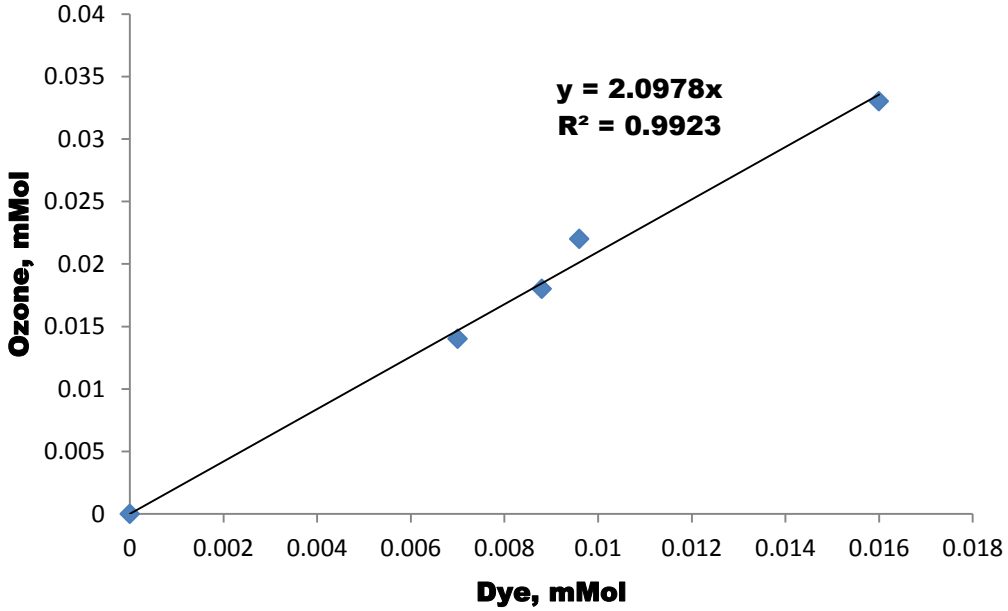

Figure 7.36 Total reaction rate vs. Ozone consumption

According to Figure 7.36, the stoichiometric ratio (n_{O3}/n_{dye}) was calculated to be approximately 2.09. As per the studies conducted by Kusvuran et al. 2010, the stoichiometric ratio (n_{O3}/n_{dye}) for BY28, MG, RB5 and RR1 was approximately 3.5, 7.1, 11 & 16.1 respectively.

7.12 Determination of Gas Hold up

The determination of gas holdup was measured with a volume expansion method. The equation was as follows:

$$\varepsilon_g = (1-\frac{V_0}{V})X100\% = (1-\frac{H_0}{H})X100\% \quad \text{..... (Eq. 7.9)}$$

Where g is gas holdup,

V_0 is valid water volume before aeration,

V is valid water volume after aeration,

H_0 is valid water height before aeration,

H is valid water height after aeration.

Table 7.10 Gas hold up at various height of bubble column

Height, cm	Height of standing water	Height of liquid and gas, cm	Gas hold up, , ε_g
20	37.8	39.1, 38.8	0.0332
40	47.3	49.3	0.0405
60	64.9	67.6	0.0416
80	80.7	84.6	0.0483
95	92.1	96.1	0.0434

From Table 7.10, it has been observed that the gas hold up increased with increase in height of the column.

7.13 Residence Time Distribution

RTD analysis is used to estimate axial dispersion coefficient from experimental tracer data which can be used to determine the mass transfer coefficient. In tracer studies, the tracer may be introduced as a pulse or as a step function. Tracer as a pulse has been introduced. The residence time distribution function E(t) of dye with time, and E(t) of dye with time (in presence of gas) is shown in Figure 7.37.

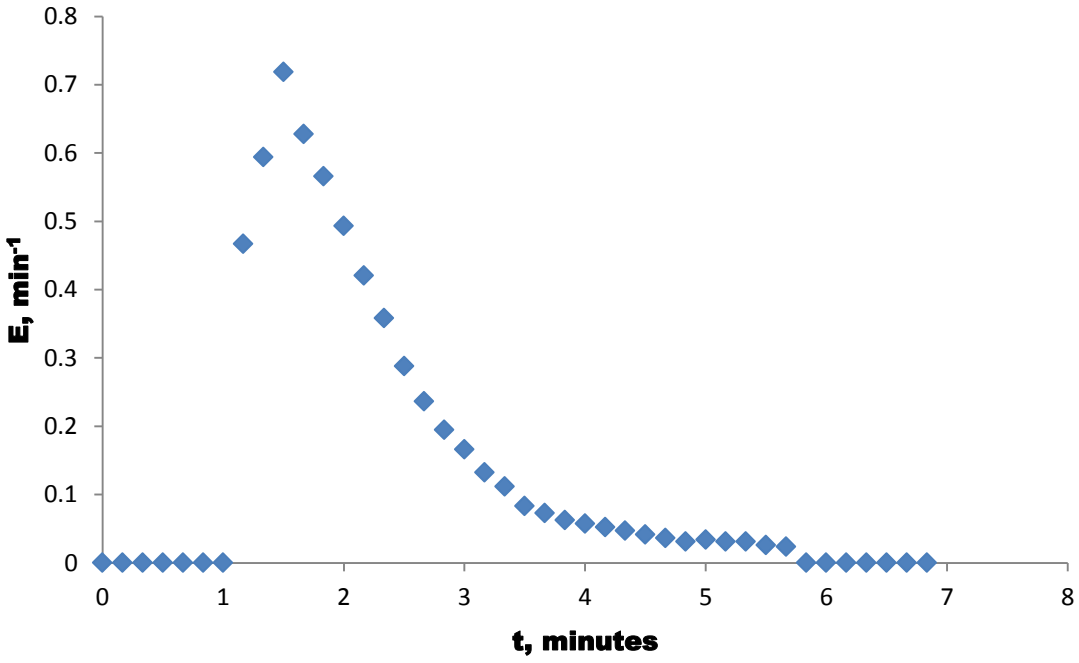

(a)

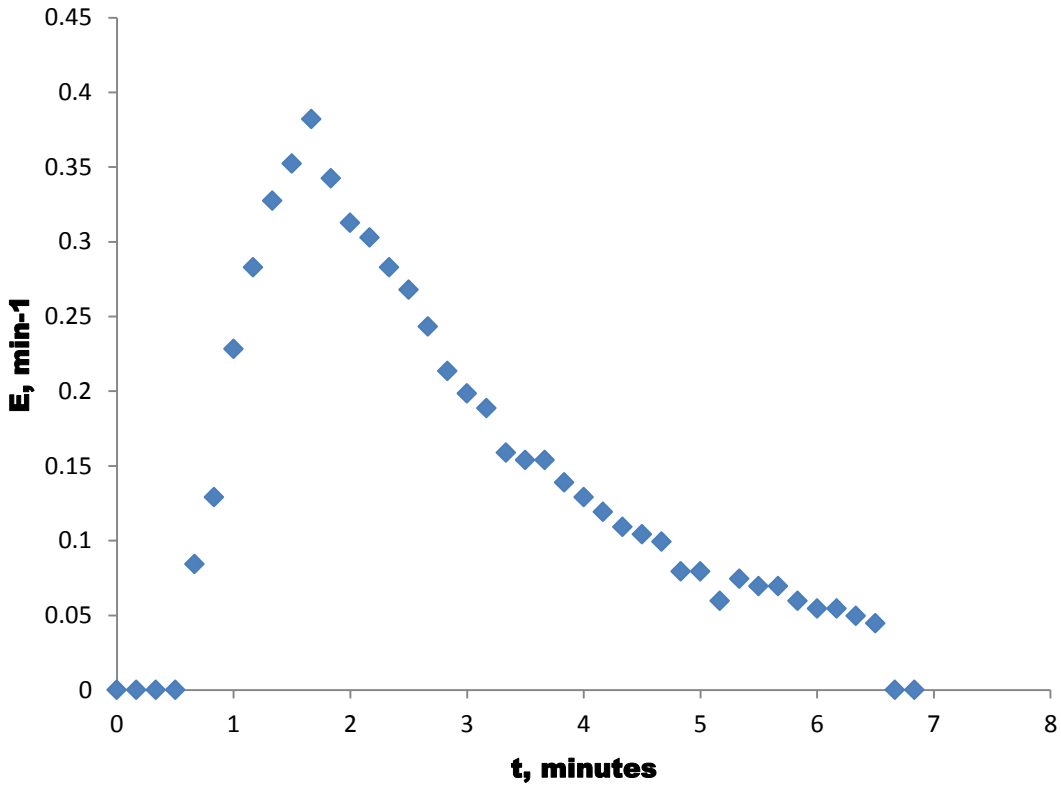

(b)

Figure 7.37 Residence time distribution function

(a) E(t) of dye with time, (b) E(t) of dye with time (in presence of gas)

Dispersion of dye

$$T_m = \frac{\int_0^\infty tCdt}{\int_0^\infty Cdt} = \frac{\sum t_i C_i \Delta t_i}{C_i \Delta t_i} \quad \text{.....(Eq. 7.10)}$$

$$\sigma^2 = \frac{\sum t_i{}^2 C_i \Delta t_i}{\sum C_i \Delta t_i} - t_m{}^2 \quad \text{.....(Eq. 7.11)}$$

Liquid flow rate, $m^3/s=6 \times 10^{-3}$, Gas flow rate, $m^3/s=60 \times 10^{-3}$

Table 7.11 Dispersion coefficient of dye

Particulars	T_m=Mean residence time, minutes	Variance =σ^2	Mean Time of passage, minutes	Peclet number=$2Tm^2/\sigma^2$	Dispersion coefficient.= U_L/P_e m^2/s
Dispersion of dye in presence of gas	2.744	2.0328	2.744	7.408	83×10^{-5} m^2/s
Dispersion of dye	2.189	0.874	2.189	10.965	56.5×10^{-5} m^2/s

The dispersion coefficient of dye in the presence of gas can be seen in Table 7.11. The studies conducted by other researchers (Ko et al. 1997) found a value of 0.056 at the liquid flow rate of 8.33×10^{-6} m^3/s and gas flow rate of 1.67×10^{-5} m^3/s.

7.14 Determination of Henry Coefficient

Markku Kuosa et al. 2006 found that the Henry constant depends on pH by the equation 7.12.

$$H = B_3 \left(\frac{pH}{pH_{ref}}\right)^{B4} \quad \text{.....(Eq. 7.12)}$$

Where,

pH_{ref} is reference value of pH

pH of 7 is taken as reference value.

B_3=7.161×10^6 $mol/m^3.Pa$ [Kuosa et al. 2004]

B_4=0.0297 (Kuosa et al., 2004)

For pH of 9 in our studies, the Henry coefficient determined was 7.161×10^6 $mol/m^3.Pa$. The Henry coefficient derived by other researchers is between 6×10^6 to 14×10^6 $mol/m^3.Pa$ [Miyahara et al. 1994; Beltran et al. 2001; Roth and Sullivan. 1981]

7.15 Determination of volumetric mass transfer coefficient

The volumetric coefficient was determined at ozone flow rate of 1LPM and turquoise dye concentration of 50 mg/l. The volumetric mass transfer coefficient can be determined by plotting a graph between ln φ vs. time as shown in equation 7.13 and Figure 7.38.

$$k_{La}\,t = \ln\left[\frac{(C_L{}^* - C_{L0})}{(C_L{}^* - C_L)}\right], \varphi = \frac{C_L{}^* - C_{L0}}{C_L{}^* - C_L} \quad \text{.....(Eq. 7.13)}$$

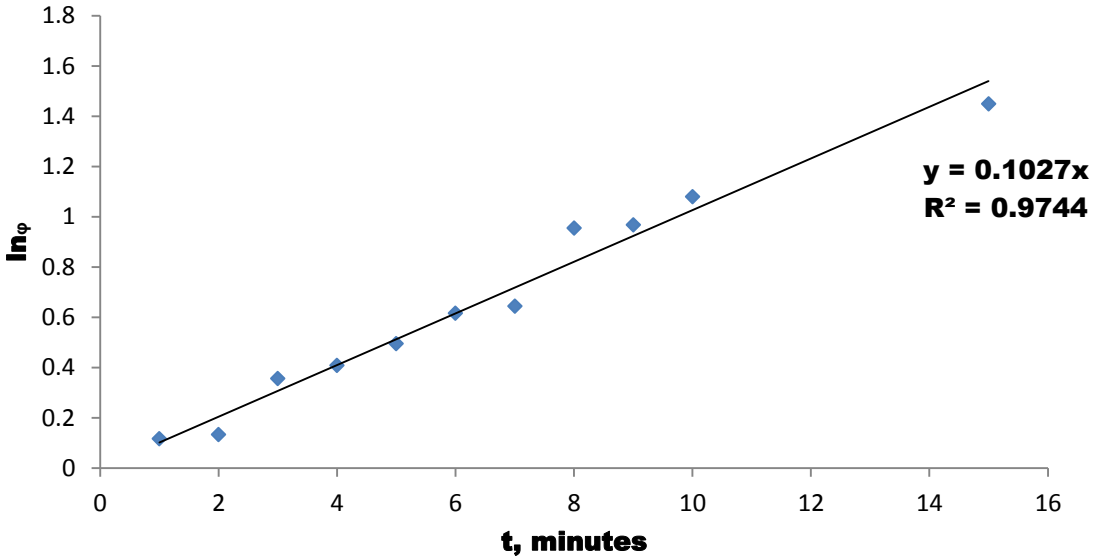

Figure 7.38 lnφ vs. time

k_{La}=0.1027 min^{-1}at

U_L= 200 ml/min=200 X 10^{-3} L/60s=200 X 10^{-6} m^3/60 s=0.33 X 10^{-5} m^3/s=0.33 X 10^{-5} X 4m^3/3.14* $(0.032m)^2$= 410 X 10-^{5} m/s=0.0041 m/s

U_L=0.0041 m/s=0.41 cm/s

U_G=1 LPM=1 X 10^{-6} m^3/60 s=4 X 10^{-6} m^3 /$(0.032m)^2$ X 60=65 X 10^{-6}

=.65 X 10^{-4} m/s=0.65 X 10^{-2} cm/s

k_{La}=0.452 X (0.3 X 10^{-5})$^{0.365}$ X (0.16 X 10^{-4})$^{0.628}$

=0.0919 X 10^{-4}

k_{La}=3.96X10^8(0.3X10^{-5})$^{1.5}$X(0.16X10^{-4})$^{0.4}$

=0.0311

Data

D_L= 83 x 10^{-5} m^2/s, D_d=56.5 x 10^{-5} m^2/s, D_G=2 x 10-^{5} m^2/s (Singer and Hull. 2000). Kinetics of dye degradation when ozone is in excess=0.7192 min^{-1}, Kinetics of ozone degradation when the dye is in excess=0.2651 min^{-1}

7.16 Modelling parameters for simulation

The modelling parameters for simulation of ozonation of turquoise blue dye in bubble column are shown in Table 7.12.

Table 7.12 Modelling parameters for simulation of ozonation in bubble column

Particulars	Value
Dispersion coefficient of dye in water, D_d m^2/s	56.5×10^{-5}
Dispersion coefficient of dissolved ozone in liquid, m^2/s	83×10^{-5}
Dispersion coefficient of ozone in the gas phase, m^2/s	2×10^{-5}
Gas hold up fraction, ε_G	0.0434
Henry constant, $mol/m^3.Pa$	7.214×10^{6}
Superficial velocity of ozone, m/s	0.02
Superficial velocity of liquid, m/s	0.004
Mass transfer coefficient, k_{La}, 1/s	0.1027

The model was validated with experimental values at various column heights ranging from 20 cm to 95 cm. The predicted value of the concentration of dye after Ozonation treatment was obtained after simulation studies with MATLAB software and compared with experimental values. The R^2 value more than 0.98 confirms the applicability of the model. The effect of column height and treatment time on the concentration of dye in water is given as Figure 7.39 & the effect of time and column height on dissolved ozone in water during ozonation is given as Figure 7.40.

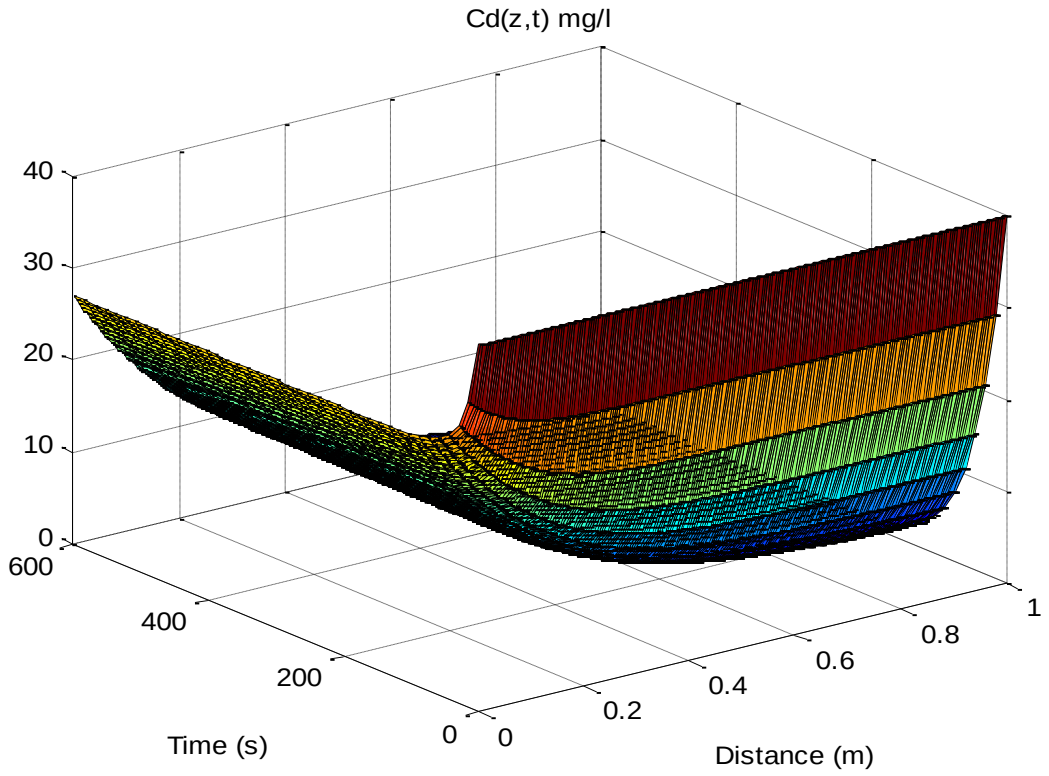

Figure 7.39 Effect of time and column height on dye degradation during ozonation

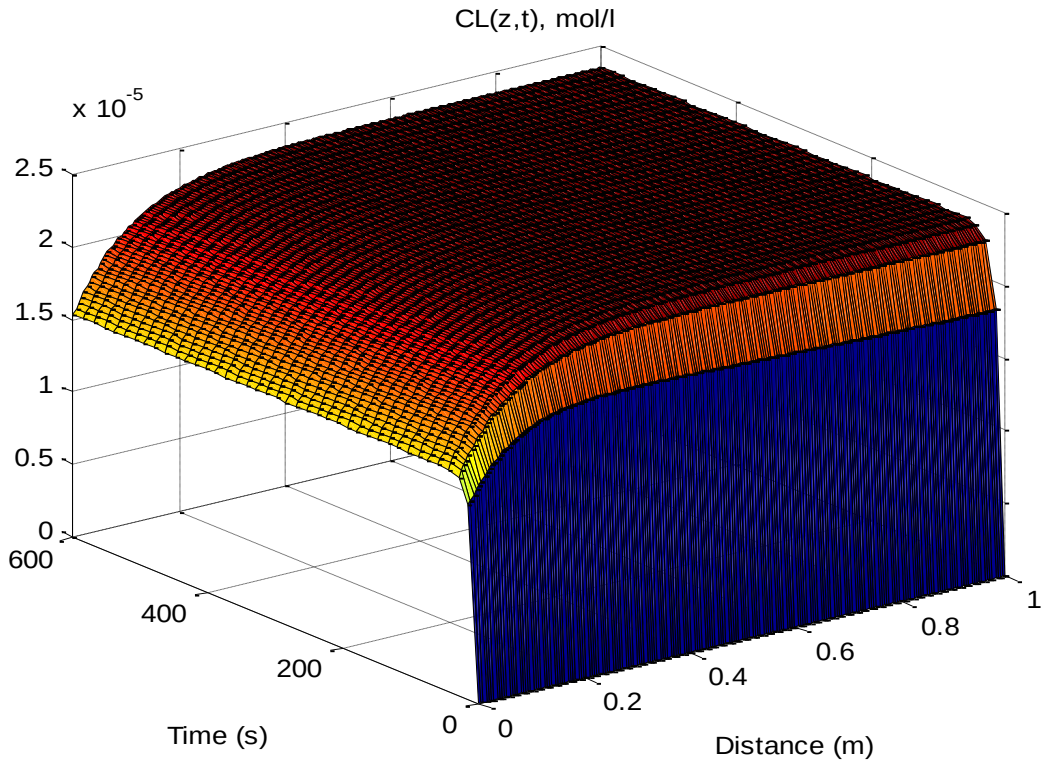

Figure 7.40 Effect of time and column height on dissolved ozone in water

It has been observed that the dye concentration at the outlet of the column decrease with an increase in the height of the column.

7.17 Comparison of experimental and predicted value of dye concentration

The predicted value of ozonation of turquoise blue dye of initial concentration of 40 mg/l obtained after simulation with the help of MATLAB software was compared with experimental values as shown in Table 7.13.

Table 7.13 Experimental and predicted values at various height of the column

Time, s	Height of column-95 cm		Height of column-80 cm		Height of column-60 cm		Height of column-40 cm	
	Exp. value	Pred. value	Exp. value	Pred. value	Exp. value	Pred. value	Exp. value	Pred. value
0	38.48	40	38.48	40	38.48	40	38.48	40
30	21.42	20.70	12.98	20.7	19.61	20.71	16.21	20.84
60	8.94	10.72	5.25	10.74	6.63	10.95	8.73	12.09
90	3.86	5.61	3.99	5.75	6.00	6.44	7.81	8.62
120	3.78	3.10	4.03	3.4	5.79	4.51	7.73	7.31
150	1.97	1.94	3.99	2.35	5.67	3.73	6.84	6.83
180	1.59	1.43	3.23	1.91	4.74	3.41	7.14	6.64
210	1.51	1.21	3.23	1.73	4.66	3.29	6.93	6.58
240	0.89	1.12	3.23	1.65	4.62	3.24	6.93	6.55
270	0.67	1.09	3.23	1.62	4.62	3.23	6.93	6.54
300	0.37	1.07	3.23	1.61	4.62	3.22	6.93	6.54
330	0.21	1.07	3.23	1.61	4.62	3.22	6.93	6.54

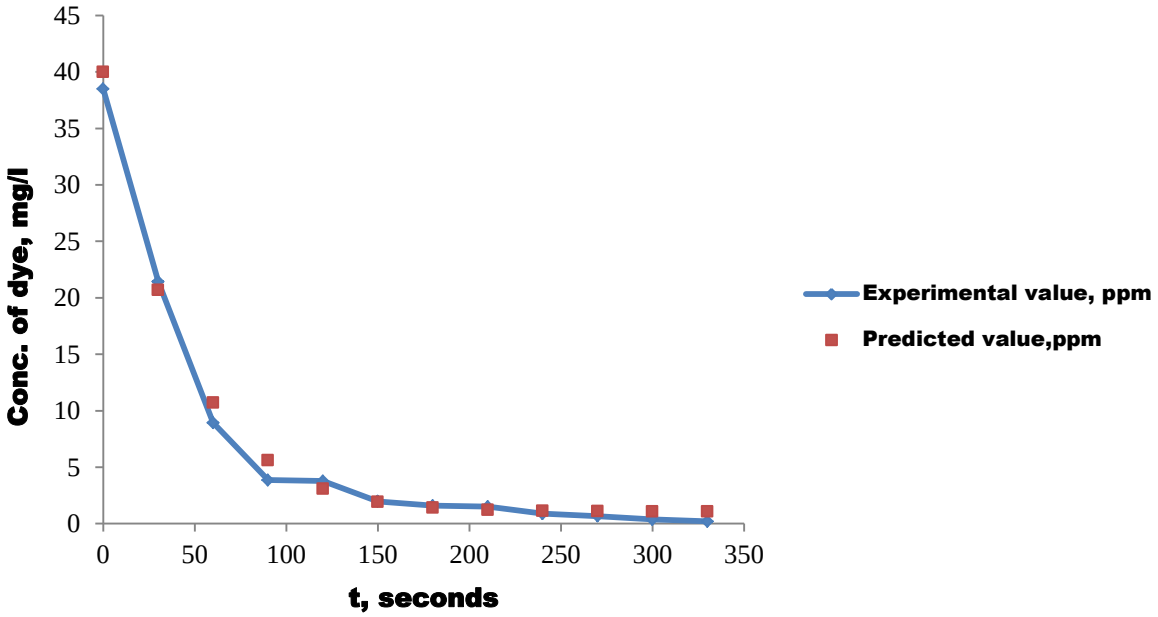

Figure 7.41 Experimental Vs. Predicted value of dye concentration

[Initial concentration 40 mg/l, column height 95 cm]

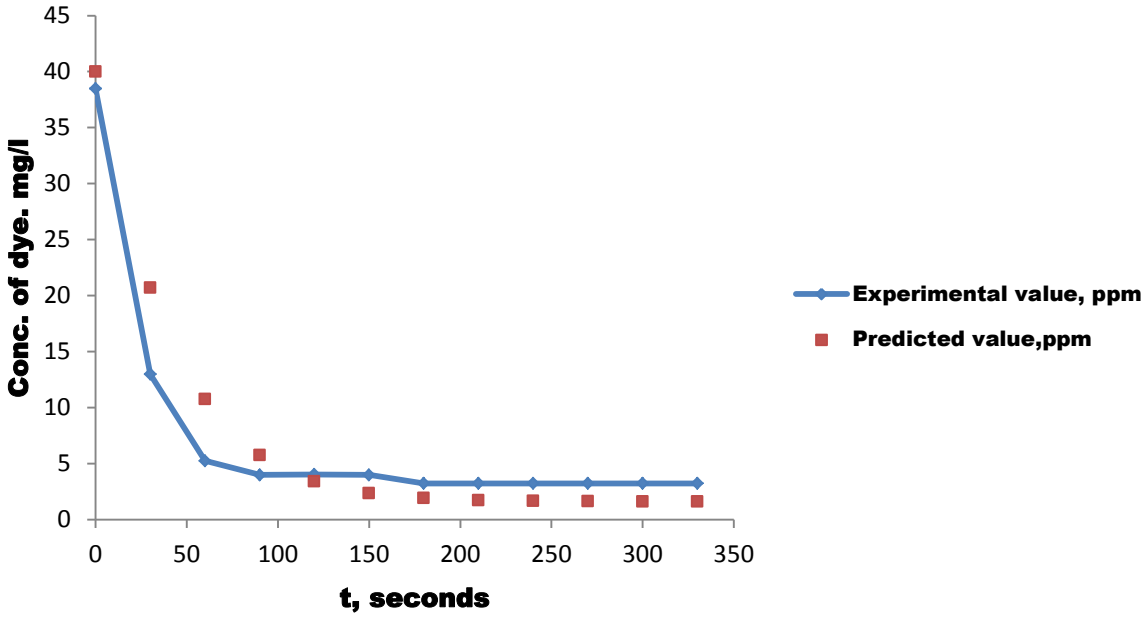

Figure 7.42 Experimental Vs. Predicted value of dye concentration

[Initial concentration 40 mg/l, column height 80 cm]

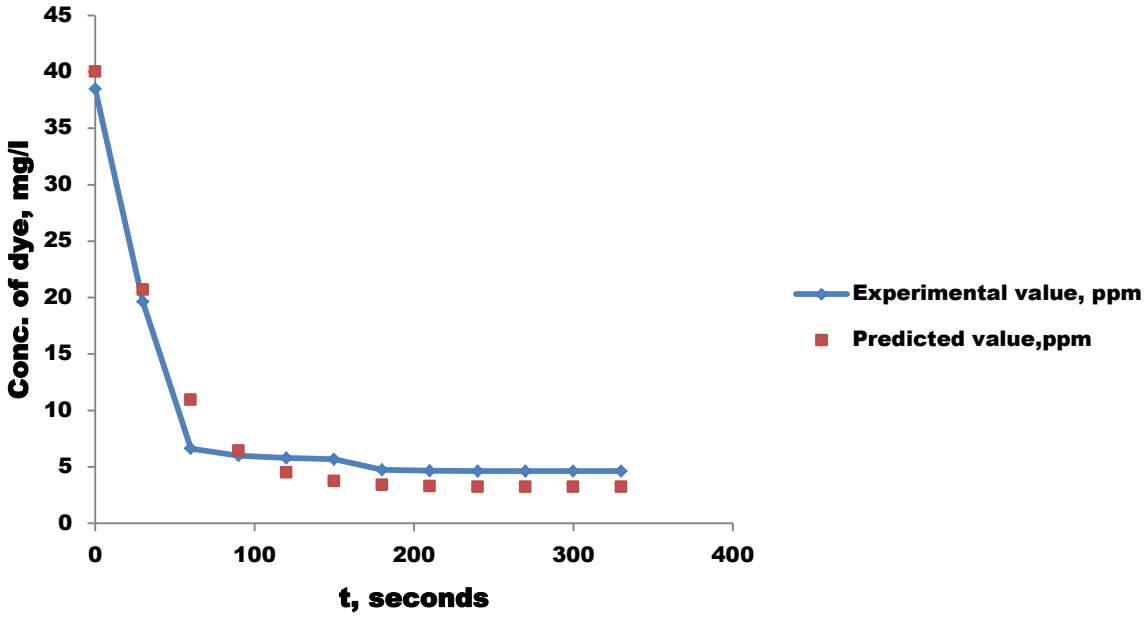

Figure 7.43 Experimental Vs. Predicted Value

[Initial concentration 40 mg/l, column height 60 cm]

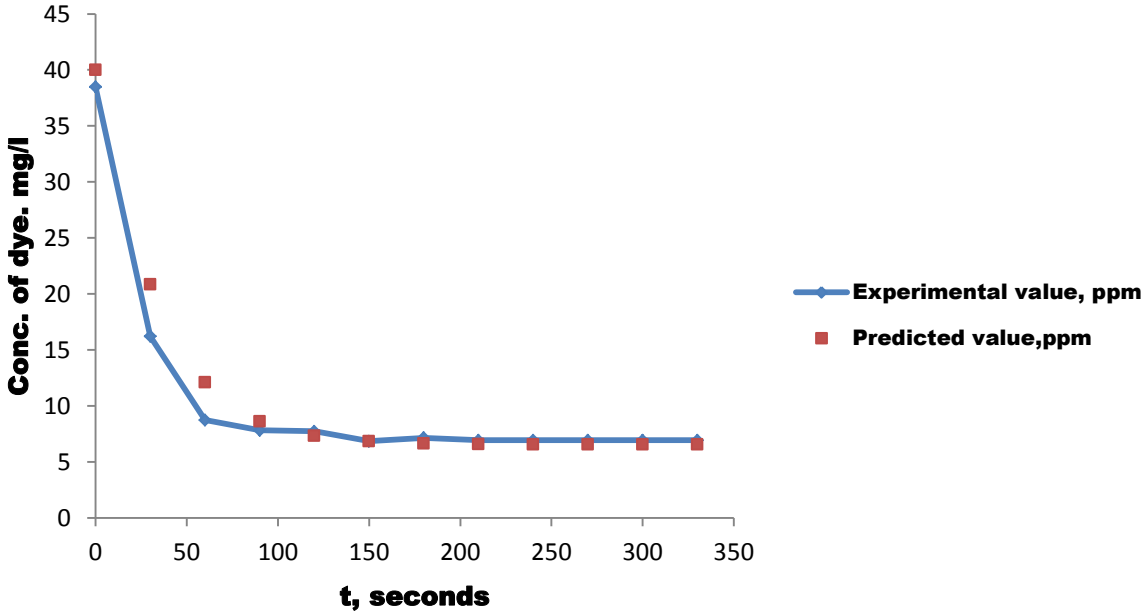

Figure 7.44 Experimental Vs. Predicted Value

[Initial concentration 40 mg/l, column height 40 cm]

The experimental vs. predicted value is shown in Figure 7.41, 7.42, 7.43 and 7.44 respectively, for column height of 95 cm, 80 cm, 60 cm and 40 cm.

7.18 Experimental and predicted values of dye concentration

The experimental and predicted value of dye concentration were compared at the column height of 95 cm and shown in Figure 7.45.

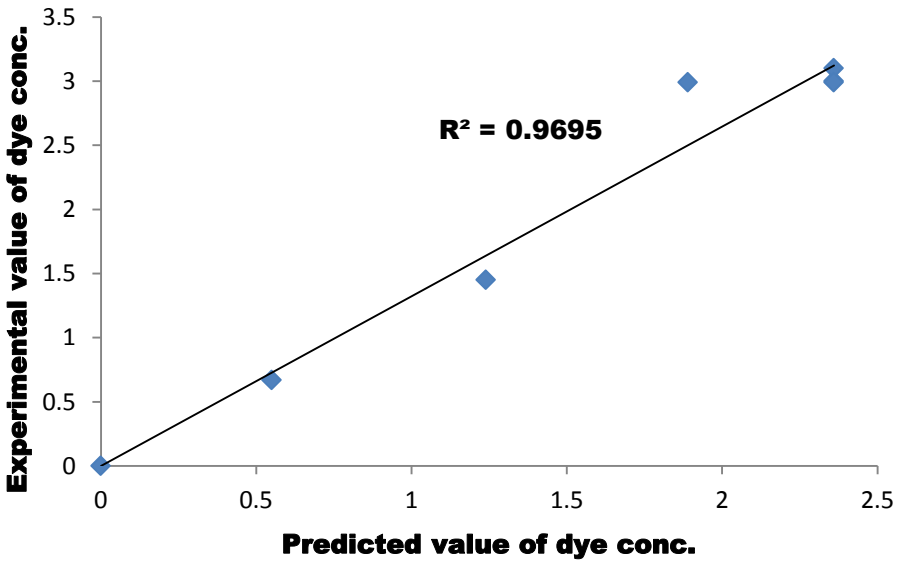

Figure 7.45 Predicted value Vs. Experimental value

It has been observed from the R^2 value of Figure 7.46 that the predicted value obtained after simulation with MATLAB software best fit the experimental value.

CHAPTER 8 MICROBIOLOGIAL TREATMENT

The black liquor of jute fiber (alkaline sulphite pulping) processes was subjected to alkaline sulphite pulping process was studies for color reduction with bacteria and fungi.

8.1 Fungal Growth

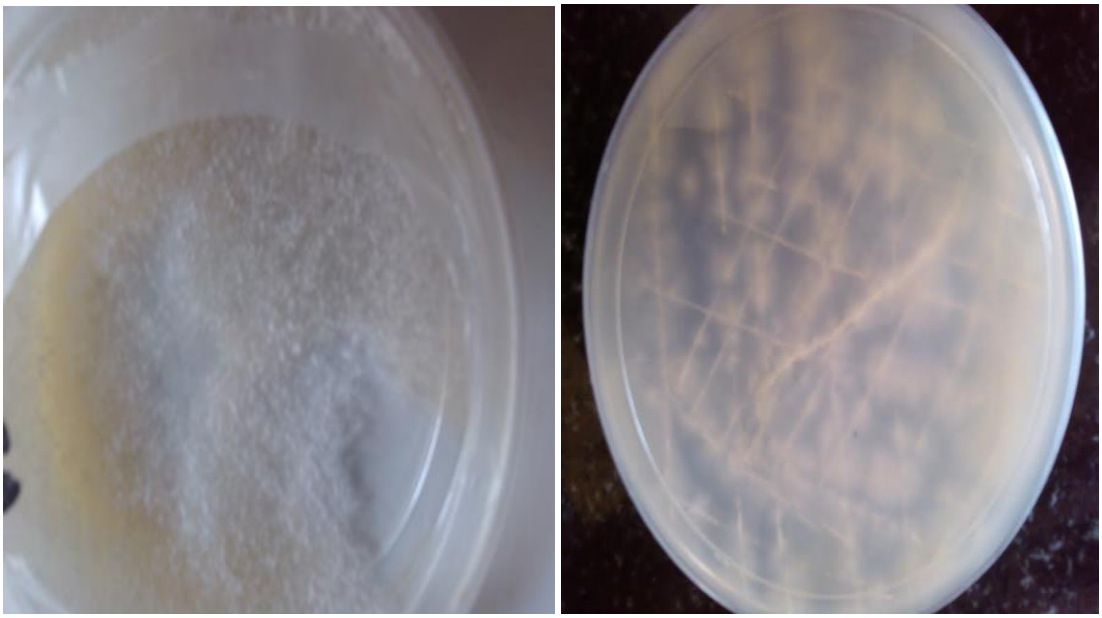

(a)*Phanerochaete Chrysosporium* **(b)*Trichoderma Reesie***

(c) *Aspergillus niger* **(d) *Aspergillus Fumigatus***

Figure 8.1 Fungal growth of cultures (a) *Phanerochaete Chrysosporium* (b)*Trichoderma Reesie* (c) *Aspergillus niger* (d) *Aspergillus Fumigatus*

8.2 Studies on black liquor treatment with bacteria and fungi

The studies were conducted with black liquor diluted 30 times to achieve initial COD-6000 mg/l and initial color of 600 mg/l with isolated bacteria and three species of fungi.

8.2.1 Studies on decolourization with bacteria and fungi

The effect of bacteria and fungi treatment on black liquor was studied for black liquor and the results are tabulated in Table 8.1.

Table 8.1 Effect of bacteria and fungi on decolourization of black liquor

Time, days	**Bacteria**	***P. Chrysosporium***	***Trichoderma Reesie***	***Aspergillus Niger***	***Pleurotus sajor caju***	***Pleurotus ostreatus***	***Coriolus Versicolor***	***Aspergillus fumigatus***	***Bacillus sp.***
0	600	600	600	600	600	600	600	600	600
4	566	568	580	578	585	590	580	590	570
5	458	473	490	486	500	510	490	470	450
7	369	375	390	380	410	420	430	390	385
9	172	178	286	200	305	315	320	210	170
11	71	66	180	150	200	210	220	177	65
12	71	60	180	150	200	210	225	170	66

The maximum decolourization of 89% was achieved with Bacillus species after almost days. The 67% reduction in color and 53% reduction in lignin was achieved at 192 hours incubation period (Chandra 2011).

8.2.2 Studies on lignin reduction with bacteria and fungi

The studies were conducted with initial lignin content of 250 mg/l and results are tabulated in Table 8.2.

Table 8.2 Effect of bacteria and fungal treatment on lignin reduction of B/L

Time, days	Bacteria	*P. Chrysosporium*	*Trichoderma Reesie*	*Aspergillus Niger*	*Pleurotus sajor caju*	*Pleurotus ostreatus*	*Coriolus Versicolor*	*Aspergillus fumigatus*	*Bacillus sp.*
0	250	250	250	250	250	250	250	250	250
4	205	221	234	225	240	242	244	230	215
5	160	170	185	175	190	195	200	181	165
7	135	149	177	156	188	190	200	165	144
9	97	115	133	125	140	142	150	120	110
11	97	66	84	69	92	95	105	80	62
12	100	65	85	70	90	96	100	78	60

The maximum reduction of lignin was observed with bacteria isolated from handmade paper industry, bacillus sp and Phanerochaete chrysosporium in the range of 61 and 78% respectively. The studies conducted by Chandra et al. 2011 found 67% reduction in lignin after 144 hours.

8.2.3 Effect of Bacteria and fungi treatment on COD of black liquor

The effect of isolated bacteria and fungi on black liquor having initial COD of 6000 mg/l is shown in Table 8.5.

Table 8.3 Effect of bacteria and fungal treatment on COD of black liquor

Time, days	Bacteria	*P. Chrysosporium*	*Trichoderma Reesie*	*Aspergillus Niger*	*Pleurotus sajor caju*	*Pleurotus Ostreatus*	*Coriolut h s Versicolor*	*Aspergillus Fumigatus*	*Bacillus sp.*
0	6000	6000	6000	6000	6000	6000	6000	6000	6000
2	5340	5500	5700	5600	5850	5800	5900	5660	5230
4	4780	4800	5000	4900	5000	5900	4900	5000	4380
5	3800	3600	4300	4000	4200	4300	4500	4600	3500
7	3000	2800	3340	3300	4000	4000	3700	3400	2700
9	1780	1500	2140	2050	2700	2700	2500	2100	1670
11	1050	810	2000	1540	2760	2550	2430	1700	1670
12	1050	820	2020	1540	2700	2550	2440	1730	1790

The COD reduction of 82% reduction was achieved with bacteria while 86% reduction was achieved with *Phanerochaete chrysosporium*.

The studies conducted by Chandra et al 2011 revealed 50% reduction in COD, 53% of lignin and 67 % of color of black liquor (initial COD of 18700 mg/l, lignin 1000 mg/l and color of 6100 Co-Pt.U) with addition of 1% glucose and 0.5% peptone(Chandra et al 2011). *Pleurotus spp.* fungi showed 57 & 76 % reduction after 14 days of incubation in final effluent with glucose at 400 and 460 nm respectively (Belem et. 2008). The laccase enzyme produced is responsible for both oxidation and polymerization reactions of phenol. The pH of the effluent after fungal and bacterial treatment reduced to acidic level. The reduction in lignin (66%), COD (75%), and color (81%) was achieved with fungi while reduction in colour (84%), COD (83%) and lignin (72%) was achieved with bacterial strain (Singh and Thakur 2004).

8.3 Solids settled after microbiological treatment

After completion of microbiological treatment, the solids were found to be settled at the bottom of Erlenmeyer flask which was quantified and the results are tabulated in Table 8.4.

Table 8.4 Effect of bacteria and fungal treatment on COD of black liquor

Particulars	**Solids, g/L**
Control (Autoclave), 35^0C	0.13
Bacteria isolated from handmade paper industry	0.948
Phanerochaete Chrysosporium	1.178
Trichoderma Reesie	0.876
Aspergillus Niger	0.991
Pleurotus Sajor Caju	0.867
Pleurotus Ostreatus	0.787
Coriolus Versicolor	0.676
Aspergillus Fumigatus	0.970
Bacillus sp.	1.098

There is maximum settled solids in *Phanerochaete Chrysosporium* with sequence of settled solids (*PC>Bacillus sp> Aspergillus Niger> Bacteria from handmade paper>Aspergillus Fumigatus>Pleurotus Sajor Caju>Pleurotus Ostreatus>Coriolus Versicolor>*and least in bacteria with 4 gpl glucose in aerobic conditions.

CHAPTER 9 SLUDGE UTILIZATION FOR MAKING ENERGY BRIQUETTES

The sludge collected from handmade paper industry was explored for its utilization as energy briquettes.

9.1 Characterization of sludge of handmade paper industry

The sludge as shown in Figure 9.1 of handmade paper industry was characterized for various parameters as given in Table 9.1.

Figure 9.1 Sludge of handmade paper industry

Table 9.1 Characterization of briquettes made with sludge

Particulars	Briquettes made with sludge only
pH	7.71
Ash,%	6.4
Organic content,%	93.6
Calorific value, MJ/kg	21.07
Density, kg/m3	980

The density of sludge of the paper industry is less than 1000 kg/$m^3$and therefore may create problem in combustion in fluidized bed reactor.

The organic matter of paper industry sludge from different paper industry sites has been reported to vary from 19 to 90 % and ash content of 1.64 to 80.2% (Abdullah et al. 2015; Tucker 2005, Report by Thapar Centre for Industrial Research & Development). As per another report, the heating value of sludge of paper industry ranged from 12.0 to 25.0 MJ/kg and ash from 0.2 to 20.2% (Scott & Smith, 1995).

9.2 Characterization of sludge of handmade paper industry mixed with banana black liquor (APP) and jute (Sulphite pulping)

The black liquor of banana (alkaline peroxide pulping) and black liquor of jute fiber was mixed with sludge of handmade paper industry and briquettes were formed. The analysis of briquettes is given in Table 9.2 and Table 9.3 respectively.

Table 9.2 Characterization of briquettes mixed with black liquor (APP)

Particulars	**Briquettes made with sludge only**	**Briquettes with 5% black liquor in sludge**	**Briquettes with 10% black liquor in sludge**	**Briquettes with 20% black liquor in sludge**	**Briquettes with 33% black liquor in sludge**	**100% black liquor (Briquettes could not be made)**
pH	7.71	7.09	7.10	7.18	7.67	9.5
Ash,%	6.4	8.70	11.0	16.25	22..5	56.26
Organic content,%	93.6	90.6	86	81.6	77.8	42.5
Calorific value,MJ/kg	21.07	21.31	21.42	21.85	22.33	26.43
Density,kg/m^3	980	928	870	775	650	1.5

Table 9.3 Characterization of briquettes mixed with black liquor (Sulphite pulping)

Particulars	Briquettes made with sludge only	Briquettes with 5% black liquor in sludge	Briquettes with 10% black liquor in sludge	Briquettes with 20% black liquor in sludge	Briquettes with 33% black liquor in sludge	100% black liquor (Briquettes could not be made)
pH	7.01	7.12	7.22	7.32	7.65	8.90
Ash,%	6.4	8,2	9.9	13,7	17.9	40.37
Calorific value, MJ/kg	21.07	21.5	21.9	22.8	23,9	28.40
Density, kg/m3	980	933	890	788	687	1.65
Sulphur content,%	nil	0.05	0.06	0.08	0.14	0.38

In an earlier study on utilization of briquettes made from a blend of rice husk and palm oil mill sludge, the calorific values of briquettes were found to range from 13.45 to 21.68 MJ/kg, ash content varied from 15.13 to 19.43% (Obi et al. 2016). The calorific value of sludge of cotton textile industry was reported to be 17.9 MJ/kg with an ash content of 8.93% (Avelar et al. 2016). The ash content determined of lignin ranged from 0.45 to 36.29% (Sameni et al. 2014). The higher heating value of hardwood lignin and softwood lignin was 21.45 and 23.50 MJ/kg respectively. The ash content of hardwood lignin and softwood lignin was 3.40 and 0.62 % respectively (Blunk & Jenkins, 200). The Sulphur content of black liquor of eucalyptus, bamboo and straw ranged from 0.2 to 5.2 % (Cardoso et al. 2009)

On the basis of fiber losses, the sludge generated from 1 T/day of the handmade paper unit would be approximately 4 kg. Taking an approximate calorific value of sludge briquettes as 22 MJ/kg (6.09 KWh/kg) an equivalent of37.08 KWh/day energy can be generated.

	
1% lignin	5% lignin
	
Lignin 20%	Lignin-33%

Figure 9.2 Briquettes made with black liquor and sludge in different ratio

CHAPTER 10 CONCLUSIONS & RECOMMENDATIONS FOR FUTURE WORK

10.1 Conclusions

There is a cluster of more than 30 handmade paper units in Sanganer, Jaipur. The wastewater discharged from these units exceeds the limits prescribed by the Central Pollution Control Board; however, the effluent of handmade paper is less polluted in comparison to paper mills. The handmade paper units utilize cotton rags as conventional raw material. Some of the handmade paper units utilize alternative ligno-cellulosic raw material like jute, Sunn hemp and Banana fiber for handmade paper making. The black liquor contributes to major pollution load. Direct dyes constitute the main colour producing component of waste water discharge from the units contributing another major pollution load.

The Fly ash as low cost adsorbent has been proven as a potential adsorbent for wastewater treatment of handmade paper industries. Batch studies have been conducted on direct black dye synthetic wastewater using fly ash of specific surface area 240 m^2/g to derive adsorption isotherms. A comparison of R^2 values in isotherms studies showed best fitting for Langmuir isotherm. The maximum adsorption capacity of fly ash was 76.33 mg/g at 318 K in batch studies. The adsorption followed first order kinetics. The negative value of ΔG_0 confirmed the feasibility of the process and spontaneous nature of adsorption of fly ash.

The Yoon Nelson and Thomas models were found to have better fitting with experimental data in fixed bed adsorption studies among the three models employed to explain the behavior of the reactor. The numerical model developed with the help of MATLAB showed excellent fitting with the experimental values.

The results of COD, Color and BOD values of treated effluent with fly ash were within prescribed norms of CPCB confirming that low cost fly ash is a potential adsorbent to treat effluent of handmade paper industry containing black dye. The adsorbed fly ash in a dosage of 5% was further utilized as additive in paper making, which showed no adverse effect on strength properties of handmade paper. From the cost analysis, fly ash has proven as a cheap alternative for treatment of waste water compared to traditional adsorbents. The major contribution lies in utilization of low cost fly ash in closed loop system.

Ozonation of synthetic samples of direct blue and red dyes was carried out in column reactors in a controlled range of operating parameters like pH, temperature and contact time in order to derive reaction kinetics. The study showed that decolourization time varied from 12 to 4 minutes for blue dye with removal increasing from 59.5% to 99% at pH of 4; the corresponding values were 12 to 6 minutes and removal efficiency increase of 73% to 99% at pH 10 respectively for the red dye at an effluent temperature of 313 K. The equilibrium time of decolourization with ozonation treatment for direct red and direct blue dye for 50 mg/l initial concentration was 6 and 4 minutes, respectively. The maximum COD removal of 45 and 54% was achieved for direct blue dye and direct red dye solutions, respectively. The decolourization of dye solutions to ozone followed the pseudo-first-order reaction with the maximum rate constant for direct red and direct blue dyes as 0.917 and 0.904 min^{-1} respectively, at pH of 10 and temperature of 313 K.

The ozonation treatment showed increase in decolourization efficiency of ozone at high pH in case of both blue and red dye. The decolourization of dye solutions with ozone is pseudo first order reaction with a maximum rate constant achieved at pH-10. The maximum rate constant for direct red and direct blue dye at pH-10 is 0.917 and 0.904 min^{-1}, respectively. The predicted values achieved with the help of MATLAB software showed good fitting with experimental values.

The black liquor of Jute fiber with sulphite pulping process having initial COD of 6000 mg/l showed the maximum decolourization of 86% with the *Phanerochaete chrysosporium* fungi.

The energy briquettes made by utilizing sludge of handmade paper industry (solid fibers) and black liquor (liquid waste) showed calorific value above 20 MJ/kg indicating a potential reuse of the waste and closing the treatment loop. Thus, from both the treatment processes, adsorption or ozone oxidation, the sludge produced may be either reused for paper making (if the hue permits) or be converted to energy briquettes thereby establishing a close loop cycle, which can be practiced at the level of small scale units.

Therefore, it can be concluded that ozonation and adsorption are potential treatment technologies for wastewater of handmade paper industry. The ozonation treatment requires initial investment but with less operational cost. The bacteria and fungi can be used in sequence with other treatment methods. The ozonation treatment can be applied after adsorption and before microbiological treatment to take care of only residual dyes for achieving economy. The sludge of handmade paper industry along with black liquor can be well used for making energy briquettes. Thus, the studies conducted on wastewater of handmade paper industry using simple and cost effective technologies can help improve the sustainability of the handmade paper industry.

10.2 Recommendations for future work

The recommendations for the future work are as given below:

- The surface charge of the dyes were not determined in the current work, however it is recommended for future work.
- Ozonation treatment may be studied for mixture of dyes.

REFERENCES

A report on opportunities for green chemistry initiatives: Pulp and Paper Industry, 2014, Office of the Principal Scientific Advisor to GOI.

Aadil, K. R., Barapatre, A., and Jha, H. (2016). "Synthesis and characterization of Acacia lignin-gelatin film for its possible application in food packaging", *Bioresources and Bioprocessing*, 3(1), 1-11.

Abdullah, R., Ishak, C. F., Kadir, W. R., and Bakar, R. A. (2015). "Characterization and feasibility assessment of recycled paper mill sludges for land application in relation to the environment", *International Journal of Environmental Research and Public Health*, 12(8), 9314–9329.

Acemiog˘ lu, B. (2004). "Adsorption of Congo red from aqueous solution onto calcium-rich fly ash", *Journal of Colloid and Interface Science*, 274, 371–379.

Adamson, A. W., and Gast, A. P. (1997). "Physical Chemistry of Surfaces", 6th ed. Wiley Interscience, New York.

Agarwal, S., Singh, K., Gupta, A. B., and Sharma, A. K. (2016). "Fly ash as low cost adsorbent for treatment of effluent of handmade paper industry-Kinetic and modelling studies for direct black dye", *Journal of Cleaner Production*, 112, 1227–1240.

Aken, P. V., Broeck, R. V. D., Degrève, J., and Dewil, R. (2015). "The effect of ozonation on toxicity and biodegradability of 2,4-dichlorophenol containing wastewater", *Chemical Engineering Journal*, http://dx.doi.org/10.1016/j.cej.2015.06.019 (Accepted Manuscript).

Alluri, V. R. G. R., Rama, Sungnanam, S. D. P., Kunjam, M., and Nethala, V. K. (2016). "Analysis of effluents released from the paper industry : Approach of its impact on agricultural soil", *International Journal of Applied Research*, *2* (7), 890–892.

APHA. (1989). “Standard Methods for the Examination of Water and Wastewater.”, 20th Edition. American Public Health Association, American Water Work Association, Water Environment Federation, Washington, D.C.

Arslan-Alaton, I. (2003). “The effect of pre-ozonation on the biocompatibility of reactive dye hydrolysates” *Chemosphere*, 51, 825–833.

Assalin, M. R., Almeida, E. S., Rosa, M. A., Moraes, S. G., and Duran, N. (2004). “Application of Ozonation Process In Industrial Wastewaters: Textile, Kraft E_1 and Whey Effluents”, *Environmental Technology*, *25*(8), 867–872.

ASTM E-1131-08, 2012, Standard Test method for compositional analysis by Thermogravimetry.

Auta, M., and Hameed, B.H. (2012). “Modified mesoporous clay adsorbent for adsorption isotherm and kinetics of methylene blue”, *Chemical Engineering Journal*, 198-199, 219–227.

Aharoni, C., Sideman, S., and Hoffer, E. (1979). “Adsorption of phosphate ions by colloid ion coated alumina”, *Journal of Chemical Technology and Biotechnology*, 29, 404–412.

Aharoni, C., and Ungarish, M. (1977). Kinetics of activated chemisorption Part 2. Theoretical
Models”, *Journal of the Chemical Society Faraday Transactions*, 73, 456-464.

Bajpai, P., and Bajpai, P. K., (1994). “Biological colour removal of pulp and paper mill wastewaters.” *Journal of Biotechnology*, 33, 211-220.

Bajpai., P. (2016). “Global Pulp and Paper Production and Consumption.”, Pulp and Paper Industry: Energy conservation, 9-14.

Bajeer, M. A., Nizamani, S. M., Hussainsherazi, S. T., and Bhanger, M. I. (2012). Adsorption and leaching potential of imidacloprid pesticide through alluvial soil”, *American Journal of Analytical Chemistry,* 3, 604-611.

Barapatre, A., and Jha, H. (2016). “Decolourization and Biological Treatment of Pulp and Paper Mill Effluent by Lignin-Degrading Fungus Aspergillus flavus Strain F10 5”, *International Journal of Current Microbiology and Applied Sciences*, 5(5), 19–32.

Belém, A., Panteleitchouk, A. V., Duarte, A. C., Rocha-Santos, T. A. P., and Freitas, A. C. (2008). “Treatment of the effluent from a kraft bleach plant with white rot fungi Pleurotus sajorcaju and Pleurotus ostreatus”, *Global Nest Journal*, 10(3), 426–431.

Beltrán, F. J., González, M., Acedo, B., and Rivas, F. J. (2000). “Kinetic modelling of aqueous atrazine ozonation processes in a continuous flow bubble contactor”, *Journal of Hazardous Materials*, 80, 189–206.

Beltrán, F. J., Aguinaco, A., and García-araya, J. F. (2010). “Kinetic modelling of TOC removal in the photocatalytic ozonation of diclofenac aqueous solutions”, *Applied Catalysis B : Environmental*, 100, 289–298.

Biermann, C. 2012, Handbook of Pulping and Papermaking, 2nd Edition, 1-754.

Bińi, A. K., Duczmal, B., and Machniewski, P. (2001). “Hydrodynamics and ozone mass transfer in a tall bubble column”, *Chemical Engineering Science*, 56, 6233–6240.

Blunk, S. L. and Jenkins, B. M. (2000), “Combustion properties of lignin residue from ligno-cellulose fermentation.”, 1-15.

Boeriu, C. G., Bravo, D., Gosselink, R. J. A., and Van Dam, J. E. G. (2004). “Characterisation of structure-dependent functional properties of lignin with infrared spectroscopy”, *Industrial Crops and Products*, 20, 205–218.

Boruah , P., Dowarah, P., Hazarika, R., Yadav, A., Barkakati, P., and Goswami, T. (2016). “Xylanase from *Penicillium meleagrinum var. viridiflavum* - a potential source for bamboo pulp bleaching”, *Journal of Cleaner Production.* doi: 10.1016/j.jclepro.2015.12.024 (Accepted manuscript).

Brebu, M., and Vasile, C. (2010). “Thermal degradation of lignin- A review”, *Cellulose Chemistry and Technology*, 44, 353–363.

Cardoso, M., de Oliveira, É. D., and Passos, M. L. (2009). "Chemical composition and physical properties of black liquors and their effects on liquor recovery operation in Brazilian pulp mills", *Fuel*, 88(4), 756–763.

Casey, J. P. (1980). " Pulp and Paper: Chemistry and Chemical Technology.", Third edition, 2, 1-576.

Central Pollution Control Board. (2006). "Development of guidelines for water conservation in pulp and paper sector", National Productivity Council, New Delhi.

Chandra, R., Abhishek, A., and Sankhwar, M. (2011). "Bacterial decolorization and detoxification of black liquor from rayon grade pulp manufacturing paper industry and detection of their metabolic products", *Bioresource Technology*, 102, 6429-6436.

Chandra, R., and Abhishek, A. (2011). "Bacterial decolorization of black liquor in axenic and mixed condition and characterization of metabolites", *Biodegradation*, 22, 603–611.

Central Pollution Control Board. (2015). "Charter for Water Recycling and Pollution Prevention in Pulp and Paper Industries (Specific to Ganga River Basin States)", Charter of paper industry, Annexure-I.

Chakradhar, B., and Shrivastava, S. (2004). "Colour removal of pulp and paper effluents", *Indian Journal of Chemical Technol*ogy 11, 617–621.

Chatterjee, A. K. (2010). "Indian fly Ashes, their characteristics, and potential for mechano-chemical activation for enhanced usability", *In: IInd International Conference on Sustainable Construction Material and Technologies*.

Chaudhari, P. K., Majumdar, B., Choudhary, R., Yadav, D. K., and Chand, S. (2010). "Treatment of paper and pulp mill effluent by coagulation", *Environmental Technology*, 31, 357–363.

Chavan, S. K., and Paul, S. A. (2013). "Waste coal fly ash utilized for removal of sulphur dye

from textile waste water: kinetics and equilibrium study", *Journal of Chemical, Biological and Physical Sciences,* 3, 1727-1734.

Chen, H. L., Chen, Y. C., Zhan, H. Y., and Fu, S. Y. (2010). "Enhanced Biodegradation of Pulping Effluents By a Statistical Experimental Design Using Microbial Consortia", *Bioresources,* 5, 1581–1594.

Chen, Y. H., Chang, C. Y., Chiu, C. Y., Yu, Y. H., Chiang, P. C., Ku, Y., and Chen, J. N. (2003). "Dynamic behavior of ozonation with pollutant in a counter current bubble column with oxygen mass transfer", *Water Research,* 37, 2583–2594.

Chongrak, K., Eric, H., Noureddine, A., and Jean, P. (1998). "Application of Methylene Blue Adsorption to Fiber Specific Surface Area Measurement", *Journal of Cotton Science*, 2:164-173.

Ciardelli, G., and Ranieri, N. (2001). "Technical Note the Treatment and Reuse of Wastewater in the Textile Industry By Means of Ozonation and Electroflocculation", *Water Research*, 35(2), 567–572.

Cibichakravarthy, G. V., Ramanathan, B., Nallapeta, A. S., Mula, and R. V. R., Rayalu, J. (2012). "Decolourization of paper mill effluent by immobilized cells of Phanerochaete Chrysosporium", *International Journal of Plant, Animal and Environmental Sciences*, 141–146.

Colindres, P., Yee-Madeira, H., and Reguera, E. (2010). "Removal of Reactive Black 5 from aqueous solution by ozone for water reuse in textile dye processes", *Desalination*, 258, 154-158.

Cotana, F., Cavalaglio, G., Nicolini, A., Gelosia, M., Coccia, V., Petrozzi, A., and Brinchi, L. (2014). "Lignin as co-product of second generation bioethanol production from ligno-cellulosic biomass", *Energy Procedia*, 45(0), 52–60.

Dangcong, P., and Qiting, J. (1993). "Anaerobic digestion of alkaline black liquor using an upflow anaerobic sludge blanket reactor", *Journal of Chemical Technology Biotechnology,* 58, 89–93.

Daniels, W. L., Stewart, B., Haering, K., and Zipper, C. (2002). "The Potential for beneficial Reuse of Coal Fly Ash in southwest virginia Mining environments", Powell River Project, Virginia Cooperative Extension, 460-134.

Dashtban, M., Schraft, H., Syed, T. A., and Qin, W. (2010). "Fungal biodegradation and enzymatic modification of lignin", *International Journal Biochemistry Molecular Biology*, 1, 36–50.

Davy, M. F., Uloth, V.C., and Cloutier, J. N. (1998). "Economic evaluation of black liquor treatment processes for incremental kraft pulp production", *Pulp & Paper Canada*, 99(2), 35–39.

Devi, T. S. R., and Gayathri, S. (2010). "FTIR and FT-Raman spectral analysis of paclitaxel drugs", *International Journal of Pharmaceutical Sciences Review and Research*, 19, 106-110.

Devi, N. L., Yadav, I. C., Shihua, Q. I., Singh, S., and Belagali, S. L. (2011). "Physicochemical characteristics of paper industry effluents - A case study of South India Paper Mill (SIPM).", *Environmental Monitoring and Assessment*, 177, 23–33.

Dhadse, S., Kumari, P., and Bhagia, L. J.(2008). "Fly ash characterization, utilization and government initiatives in India - A review.", *Journal of Scientific & Industrial Research*, 67, 11–18.

Dhanushree, M. S., and Kousar, H. (2015). "An Overview of certain Physico-chemical Parameters of Paper Mill Effluent Department of Post Graduate Studies and Research in Environmental Science , Kuvempu University , 4, 195–197.

Dhaouadi, H., Poncin, S., Hornut, J. M., and Midoux, N. (2008). " Gas – liquid mass transfer in bubble column reactor : Analytical solution and experimental confirmation.", *Chemical Engineering & Processing*, 47, 548–556.

Dogruel, S., Genceli, E. A., Babuna, F. G., and Orhon, D. (2006). " An investigation on the optimal location of ozonation within biological treatment for a tannery wastewater.", *Journal of Chemical Technology and Biotechnology*, 81, 1877–1885.

Dubinin, M. M. (1960). "The potential theory of adsorption of gases and vapours for adsorbents with energetically nonuniform surfaces.", *Chemical Reviews*, 60, 235–241.

El-Din, M. G., and Smith, D. W. (2003). "Mass transfer analysis in ozone bubble columns.", *Journal of Environmental Engineering Science*, *2*, 63–76.

EPA Notifications' 64(E), dated 18 Jan 1998; Environment Protection rules 1986

Erol, F., Özbelge, T. A., and Özbelge, H. Ö. (2009). "Modeling of catalytic ozonation process in a three-phase reactor.", *Journal of Environmental Science and Health Part A : Toxic / Hazardous Substances and Environmental Engineering*, 44, 295-306.

Fanchiang, J. M., Tseng, and D. H. (2009). " Degradation of anthraquinone dye C.I. Reactive Blue 19 in aqueous solution by ozonation.", *Chemosphere* 77, 214–221.

Faria, P. C. C., Orfao, J. J. M., Pereira, and M. F. R. (2009). "Activated carbon and ceria catalysts applied to the catalytic ozonation of dyes and textile effluents.", *Applied Catalysis B: Environmental*, 88, 341–350.

Filipkowska, U., Klimiuk, E., Kuczajowska-Zadrożna, M., Kuś, S. (2004). "The Removal of Reactive Dyes from Binary Mixtures Using Chitin.", *Polish Journal of Environmental Studies*, 13, 65-661.

Font, X., Caminal, G., Gabarrell, X., Romero, S., and Vicent, M. T. (2003). "Black liquor detoxification by laccase of Trametes versicolour pellets.", *Journal of Chemical Technology and Biotechnology*, 78, 548–554.

Fracaro, G., Vakkilainen, E., Hamaguchi, M., De Souza, and S. N. M. (2012). "Energy efficiency in the Brazilian pulp and paper industry.", *Energies* 5, 3550–3572.

Freundlich, H. M.F. (1906). "Over the adsorption in solution.", *The Journal of Physical Chemistry*, 57,385-471.

Garg, V. K., Gupta, R., Kumar, R., and Gupta, R. K. (2004). "Adsorption of chromium from aqueous solution on treated sawdust.", *Bioresources Technology*, 92, 79–81.

Giri, K., Patel, R. K., and Mahapatra, S. S. (2011). “Artificial neural network (ANN) approach for modeling of arsenic (III) biosorption from aqueous solution by living cells of Bacillus cereus biomass.”, *Chemical Engineering Journal*, 178, 15-25.

Gomes, A. C., Fernandes, L. R. and Simões, R. M. S. (2012). “Oxidation rates of two textile dyes by ozone: Effect of pH and competitive kinetics.”, *Chemical Engineering Journal*, 189–190, 175–181.

Grover, R., Marwaha, S. S., and Kennedy, J. F. (1999). “Studies on the use of an anaerobic baffled reactor for the continuous anaerobic digestion of pulp and paper mill black liquors.”, *Process Biochemistry*, 34, 653–657.

Gong, X., Takagi, S., Huang, H., and Matsumoto, Y. (2007). “A numerical study of mass transfer of ozone dissolution in bubble plumes with an Euler – Lagrange method.”, *Chemical Engineering Science*, 62, 1081–1093.

Guendy, H. R. (2007). “Ozone treatment of textile wastewater relevant to toxic effect elimination in marine environment.”, *Egyptian Journal of Aquatic Research*, 33, 98–115.

Gupta, G., Prasad, G., Panday, K. K., and Singh, V. N. (1988). “Removal of chrome dye from
aqueous solutions by fly ash.”, *Water, Air & Soil Pollution*, 37, 13-24.

Hameed, B. H., Ahmad, A. A., and Aziz, N. (2007). “Isotherms, kinetics and thermodynamics of acid dye adsorption on activated palm ash.”, *Chemical Engineering Journal*, 133(1–3), 195–203.

Han, R., Ding, D., Xu, Y., Zou, W., Wang, Y., Li, Y., and Zou, L. (2008). “Use of rice husk for the adsorption of congo red from aqueous solution in column mode.”, *Bioresource Technology*, 99(8), 2938–2946.

Han, Z.-X., Zhu, Z., Wu, D., Wu, J., and Liu, Y. (2014). "Adsorption Kinetics and Thermodynamics of Acid Blue 25 and methylene blue dye solutions on natural sepiolite.", *Synthesis and Reactivity in Inorganic, Metal-Organic and Nano-Metal Chemistry*, 44(1), 140–147.

Hariharan, S., and Nambisan, P. (2013). "Optimization of Lignin Peroxidase, Manganese Peroxidase, and Lac Production from Ganoderma lucidum Under Solid State Fermentation of Pineapple Leaf.", *Bioresources*, 8(1), 250–271.

Hasan, S. H., and Srivastava, P. (2011). "Biosorptive Abatement of Cd 2 + by Water Using Immobilized Biomass of Arthrobacter sp . : Response Surface Methodological Approach.", *Industrial & Engineering Chemistry Research*, 247–258.

He, S. H., Li, J., Xu, J., and Mo, L. (2016). " Enhanced Removal of COD and Colour in Paper-making Wastewater by Ozonation Catalyzed by Fe Supported on Activated Carbon.", *Bioresources*, 11 (4), 8396–8408.

Heidrich, C., Feuerborn, H., and Weir, A. (2013). Coal Combustion Products : a Global Perspective. *World of Coal Ash*, 17.

Helmy, S. M., Rafie, S. E., and Ghaly, M. Y. (2003). " Bioremediation post-photo-oxidation and coagulation for black liquor effleunt treatment.", *Desalination*, 158 , 331-339.

Hoa, D. T. and Man, T. D. (2006). " Study on treatment of alkaline black liquor using sulphate reducing bacteria.", *Advances in Natural Sciences*, 7(1), 139–145.

Hoigné, J., and Bader, H. (1983). "Rate constants of reactions of ozone with organic and inorganic compounds in water-I. Non-dissociating organic compounds.", *Water Research*, 17, 173-183.

Ho, Y. S., and McKay, G. (1998). "Sorption of dye from aqueous solution by peat.", *Chemical Engineering Journal*, 70, 115–124.

Hu, Z., Que, Y., Gao, Y., Yin, Y., and Zhao, Y. (2015). "Using Black Liquor from the Soda Pulping Process for Protein Production by Candida utilis.", *10*(3), 3908–3921.

ISO-11358-1:2014, Plastics-Thermogravimetry (TG) of polymers-Part I General Principles

Irfan, M., Butt, T., Imtiaz, N., Abbas, N., Ahmad, R., and Shafique, A. (2013). "The removal of COD, TSS and colour of black liquor by coagulation – flocculation process at optimized pH, settling and dosing rate.", *Arabian Journal of Chemistry*, 1-12.

Jaganathan, B., Hossain, S. K. M., Begum, K. M. M. S., and Anantharaman, N. (2009). "Aerobic Pollution Abatement of Pulp mill Effluent with the White Rot fungus *Phanerochaete chrysosporium* in Three-phase Fluidized Bed Bioreactor.", *Chemical Engineering Research*, 13, 13–16.

Jogarao. (2016). "How to recover more used paper for recycling.", *Indian Pulp and Paper Technical Association*, 28 (1), 84-87.

Kahraman, S., Dogan, N., and Erdemoglu, S. (2008). "Use of various agricultural wastes for the removal of heavy metal ions, *International Journal of Environment and Pollution*, 34, 275–284.

Kamali, M., Gameiro, T., Costa, M. E. V, and Capela, I. (2016). "Anaerobic digestion of pulp and paper mill wastes - An overview of the developments and improvement opportunities.", *Chemical Engineering Journal*, 298, 162–182.

Kannan, N., and Sundaram, M. M. (2001). "Kinetics and mechanism of removal of methylene blue by adsorption on various carbons—a comparative study.", *Dyes and Pigments*, 51, 25–40.

Kao, P. N., Tzeng, J. H., and Huang, T. L. (2000). "Removal of chlorophenols from aqueoussolution by fly ash.", *Journal of Hazardous Materials*, 76, 237-249.

Kara, S., Aydiner, C., Demirbas, E., Kobya, M., and Dizge, N. 2007). "Modeling the effects of adsorbent dose and particle size on the adsorption of reactive textile dyes by fly ash.", *Desalination*, 212 (2007) 282–293.

Kavitha, D., and Namasivayam, C. (2007). “Experimental and kinetic studies on methylene blue adsorption by coir pith carbon.”, *Bioresources Technology*, 98, 14–21.

Kesalkar, V. P., Khedikar, I. P., and Sudame, A. M. (2012). “Physico-chemical characteristics of wastewater from Paper Industry.”, *International Journal of Engineering Research and Applications*, 2 (4), 137–143.

Khan, T. A., Singh, V. V., and Kumar, D. (2004). Removal of some basic dyes from artificial textile wastewater by adsorption on Akash Kinari coal. *Journal of Scientific & Industrial Research*, 63, 355-364.

Khan, H., Ahmad, N., Yasar, A., and Shahid, R. (2010). “Advanced oxidative decolorization of red Cl-5B:Effects of dye concentration, process optimization and reaction kinetics.”, *Polish Journal of Environmental Studies*, 19(1), 83–92.

Khosla, E., Kaur, S., and Dave, P. N. (2013). “Tea waste as adsorbent for ionic dyes.”, *Desalination and Water Treatment*, 51, 6552–6561.

Kirk, T. K., and Cullen, D. (1998). “Enzymology and molecular genetics of wood degradation by white-rot fungi.” In: Young RA, Akhtar M (eds) Environmentally friendly technologies for the pulp and paper industry. Wiley, New York, 273–307.

Ko, D.-S., Sauer, K., Nord, S., Müller, R., and Wolfrum, J. (1997). “Determination of the diffusion coefficient of dye in solution at single molecule level.”, *Chemical Physics Letters*, 269(1–2), 54–58.

Koch, M., Yediler, A., Lienert, D., Insel, G., and Kettrup, A. (2002). “Ozonation of hydrolyzed azo dye reactive yellow 84 (CI).”, *Chemosphere* 46, 109–113.

Kolovea, E. P., The Use of Fly Ash for Lead Removal from Industrial Wastes, PhD Dissertation, Aristotle University of Thessaloniki, Thessaloniki, Greece, 1982, 76–79.

Konsowa, A. H., Ossman, M. E., Chen, Y., and Crittenden, J. C. (2010). “Decolourization of industrial wastewater by ozonation followed by adsorption on activated carbon.” *Journal of Hazardous Materials*, 176, 181–185.

Kozakova, Z., Nejezchleb, M., Krcma, F., Halamova, I., Caslavsky, J., and Dolinova, J. (2010). "Removal of organic dye direct red 79 from water solutions by DC diaphragm discharge: Analysis of decomposition products.", *Desalination*, 258, 93–99.

Kulshrestha, N. K. (1988). "Analysis of Financial Statements of Indian Paper Industry." *Navman Prakashan*, 1-2.

Kumar, V., Mathur, M., Sinha, S. S., and Dhatrak, S. (2005). "Fly Ash: an Environment Savior.", Fly Ash India. TIFAC, New Delhi. IVth 1.1-1.4.

Kumar, P., Teng, T. T., Chand, S., and Wasewar, K. L. (2011). "Treatment of Paper and Pulp Mill Effluent by Coagulation.", International Journal of Chemical, Molecular, Nuclear, Materials and Metallurgical Engineering, 5(8), 715–720.

Kumar, A., Chaudhary, P., and Verma, P. (2013). "Adsorption of reactive red 194 dye from textile effluent by using class F fly ash.", *Scholars Journal of Applied Medical Sciences*, 1, 111-116.

Kundu, S., and Gupta, A. K. (2006). "Arsenic adsorption onto iron oxide-coated cement (IOCC): regression analysis of equilibrium data with several isotherm models and their optimization.", *Chemical Engineering Journal*, 122, 93-106.

Kuosa, M., Haario, H., and Kallas, J. (2006). "Axial Dispersion Model for Estimation of Ozone Self- Decomposition Axial Dispersion Model for Estimation of Ozone Self-Decomposition.", *Ozone : Science & Engineering : The Journal of the International Ozone Association*, 27, 409-417.

Kuosa, M., Laari, A., and Kallas, J. (2004). "Determination of the Henry's coefficient and mass transfer for ozone in a bubble column at different pH values of water.", *Ozone: Science & Engineering*, 26 (3), 277–286.

Kusvuran, E., Gulnaz, O., Samil, A., and Erbil, M. (2010). "Detection of double-bond ozone stoichiometry by an iodimetric method during ozonation processes.", *Journal of Hazardous Materials*, 175, 410-416.

Kuzhali, S. S., Manikandan, N., and Kumuthakalavalli, R. (2012). "Physico chemical and biological parameters of paper industry effluent.", *Journal of Natural Product and Plant Resources*, 2(3), 445–448.

Lafi, W. K., and Qodah, Z. A. (2006). "Combined advanced oxidation and biological treatment processes for the removal of pesticides from aqueous solutions.", *Journal of Hazardous Materials*, 137 (2006) 489–497.

Lakdawala, M. M., and Oza, B. N.(2011). "Removal of BOD contributing components from sugar Industry waste water using bagasse fly ash- waste material of sugar Industry.", *Der Chemica Sinica*, 2 (4), 244-251.

Langlais, B., Reckhow, D. A., and Brink, D. R. (1991). "Ozone in water treatment-application and engineering.", Lewis Publisher, American Water Works Association Research Foundation, Michigan.

Lee, S. H., Kim, H. J., Sakai, E., and Daimon, M. (2003). "Effect of particle size distribution of fly ash-cement system on the fluidity of cement pastes.", *Cement and Concrete Research*, 33, 763–768.

Li, H., Cao, X., Zhang, C., Qing, Y., Zhao, Z., Niu, X., Sun, X., Liu, Y., Ma, L., and Li, Z. (2017). "Enhanced adsorptive removal of anionic and cationic dyes from single or mixed dye solutions using MOF PCN-222.", *Royal Society of Chemistry Advances*, 7, 16273-16281.

Lin, S. H., and Lin, C. M. (1993). "Treatment of Textile Waste Effluents by Ozonation and Chemical Coagulation.", *Water Research*, 27 (12), 1743-1748.

Lin, S. Y. and Dence, C. W. (1992). " Methods in lignin chemistry.", Springer-Verlag, 1-568.

Lokeshappa, B., and Dikshit, A. K. (2011). "Disposal and management of fly ash.", Internation Conference on Life Science and Technology (IPCBEE). 3, Singapore.

Loutfi, H., Blackwell, B., and Uloth, V. (1991). "Lignin recovery from kraft black liquor: Preliminary process design." *TAPPI Journal*, 74(1), 203–210.

Lu, X., Yang, B., Chen, J., and Sun, R. (2009). "Treatment of waste water containing azo dye reactive brilliant red X-3B using sequential ozonation and upflow biological and aerated filter press.", *Journal of Hazardous Materials*, 161, 241–245.

Mandavgane, S. A. and Yenkie, M. K. N. (2011). "Effect of pH on the medium on degradation of aqueous ozone.", *Rasayan J Chem*, 3, 544-547.

Marce, M., Domenjoud, B., Esplugas, S., and Baig, S. (2016). "Ozonation treatment of urban primary and bio treated wastewaters : Impacts and modeling.", *Chemical Engineering Journal*, 283, 768–777.

Mall, I. D., Srivastava, V. C., and Agarwal, N. K. (2006). "Removal of Orange-G and Methyl Violet dyes by adsorption onto bagasse fly ash - Kinetic study and equilibrium isotherm analyses.", *Dyes and Pigments*, 69, 210–223.

Maroto-Valer, M. M., Taulbee, D. N., and Hower, J. C. (2001). "Characterization of differing forms of unburned carbon present in fly ash separated by density gradient centrifugation.", *Fuel*, 80, 795–800.

Mehmet, F. S., and Hasan, Z. S. (2002). "Ozone treatment of textile effluents and dyes: Effect of applied ozone dose, pH and dye concentration.", *Journal of Chemical Technology and Biotechnology*, 77, 842–850.

Meric, S., Selcuk, H., and Belgiorno, V. (2005). "Acute toxicity removal in textile finishing waste water by Fenton's oxidation, ozone and coagulation–flocculation processes.", *Water Research*, 39, 1147–1153.

Meza, P. R., Felissia, F. E., and Area, M. C. (2010). "Reduction of the recalcitrant COD of high yield pulp mills effluents by AOP. Part 1. Combination of ozone and activated sludge.", Bioresources, 6(2), 1053-1068.

Mittal, A., Jhare, D., and Mittal, J. (2013). “Adsorption of hazardous dye Eosin Yellow from aqueous solution onto waste material De-oiled Soya: Isotherm, kinetics and bulk removal.”, *Journal of Molecular Liquids*, 179, 133–140.

Mittal, A., and Lishakurup, M. J. (2007). “Freundlich and Langmuir adsorption isotherms and kinetics for the removal of Tartrazine from aqueous solutions using hen feathers.”, *Journal of Hazardous Materials*, 146, 243-248.

Mitani, M. M., Keller, A. A., Sandall, O. C., and Rinker, R. G. (2005). “Mass transfer of ozone using a microporous diffuser reactor system.”, *Ozone Science and Engineering*, 27, 45–51.

Nassar, M. (2003). “Thermal Behavior of Bagasse Kraft Black Liquor.”, *Energy Sources*, *25*(8), 837–844.

Negrão, D. R., Sain, M., Leão, A. L., Sameni, J., Jeng, R., De Jesus, J. P. F., and Monteiro, R. T. R. (2015). “Fragmentation of lignin from organosolv black liquor by white rot fungi.”, *BioResources*, *10*(1), 1553–1573.

Nouri, H., and Ouederni, A. (2013). “Modeling of the Dynamics Adsorption of Phenol from an Aqueous Solution on Activated Carbon Produced from Olive Stones.”, *International Journal of Chemical Engineering*, 4, 254–261.

Nwabanne, J. T., and Igbokwe, P. K. (2012). “Adsorption performance of packed bed column for the removal of Lead (ii) using oil Palm Fibre.”, *International Journal of Applied Science and Technology*, 2 (5), 106-115.

Obi, O. F., and Okongwu, K. C. (2016). Characterization of fuel briquettes made from a blend of rice husk and palm oil mill sludge. *Biomass Conversion and Biorefinery*.

Ohman, F. (2006). “Precipitation and separation of lignin from kraft black liquor.” Ph.D. thesis, Division of Forest Products and Chemical Engineering, Chalmers University of Technology, Sweden.

Öhman, F., Wallmo, H., and Theliander, H. (2007). “Precipitation and filtration of lignin from black liquor of different origin.”' *Nordic Pulp & Paper Research Journal* 22(2), 188-193.

Olalekan, A. O., Olatunya, A. P., Dada, A. M., and Dada, O. (2012). “Langmuir, Freundlich, Temkin and Dubinin-Radushkevich isotherms studies of equilibrium sorption of Zn2+ unto phosphoric acid modified rice husk.”, *International Organization of Scientific Research Journal of Applied Chemistry*, 3, 38–45.

Olsson, M. R., Axelsson, E., and Berntsson, T. (2006). “Exporting lignin or power from heat-integrated kraft pulp mills: A techno-economic comparison using model mills.” *Nordic Pulp & Paper Research Journal*, 21(4), 476–484.

Olya, M. E., Pirkarami, A., and Mirzaie, M. (2013). “Adsorption of an azo dye in an aqueous solution using hydroxyl-terminated polybutadiene (HTPB).”, *Chemosphere*, 91(7), 935–940.

Olya, M. E., Nezhad, B. Z., and Khodadadi, M. R., (2016) . “Synthesis , characterization and application of Al-Ag / ZnO nano photocatalyst for dye degradation in a new multi layered cylindrical photoreactor.”, *Mediterranean Journal of Chemistry*, 13, 2013–2015.

Omomnhenle, S., Ofomaja, A., and Okiemen, F. E. (2006). “Sorption of Methylene Blue by Unmodified and Modified Citric Acid Saw Dust.”, *Chemical Society of Nigeria*, 30 (1 & 2): 161- 164.

Ong, S.T., Lee, C.K., and Zainal, Z. (2007). “Removal of basic and reactive dyes using ethylene diamine modified rice hull.”, *Bioresources Technology*, 98, 2792–2799.

Ordoño, E., and Rollon, A. (2012). “The Effect of Ozonation Pre-treatment in Enhancing the Biodegradability of Effluent from Distillery of Ethanol Fermented from Molasses.”, *International Journal of Engineering and Applied Sciences*, 1(2), 47–52.

Ozcan, A.S., and Erdem, B. (2004). “Adsorption of Acid Blue 193 from aqueous solutions onto Na-bentonite and DTMA-bentonite.”, *Journal of Colloid and Interface Science*, 280, 44–54.

Palma C., Moreira M. T., Mielgo I., Feijoo G. and Lema J. M. (1999). “Use of a fungal bioreactor as a post treatment step for continuous decolourisation of dyes.”, *Water Science & Technology*, 40, 131-136

Paprocki, A., Dos Santos, H. S., Hammerschitt, M. E., Pires, M., and Azevedo, C. M. N. (2010). “Ozonation of azo dye acid black 1 under the suppression effect by chloride ion.”, *Journal of The Brazilian Chemical Society*, 21(3), 452–460.

Pengthamkeerati, P., Satapanajaru, T., Chatsatapattayakul, N., Chairattanamanokorn, P., and Sananwai, N. (2010). “Alkaline treatment of biomass fly ash for reactive dye removal from aqueous solution.”, *Desalination*, 261, 34–40.

P_erez-Marín, A. B., Meseguer, V. Z., Ortuno, J. F., Aguilar, M., S_aez, J., and Llorens, M. (2007). “Removal of cadmium from aqueous solutions by adsorption onto orange waste.”, *Journal of Hazardous Materials. B.*, 139, 122-131.

Prasad, D.Y. (1992). “The Anaerobic Biodegradation of a Bagasse- Based Paper-Mill Waste in Fixed-Film Reactor.”, *Journal of Chemical Technology & Biotechnology*, 53, 67–72.

Rachakornkij, M., Ruangchuay, S., and Teachakulwiroj, S. (2004). “Removal of reactive dyes from aqueous solution using bagasse fly ash.”, *Songklanakarin Journal of Science and Technology*, 26(Suppl. 1), 13-24.

Rahchamani, J., Zavvarmousavi, H., and Behzad, M. (2011). “Adsorption of methyl violet from aqueous solution by polyacrylamide as an adsorbent: Isotherm and kinetic studies.”, *Desalination* 267, 256-260.

Ramezanianpour, A. (2014). “Cement Replacement Materials.”, Geochemistry/Mineralogy, Springer-Verlag, Berlin Heidelberg, 48–50.

Raschip, I. E., Hitruc, G. E., Vasile, C., and Popescu, M. (2013). “International Journal of Biological Macromolecules Effect of the lignin type on the morphology and thermal properties of the xanthan / lignin hydrogels.”, 54, 230–237.

Rastegarfar, N., Behrooz, R., and Bahramifar, N. (2015). “Electrocoagulation treatment of black liquor from soda-AQ pulping of wheat straw.”, *Environmental Monitoring and Assessment*, *187*(2), 45.

Regti, A., Kassimi, A. E., Laamari, M. R., and Haddad, M. E. (2016). “ Competitive adsorption and optimization of binary mixture of textile dyes: A factorial design analysis.”, *Journal of the Association of Arab Universitites for Basic and Applied Sciences* (doi:10.1016/j.aubas.2016.07.005).

Report on Fly Ash Generation at Coal/Lignite Based Thermal Power Stations and its Utilization in the Country for the Year 2015. Central Electricity Authority. New Delhi, 1.

Rhim, J. A., and Yoon, J. H. (2005). “Mass Transfer Characteristics and Overall Mass Transfer Coefficient in the Ozone Contactor.”, *Korean Journal of Chemical Engineering*, 22 (2), 201–207.

Rodríguez-Mirasol, J., Cordero, T., and Rodriguez, J. J. (1996). “High temperature carbons from lignin.” *Carbon*, 34, 43–52.

Rytioja, J., Hildén, K., Yuzon, J., Hatakka, A., de Vries, R. P., and Mäkelä, M. R. (2014). Plant-Polysaccharide-Degrading Enzymes from Basidiomycetes. *Microbiology and Molecular Biology Reviews*, *78*(4), 614–649.

Saakshy, Sharma, A. K., and Jain, R. K. (2008). “Waste water for hanmade paper making: Preliminary Observations.”, *Hydro* , 1125-1128.

Saakshy, Sharma., A. K., and Jain., R. K. (2013). “ Application of natural dyes: An emerging environment friendly solution to the handmade paper industry.”, R.C Kuhad and A. Singh (eds.) Biotechnology for Environmental Management and Resource Recovery, 279-288.

Saakshy, Sunita, Khan, M. E., Kumar, A., and Sharma, A. K. (2015), "A Peep in to Indian Handmade Paper Industry.", Handmade Paper & Products Souvenir Paperex, 45-62.

Sağ, Y., and Aktay, Y. (2000). "Mass transfer and equilibrium studies for the sorption of chromium ions onto chitin.", *Process Biochemistry, 36*(1–2), 157–173.

Sameni, J., Krigstin, S., Rosa, D. dos S., Leao, A., and Saini, M. (2014). "Thermal characteristics of lignin residue from industrial processes.", *BioResources*, *9*(1), 725–737.

Sammons, R. J., Harper, D. P., Labbe, N., Bozell, J. J., Elder, T., and Rials, T.G. (2013). "Characterization of Organosolv Lignins using Thermal and FT-IR Spectroscopic Analysis.", *Bioresources*, 8 (2), 2752–2767.

Santamarina, J. C., Klein, K. A., Wang, Y. H., and Prencke, E. (2002). "Specific surface: Determination and relevance.", *Canadian Geotechnical Journal*, 39, 233-241.

Saravanan, M., Anbu, J., Maharajan, G., and Pillai, K. S. (2008). "Targeted delivery of diclofenac sodium via gelatin magnetic microspheres formulated for intra-arterial administration.", *Journal of Drug Targeting*, 366–378.

Saroj, S., Kumar, K., Pareek, N., Prasad, R., and Singh, R. P. (2014). "Biodegradation of azo dyes Aci red 183, direct blue 15 and direct red 75 by the isolate penicillium oxalicum SAR-3.", *Chemosphere*, 107, 240–248.

Scott, G. M., and Smith, A. (1995). "Sludge characteristics and disposal alternatives for recycled fibre plants.", *Recycling Symposium*, 239-249.

Selcuk, H. (2005). "Decolourization and detoxification of textile wastewater by ozonation and coagulation processes.", *Dyes and Pigments*, 64, 217–222.

Selvam, K., and Priya, M. S. (2012). "Biological Treatment of Pulp and Paper Industry Effluent by White Rot Fungi Schizophyllum commune and Lenzites eximia.", *International Journal of Pharmaceutical & Biological Archives*, 3(1), 121-126.

Senapati, M. R. (2011). “Fly ash from thermal power plants: Waste management and Review.”, *Current Science*, 100, 1791-1794.

Sevimli, M. F., and Sarikaya, H. Z. (2002). “Ozone treatment of textile effluents and dyes: Effect of applied ozone dose, pH and dye concentration.”, *Journal of Chemical Technology and Biotechnology*, 77, 842–850.

Shah, A.K., Ali, Z. M., Memon, A. R., Laghari, A. J., Mughal, M. A., Shah, S. F. A., and Hussain, S. (2013). “Exploitation of low cost coal fly ash adsorbent with coagulants for the treatment of industrial complex nature dyes waste water.”, *International Journal of Scientific & Industrial Research*, 4 (9).

Sharma, A., and Ramotra, A. (2014). “Physico – Chemical Analysis of Paper Industry Effluents in Jammu city (J&K).”, *International Journal of Scientific and Research*, 4 (10), 10–13.

Shawaqfaha, M., Al Momanib, F. A., and Al-Anber, Z. A. (2012). “Ozone treatment of aqueous solutions containing commercial dyes.”, *AFINIDAD LXIX*, 559, 229–234.

Shu, H. Y., and Huang, C. R. (1995). “Degradation of commercial azo dyes in water using ozonation and UV enhanced ozonation process.”, *Chemosphere*, 31 (8), 3813-3825,

Singh, P., and Thakur, I. S. (2004). “Removal of colour and detoxification of pulp and paper mill effluent by microorganisms in two step bioreactor.”, *Journal of Scientific & Industrial Research*, 63, 944–948.

Sjostorm. E., (1993). “Wood Chemistry: Fundamentals & Applications.” 1-240.

Skousen, J., Yang, J. E., Lee, J. S., and Ziemkiewicz, P. (2013). “Review of fly ash as soil amendment.”, *Geosystem Engineering*, 16 (3), 249-256.

Smook., G. A. (1992) Handbook for Pulp and Paper Technologists, 2nd Edition, Angus Wilde Publications.

Somensi, C. A., Simionatto, E. L., Bertoli, S. L., Wisniewski, A., and Radetski, C. M. (2010). "Use of ozone in a pilot-scale plant for textile wastewater pre-treatment: Physico-chemical efficiency, degradation by-products identification and environmental toxicity of treated wastewater.", *Journal of Hazardous Materials,* 175, 235–240.

Somppi, J. L. (1998). "Experimental studies on pulp and paper mill sludge ash behaviour in fluidized bed combustors.", VTT Publications.

Sonar, S. K., Niphadkar, P. S., Mayadevi, S. M., and Joshi, P. N. (2014). "Preparation and characterization of porous fly ash/NiFe2O4 composite: Promising adsorbent for the removal of Congo red dye from aqueous solution.", Material Chemistry and Physics, 148, 371–379.

Sotelo, J. L., Ovejero, G., Rodriguez, A., S., and Garcia, J., (2012). Removal of atenolol and isoproturon in aqueous solutions by adsorption in a fixed-bed column.", *Industrial & Engineering Chemistry Research*, 51, 5045–5055.

Sridhar, R., Sivakumar, V., and Thirugnanasambandham, K. (2016). "Response surface modeling and optimization of upflow anaerobic sludge blanket reactor process parameters for the treatment of bagasse based pulp and paper industry wastewater.", *Desalination and Water Treatment*, 57, 4345–4356.

Standard Methods of Examination of Water & Waste water (1999) American Public Health Association, American Water Works Association, Water Environment Federation, 1-541.

Sundrarajan, M., Vishnu, G., and Joseph, K. (2007). "Decolourisation of exhausted reactive dye bath using ozonator for reuse.", *International Journal of Environmental Science and Technology*, 4, 263–270.

Swamy, N. K., Singh, P., and Sarethy, I. P. (2016). "Effect of Sequential Treatment of Paper Industry Wastewater using Aluminium Chloride and Pseudomonas putida.", *Indian Journal of Advances in Chemical Science,* 226–229.

Swamy, N. K., Singh, P., and Sarethy, I. P. (2016). “Effect of Sequential Treatment of Paper Industry Wastewater using Aluminum Chloride and Pseudomonas putida.”, *Indian Journal of Advances in Chemical Science,* S1,226–229.

Tapalad, T., Neramittagapong, A., Neramittagapong, S., and Boonmee, M. (2008). “Degradation of congo red dye by ozonation.”, *Chiang Mai Journal of Science,* 35(1), 63–68.

Taty-Costodes, V. C., Fauduet, H., Porte, C., and Ho, Y. S. (2005). “Removal of lead (II) ions from synthetic and real effluents using immobilized Pinus sylvestris sawdust: Adsorption on a fixed-bed column.”, *Journal of Hazardous Materials*, *123*(1–3), 135–144.

Tehrani-Bagha, A. R., Mahmoodi, N. M., and Menger, F. M. (2010). “Degradation of a persistent organic dye from colored textile waste water by ozonation.”, *Desalination,* 260, 34–38.

Temkin, M. I., and Pyzhev, V. (1940). “Kinetics of ammonia synthesis on promoted iron catalyst.”, *Acta Physico-Chimica Sinica*, 12, 327-356.

Terry, A. P. (2010). “Application of ozone and oxygen to reduce chemical oxygen demand and hydrogen sulfide from a recovered paper processing plant.”, International Journal of Chemical Engineering, 1-6.

Thapar Centre for Industrial Research & Development, 2011, Secondary Sludge Treatment and Disposal in Pulp & Paper Industry, Indian Paper Manufacturers Association, 1-104.

Tiwari, G., and Bose, P. (2007). “Determination of ozone mass transfer coefficient in a tall continuous flow counter-current bubble contactor.”, *Chemical Engineering Journal*, 132, 215–225.

Tucker, P., 2005, Co-composting paper mill sludges with fruit and vegetable wastes, University of Paisley, 1-167.

Turhan, K., and Turgut, Z. (2012). “Treatment and degradability of direct dyes in textile wastewater by ozonation: A laboratory investigation.”, *Desalination and Water Treatment*, 11, 184-191.

Turhan, K., and Ozturkcan, S. A. (2013). “Decolourization and degradation of reactive dye in aqueous solution by ozonation in a semi-batch bubble column reactor.”, *Water, Air & Soil Pollution*, 224, 1353.

Turhan, K., Durukan, I., Ozturkcan, S. A., and Turgut, Z. (2012). “Decolorization of textile basic dye in aqueous solution by ozone.”, *Dyes and Pigments,* 92, 897–901.

Ukiwe, L. .N., Ibeneme, S. I., Duru, C. E., Okolue, B. N., Onyedika, G. O., and Nweze, C. A. (2014). “Chemical and electrocoagulation techniques in coagulation-floccculationin water and wastewater treatment- A review.”, *International Journal of Recent Research & Applied Studies*, 18 (3), 285-294.

Uloth, V. C., and Wearing, J. T. (1989). “Kraft lignin recovery-Acid precipitation versus ultrafiltration: Laboratory test results.”, Pulp & Paper-Canada, 90(9), 67-71.

Usharani, K., Muthukumar, M., and Kadirvelu, K. (2012). “Effect of pH on the degradation of aqueous organophosphate (methylparathion) in wastewater by ozonation.”, *International Journal of Environmental Research,* 6(2), 557–564.

Varasavanan, T., and Sreekrishnan, T. R. (2005). “Bio-physico-chemical treatment for removal of colour from pulp and paper mill effluents.”, *Journal of Scientific & Industrial Research*, 64, 61-64.

Vargas, J., and Halog, A. (2015). “Effective carbon emission reductions from using upgradedfly ash in the cement industry.”, *Journal of Cleaner Production*, 103, 948-959.

Verma, G., Singh, R. K., and Sahu, V. (2013). “A comparative study on the removal of heavymetals by adsorption using fly ash and sludge: A review.”, *International Journal of Application or Innovation in Engineering and Management*, 2(7), 45-56.

Vijayaraghavan, K., Padmesh, T. V. N., Palanivelu, K., and Velan, M. (2006). "Biosorption of nickel (II) ions onto Sargassumwightii: application of two-parameter and three parameter isotherm models.", *Journal of Hazardous Materials B*, 133, 304-308.

Vilela, N., Augusta, A., and Rezende, P. (2016). "Evaluation of briquettes made from textile industry solid waste.", *91*.

Vimonses, V., Lei, S., Jin, B., Chow, C. W. K., and Saint, C. (2009). "Kinetic study and equilibrium isotherm analysis of Congo Red adsorption by clay materials.", *Chemical Engineering Journal*, 148, 354–364.

Wallberg, O., Linde, M., and Jönsson, A.S. (2006). "Extraction of lignin and hemicelluloses from kraft black liquor.", *Desalination*, 199, 413–414.

Wang, X. J., Chen, S. L., Gu, X. Y., Wang, K. Y., and Qian, Y. Z. (2008). "Biological aerated filter treated textile washing wastewater for reuse after ozonation pre-treatment.", *Water Science & Technology*, 58, 919–923.

Watkins, D., Hosur, M., Tcherbi-narteh, A., and Jeelani, S. (2014). "Extraction and characterization of lignin from different biomass resources.", *Journal of Materials Research and Technology*, 4(1), 26-32.

Webber, T. W., and Chakravorti, R. K. (1974). "Pore and solid diffusion models for fixed-bed adsorbers.", *AIChE Journal*, 20(2), 228-238.

Wen-bo, Yang., Huan-zhen, Mu., and Yan-chu, Huang. (2003). "Treatment of the black liquor from the paper making industry by acidification and reuse.", *Journal of Environmental Sciences*, 15 (5), 697-700.

Wesche, K. (1990). "Fly Ash in Concrete Properties and Performance.", RILEM Report.International Union of Testing and Research Laboratories, France.Chapman andHall, London, 7.

www.knhpi.org.in

www.fao.org/forestry/statistics;

www.paperindustryworld.com;
www.statistica.com
www.ibisworld.com/industry/global/global-paper-pulp-mills.htm
www.fao.org
www.flyash2012missionenergy.org
www.ntpc.co.in
www.intechopen.com

White, S. C. and Case, E. D. (1990). "Characterization of fly ash from coal-fired power plants.", *Journal of Materials Science, 25*, 5215–5219.

Wu, J., and Wang, T. (2001). "Ozonation of aqueous azo dye in a semi-batch reactor.", *Water Research,* 35 (4), 1093–1099.

Yadav, S., Agnihotri, S., Gupta, S., and Tripathi, R. K. (2014). "Incorporation of STP sludge and Fly ash in brick manufacturing: An attempt to save the environment.", International Journal of Advance Research in Science and Technology, 3, 138–144

Yamada, K., Haraguchi, K., Gacho, C. C., Wongsiri, B. P., and Pena, M. L. (2003). "Removal of dyes from Aqueous solutions by sorption with coal fly ash.", In: International Ash Utilization Symposium. Centre for Applied Energy Research. Univ. of Kentucky.

Yang, Q., and Wu, S. (2009). "Thermogravimetric characteristics of wheat straw lignin.", *Cellulose Chemistry and Technology, 43*, 133–139.

Yasar, A. (2007). "Ozone for color and COD removal of raw and anaerobically biotreated combined industrial wastewater.", *Polish Journal of Environment Studies*, 16(2), 289–294.

Yong, K., Wu, J., and Andrews, S. (2005). "Heterolytic catalytic ozonation of aqueous reactive dye.", *Ozone: Sciece & Engineering*, 27, 257–263.

Zaied, M., and Bellakhal, N. (2009). “Electrocoagulation treatment of black liquor from paper industry.” *Journal of Hazardous Materials*, 163, 995–1000

Zhao, H., Sun, W., Wu, X., and Gao, B. (2015). “The properties of the self-compacting concrete with fly ash and ground granulated blast furnace slag mineral admixtures.”, *Journal of Cleaner Production*, 95, 66-74.

Zhang, Z., O’Hara, I. M., Kent, G. A., and Doherty, W. O. S. (2013). “Comparative study on adsorption of two cationic dyes by milled sugarcane bagasse.”, *Industrial Crops and Products*, *42*, 41–49.

Zhang, J., Tejada-martínez, A. E., and Zhang, Q. (2014). “Developments in computational fluid dynamics-based modeling for disinfection technologies over the last two decades : A review, *Environmental Modelling & Software*, 58, 71-85.

Zheng, T., Wang, Q., Zhang, T., Shi, Z., Tian, Y., Shi, S., Smale, N., and Wang, J. (2015). “Microbubble enhanced ozonation process for advanced treatment of wastewater produced in acrylic fiber manufacturing industry.”, *Journal of Hazardous Materials*, 287, 412–420.

Zimmermann, S. G., Wittenwiler, M., Hollender, J., Krauss, M., Ort, C., Siegrist, H., and Gunten, U. V. (2010). “Kinetic assessment and modeling of an ozonation step for full-scale municipal wastewater treatment : Micropollutant oxidation , by-product formation and disinfection.”, *Water Research*, 45, 605-617.

APPENDIX

Colour Vs. Absorbance graph

Color. PCU	Absorbance
0	0
50	0.019
100	0.032
200	0.0754
300	0.106
400	0.142
500	0.17

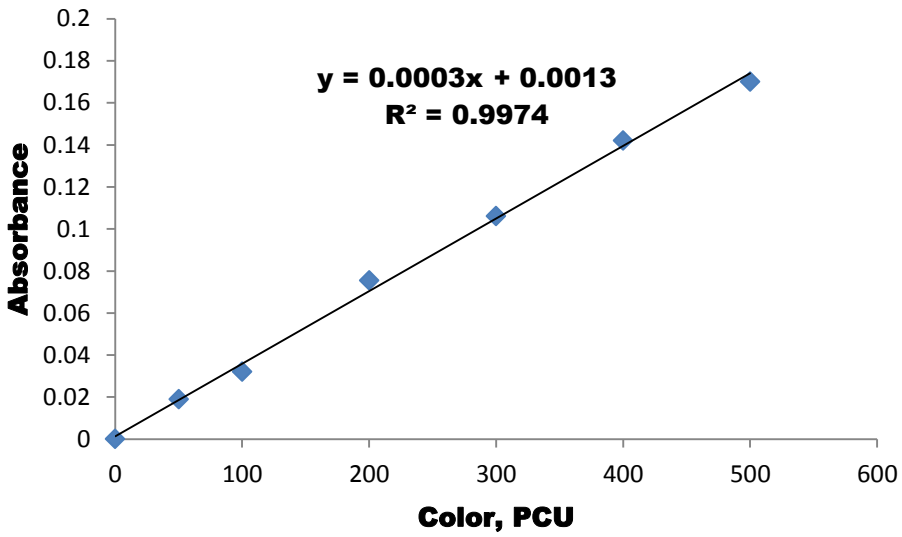

Chemical oxygen demand Vs. Absorbance graph

COD, mg/l	Absorbance
0	0
31.25	0.007
62.5	0.014
125	0.038
250	0.076
500	0.157

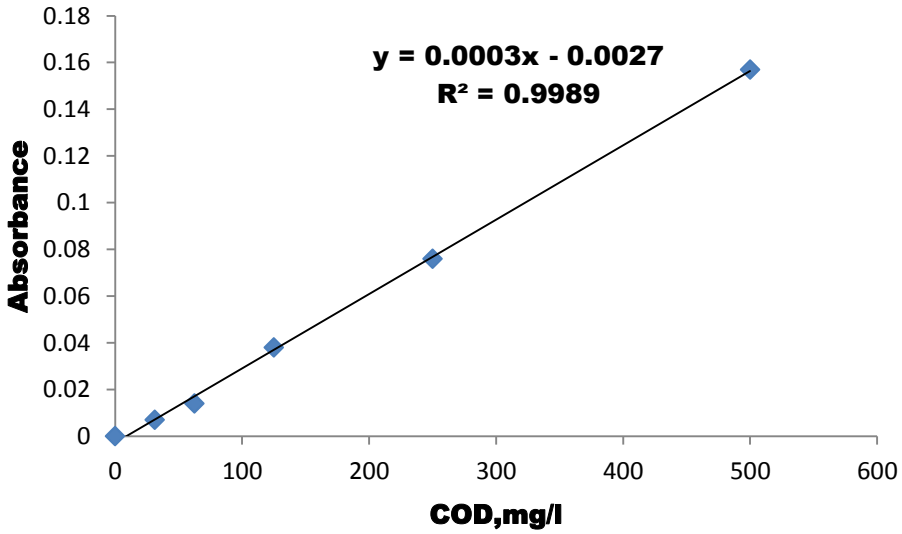

Calibration curve of dyes

Direct Red dye

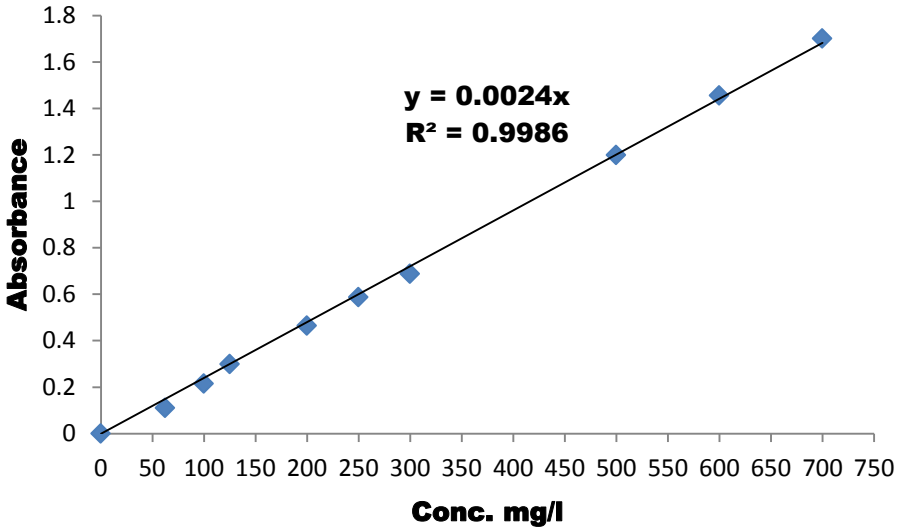

Standard calibration graph of direct red dye

Direct Blue dye

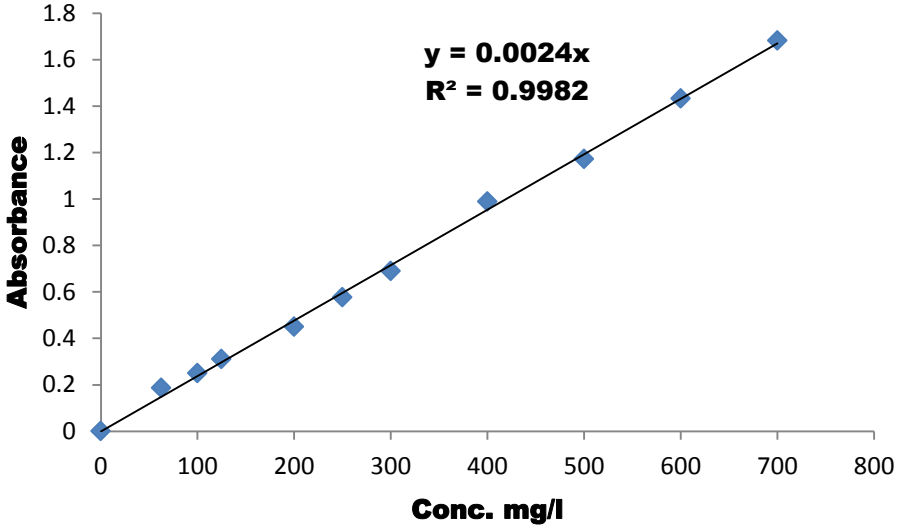

Standard calibration graph of direct blue dye

Direct Black dye

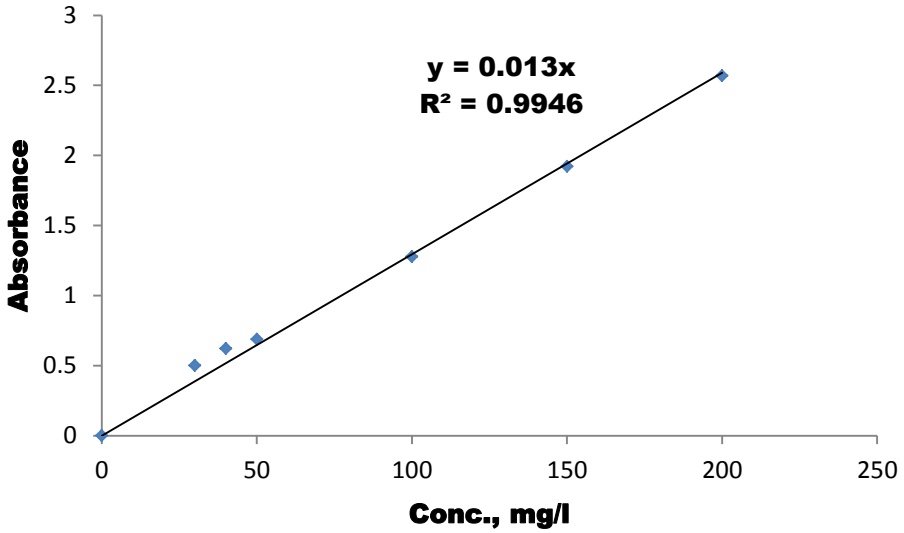

Standard calibration graph of direct black dye

Turquoise blue dye

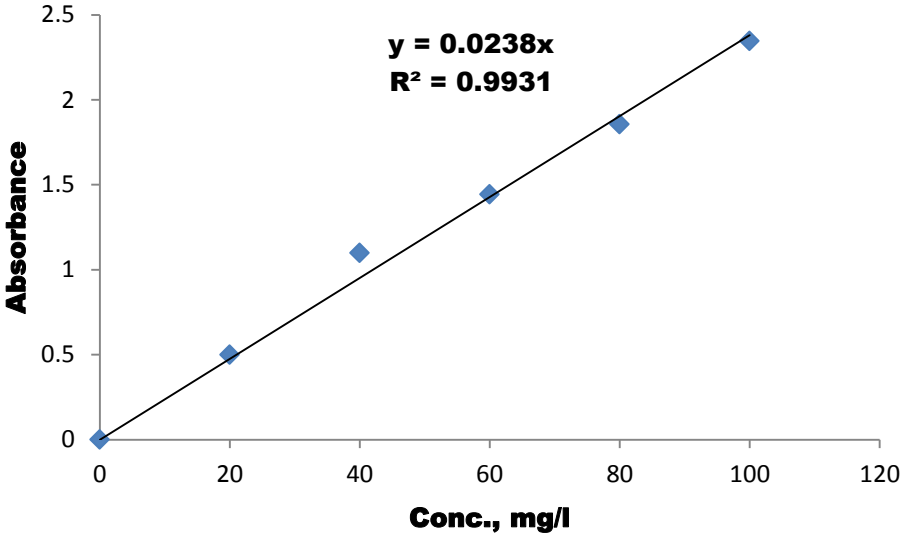

Standard calibration graph of turquoise dye

Matlab programme for Ozonation

```
function pdex4
m = 0;
x = linspace(0,1, 201);
t = linspace(0,600,41);

sol = pdepe(m,@pdex4pde,@pdex4ic,@pdex4bc,x,t);
u1 = sol(:,:,1);  %CG
u2 = sol(:,:,2);  %CL
u3 = sol(:,:,3);  %Cd

figure(1)
surf(x,t,u1)
title('CG(z,t) mol/l')
xlabel('Distance (m)')
ylabel('Time (s)')

figure(2)
surf(x,t,u2)
title('CL(z,t), mol/l')
xlabel('Distance (m)')
ylabel('Time (s)')

figure(3)
surf(x,t,u3)
title('Cd(z,t) mg/l')
xlabel('Distance (m)')
ylabel('Time (s)')

% --------------------------------------------------------------
function [c,f,s] = pdex4pde(x,t,u,DuDx)
global epsG uG uL
Ed=56.5e-5; %Dispersion Coefficient of dye in water, m2/s
EL=83e-5; %Dispersion Coefficient of Dissolved Ozone in Liquid, m2/s
EG= 2e-5; %Dispersion Coefficient of ozone in gas phase, m2/s, Ref.:
Singer, Hull
epsG = 0.0434; %Gas holdup, fraction
HenryConstant=7.2146e6; %pO3=H*CLstar, pO3 is in Pa, CLstar in
mol/liter
MW= 48; %Mol wt of ozone
Rgas = 8.314; %J/mol-K
T= 298; %K
uG=0.02; %superficial vel of ozone, m/s
uL=0.004; %superficial vel of liquid, m/s
kLa = 0.1027; %mass transfer coeff., 1/s

CG=u(1); %mol/liter
CL=u(2); %mol/liter
Cd=u(3); %mg/liter

CLstar=Rgas*T*CG/(MW*HenryConstant);

rd =-(1.3169/60)*Cd; %To be corrected, time in s
rO3= -(0.2166/60)*CL; %To be corrected, time in s



c = [1; 1;1];
f(1)= EG*DuDx(1) - uG*CG/epsG;
```

```
f(2)= EL*DuDx(2) - uL*CL/(1-epsG);
f(3)=Ed*DuDx(3)- uL*Cd/(1-epsG);

f = [f(1);f(2);f(3)];

s(1)=-kLa*(CLstar-CL)/epsG;
s(2)=kLa*(CLstar-CL)/(1-epsG) +rO3;
s(3)=rd;

s=[s(1);s(2);s(3)];

% --------------------------------------------------------------
function u0 = pdex4ic(x);
CG=0;%initial ozone conc. in gas
CL=0; %initial dissolved ozone conc. in liquid
Cd=40; %Dye Conc. initially, mg/L
u0 = [CG; CL; Cd];

% --------------------------------------------------------------
function [pl,ql,pr,qr] = pdex4bc(xl,ul,xr,ur,t)
global epsG uL uG
CGRight=ur(1);
CLRight=ur(2);
CdRight=ur(3);

CGin = 3.41; %mol/L
CLin= 0; %dissolved ozone in water at inlet, mol/L
Cdin= 40; %dye conc. at inlet, mg/L

pl = [uG*CGin; uL*CLin; uL*Cdin];
ql = [epsG ;(1-epsG);(1-epsG)];
pr = [uG*CGRight/epsG;uL*CLRight/(1-epsG);uL*CdRight/(1-epsG)];
qr = [1;1;1];
```

Matlab program for adsorption

```
function [t z cb q]=FixedBedAds()
N=101; %No. of FD points along the bed
BedLength=0.024; %m
dz=BedLength/(N-1);
z=0:dz:BedLength;

cbinit=zeros(1,N);
qinit=zeros(1,N);
yinit=[cbinit;qinit];
tspan=[0,20];
[t y]=ode15s(@(t,y)diffeq(t,y,N,dz),tspan,yinit);
cb(:,1:N)=y(:,1:N);
q(:,1:N)=y(:,N+1:2*N);
figure(1),plot(t,cb(:,end)), title('Bulk Concentration'),
xlabel('Time(s)'),ylabel('Bulk Conc. (mg/m^3)')
figure(2),plot(t,q (:,end)), title('Solid Concentration'),
xlabel('Time(s)'),ylabel('solid Conc. (mg/g)')


function dydt=diffeq(t,y,N,dz)

DL=56.5e-5; %Dispersion coefficient, m2/s
vel=0.01836; %Superficial Velocity, m/s, check it
cbin=50E-3; %mg/m3, inlet dye conc.
K=0.396e-3;
qm=27.39; %mg/g
eps=0.514;
Rp=18e-5;%m
rhop=750e3;%g/m^3
kf=1.99;% External mass transfer coefficient m/s, check it

cb(1:N)=y(1:N);
for i=1:N, q(i)=y(i+N);end

for i=1:N,
   if i==1,
       dcbdz=(cb(1)-cbin)*vel/DL;
       d2cbdz2=(1/dz^2)*(2*cb(2)-2*cb(1)-
2*vel*dz*cb(1)/DL+2*vel*dz*cbin/DL);
   end

   if i>1 && i<N,
    dcbdz=(cb(i+1)-cb(i-1))/(2*dz);
    d2cbdz2=(cb(i+1)-2*cb(i)+cb(i-1))/dz^2;
   end

   if i==N,
       dcbdz=0;
       d2cbdz2=2*(cb(N-1)-cb(N))/dz^2;
   end
   cs=q(i)/(K*(qm-q(i)));
   dqdt(i)=3*kf*(cb(i)-cs)/(Rp*rhop);
   dcbdt(i)=DL*d2cbdz2-vel*dcbdz-(1-eps)*dqdt(i)/eps;

end

dydt=[dcbdt,dqdt]';
```